

ENERGY ANISOTROPIES OF PROTON-LIKE ULTRA-HIGH ENERGY COSMIC RAYS

Jon Paul Lundquist

Thesis Defense
September 22, 2017



INTRODUCTION

PART ONE

- ▶ Overview of Ultra-high Energy Cosmic Rays (UHECR)
 - ▶ Sources and propagation
 - ▶ Previous Results
 - ▶ Anisotropy
 - ▶ Energy Spectrum
 - ▶ Composition
 - ▶ Extensive Air Showers
 - ▶ Telescope Array Project and UHECR Detection

PART TWO

- ▶ Anisotropy Studies
 - ▶ ~~Kernel Density Estimation Hotspot Analysis (not enough time)~~
 - ▶ Energy Spectrum Anisotropy
 - ▶ Energy-Distance Correlation
 - ▶ Hot/Coldspot Summary Analysis

PART THREE

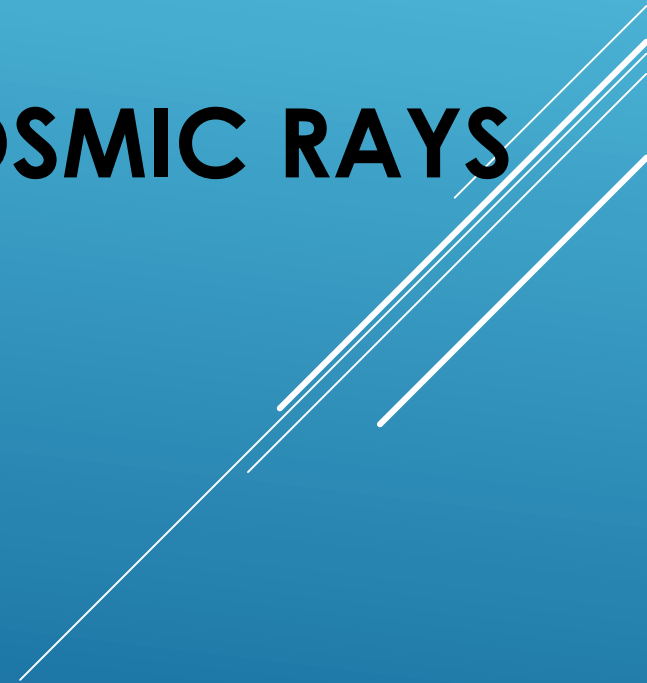
- ▶ Composition Study
 - ▶ Pattern Recognition Analysis
 - ▶ Composition
 - ▶ L-test and the Shift plot

GOALS

- ▶ Remove model dependencies – assumptions and parameters – whenever possible.
 - ▶ Requires the development of new statistical methods.
- ▶ Anisotropy – magnetic deflection as a signature of a source instead of a confounding variable
- ▶ Combine UHECR energy, anisotropy, and composition into one picture.

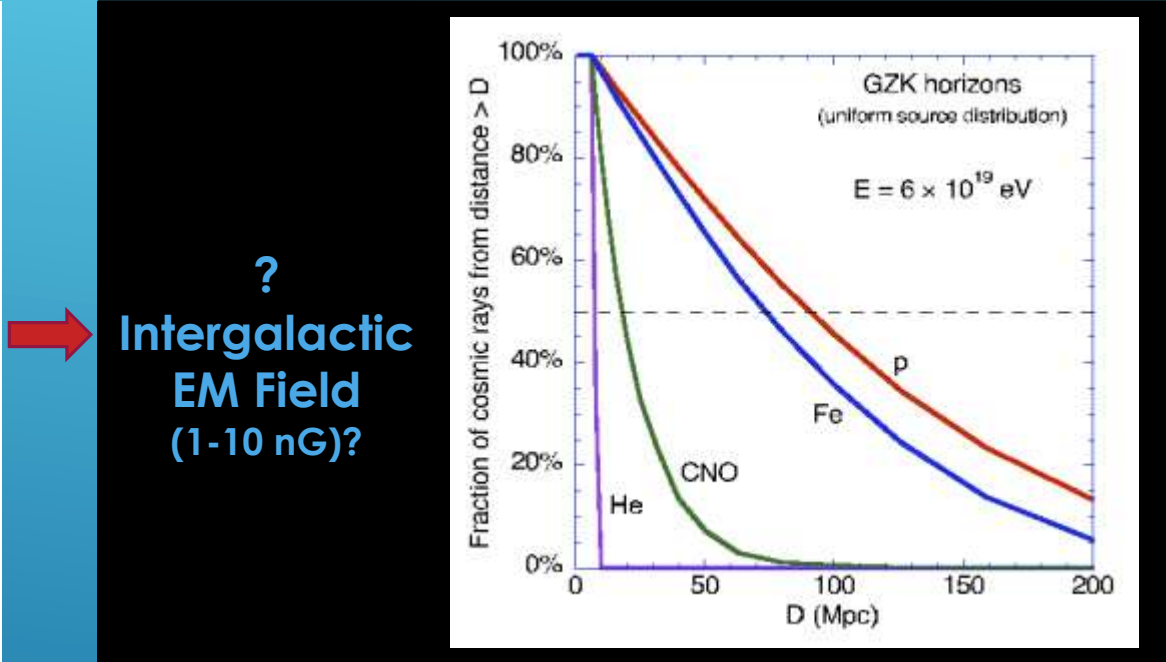
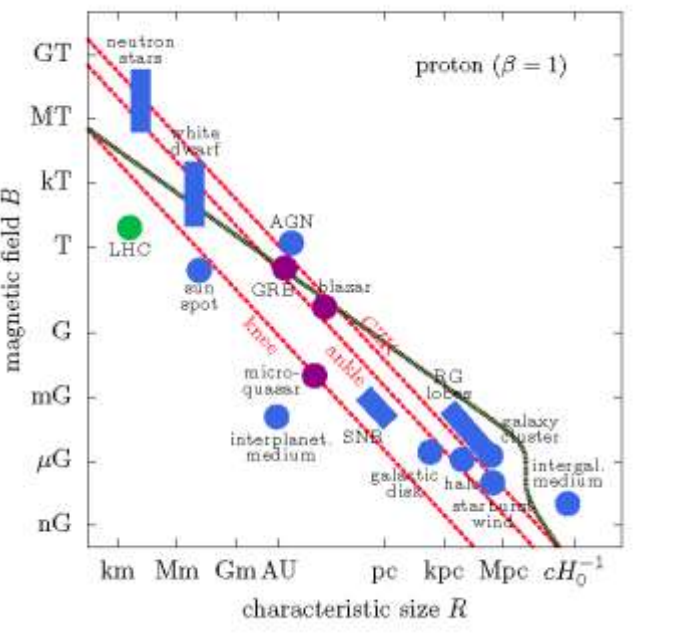
PART ONE

OVERVIEW OF ULTRA-HIGH ENERGY COSMIC RAYS

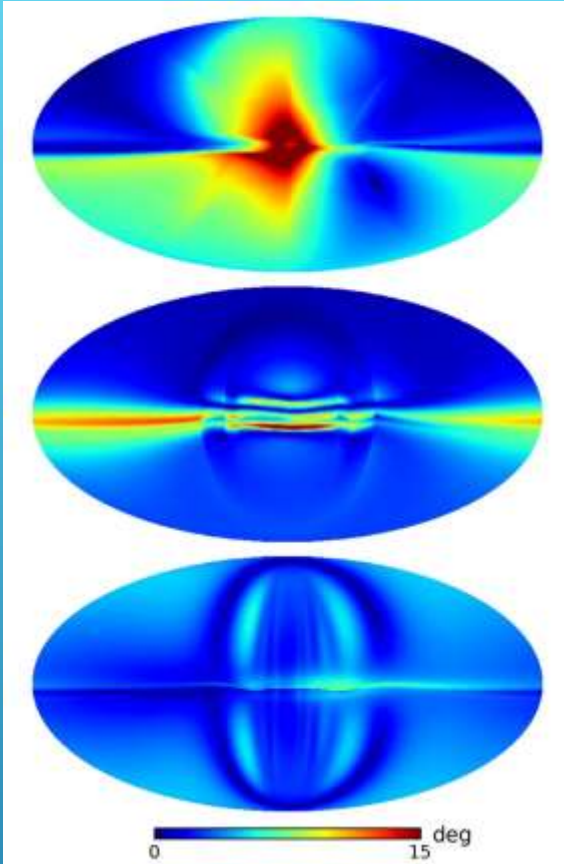


SOURCES AND PROPAGATION

SOURCES



?
Intergalactic
EM Field
(1-10 nG)?



Intragalactic EM Field

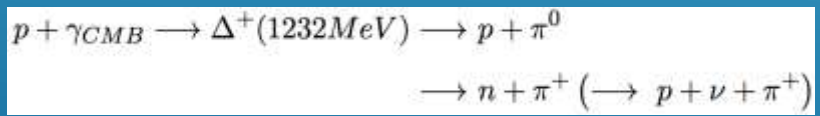
Larmor radius energy limitation

$$E < \frac{E_{max}}{10^{18} \text{ eV}} \cong \frac{1}{2} \beta \cdot Z \cdot \frac{B}{\mu\text{G}} \cdot \frac{L}{\text{kpc}}$$

Relates: energy, sources, composition

$$\delta = \frac{s}{R_{Larmor}} = 0.5^\circ Z \frac{L}{\text{kpc}} \frac{B}{\mu\text{G}} \frac{10^{20}}{E}$$

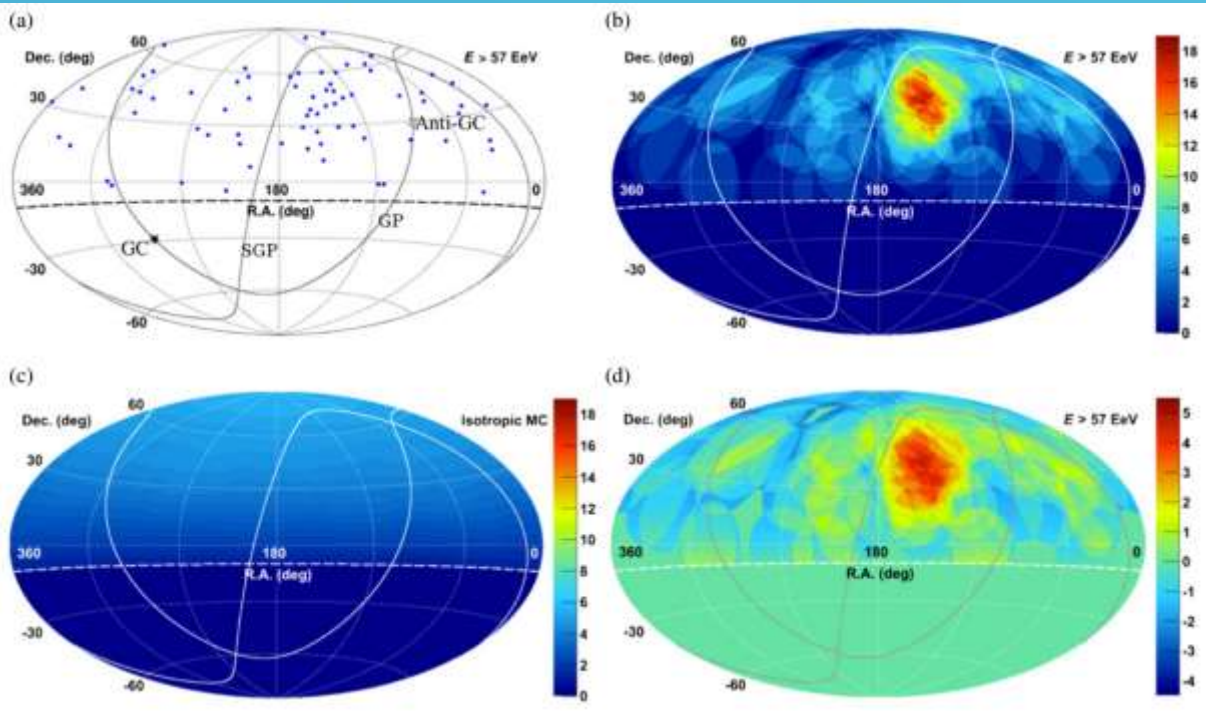
Greisen-Zatsepin-Kuzmin limit
Cosmic Microwave Background



Total Deflection
 $\langle \delta \rangle \approx \sim 10^\circ$ -- $\delta \lesssim 50^\circ$ for $E = 10^{20}$

PREVIOUS RESULTS - ANISOTROPY

TA Hotspot

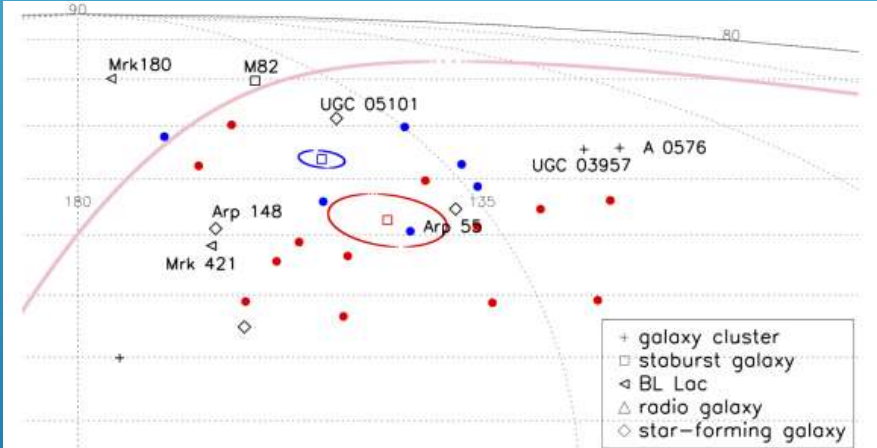


3.4 σ significance of the anisotropy observation

Hotspot near the supergalactic plane:

- Ursa Major cluster (20 Mpc from Earth)
- Coma cluster (90 Mpc)
- Virgo cluster (20 Mpc)

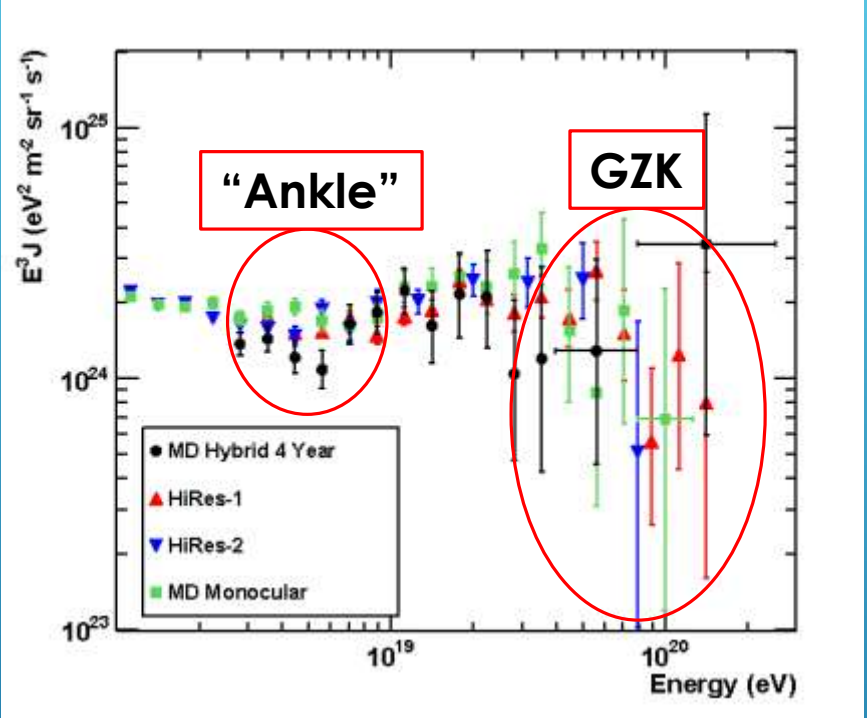
The angular distance to the supergalactic plane is $\sim 17^\circ$.



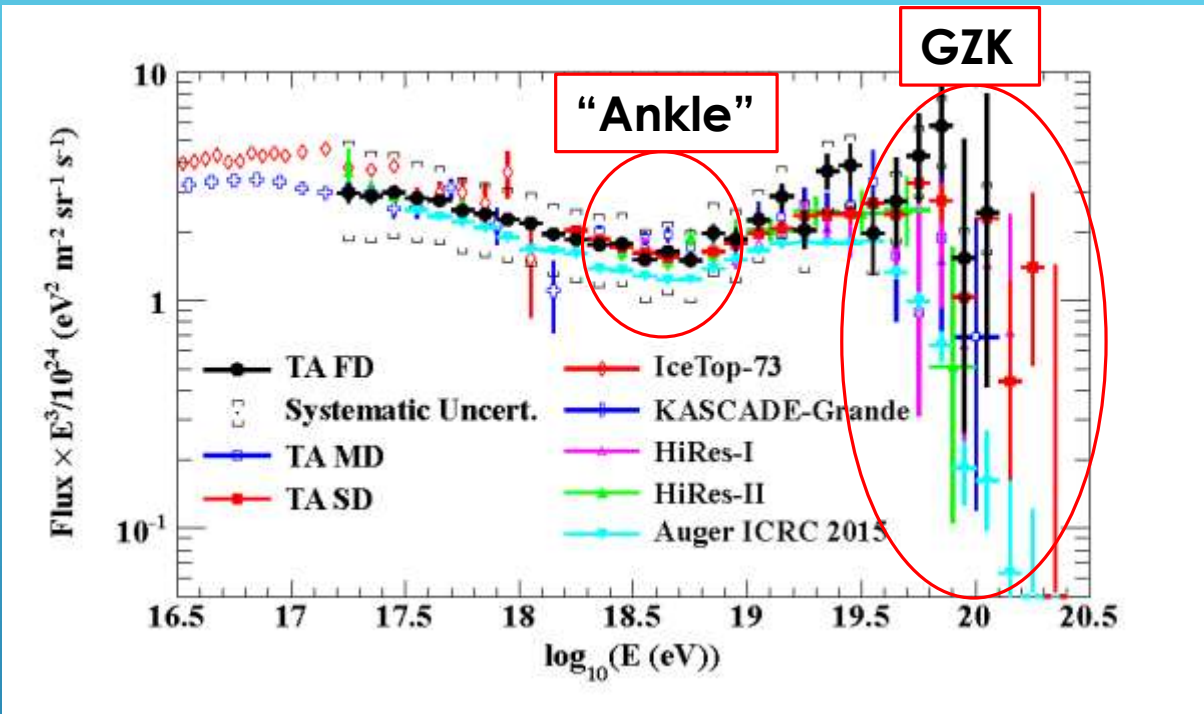
“A Monte Carlo Bayesian Search for the Plausible Source of the Telescope Array Hotspot” He, H.N. et al.

FIG. 2: The 19 events at the hotspot in the equatorial coordinates are denoted by filled circles (red: $E < 75\text{EeV}$; blue: $E > 75\text{EeV}$). Reconstructed positions of shifted sources for two groups of the hotspot events are denoted by the open squares; the errors are shown by ellipses of the corresponding color.

PREVIOUS RESULTS – ENERGY SPECTRUM



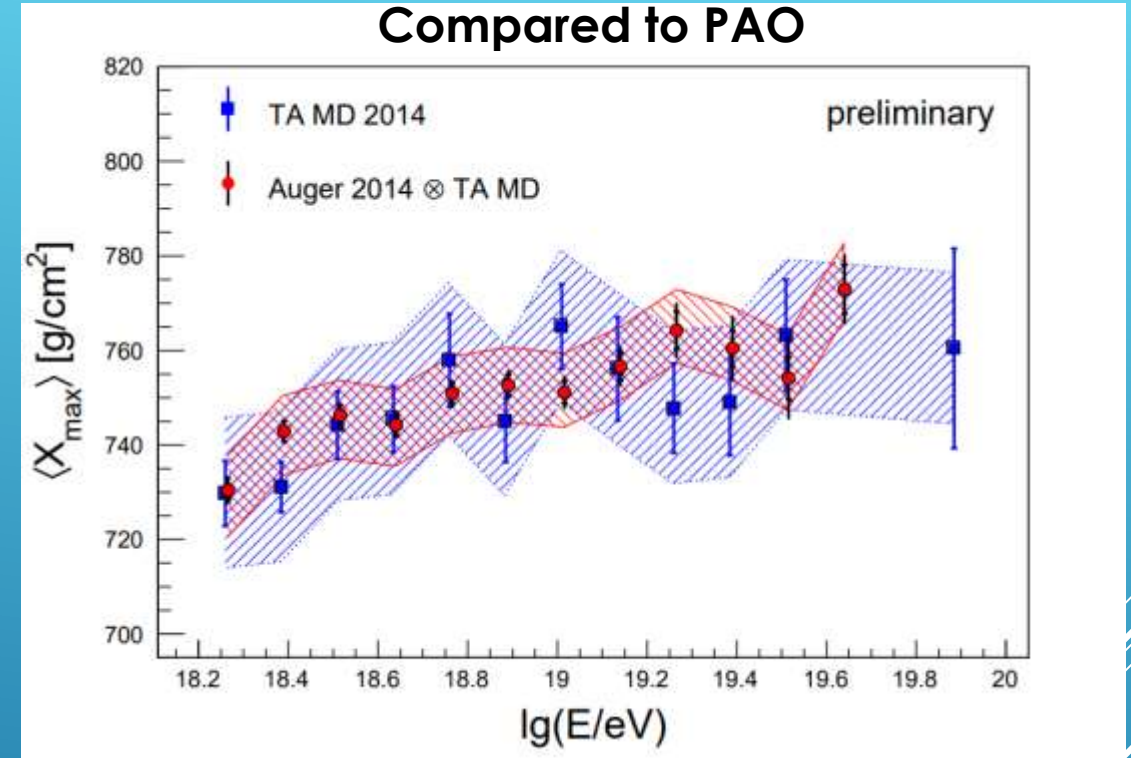
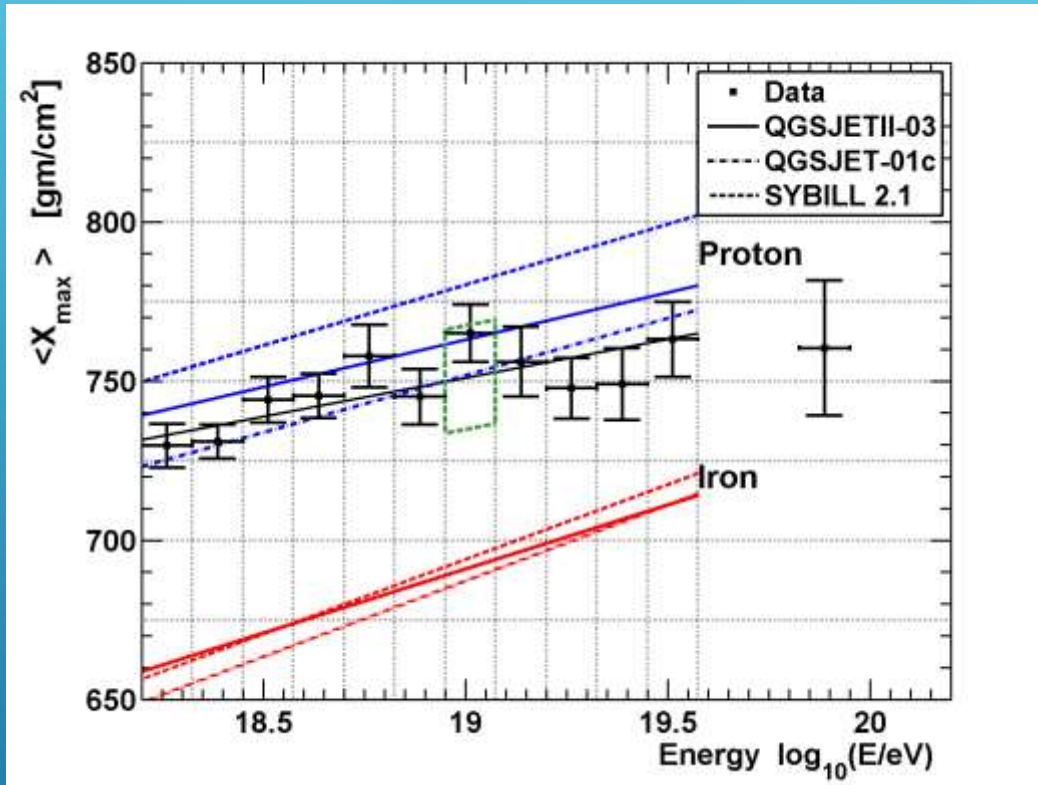
Good Agreement
Between TA Detectors



Good Agreement
Between Experiments

"Ankle" is approximately the end of galactic sources

PREVIOUS RESULTS - COMPOSITION



Published 5 year data result from this thesis work

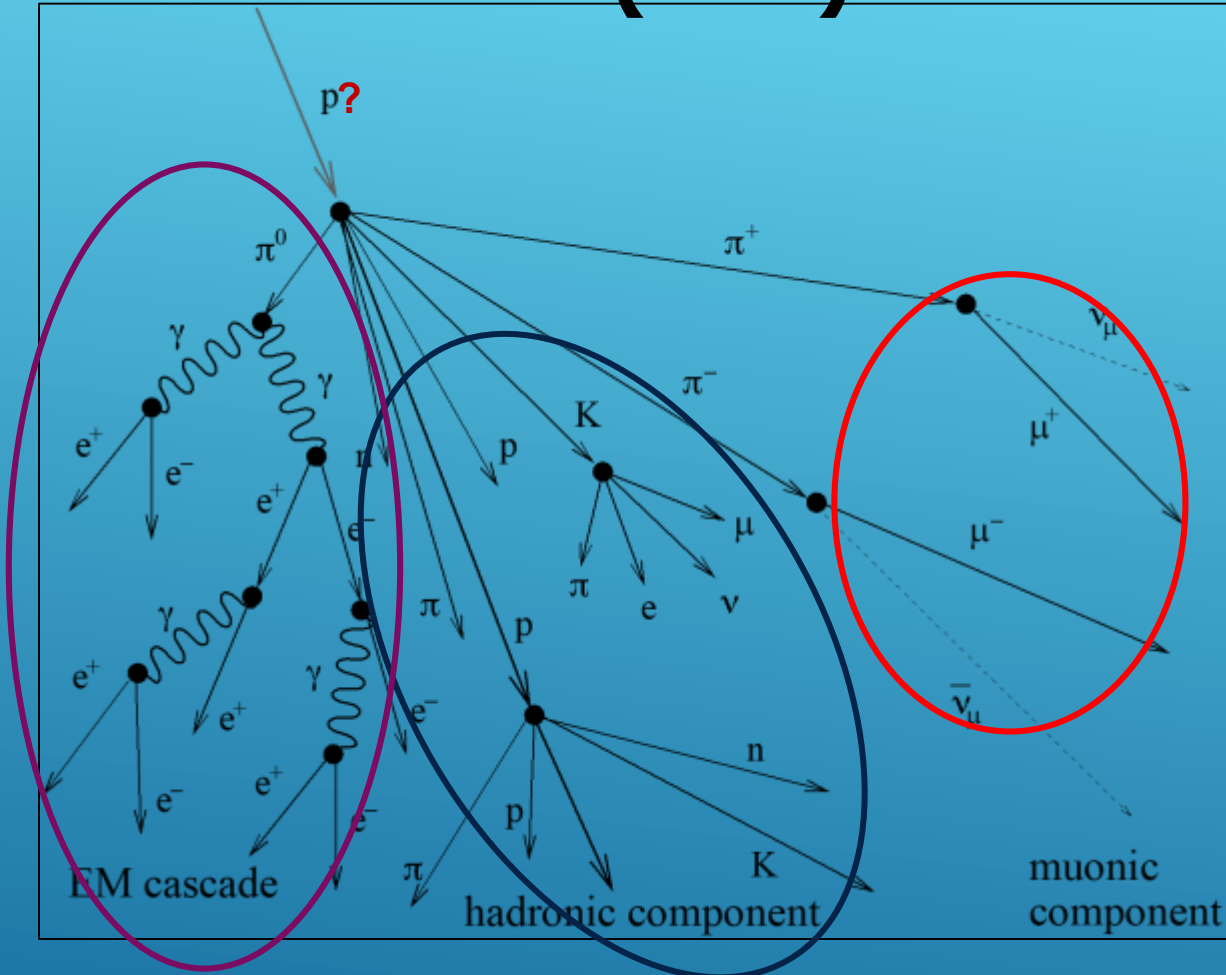
- proton-dominant *depending on model*

- PAO reports heavier at higher energies
 - Data of TA and PAO agree
- *Result of different simulations or North/South anisotropy?*

EXTENSIVE AIR SHOWERS (EAS)

UHECR studied indirectly using extensive air shower

EM Cascade is the largest contribution.



- Muons created early in shower -- charged Pion decays.
- Muons and neutrinos are “missing energy”

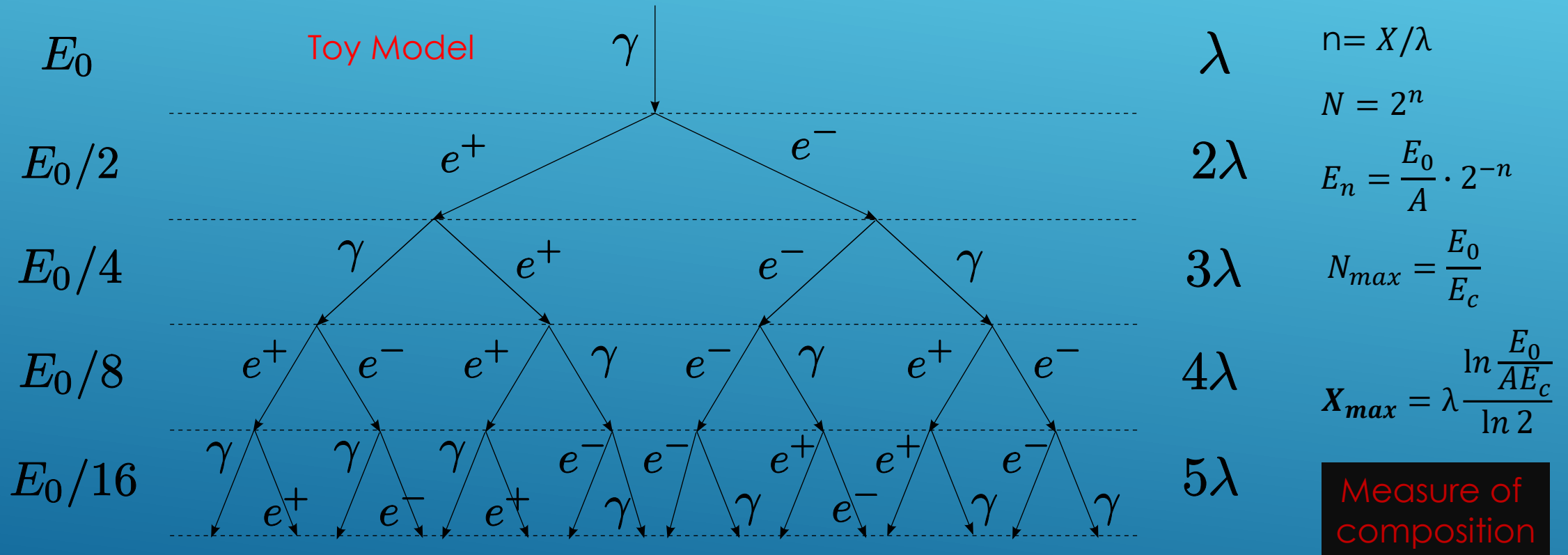
- Collisions result in Pions, Kaons (~8%), and Nucleons (~4-5%)
- 1/3 of the Pions (π^0) decay into two photons and contribute to EM cascade in each generation.
- Kaons contribute ~8% to EM cascade in later generations.

HEITLER MODEL

Radiation length, λ (36.5 g/cm² in air), is about the same for pair production and Bremsstrahlung radiation.

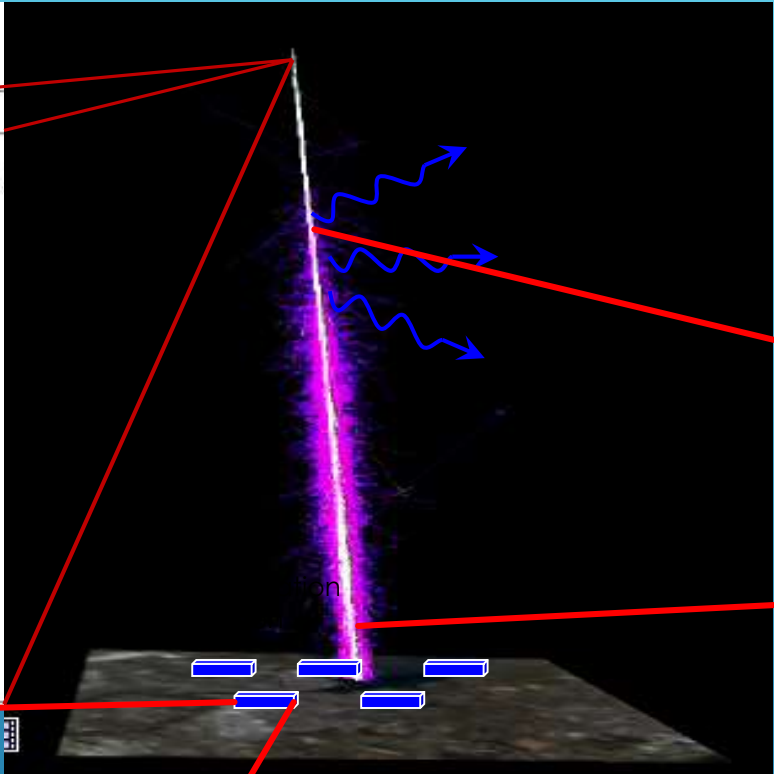
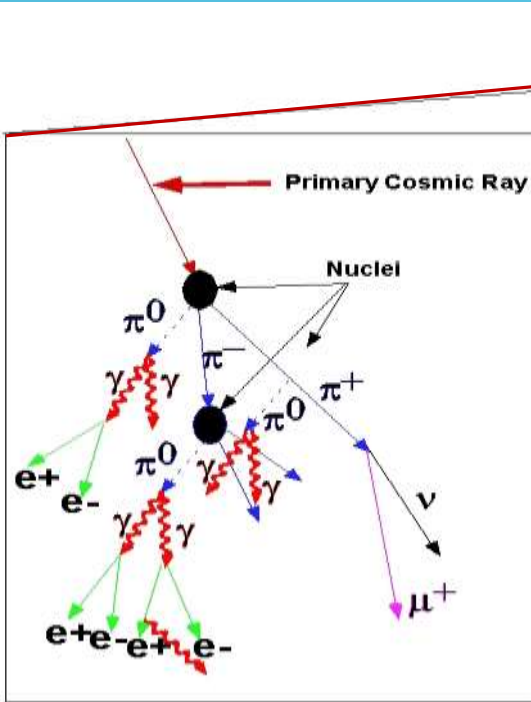
Mean energy per particle

Distance

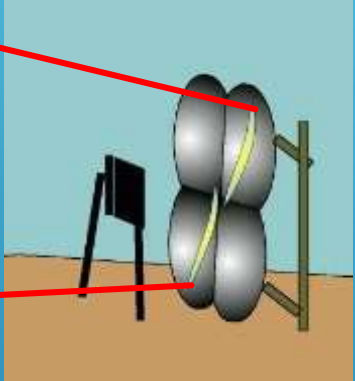


X_{max} : shower depth with maximum particles.
The shower then decreases in size due to ionization losses.

INDIRECT DETECTION



- Fluorescence from charged particle excitation of nitrogen.



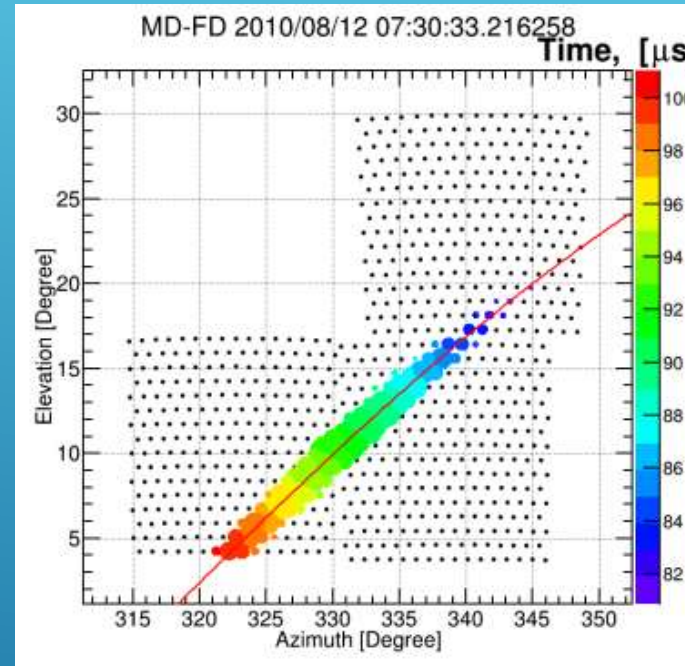
- Charged particles activate scintillator plastic. Picked up by photomultiplier tubes.

SIMULATION, DETECTION, RECONSTRUCTION

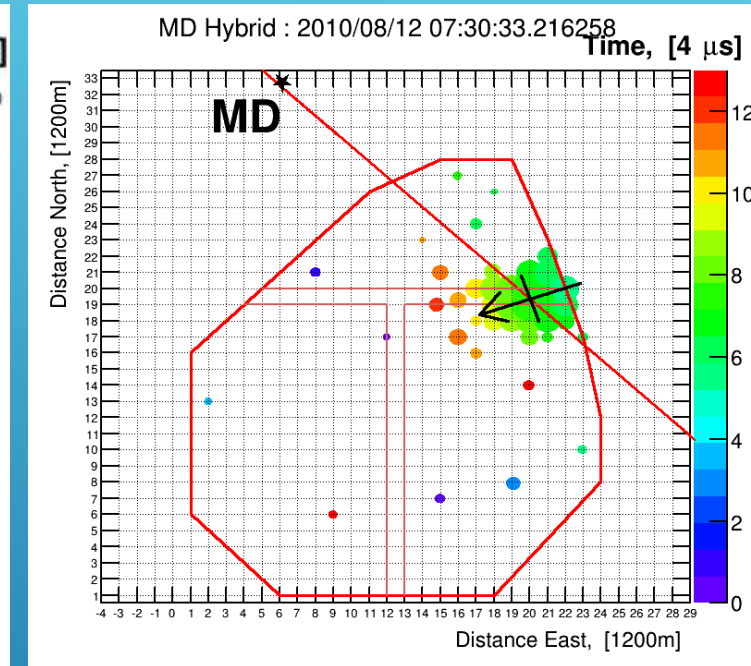
Reconstructions used from previous works



CORSIKA Simulated Air
Shower 10^{15} eV 45° inclination
Red – $e^{+/-}$, γ
Green – $\mu^{+/-}$
Blue – Hadrons ($\pi^{0/+/-}$, $K^{0/+/-}$, p, n)



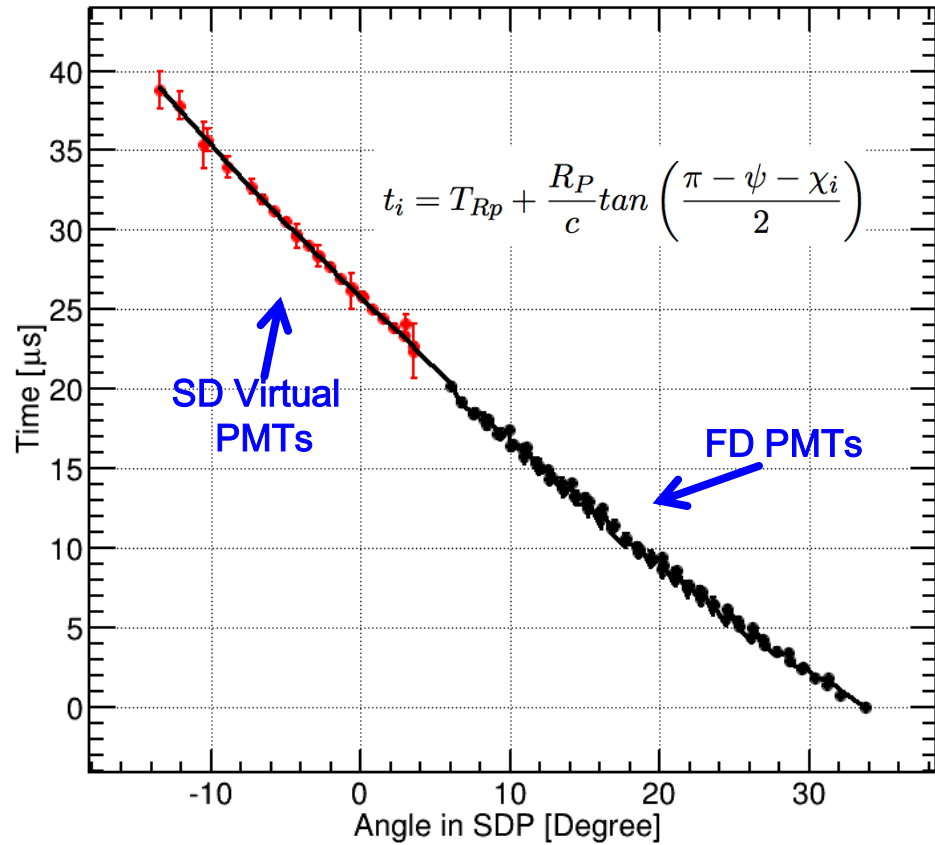
Fluorescence Detector



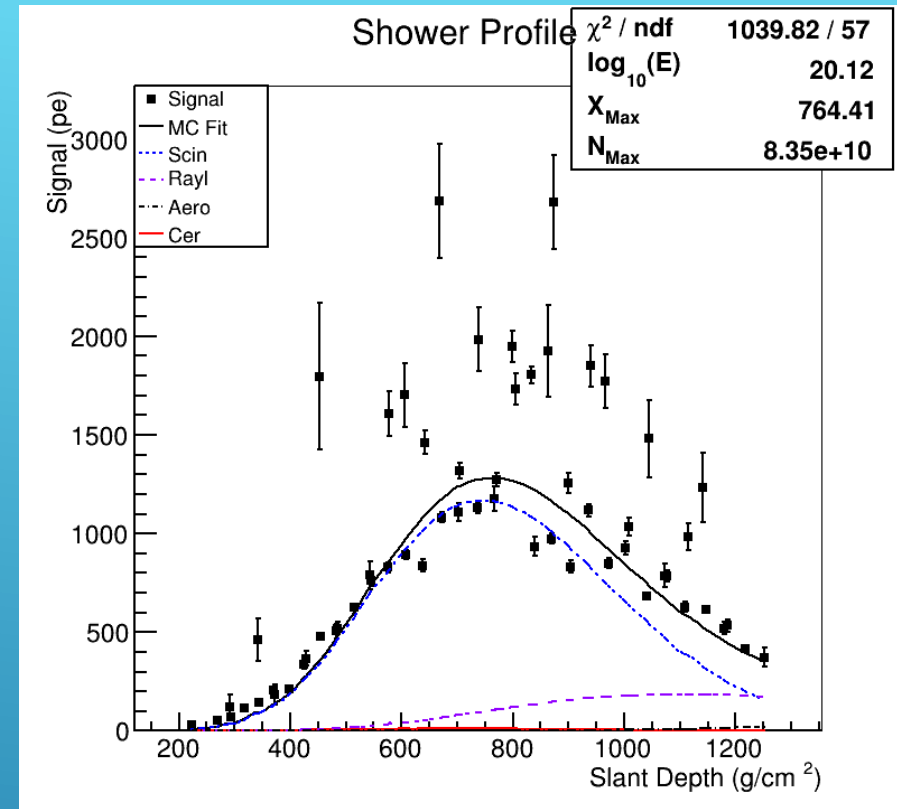
Surface Detector

RECONSTRUCTION

Time vs Angle (Hybrid)



Viewing angle converted to slant depth using atmospheric profile



Fit to GH profile and search for the reconstructed Monte Carlo event that matches the data

$$N(X) = N_{\max} \left(\frac{X - X_0}{X_{\max} - X_0} \right)^{\frac{X_{\max} - X_0}{\lambda}} \exp\left(\frac{X_{\max} - X}{\lambda} \right)$$

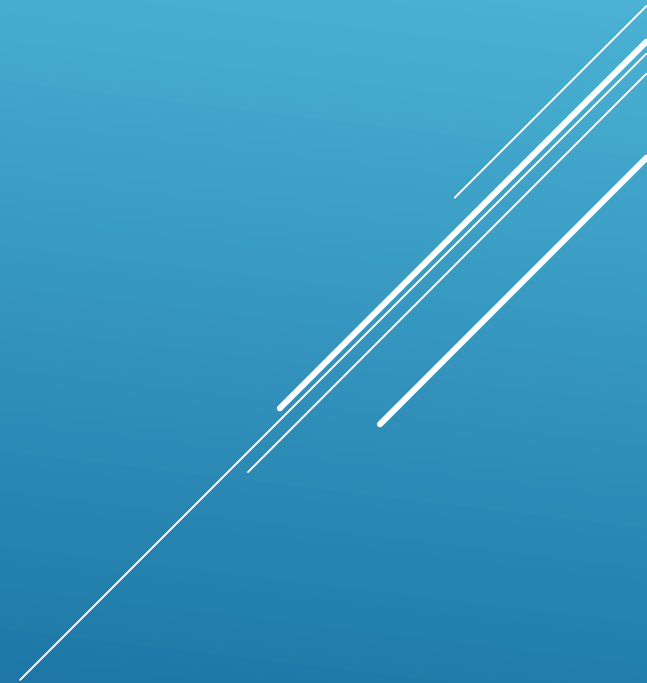
Take energy from MC event which minimizes

$$\chi_{Profile}^2 = \sum_i \frac{1}{\sigma_i^2} \left(S_i^{(m)} - S_i^{(p)} \right)^2$$

S_i are measured and predicted tube signals

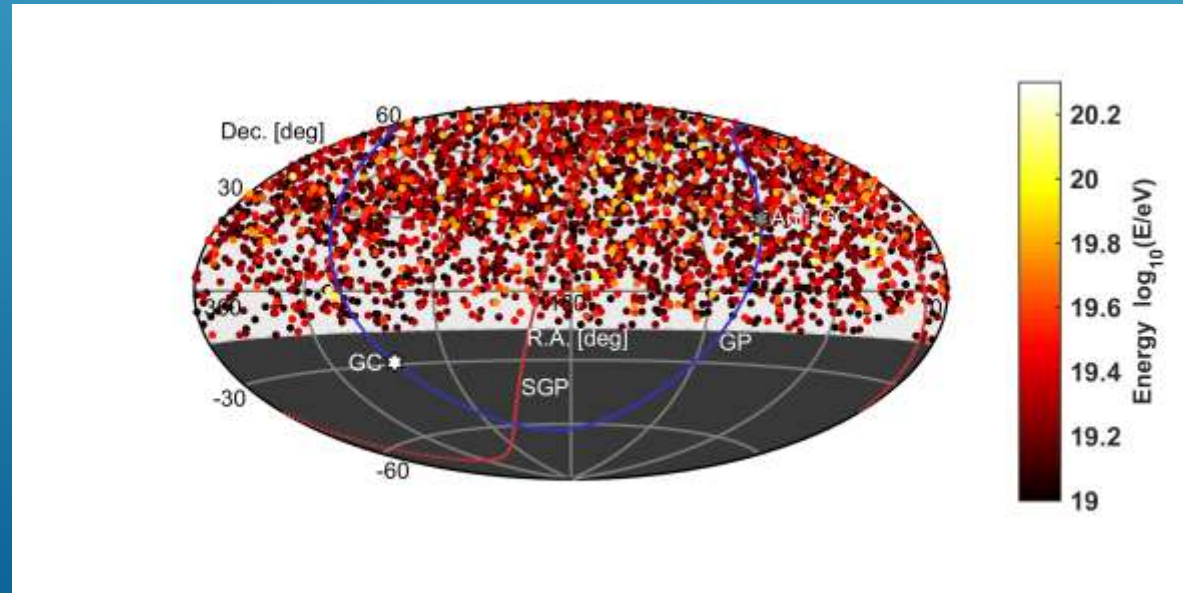
PART TWO

ANISOTROPY STUDIES



DATA SUMMARY

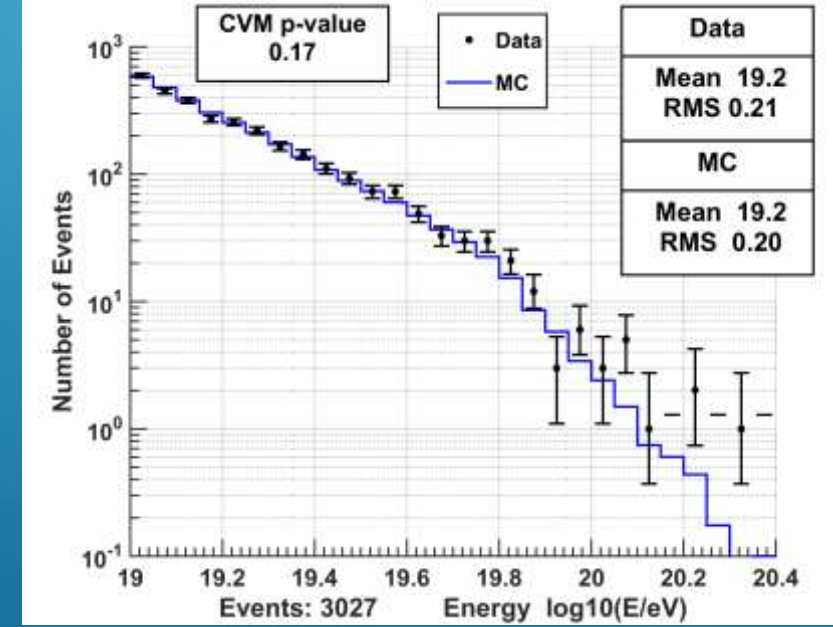
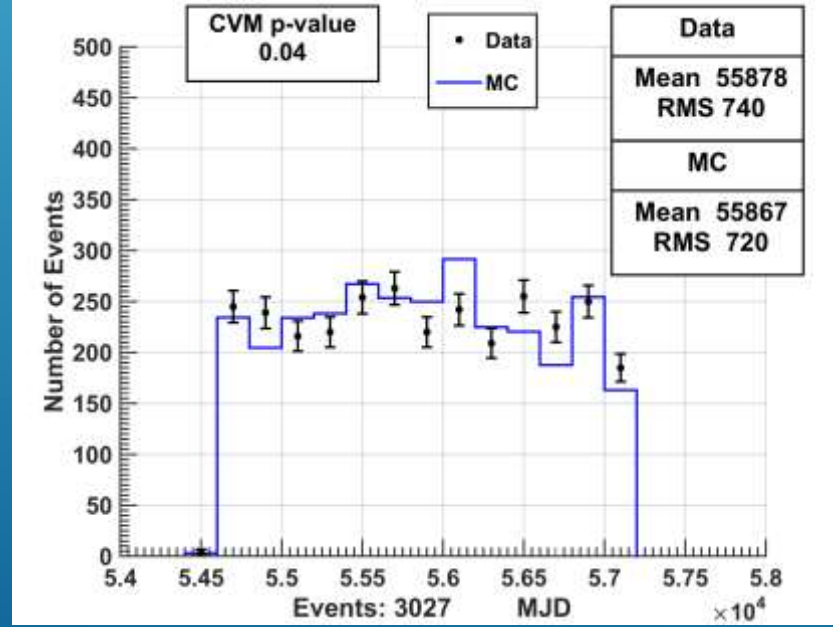
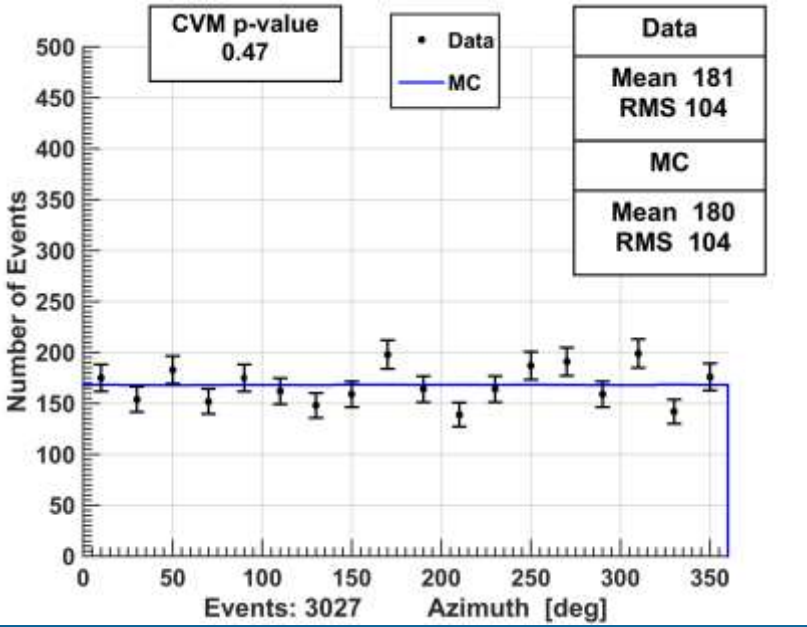
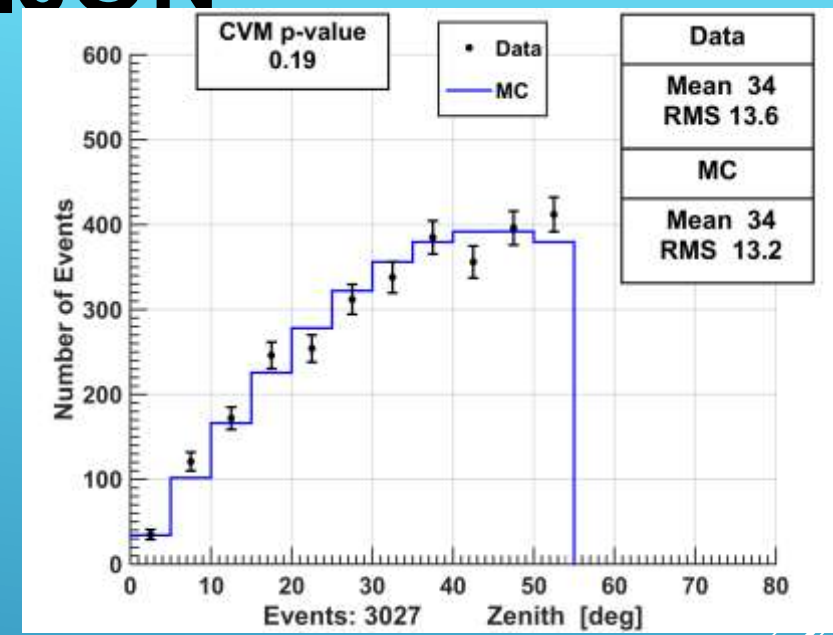
- ▶ **Data:**
 - 7 years surface detector data (*from ICRC hotspot*).
Detector. ≥ 4 , Zenith angle $< 55^\circ$, Pointing Error $< 10^\circ$
 - ▶ **Additional cuts (due to lower energy):**
 - ▶ Pointing direction error $< 5^\circ$, boundary > 1.2 km , Lateral fit $\chi^2 < 10$
 - ▶ $E \geq 10^{19.0}$ eV - 3027 events



ISOTROPIC MONTE-CARLO COMPARISON

- $\sin(\theta) \cdot \cos(\theta)$ – Zenith distribution from detector geometry
- Flat Azimuthal angle distribution.
- On-time simulated – sampling 250,000 event times ($E > 17.7$ EeV).
- Energy sampled from reconstructed HiRes spectrum.

($E > 20$ EeV, $p = 0.48$)



Uniform Azimuth

Time taken from data

Reconstructed HiRes Spectrum

ENERGY SPECTRUM ANISOTROPY

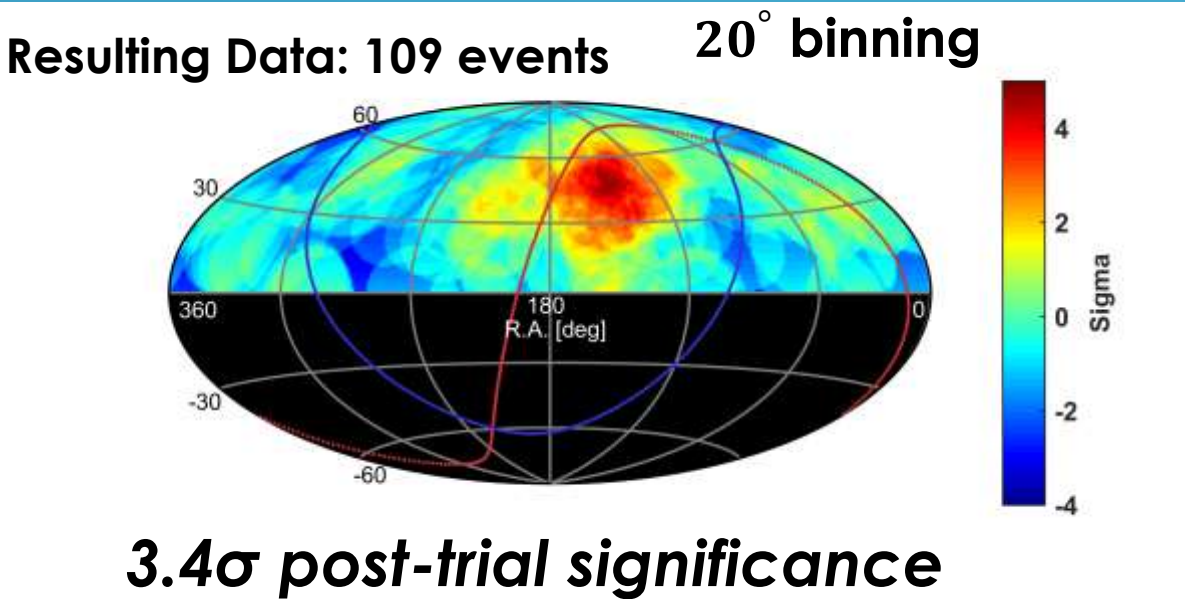
Is there a location on the sky which has a significantly different overall spectrum? Signature of sources, magnetic deflection or both.

7-YEAR DATA HOTSPOT RESULT

Period : 2008 May – 2015 May

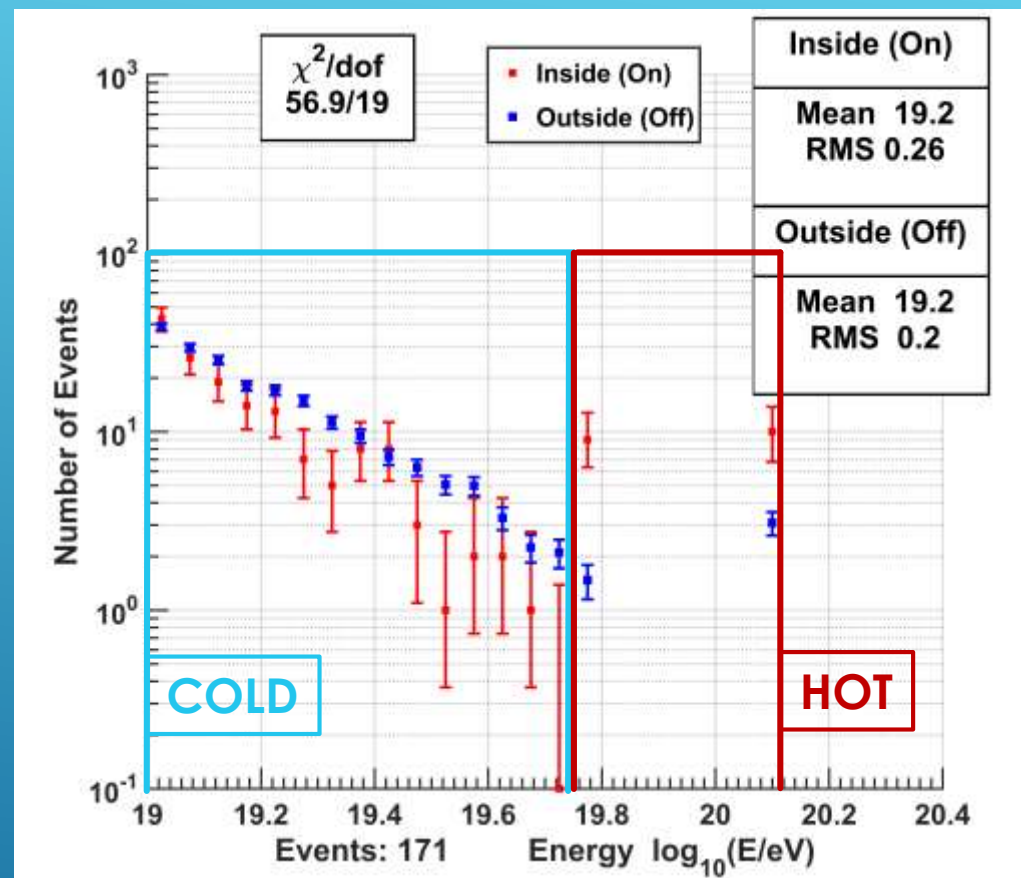
Cuts:

- # of used detectors ≥ 4
- Zenith angle $< 55^\circ$
- Pointing Error $< 10^\circ$
- Energy Threshold $\geq 57\text{EeV}$



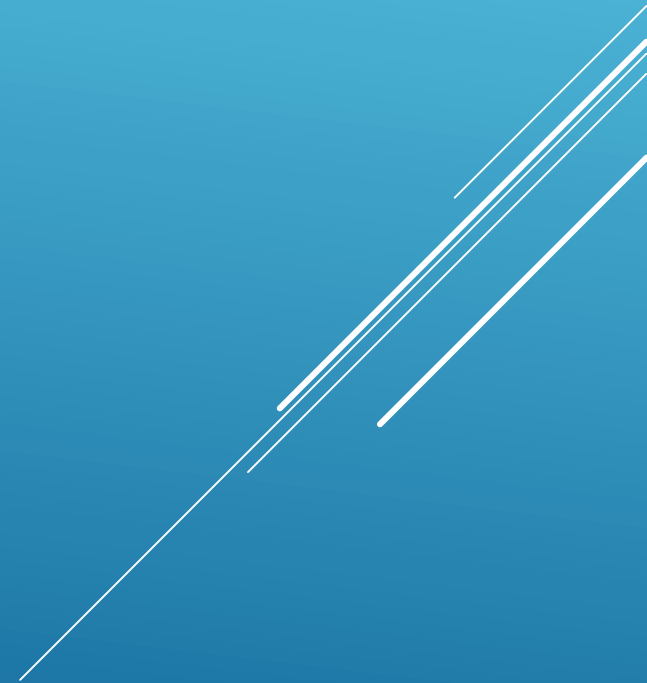
Max. significance 5.1σ
148.5° R.A, 44.5° Dec.
(17° from SGP)

Tighter Cuts, 20° bin



Energy distribution shows
an overall deficit of events

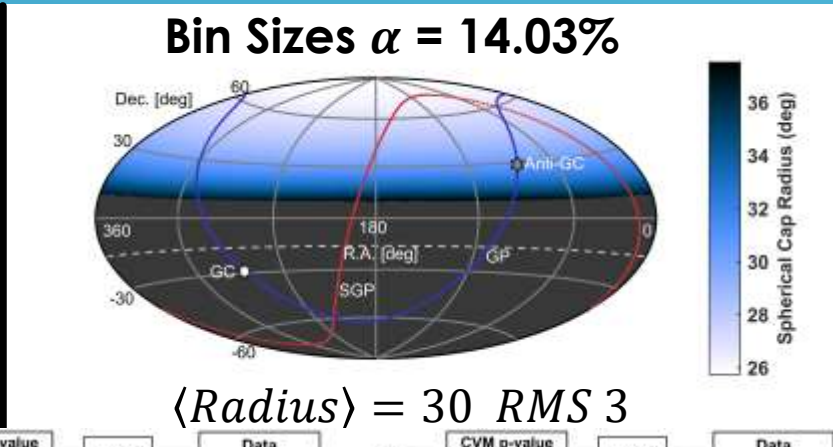
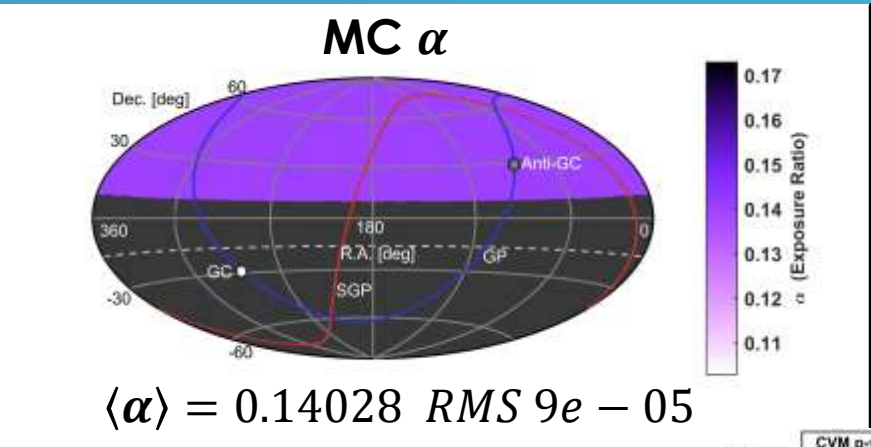
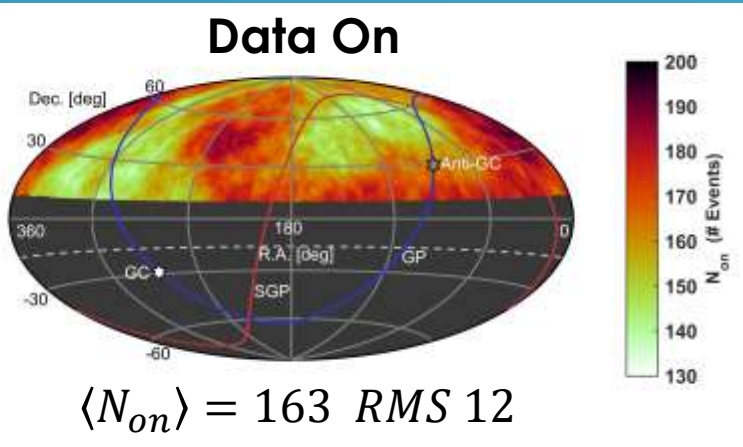
METHOD



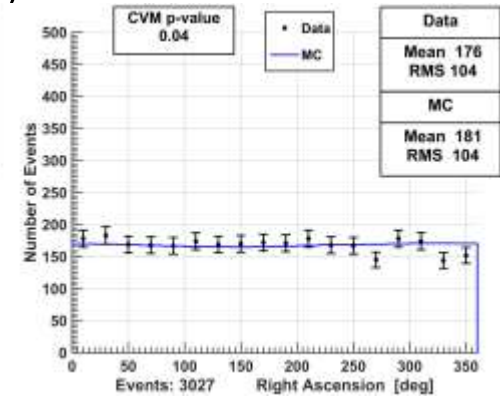
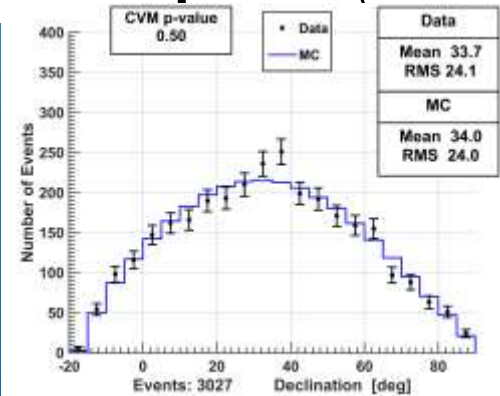
ESTIMATED BACKGROUND – EQUAL EXPOSURE

- Likelihood and χ^2 tests are sample size biased
 - Need to control statistics
- Equal exposure binning samples the sky equally.
 - “On” exposure such that bin size average = 15°, 20°, 25°, 30°

$$\alpha = N_{on}^{MC} / N_{off}^{MC} = \text{constant}$$

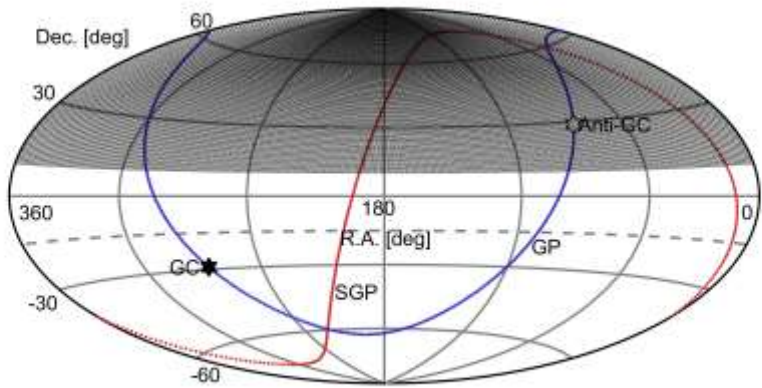


- 30° <bin>, $E \geq 10^{19.2}$ eV
- Maximum pre-trial significance for mean bin size of 30°
- Energy threshold scanned - $10^{19.0}$, $10^{19.1}$, $10^{19.2}$, $10^{19.3}$ eV.

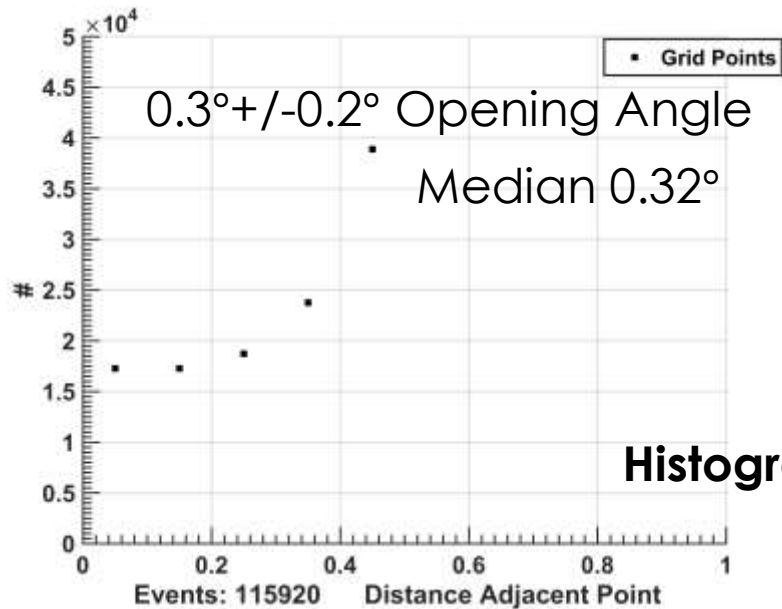


OVERSAMPLING GRID

0.5°x0.5° in RA and Decl.



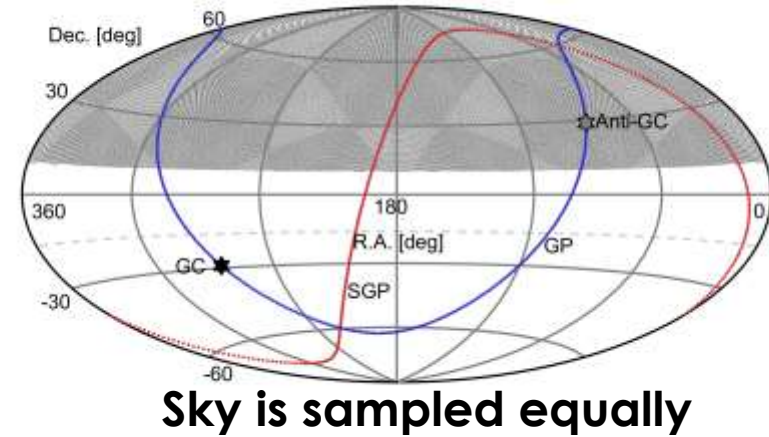
Changing sampling -- declination bias



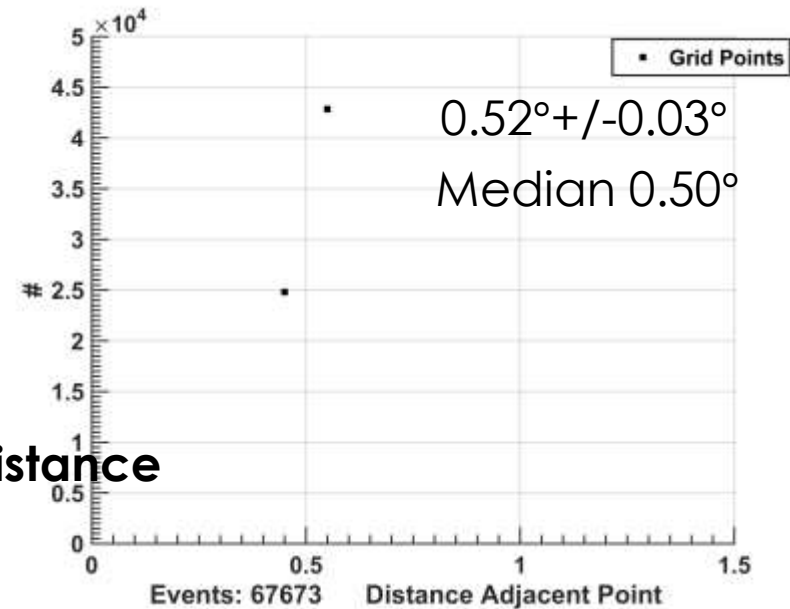
Histograms of closest grid distance

*N. A. Teanby (2006) "An icosahedron-based method for even binning of globally distributed remote sensing data" COMPUTERS & GEOSCIENCES, 32 (9), 1442-1450.

Used here
0.5°x0.5° in Opening Angle*

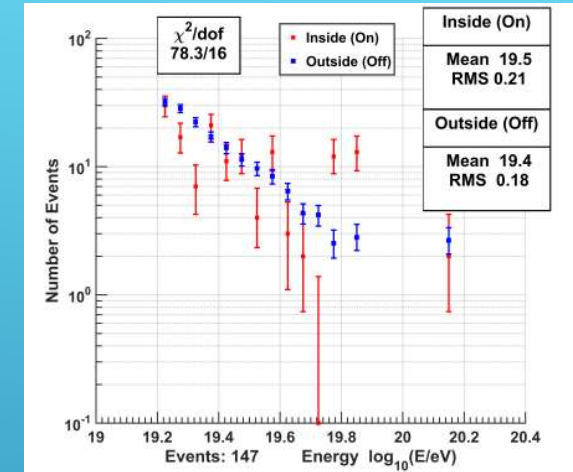


Sky is sampled equally



POISSON LIKELIHOOD GOODNESS-OF-FIT

- Compare energy distribution “On” (inside) to “Off” (outside)
 - “Off” Normalized to N_{bg} (expectation)
- Energy bins of $0.05 \log_{10}(E/eV)$
 - Less than mean energy resolution



$$\chi_k^2 \simeq 2n_{on} \log \frac{n_{on}}{n_{bg}} + n_{bg} - n_{on}$$

- n_{on} # data in bin
- n_{bg} expectation
- Degrees of freedom:
 - # bins
 - +1 for fluctuating background
 - +1 for variable number of bins

$$\sum n_k^{bg} = N_{bg} = \alpha N_{off}^{data}$$

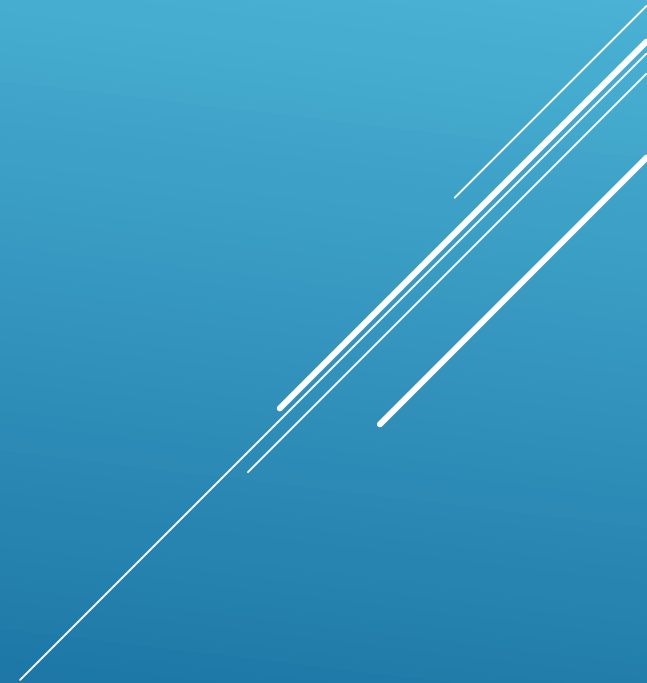
- N_{off} Normalized to expectation

Test Used Previously by T.A. In:

Study of Ultra-High Energy Cosmic Ray Composition Using Telescope Array's Middle Drum Detector and Surface Array in Hybrid Mode, *Astroparticle Phys.* **64**, 49 (2014).

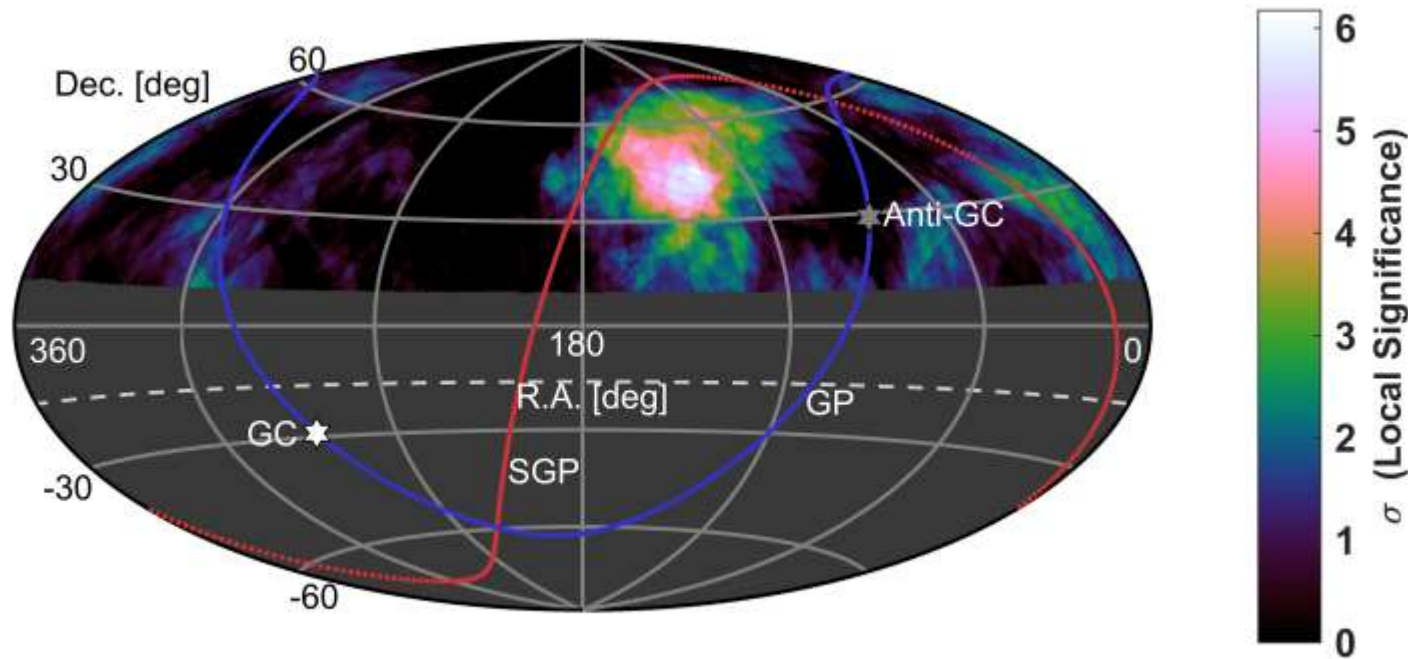
• Good reference <http://www.fysik.su.se/~conrad/James/james.5.gof.pdf> or Particle Data Group book

RESULT



ENERGY SPECTRUM ANISOTROPY – 30° <BIN>

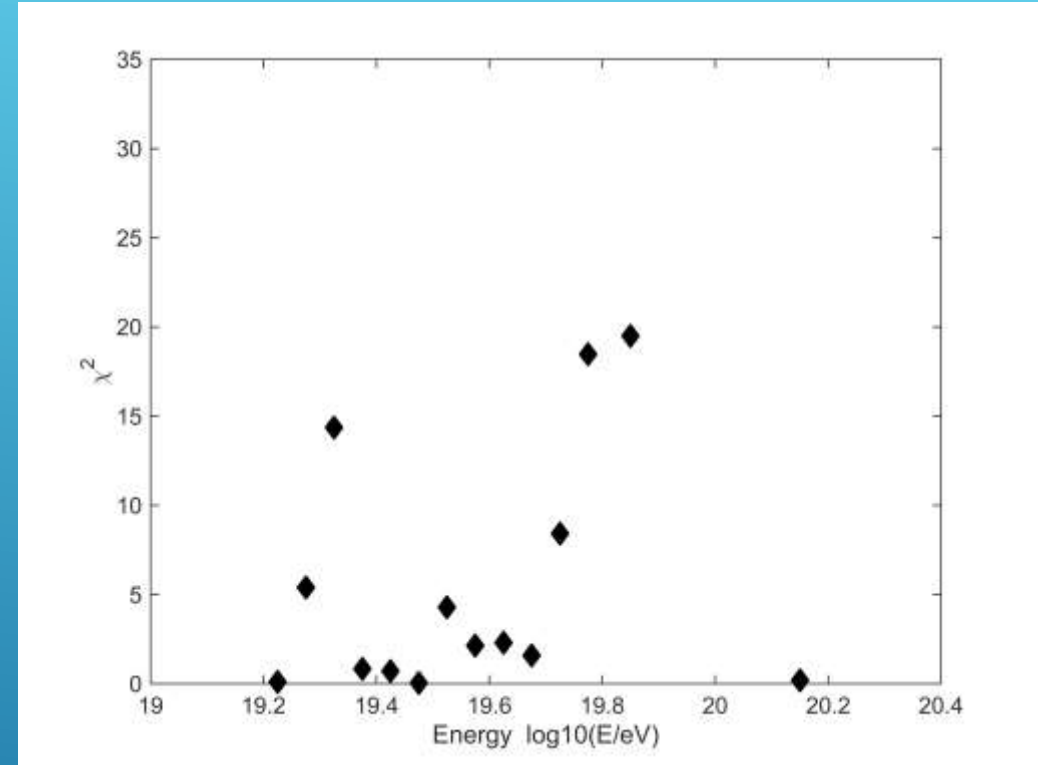
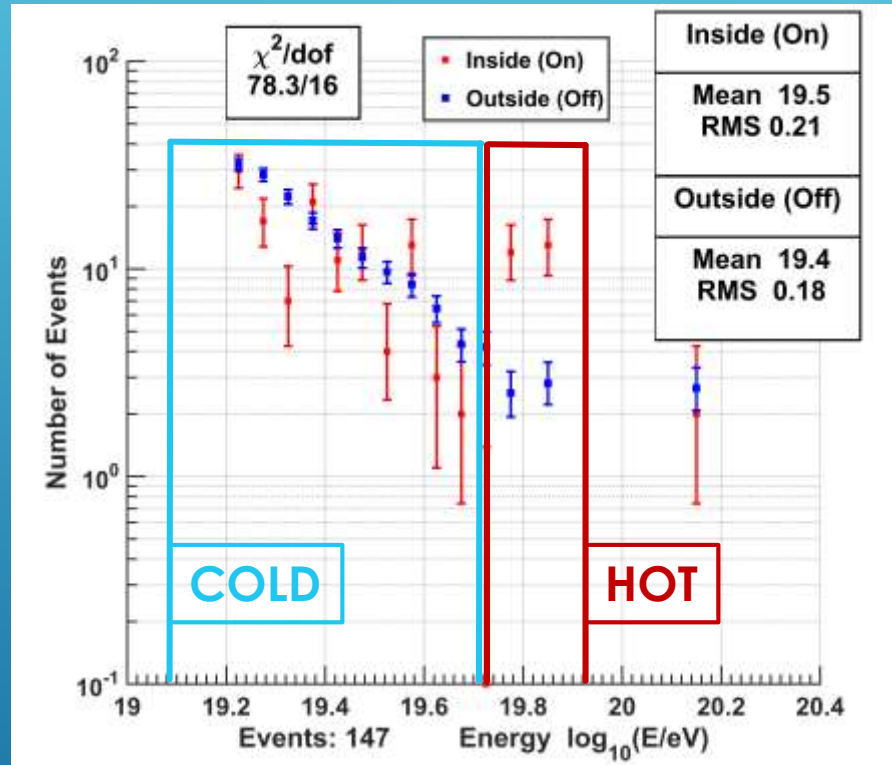
- σ deviation — “On” data compared to “Off” data



30° <bin>, $E \geq 10^{19.2}$ eV

- Maximum: 6.17σ
- 138.8° R.A., 44.8° Decl.
- Bin size: 28.43°
- # Events: 147
- 6.8° from “hotspot”

ENERGY COMPARISON – MAX. LOCAL SIGMA



- Max. local σ (6.17) location — 138.8° R.A., 44.8° Decl.
- 28.43° radius cap bin
- $E \geq 10^{19.2}$ eV
- Expected Background: $N_{bg} = 166.2$

Bin Chi Squares

$$\chi_k^2 \simeq 2n_{on} \log \frac{n_{on}}{n_{bg}} + n_{bg} - n_{on}$$

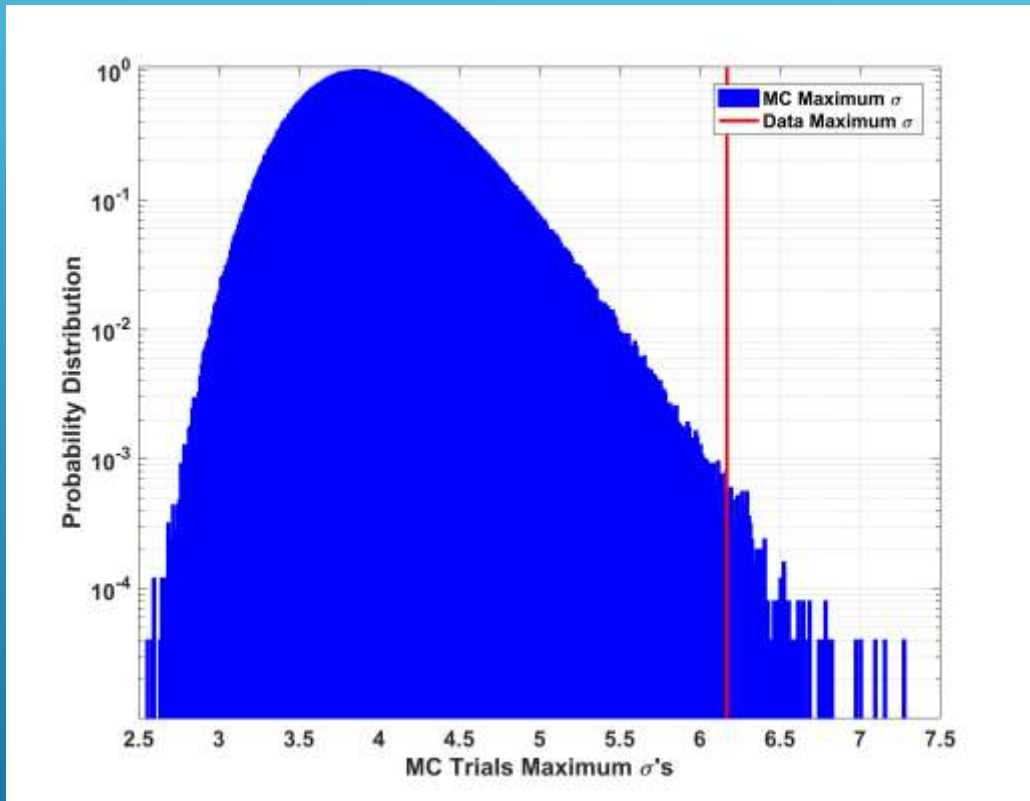
GLOBAL SIGNIFICANCE

- Count simulations with $\sigma \geq 6.17$
- **MC TEST Penalties**
 - *Bin scan - 15°, 20°, 25°, 30° average bin sizes*
 - *Not enough events inside bins less than 15°*
 - *Not enough events outside bins greater than 30°*
 - *Energy threshold scan - $10^{19.0}$, $10^{19.1}$, $10^{19.2}$, $10^{19.3}$ eV.*
 - *Not enough events for cuts $> 10^{19.3}$ eV*
- Max. σ of $4*4 = 16$ is counted as 1 MC.

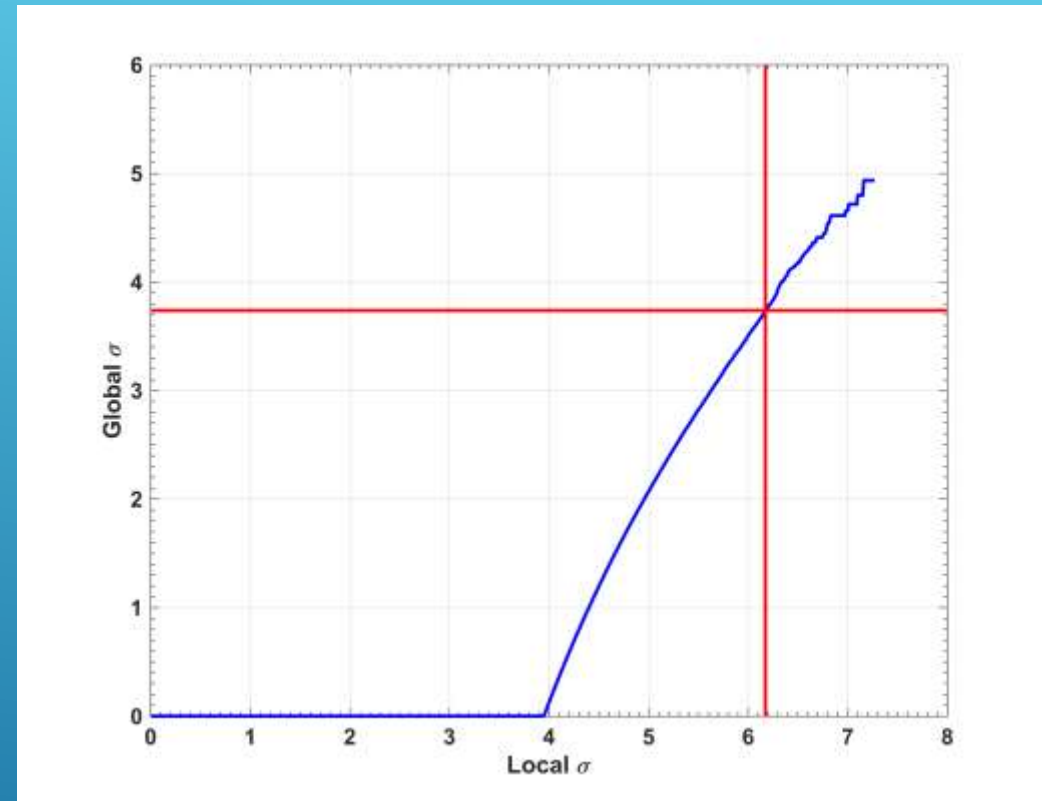
Result: from 2,500,000 sets of 16 maps **232 passed for $3.74\sigma_{global}$**

*One sided probability with 16 times scan penalty

SPECTRUM ANISOTROPY – GLOBAL SIGNIFICANCE

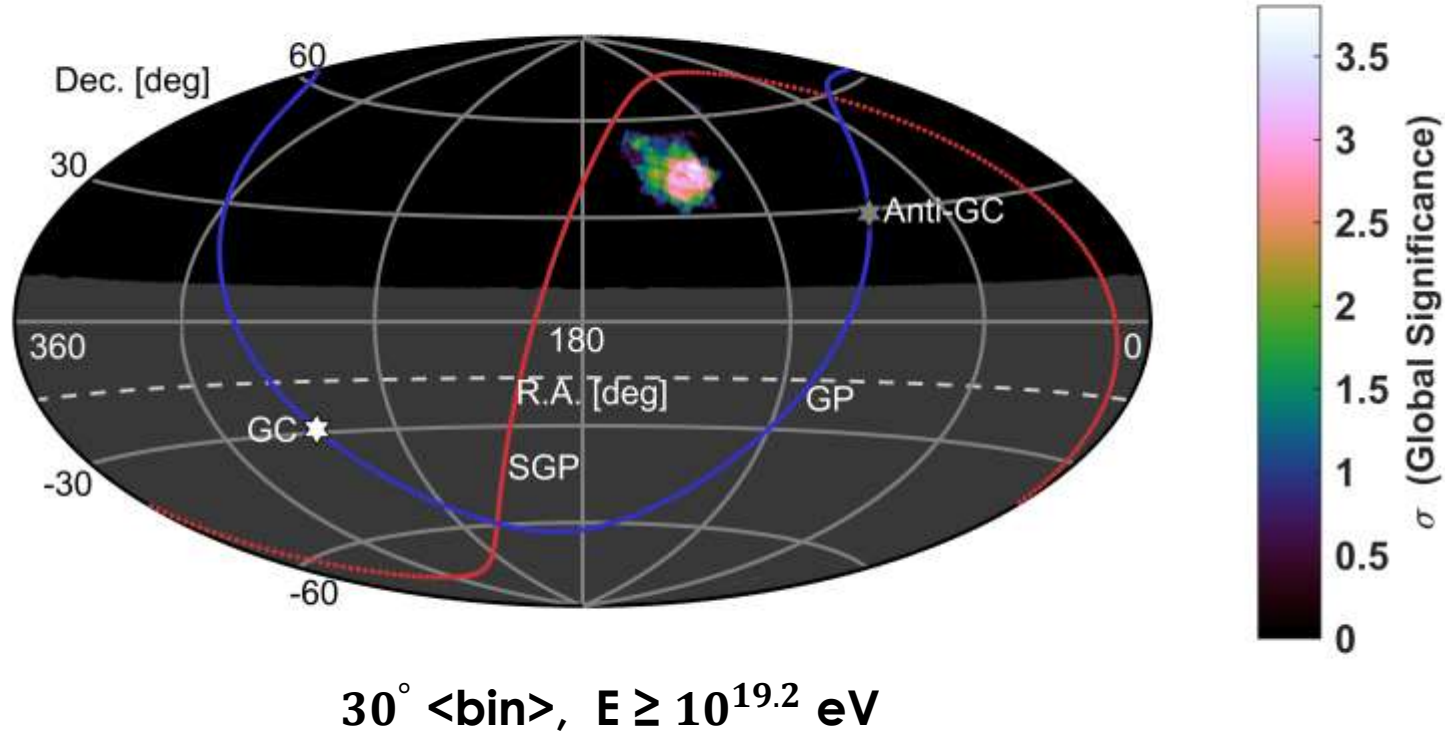


MC trials maximum distribution



Local sigma to Global post-trial sigma

SPECTRUM ANISOTROPY – GLOBAL SIGNIFICANCE

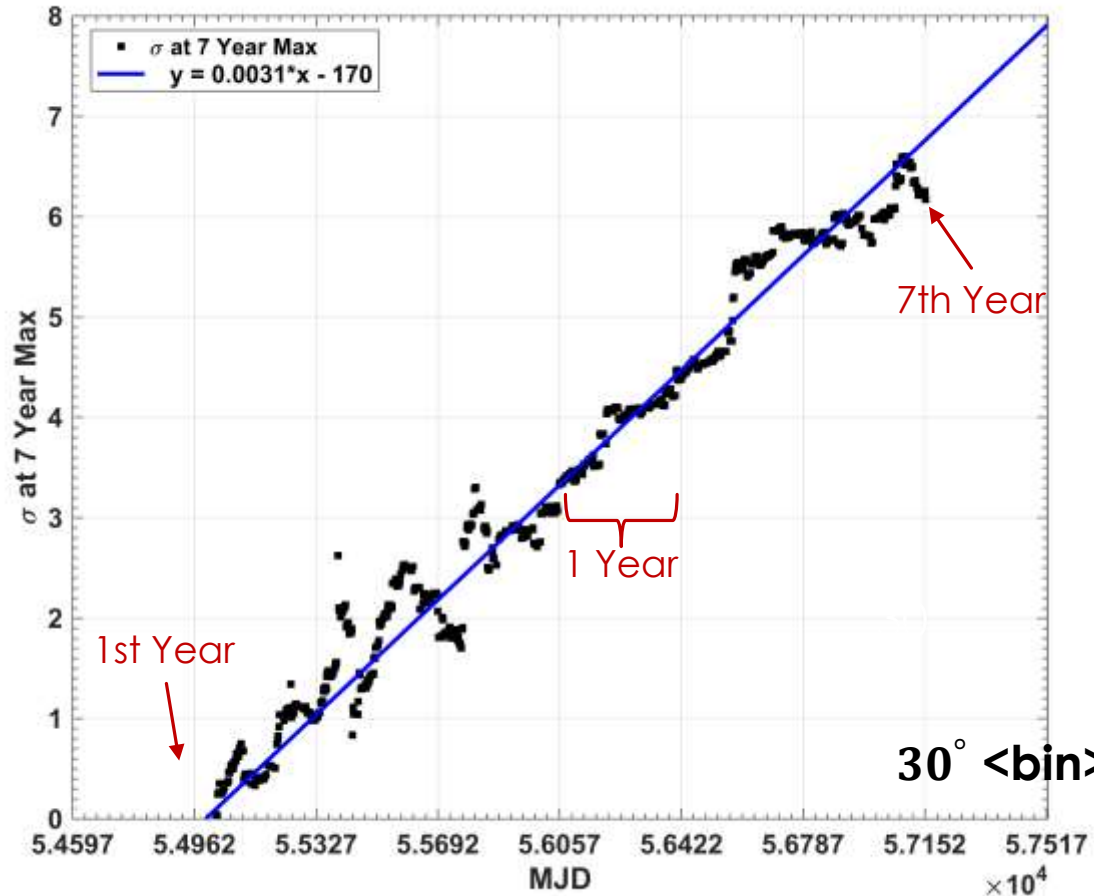


- 138.8° R.A., 44.8° Decl.
- Local sigma: 6.17σ
- **Global sigma: 3.74σ**

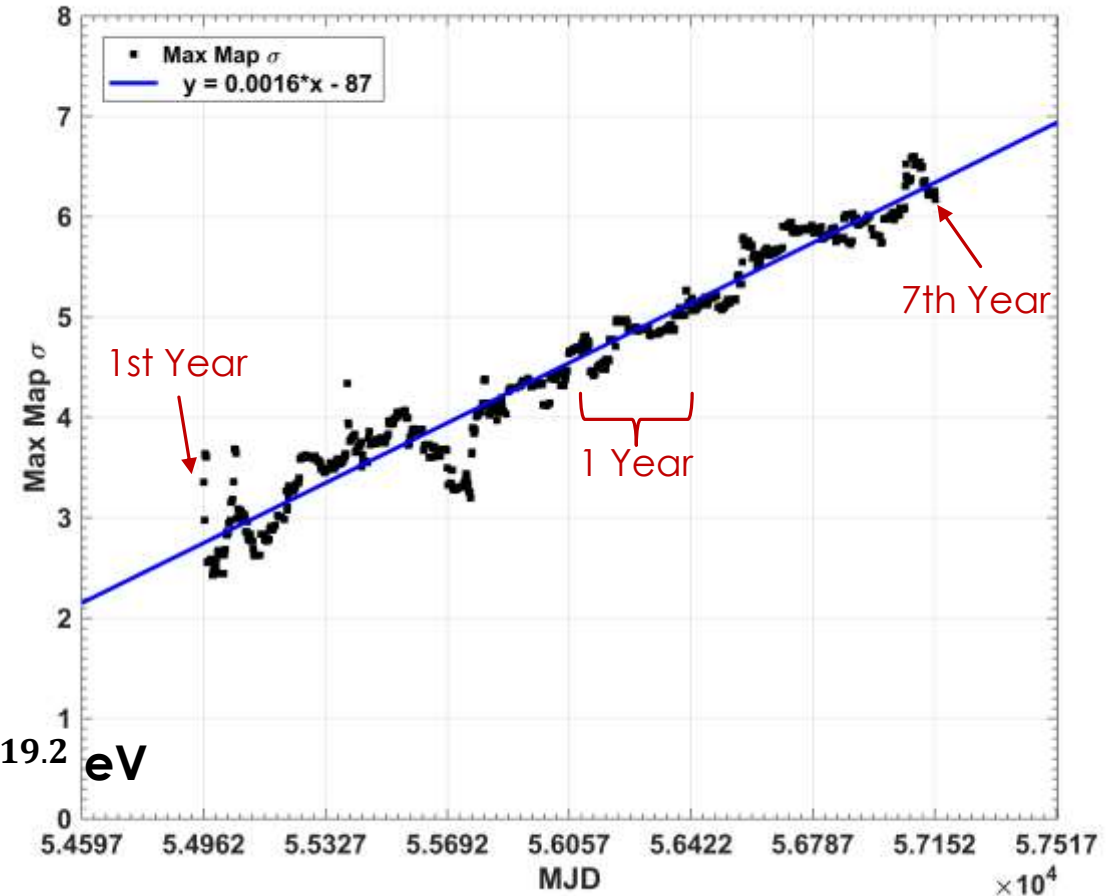
Rough estimate of radius: 1659 grid points $\sigma > 0.7$. $\sqrt{((1659 * 0.5) / \pi)} \approx 15^\circ$

INTEGRAL DAY SIGNIFICANCE

- Blue line is linear fit



$30^\circ < \text{bin} >, E \geq 10^{19.2} \text{ eV}$



- σ_{local} at 7 year max location — +1 σ /year
 - Linear correlation 0.989

- Maximum σ_{local} on map
- Linear correlation 0.976

POSSIBLE CAUSES

- Possible source:
 - M82 starburst galaxy most likely source
 - “A Monte Carlo Bayesian Search for the Plausible Source of the Telescope Array Hotspot”
<https://arxiv.org/abs/1411.5273>
 - “Ultra-high-energy-cosmic-ray hotspots from tidal disruption events”
<https://arxiv.org/abs/1512.04959>
- Possible magnetic field:
 - Supergalactic magnetic sheet increases post-GZK flux ($E > 50 \text{ EeV}$) and deflects ($E < 50 \text{ EeV}$)
 - “The supergalactic structure and the origin of the highest energy cosmic rays”
<https://arxiv.org/abs/astro-ph/9709250>
 - “Cosmic Magnetic Fields in Large Scale Filaments and Sheets”
<https://arxiv.org/pdf/1512.04959v2.pdf>

ENERGY SPECTRUM ANISOTROPY CONCLUSION

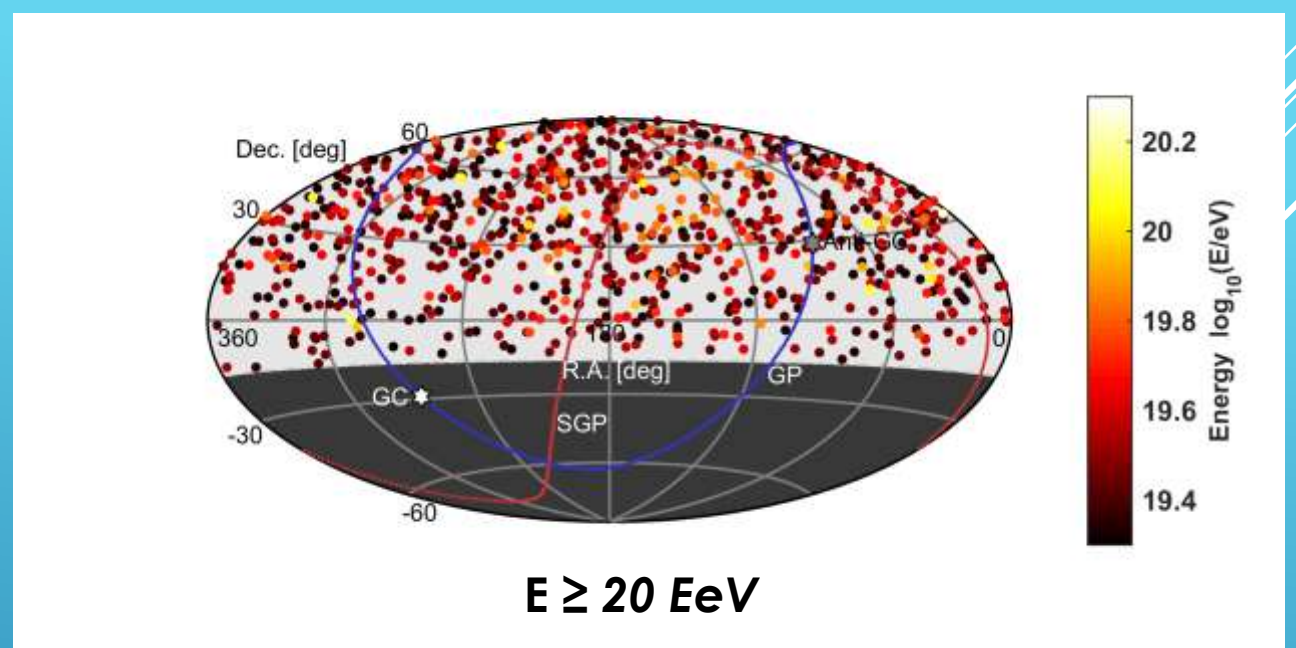
- There is a **3.74 σ** Energy Spectrum Anisotropy ($E \geq 10^{19.2}$ eV) at 138.8° R.A., 44.8° Decl.
 - Deficit at low energies and excess at high energies
 - It has been increasing in significance every year.
- Evidence of magnetic deflection of UHECR

ENERGY-DISTANCE CORRELATION

Is there a direct signature of magnetic deflection?



GOAL



- **Anisotropy search with fewest assumptions**
 - Magnetic fields deflect low energy more than high energy.
 - Single dominant source
- **No assumptions for:**
 - source distribution
 - event composition
 - magnetic field configurations.

SOME PREVIOUS STUDIES

Most similar to this analysis

- *Search for signatures of magnetically-induced alignment in the arrival directions measured by the Pierre Auger Observatory* Astroparticle Phys. Vol 35, Issue 6, Jan. 2012, 354-361
 - Parameters:
 - 20 EeV threshold – **USED IN THIS ANALYSIS**
 - **Lots of other parameters:**
 - Linear correlations with inverse energy
 - directional with limit on transverse spread
 - 20 deg. distance limit
 - one event $E > 45$ EeV required
 - limit on minimum correlation
 - There are a number of other hidden parameters as well...

“...there is no significant evidence for the existence of correlated multiplets in the present data set.”

SOME PREVIOUS STUDIES

- *Search for patterns by combining cosmic-ray energy and arrival directions at the Pierre Auger Observatory*
Aab, A., et al. European Physical Journal C (2015) 75: 269.
 - Parameters:
 - 5 EeV cut
 - **Lots of other parameters:**
 - Number of iterations
 - Cone size
 - 60 EeV events as center of cones.

“...using observables sensitive to patterns characteristic for deflections in cosmic magnetic fields. No such patterns have been found within this analysis.”

<https://arxiv.org/pdf/1410.0515v4.pdf>

METHOD



ENERGY-DISTANCE RANKED CORRELATION

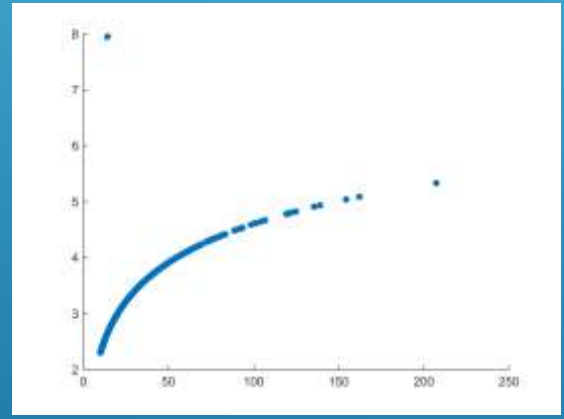
B is a test point

C is an event with Energy \geq B

a is the Opening Angle

For each event (i) Kendall's τ correlation $F_i[E_j(E_j > E_i), \theta_{ij}(E_j > E_i)]$

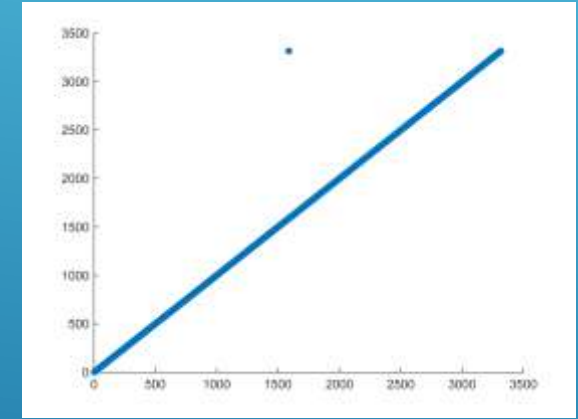
$$\tau = \frac{(\text{number of concordant pairs}) - (\text{number of discordant pairs})}{\frac{1}{2}n(n-1)}$$



Linear Corr: 0.903

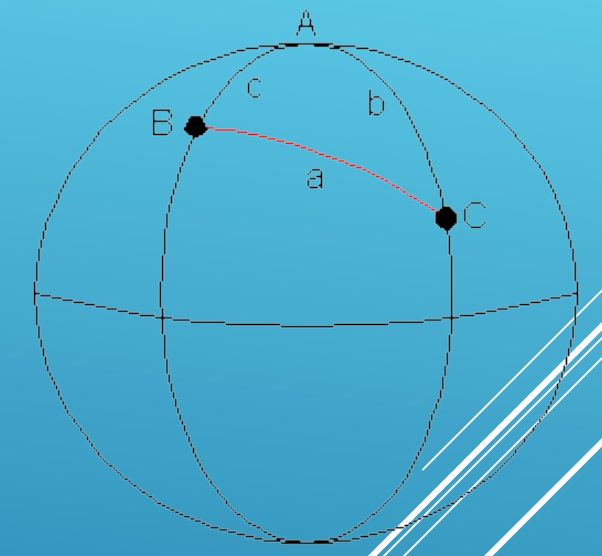
Outlier decreases corr: ~ 0.02

**Robust
against
outliers**



Rank Corr: 0.9994

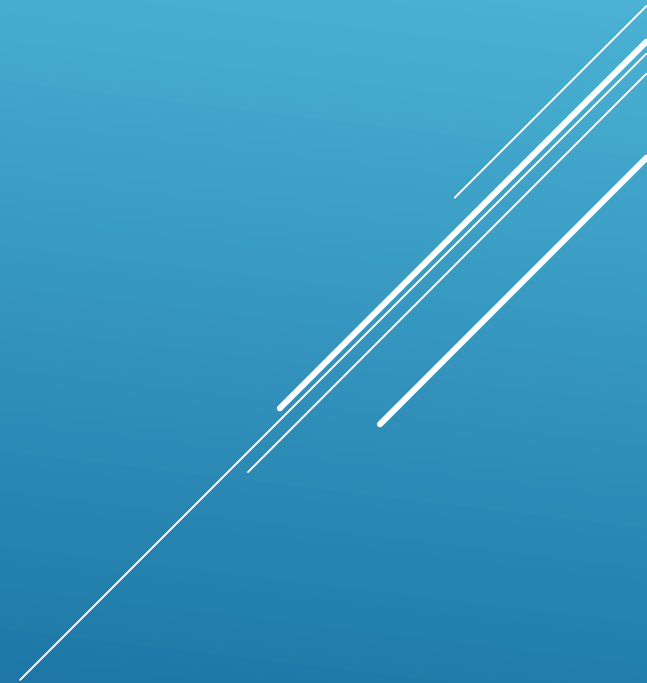
Outlier decreases corr: 0.0006



$$\Delta\sigma = \arccos(\mathbf{n}_1 \cdot \mathbf{n}_2)$$

- ▶ No binning
- ▶ **Each event becomes a test point.** Test parameters (location and energy cut) decided by the data. Removes free parameters.

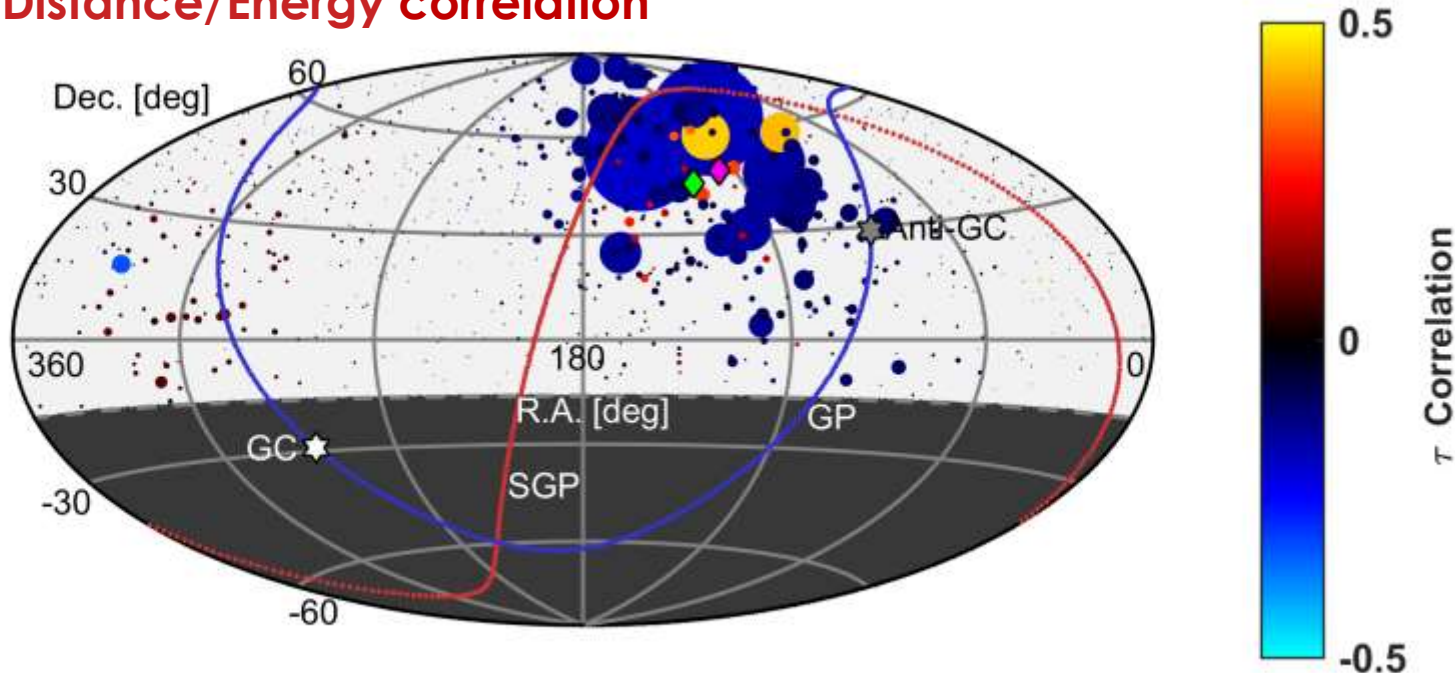
RESULT



DATA RESULT

- ▶ Each test point (i) calculate Kendall's τ correlation $F_i[E_j(E_j > E_i), \theta_{ij}(E_j > E_i)]$
 - **Negative Correlation:** Energy Increases (decreases) \rightarrow Angle decreases (increases)
 - **Positive Correlation:** Energy Increases (decreases) \rightarrow Angle Increases (decreases)

- Size proportional to **1/p-value**
- Color is **Distance/Energy correlation**

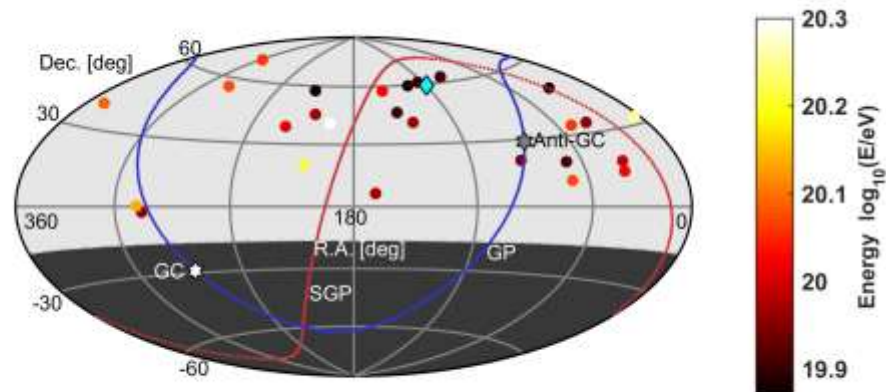
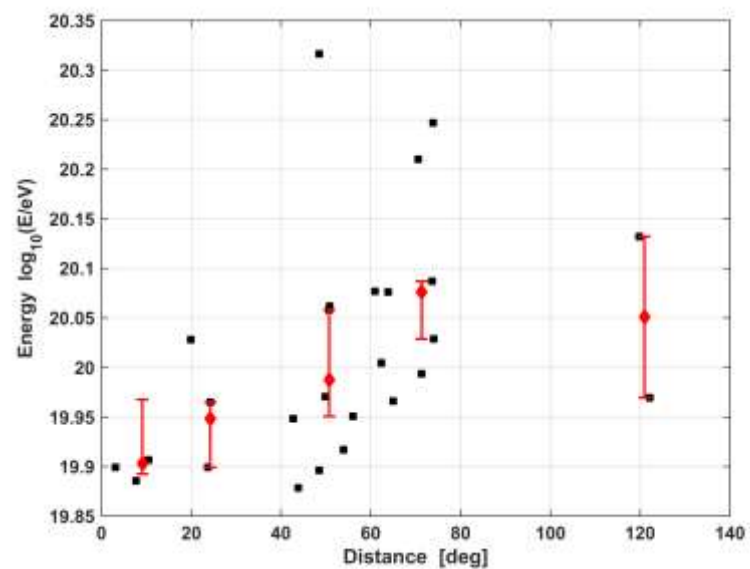


*Each Test Point sample size is different

Events with
 $E \geq 20 \text{ EeV}$

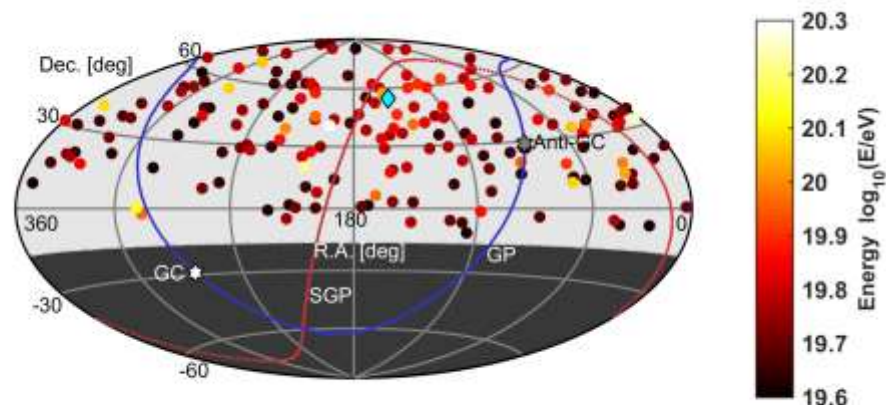
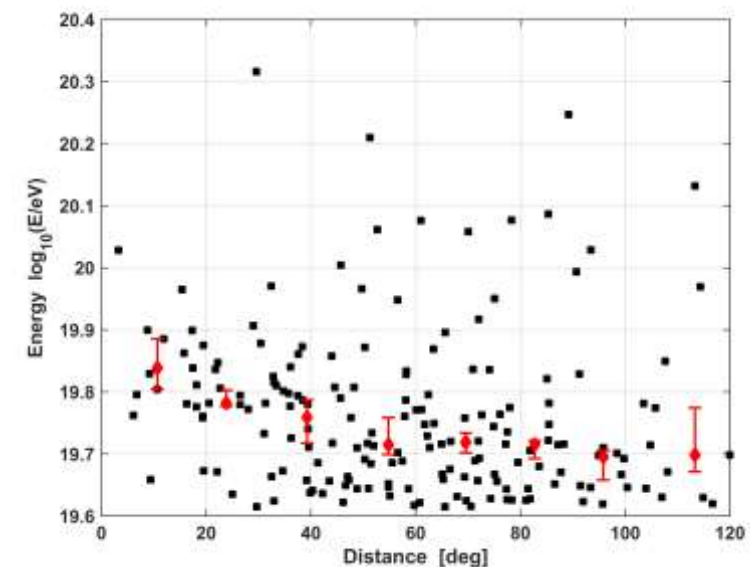
- Spectrum Anisotropy center:
138.8° R.A., 44.8° Dec.
- Correlation Weighted
(1/p) Average:
126.2° R.A. , 48.4° Dec.

2 MOST SIGNIFICANT POINTS



R.A. 119.6, Dec. 59.2
 $E \geq 75.0$ EeV

tau	p-val	σ -local	σ -global
0.452	0.000927	2.9	2.46



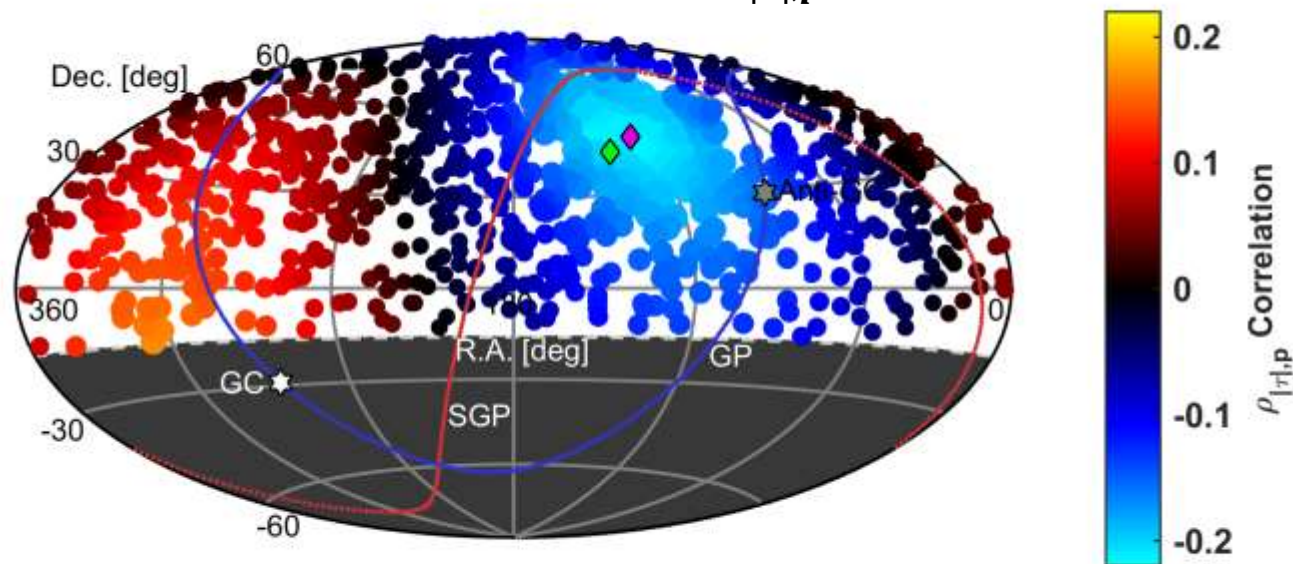
R.A. 154.6, Dec 54.6
 $E \geq 41.2$ EeV

tau	p-val	σ -local	σ -global
-0.188	0.000167	3.4	2.33

Localization of Effect with Unbinned Data

- For each *test point* (*i*) PARTIAL LINEAR correlation of all *test points* $|\tau|_s - F_i[|\tau_j|, \theta_{ij}]$
 - ▶ Account for differing sample size by controlling for p-value
- **Negative Correlation:** Correlations decrease from that point. A “source.”
- **Positive Correlation:** Correlations increase from that point.

- Size proportional to $1/p$, Color is $\rho_{|\tau|,p}$



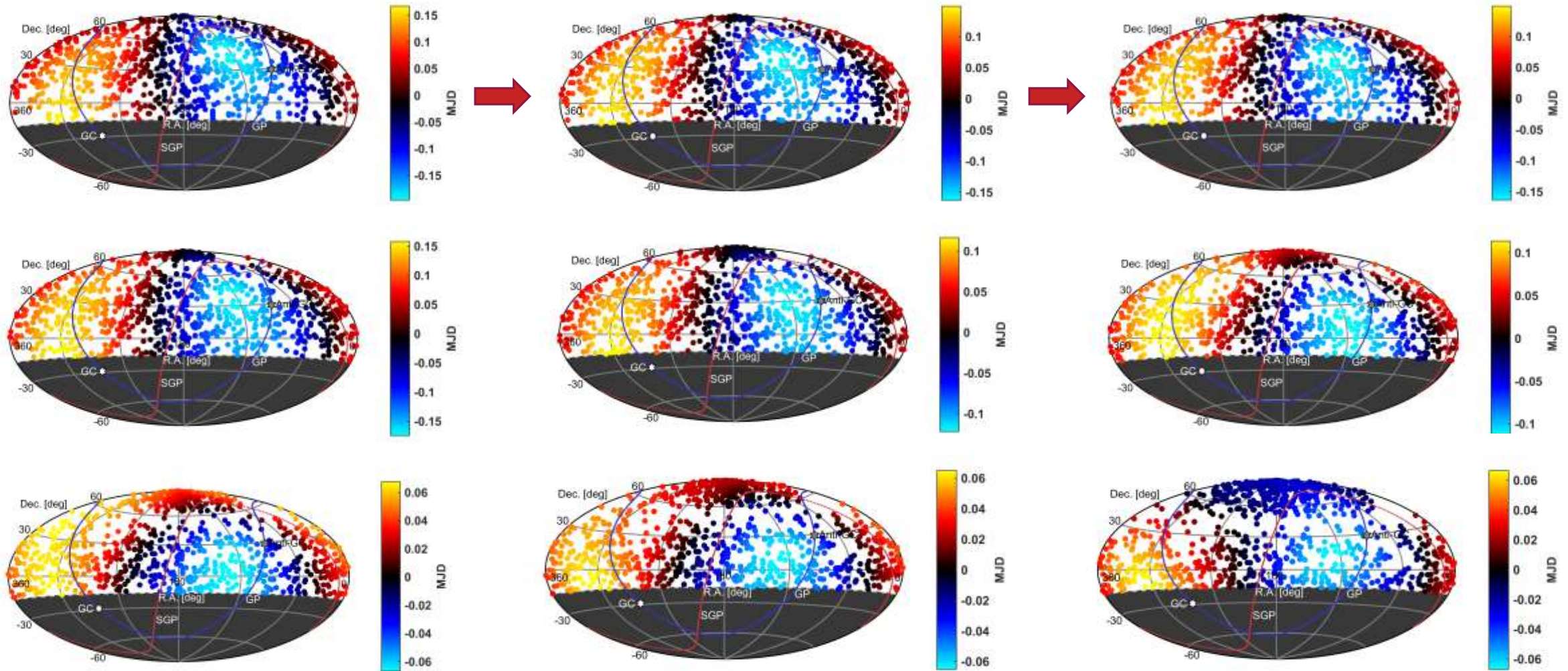
Correlation of correlations
assumes single source

- Circular Mean Weighted by τ 's $1/p$
 - 126.2° R.A. , 48.4° Dec.
 - Maximum $|\rho_{|\tau|,p}|$:
 - 125.9° R.A., 49.7° Dec.

*Each test point sample size is the same

NOT A MEASURE OF DENSITY

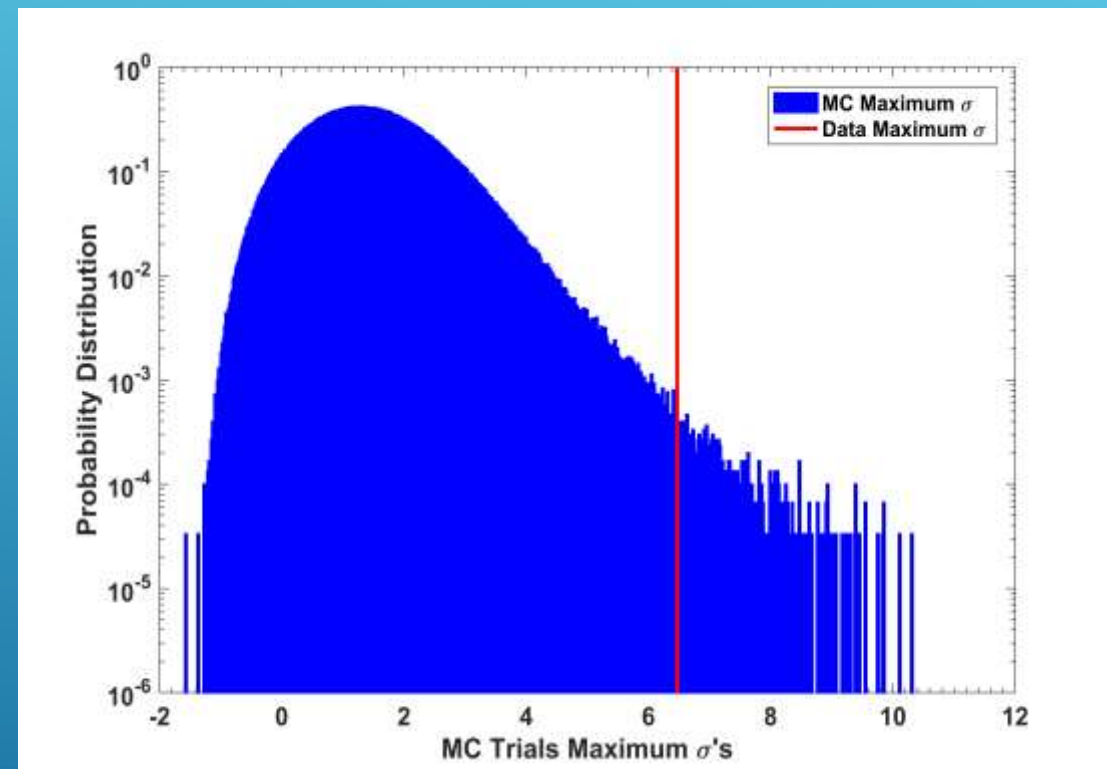
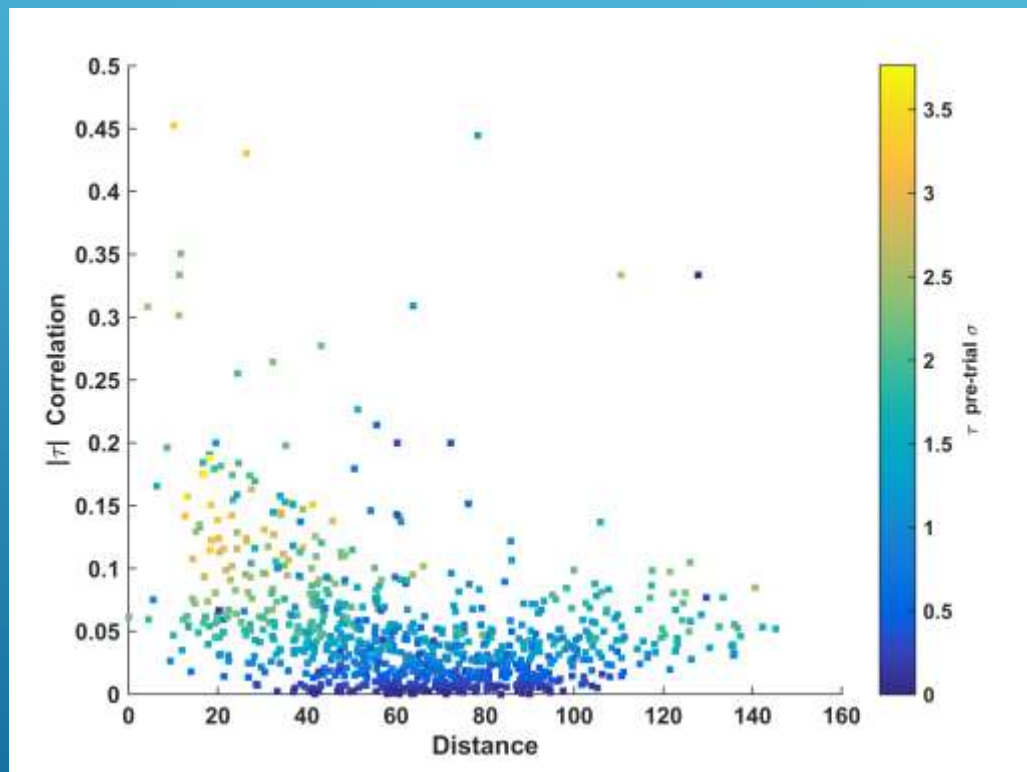
- Data declination is subtracted and folded up toward top of FOV to see how location is tracked
 - Steps of -5 deg. Left to right, top to bottom.



CORRELATION ANISOTROPY SIGNIFICANCE TEST

Single parameter search in MC – use $\sigma_{\rho|\tau,p}$

- $\sigma_{\rho|\tau,p} = 6.47\sigma$ $\rho_{|\tau|,p} = -0.22$
- 125.9° R.A., 49.7° Dec. – 9.4° from *Energy Spectrum Anisotropy* maximum

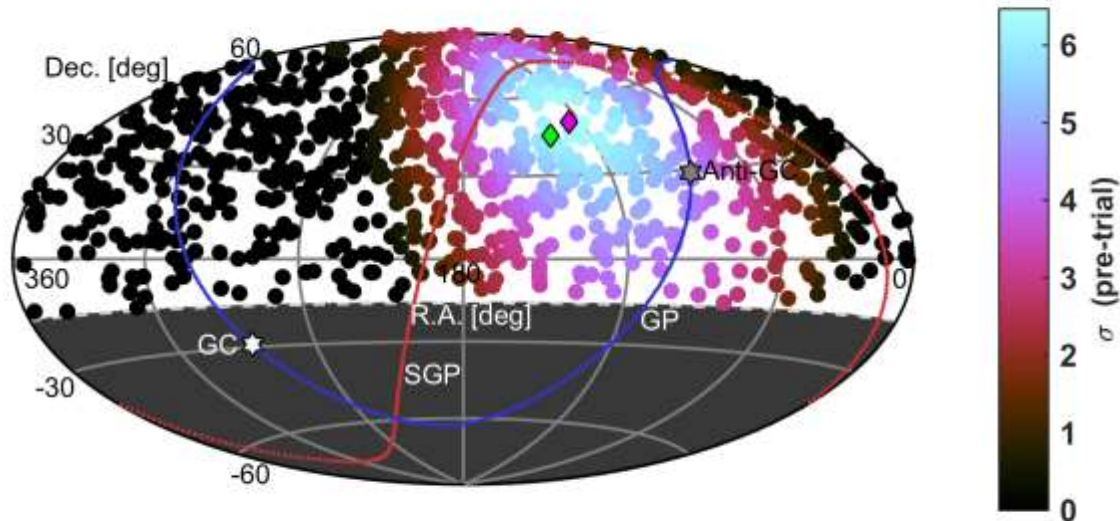


Count MC (or energy scrambled data) with $\sigma \geq \sigma_{data}$ for $\rho_{|\tau|,p} < 0$

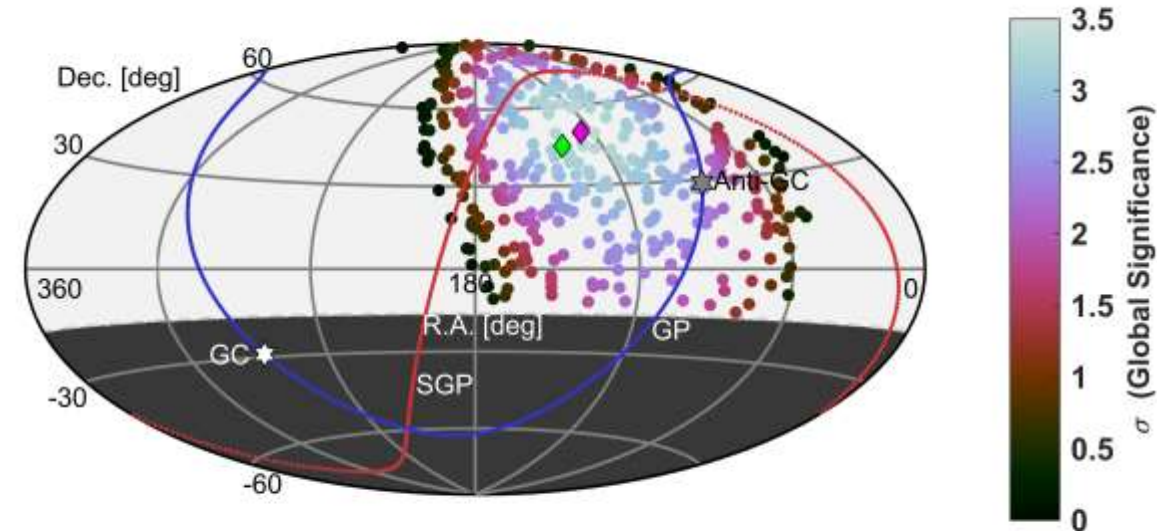
Result: 556 (or 521) counts out of 1,500,000 - that's 3.37σ

CORRELATION ANISOTROPY SIGNIFICANCE TEST

Pre-trial significance



Post-trial significance (zeros removed)



Count MC (or energy scrambled data) with $\sigma \geq \sigma_{data}$ for $\rho_{|\tau|,p} < 0$
Result: 556 (or 521) counts out of 1,500,000 - that's 3.37σ

INTEGRAL DAY SIGNIFICANCE

8 year estimate $\sim 4\sigma_{global}$



- σ_{local} at 7 year max location — +1 σ /year
 - Linear correlation 0.910 (0.944 after 5th year)

- Maximum σ_{local} on map
- Linear correlation 0.905 (0.935 after 5th year)

ENERGY-DISTANCE CORRELATION CONCLUSION

- There is a **3.37 σ** Energy/Distance Correlation Anisotropy ($E \geq 10^{19.3}$ eV) located at 125.9° R.A., 49.7° Dec.
 - It has increased in significance 6 out of 7 years.
- Direct evidence of magnetic deflection of UHECR

COMBINED MEASURE OF ENERGY SPECTRUM ANISOTROPY AND ENERGY/POSITION CORRELATION

- Energy Spectrum Anisotropy significance: 3.74σ
- Energy-Distance Correlation Anisotropy significance: 3.37σ
- *Stouffer's Method combined significance*: 5.03σ

NEXT UP:

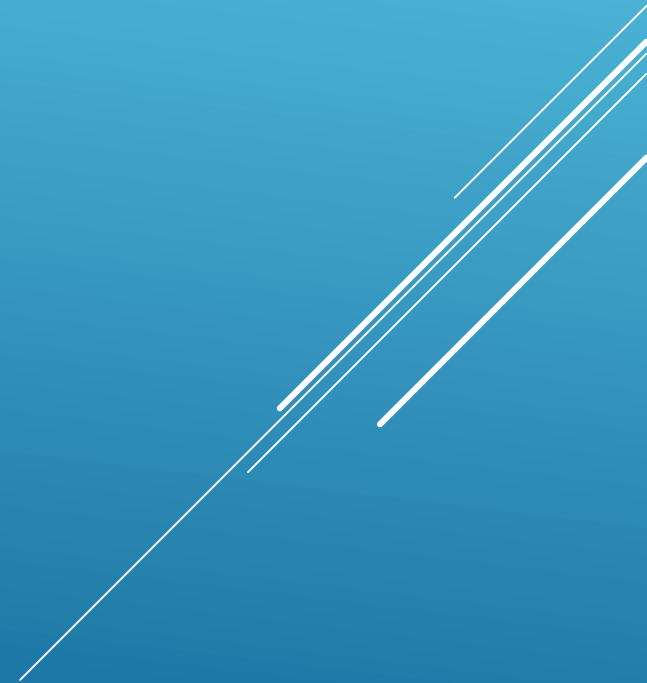
- Hot/Coldspot Anisotropy (a result of Spectrum AND Position Correlation): 5.4σ

HOT/COLDSPOT SUMMARY ANALYSIS

Is there a direct signature of magnetic deflection?

A decorative graphic consisting of several parallel white lines of varying lengths, slanted diagonally from the bottom right towards the top right, located in the lower right quadrant of the slide.

METHOD



LI-MA SIGNIFICANCE

- Compare N events “On” (inside) to expectation – How significant is the excess or deficit?
- Derived by Poisson likelihood ratio and approximation to χ^2 (like the Poisson Likelihood GOF)

$$S = \text{sign}(N_{on} - N_{bg})\sqrt{2} \left\{ N_{on} \ln \left[\frac{1 + \alpha}{\alpha} \left(\frac{N_{on}}{N_{on} + N_{off}} \right) \right] + N_{off} \ln \left[(1 + \alpha) \left(\frac{N_{off}}{N_{on} + N_{off}} \right) \right] \right\}^{1/2}$$

- N_{on} = # data in bin
- N_{off} = # data outside bin
- α = ratio of N_{on} / N_{off} for simulated isotropy
- N_{bg} expectation

$$N_{bg} = \alpha N_{off}^{data}$$

- N_{off} Normalized by exposure ratio

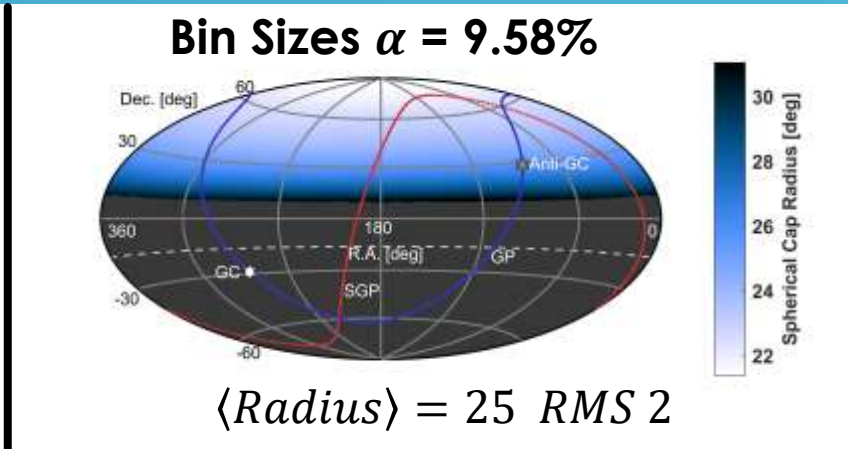
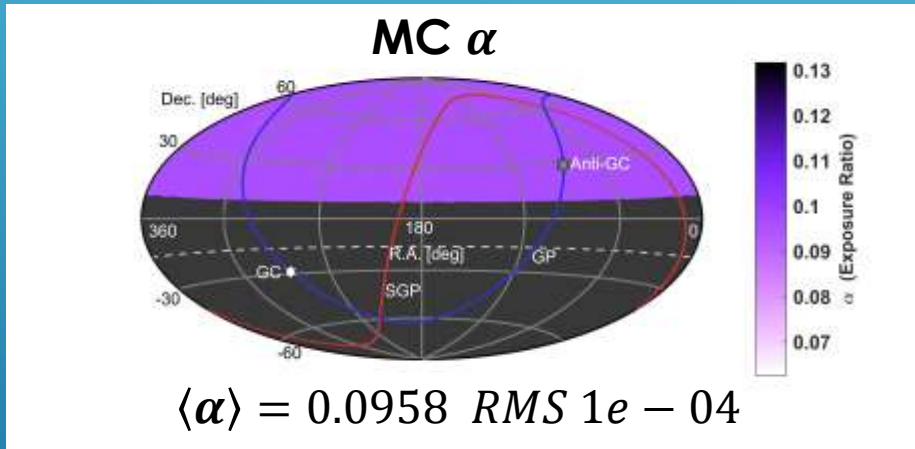
Test Used Previously by T.A. In:

INDICATIONS OF INTERMEDIATE-SCALE ANISOTROPY OF COSMIC RAYS WITH ENERGY GREATER THAN 57 EeV IN THE NORTHERN SKY MEASURED WITH THE SURFACE DETECTOR OF THE TELESCOPE ARRAY EXPERIMENT

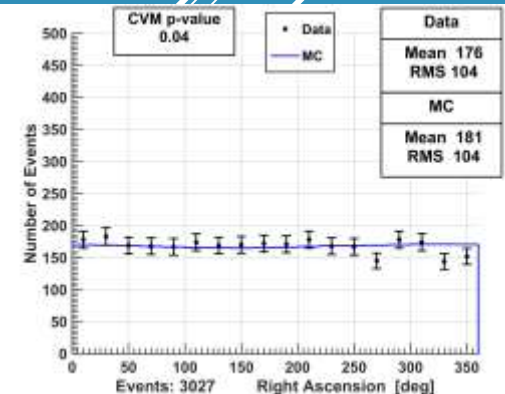
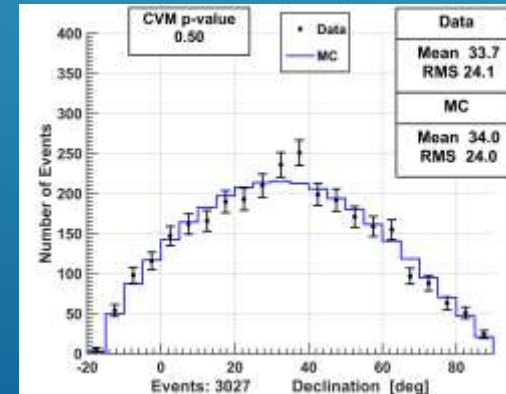
ESTIMATED BACKGROUND – EQUAL EXPOSURE

- Equal exposure binning samples the sky equally.
 - “On” exposure such that bin size average = 15°, 20°, 25°, 30°
- Maximum Li-Ma significance for mean bin size of 25°

$$\alpha = N_{on}^{MC} / N_{off}^{MC} = \text{constant}$$



25° <bin>

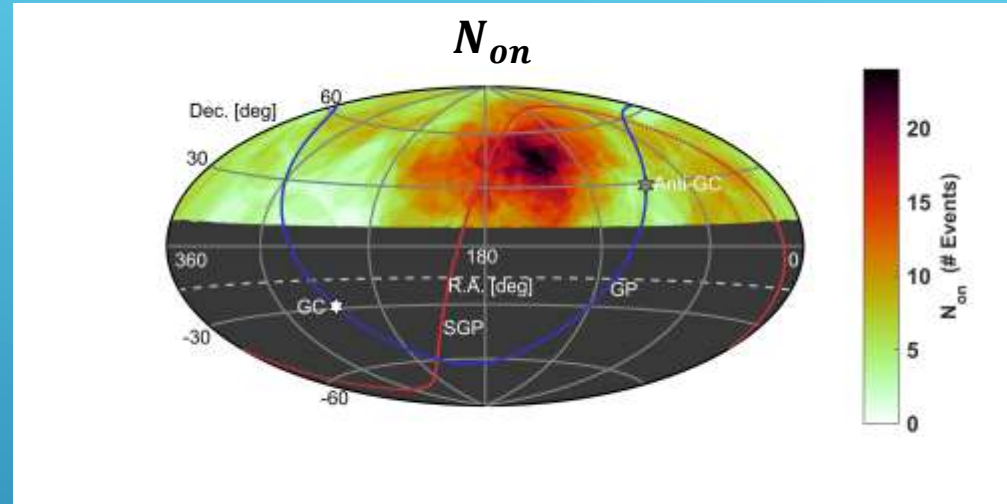
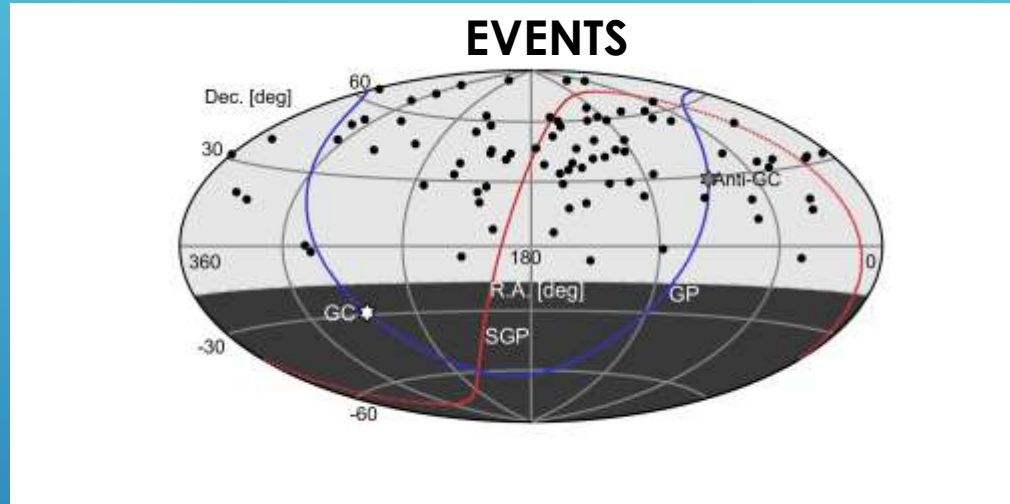


RESULT

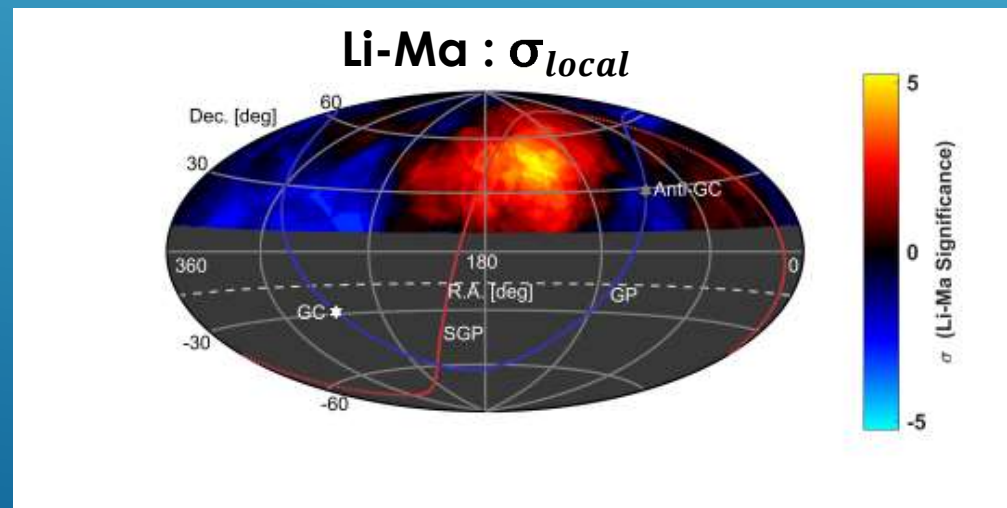
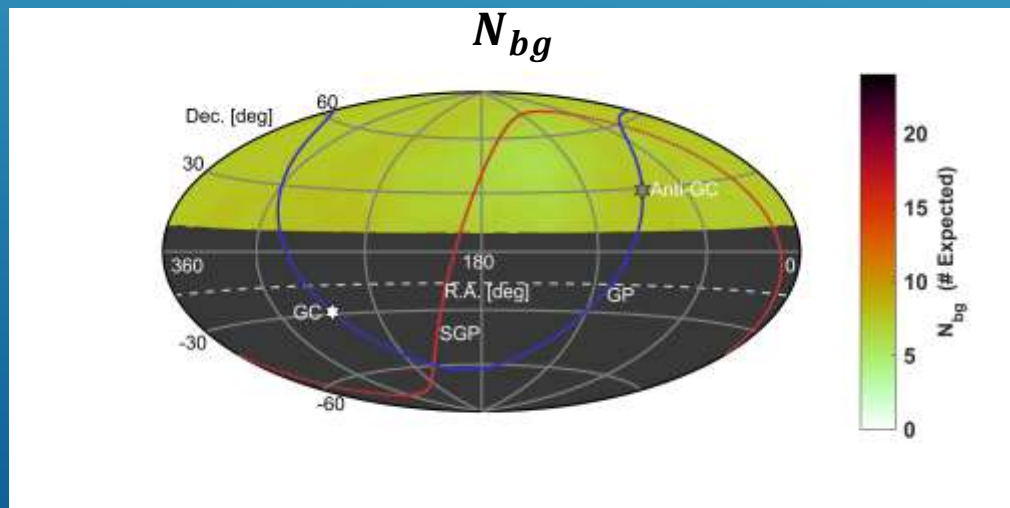


TWO ENERGY BIN LI-MA STATISTICS

Data: $E \geq 57 \text{ EeV}$ ($10^{19.75}$) – a priori choice from previous studies



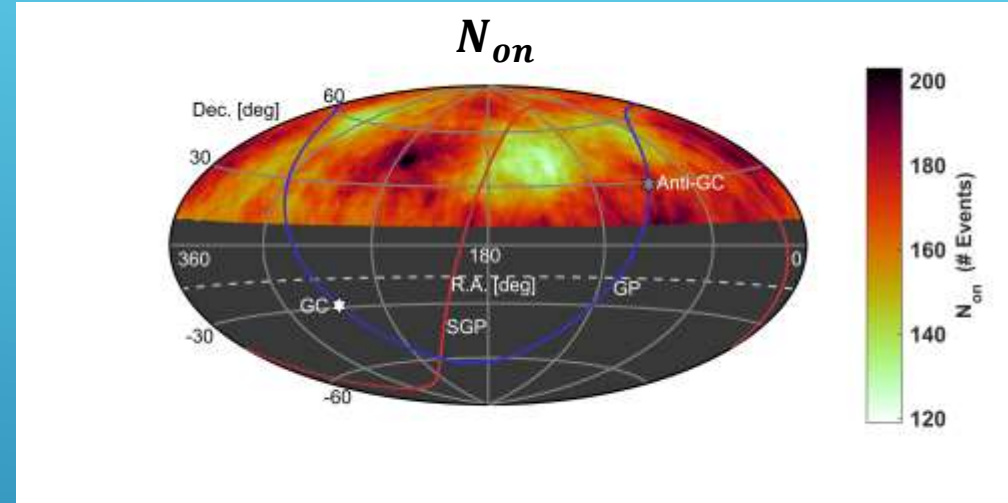
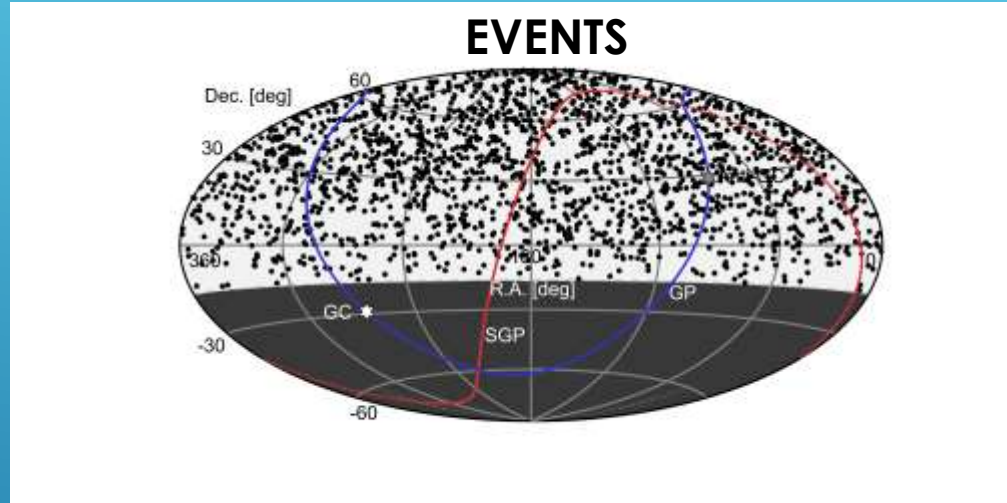
Events in
25 <bin>



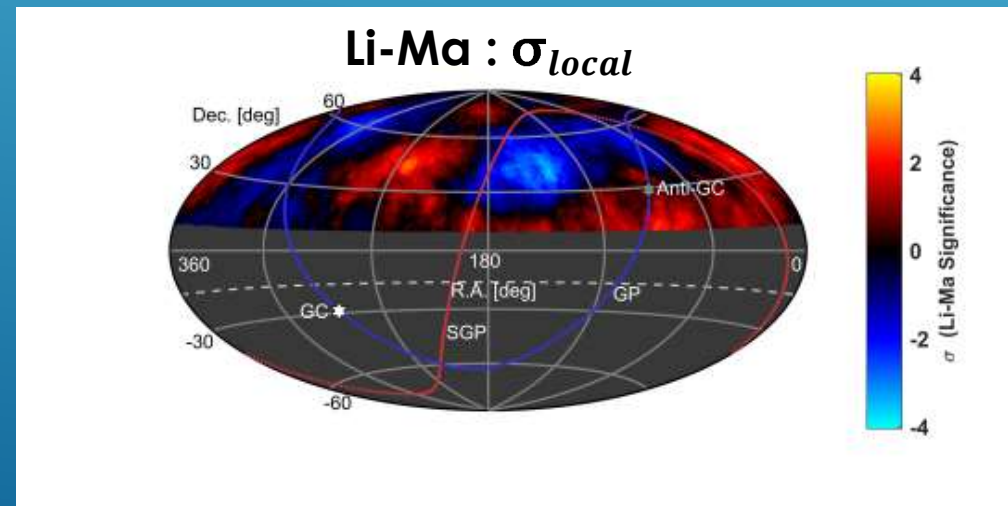
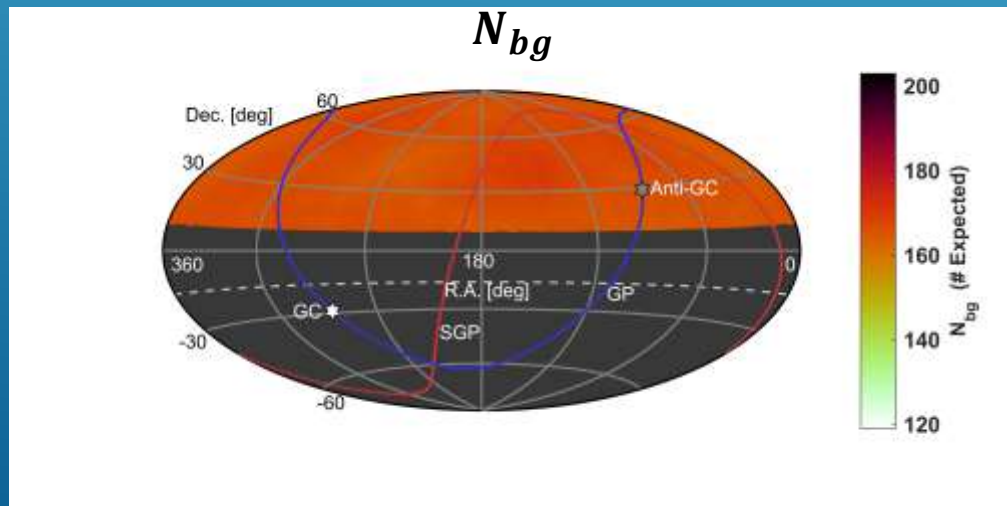
Pre-trial
significance

TWO ENERGY BIN LI-MA STATISTICS

Data: $10^{19.1} \leq E \leq 10^{19.75}$



Events in
25 <bin>



Pre-trial
significance

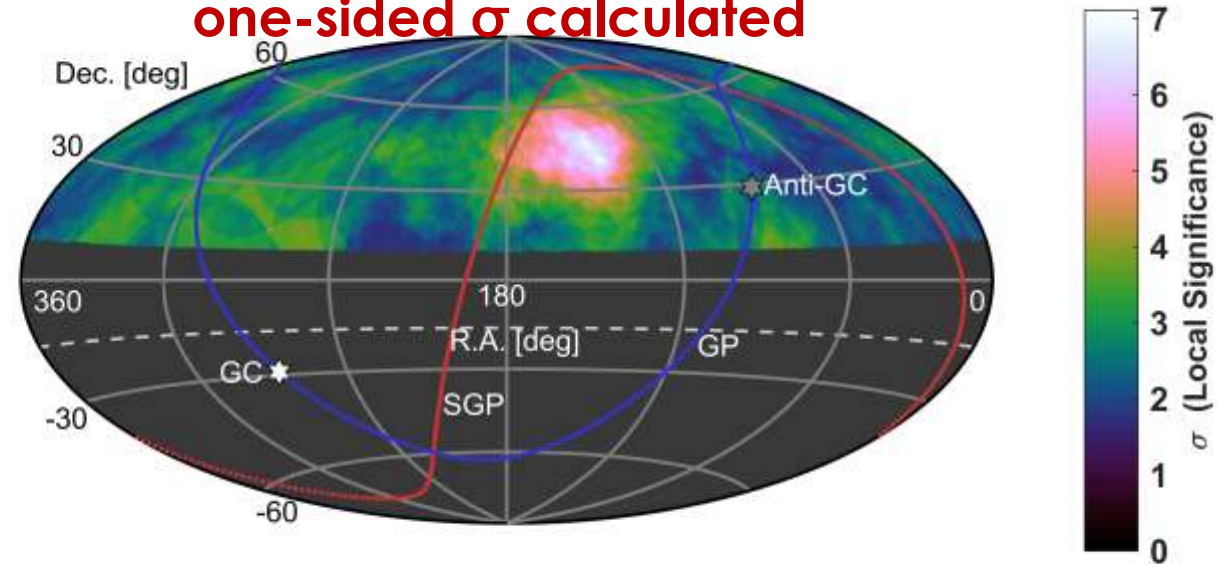
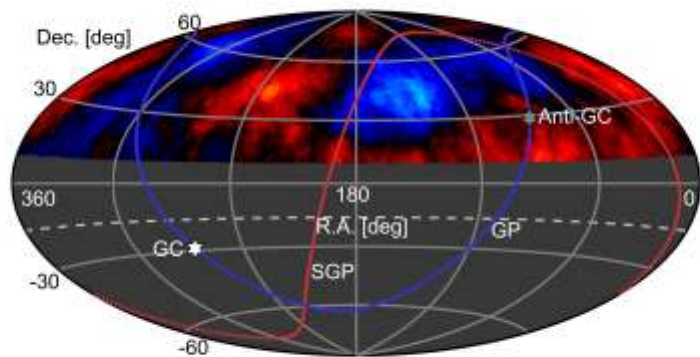
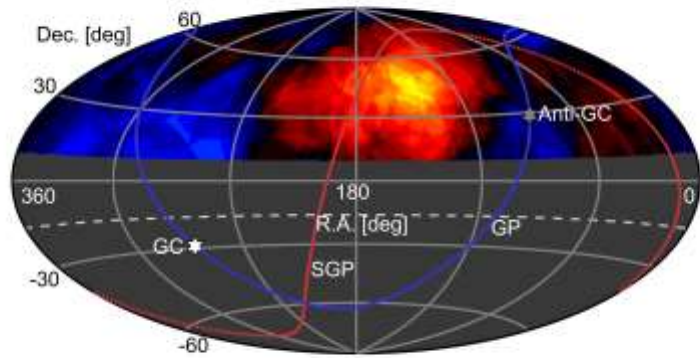
- Energy threshold scanned- $10^{19.0}$, $10^{19.1}$, $10^{19.2}$, $10^{19.3}$ eV.

COMBINED LI-MA STATISTICS

High Energy HOTSPOT

- ▶ Maximum $\sigma_{local} = 7.11$ at 142° R.A., 40° Dec.
- ▶ 5° from Energy Spectrum Anisotropy
- ▶ 16 degrees from supergalactic plane

Combined σ : two-sided test probabilities multiplied
one-sided σ calculated



Cap with maximum joint significance (p-values multiplied)
HOT excess = $5.24 \sigma_{local}$ and COLD deficit = $-4.03 \sigma_{local}$

Low Energy COLDSPOT

EVIDENCE OF CAUSAL CONNECTION

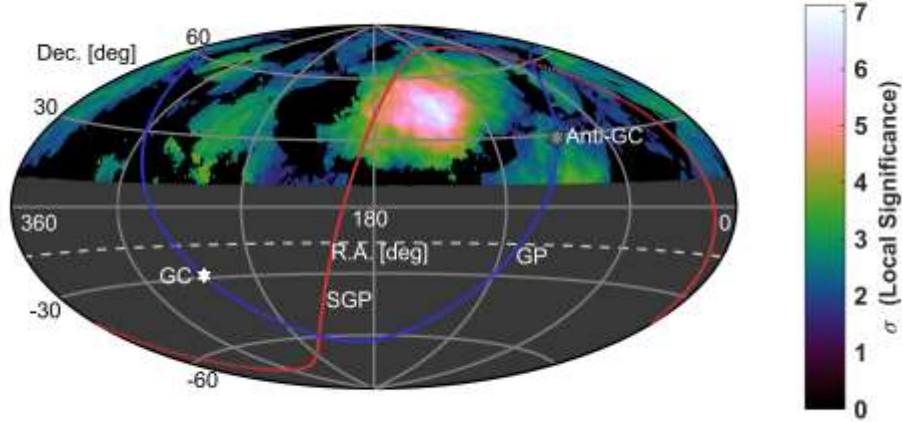
Evidence for physical cause resulting in an **excess** at same point as **deficit**

- **Energy-Distance Correlation Anisotropy is direct evidence.**
- **Measured independently the Hotspot and Coldspot have the same size $\sim 25^\circ$**

SUPERGALACTIC PLANE SHIFT

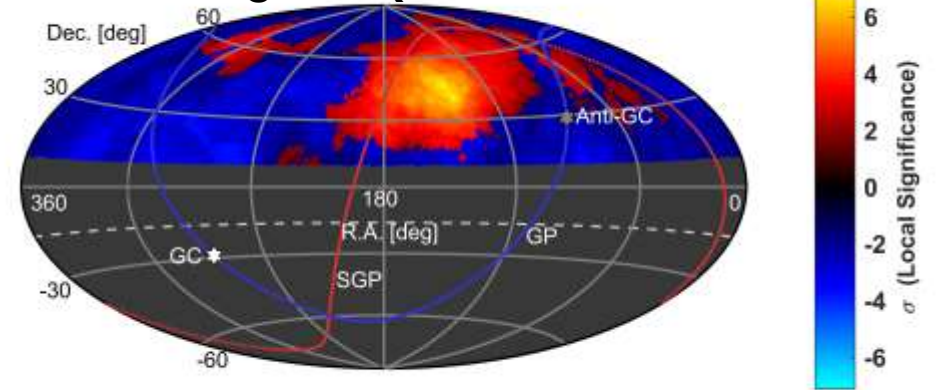
Supergalactic magnetic sheet increase flux of post-GZK particles ($E > 50 \text{ EeV}$) and deflects ($E < 50 \text{ EeV}$)
– suggested by (Biermann, Kang, Ryu)^{1 2}

Event Density Asymmetry – Hot/Cold and Cold/Hot

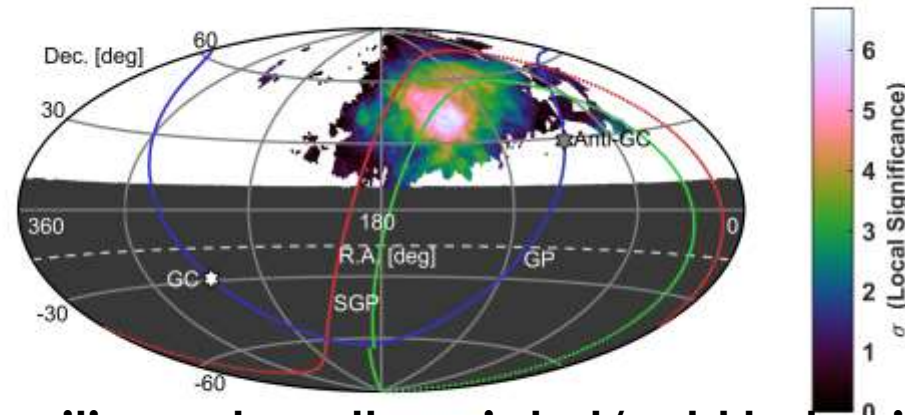


Test for post-trial significance

Hot/Cold positive
All other situations negative (Hot/Hot, Cold/Cold, Cold/Hot)



Looks like supergalactic plane



Sky positions where there is hot/cold behavior
 $30^\circ < \text{bin} >$

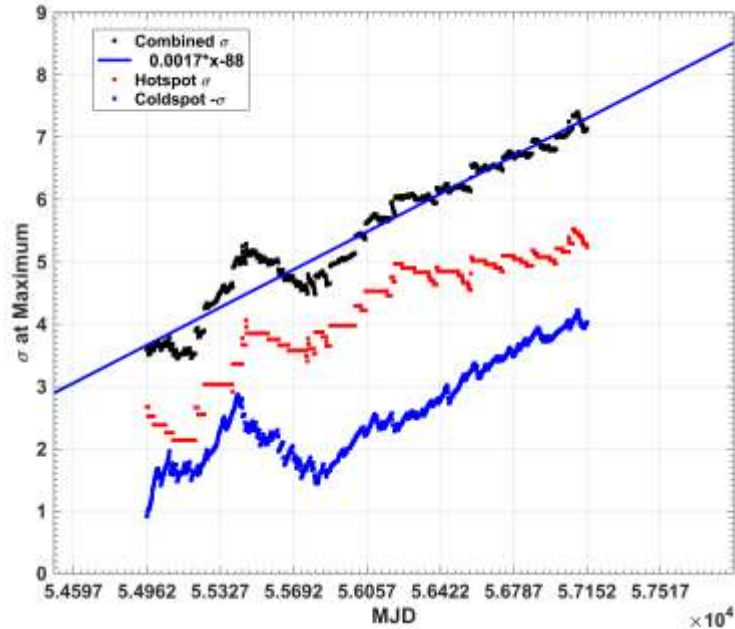
Green line is linear in SG
weighted by energy anisotropy σ^2
of Hot/Coldspot points.

Result is SGP shifted -16°

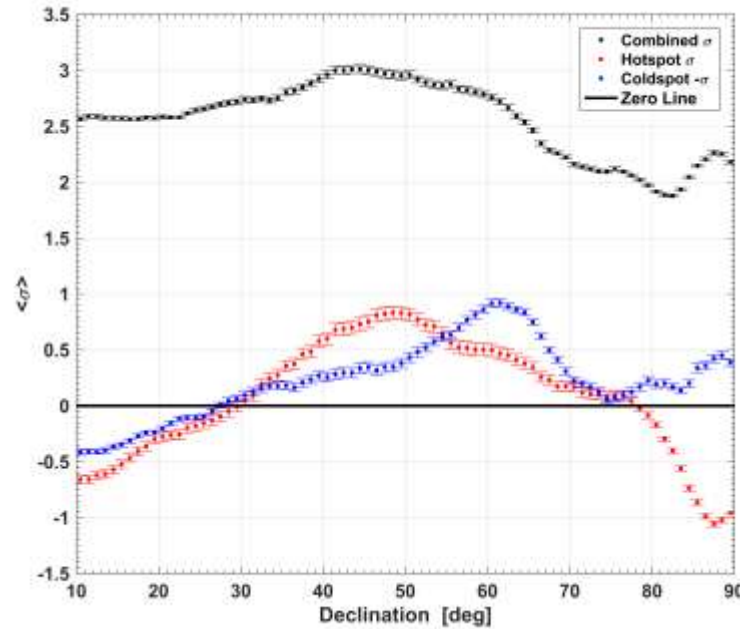
TWO ENERGY BIN CORRELATIONS

These analyses can be done due to equal opening angle grid

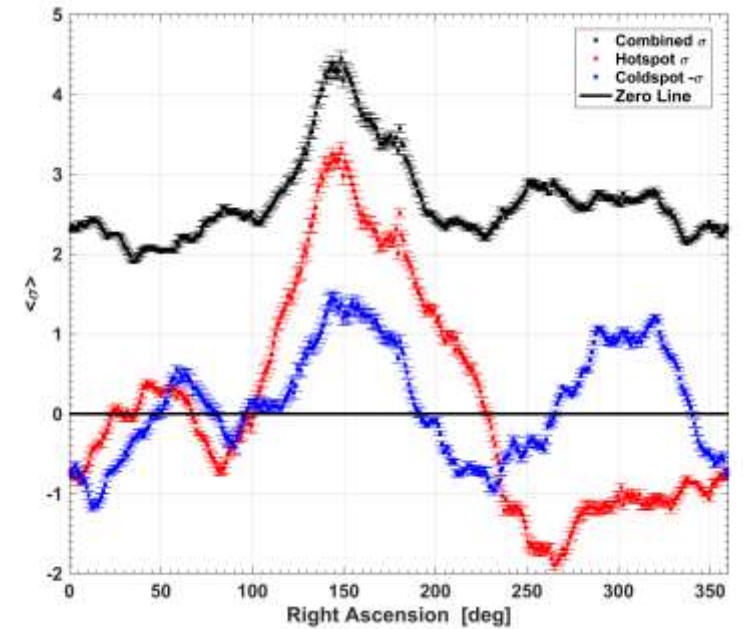
Li-Ma σ_{local} for Combined, Low Energy Bin, and High Energy bin



Correlated in time
(Integral day data σ_{local}
at max. point)



Correlated in Declination
(1° Dec. bins average σ_{local})

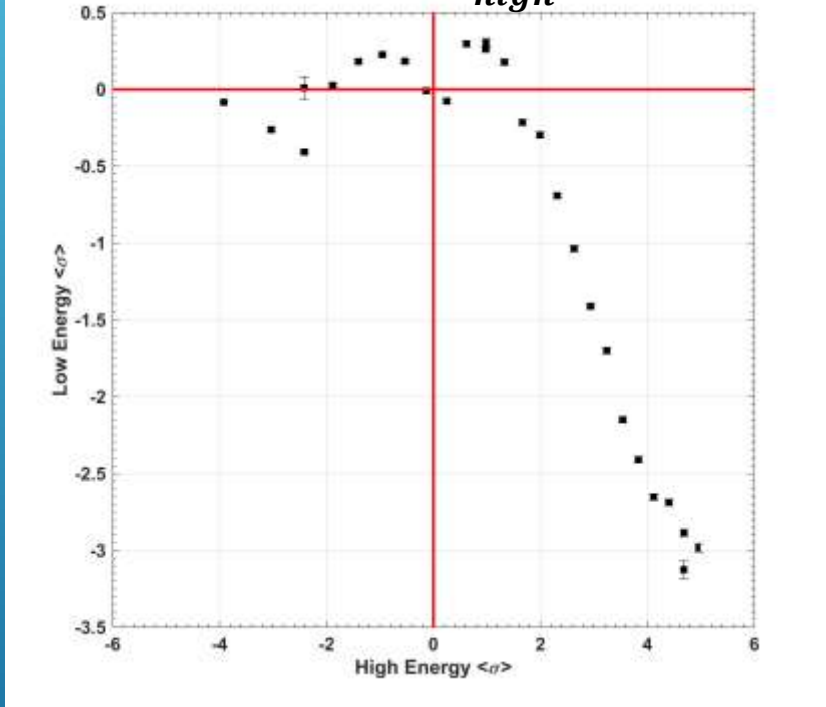


Correlated in Right Ascension
(1° Dec. bins average σ_{local})

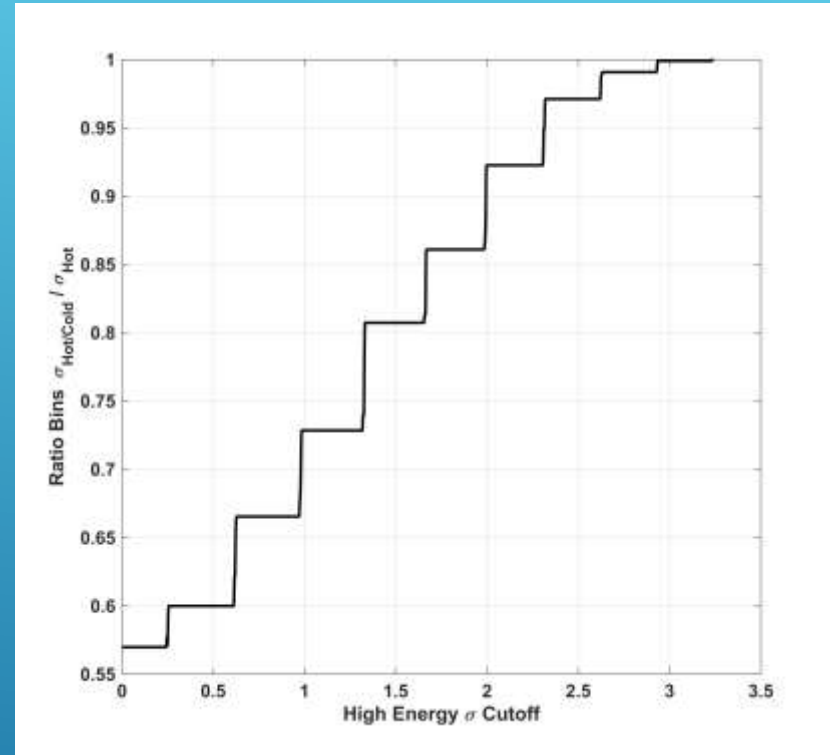
TWO ENERGY BIN CORRELATIONS

Li-Ma σ_{local} for Low Energy Bin, and High Energy bin

Linear Correlation $\sigma_{high} > 0$: -0.625



Excesses directly correlated with deficits
(average of grid points
within $0.1 \sigma_{high}$ bins)



Grid points with Hot/Coldspot divided by # Hotspot
Versus high energy bin σ_{high} cutoff
(100% of grid points with $\sigma_{high} > 3.24$ are a Hot/Coldspot)

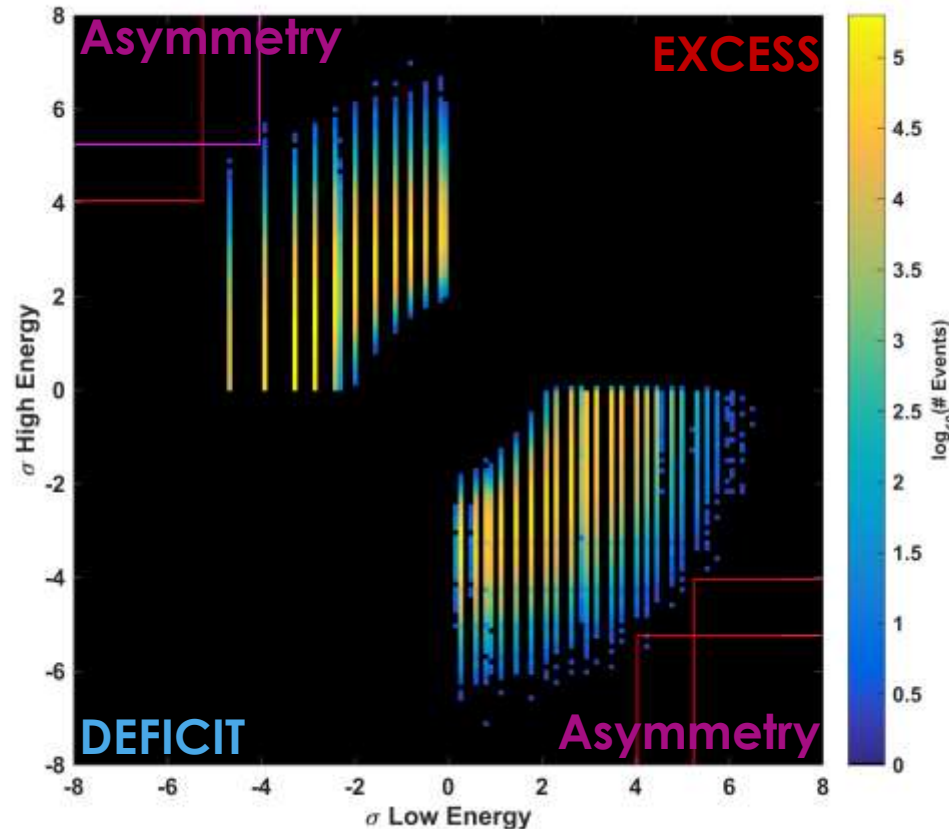
EVENT DENSITY ASYMMETRY SIGNIFICANCE



EVENT DENSITY ASYMMETRY SIGNIFICANCE

- ▶ Testing MC trials for combined significance underestimates significance
 - ▶ Maxima with excess/deficit in both bins are not signatures of magnetic deflection
- ▶ Significance of MC is found from separate energy bin σ thresholds.

MC sets outside
of four bounds
pass the test



MC Sets scanned
same bin sizes and energy thresholds
as data

- **3** isotropic MC have equal or greater event density asymmetry out of $16 * 87.89$ million
 - **5.4 σ** significance

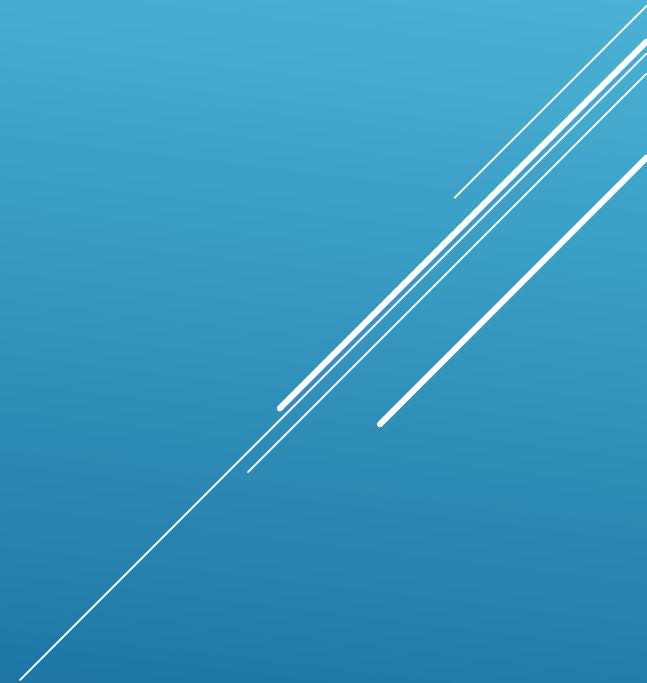
COMBINED MEASURE OF ENERGY SPECTRUM ANISOTROPY AND ENERGY/POSITION CORRELATION

- Energy Spectrum Anisotropy significance: **3.74 σ** (parameters scanned and accounted for)
- Energy-Distance Correlation Anisotropy significance: **3.37 σ** (parameters not scanned)
 - *Stouffer's Method combined significance: 5.03 σ*
- Hot/Coldspot Anisotropy (a result of Spectrum AND Position Correlation): **5.4 σ**

CONCLUSION

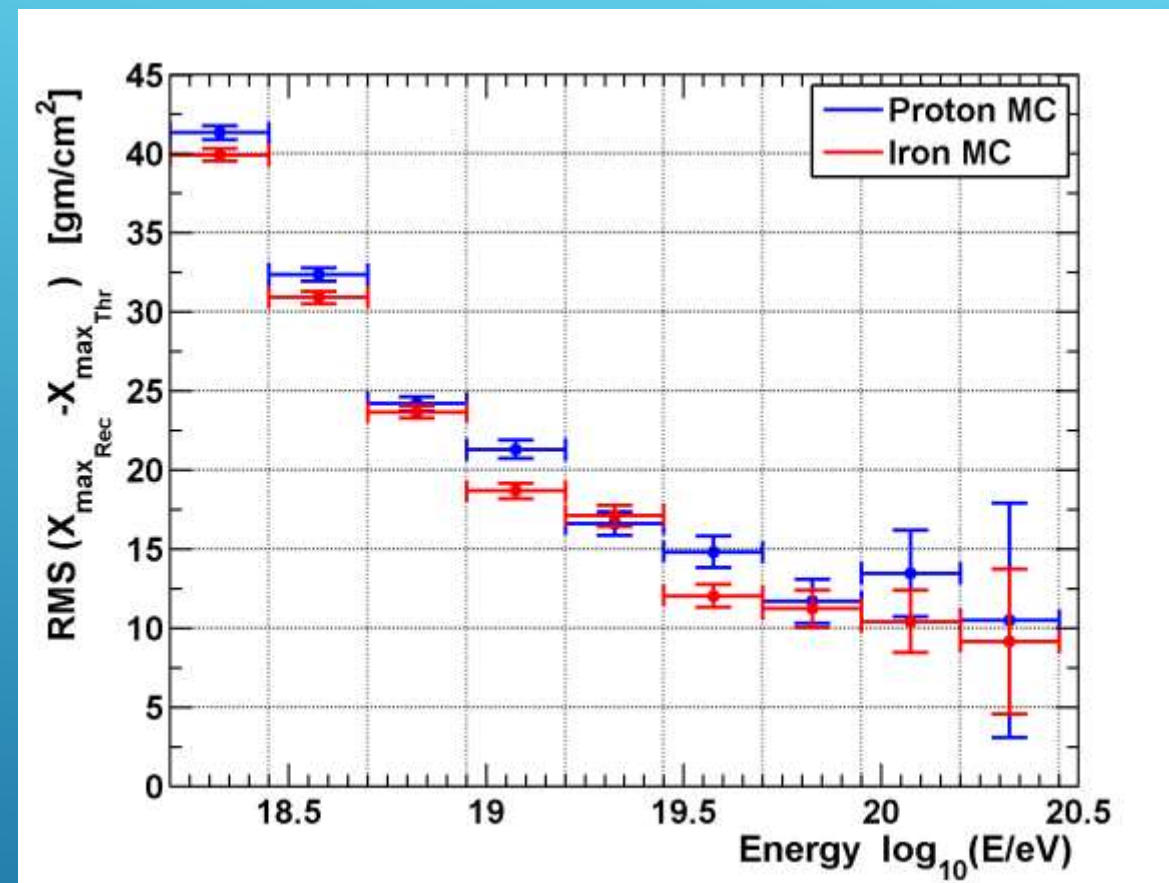
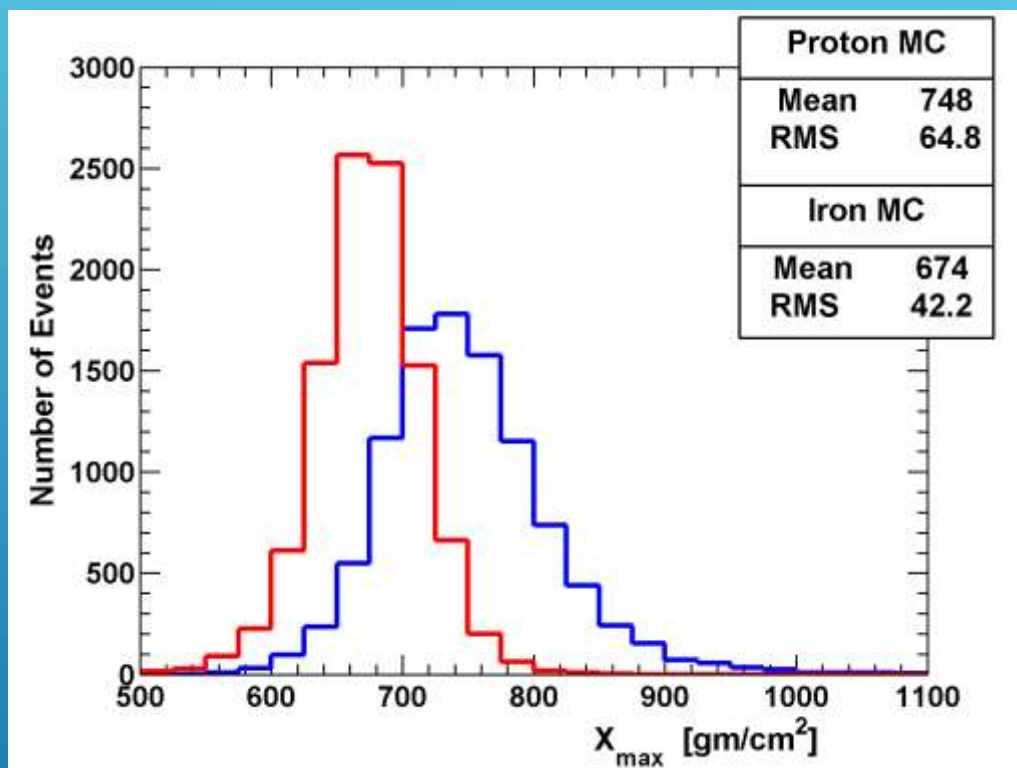
- ▶ Hot/Coldspot Event Density Asymmetry (energy-position correlation)
 - ▶ **Post-trial $\sigma = 5.4$**
- ▶ The previously reported Hotspot is correlated with a deficit of low energy events. This **observation** is suggestive of magnetic deflection.

PART TWO
COMPOSITION STUDY



**PATTERN RECOGNITION ANALYSIS
&
QUALITY FACTOR ANALYSIS**

XMAX RESOLUTION – ENERGY DEPENDENCE

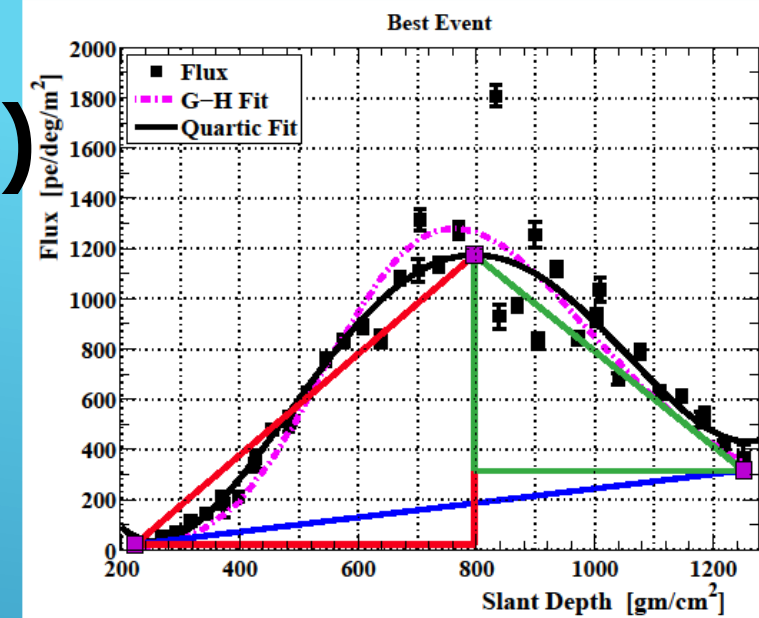


- Protons deeper and wider than iron.
 X_{\max} (peak) gives composition information

- Energy dependence of resolution is important if there is a change in composition

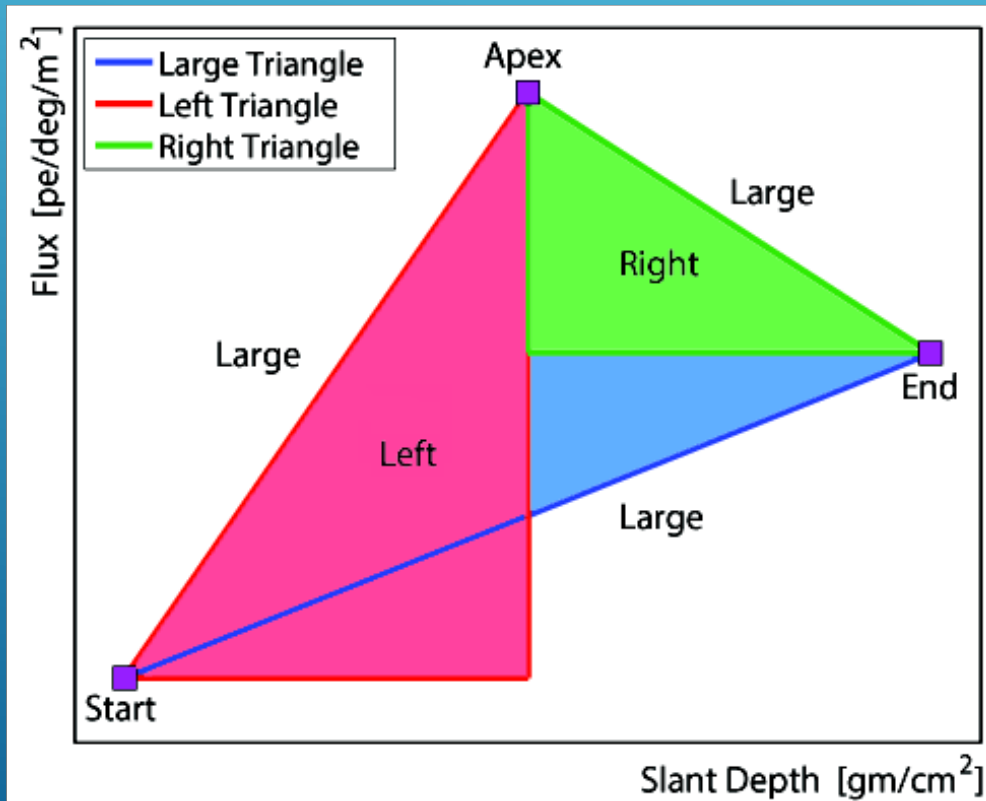
PATTERN RECOGNITION ANALYSIS (PRA)

- ▶ No model needed to see increase and decrease in signal
- ▶ Fit shower profiles to triangles
 - ▶ Extract features from triangles. Describes shape of event. (Length of sides, angles, etc.)
- ▶ Brains are good at pattern recognition: use them to create **training set** of known good and bad events.
- ▶ Training set is used to find useful features, and cut values, for a yes/no determination.
 - ▶ The result agrees with the human observers on the **97.2% to 99.6%** percent level.

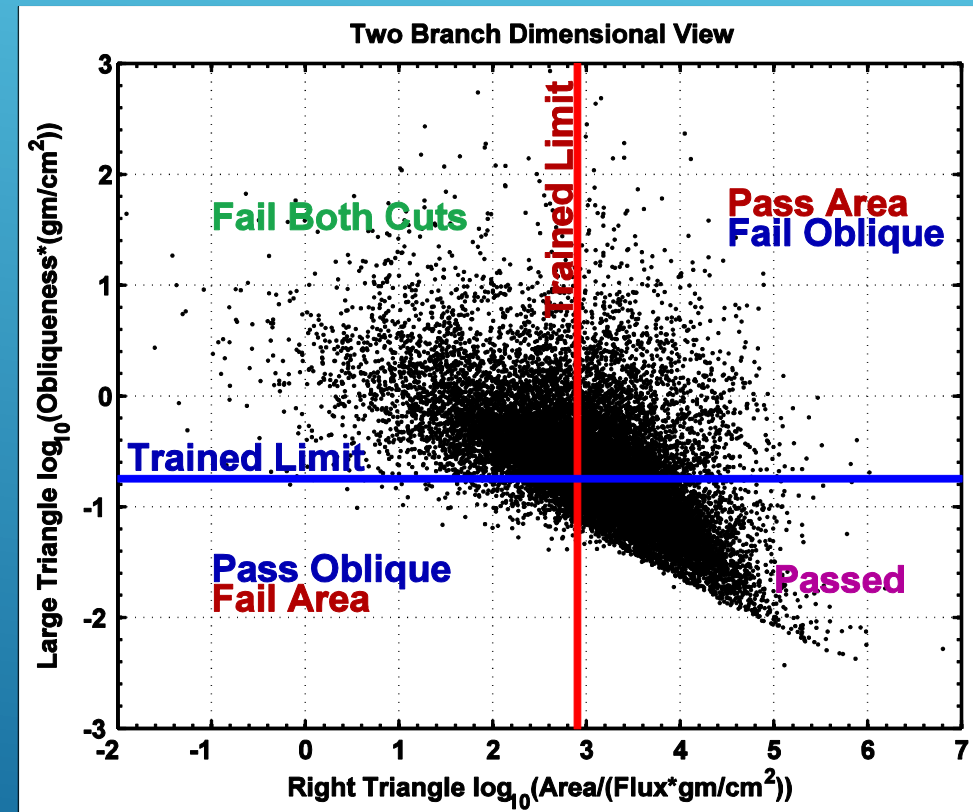


BINARY PRA

- ▶ Example of cut on two features extracted from triangles. (These two cut the most events)
 - ▶ Obliqueness: perimeter/area of the large triangle.
 - ▶ Right triangle area: $1/2 * \text{Slantdepth} * \text{Flux}$ of the triangle sides.



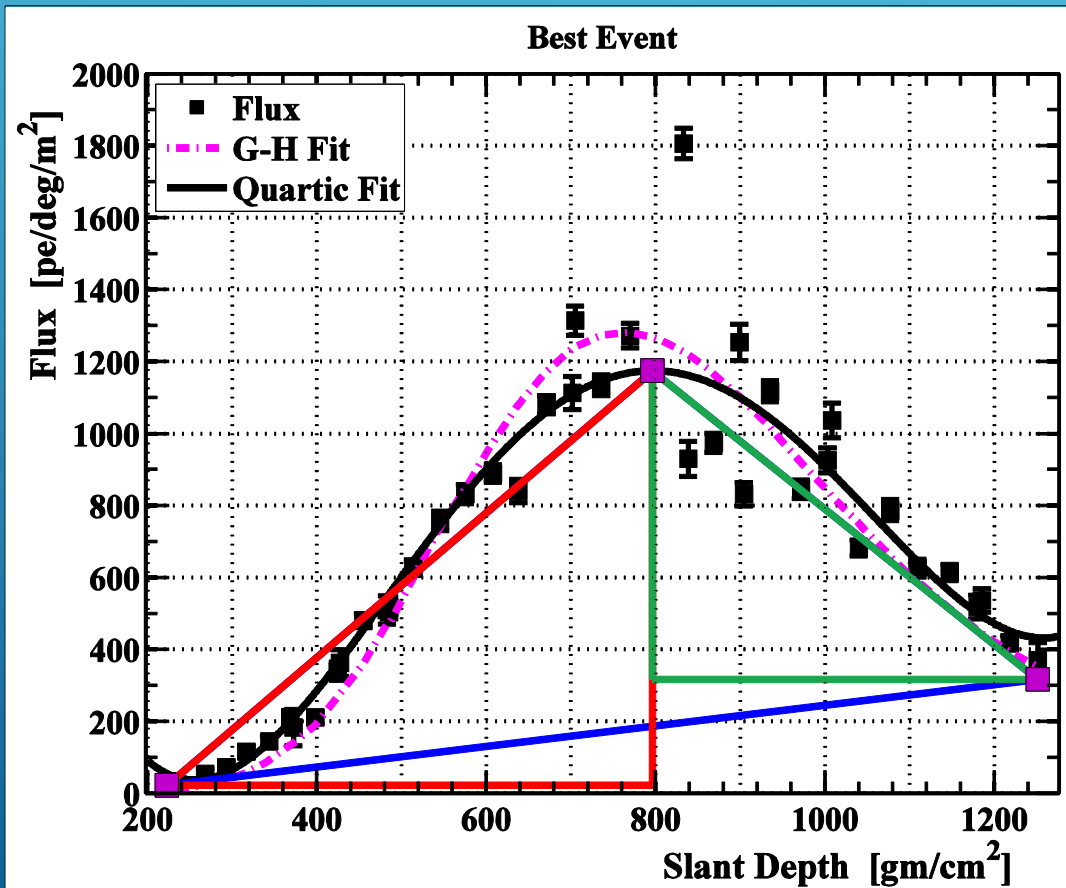
Triangle Labels



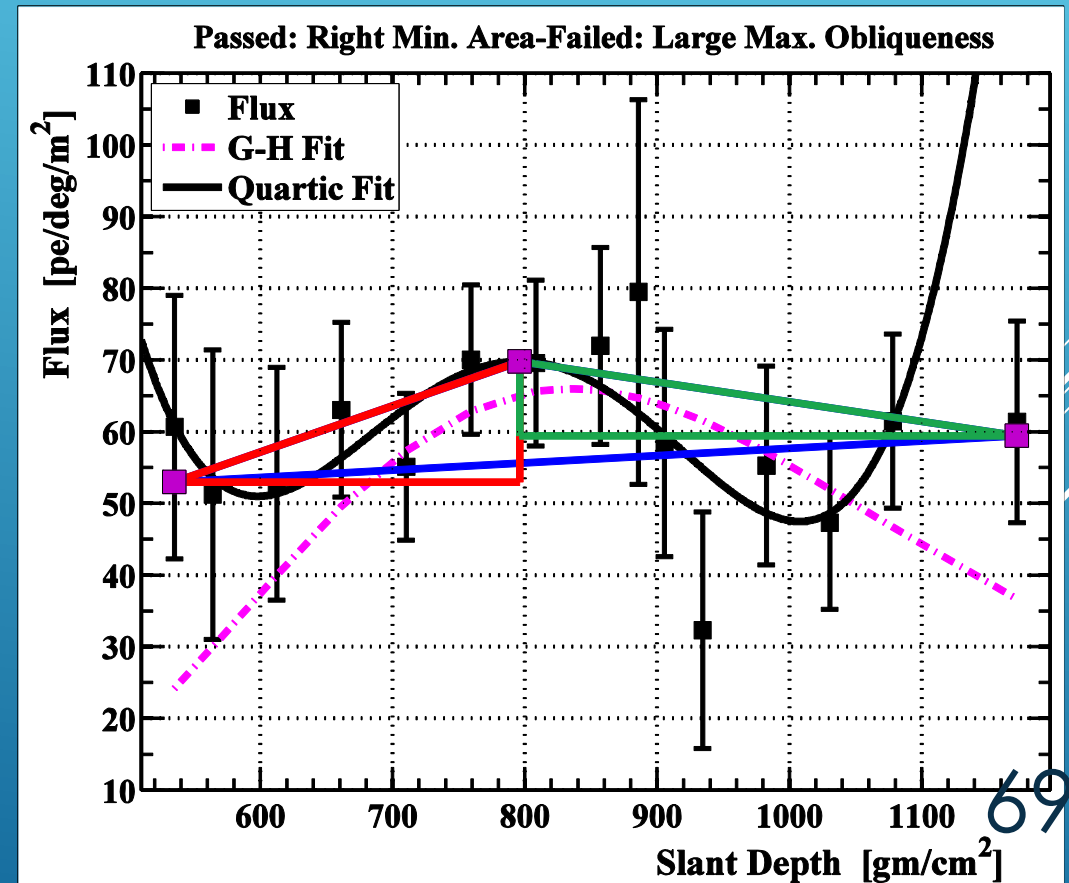
2d view of two cuts

BINARY PRA

- ▶ PRA determines whether an event has an acceptable profile and returns a binary yes/no answer.



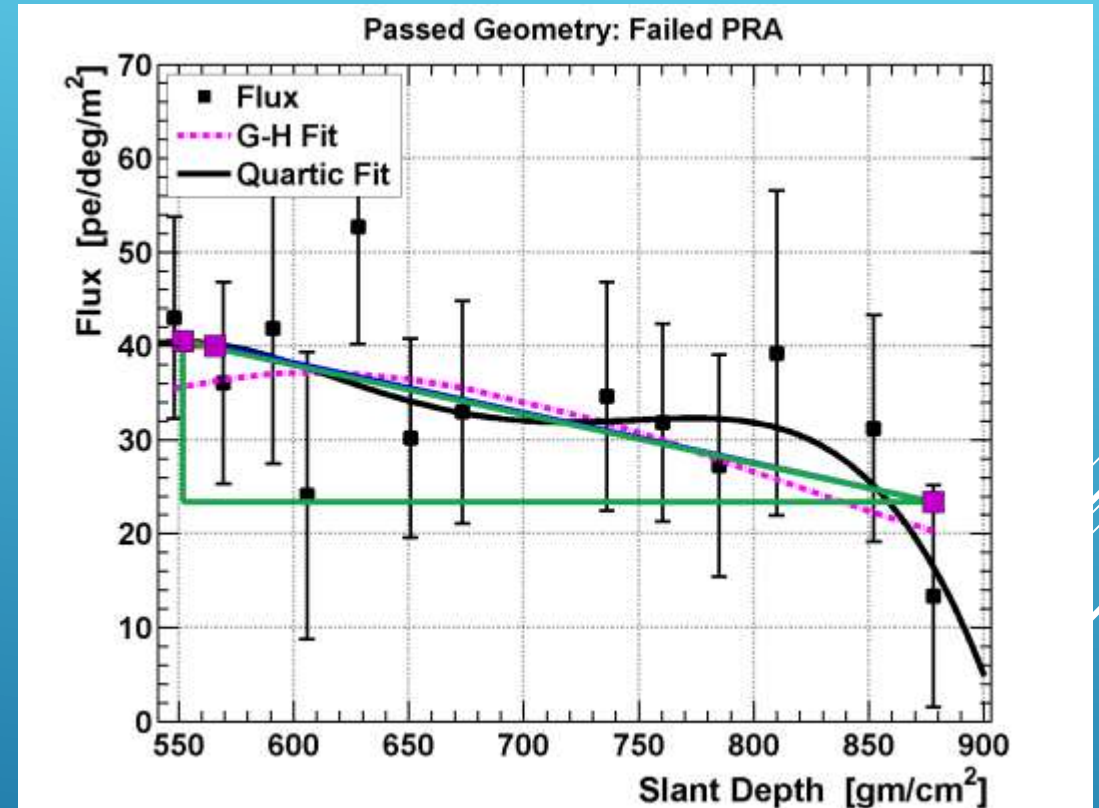
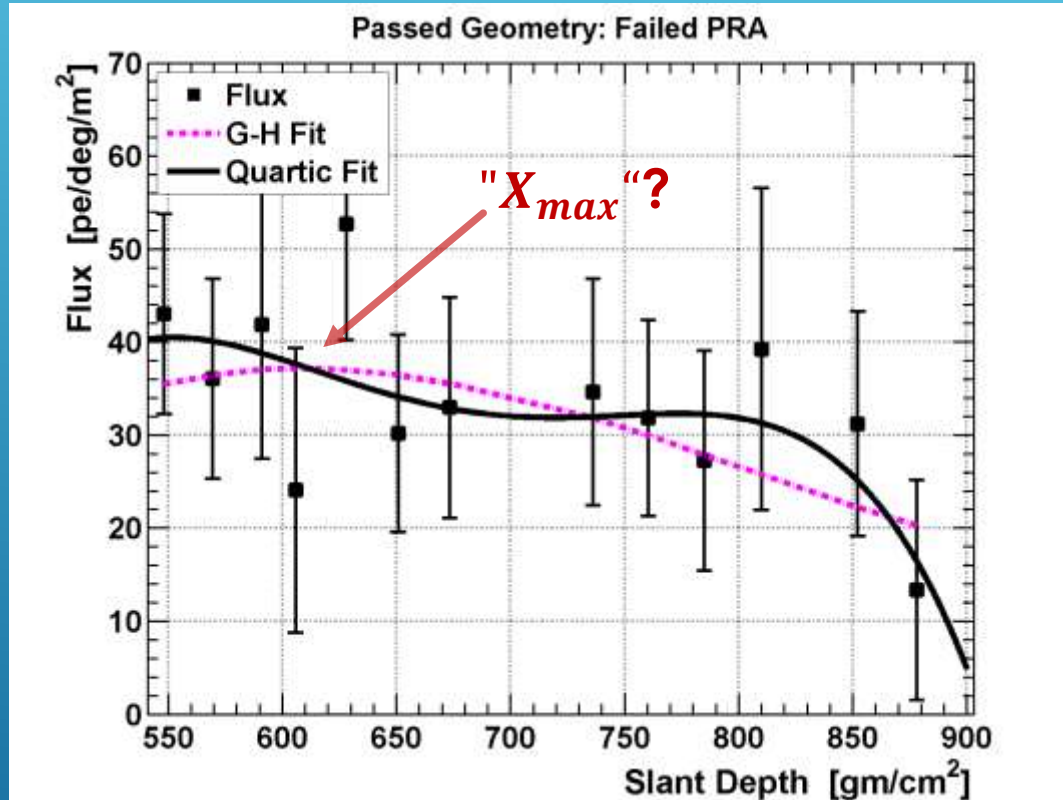
Good (1)



Bad (0)

FAILED PRA – PASSED GEOMETRY CUTS

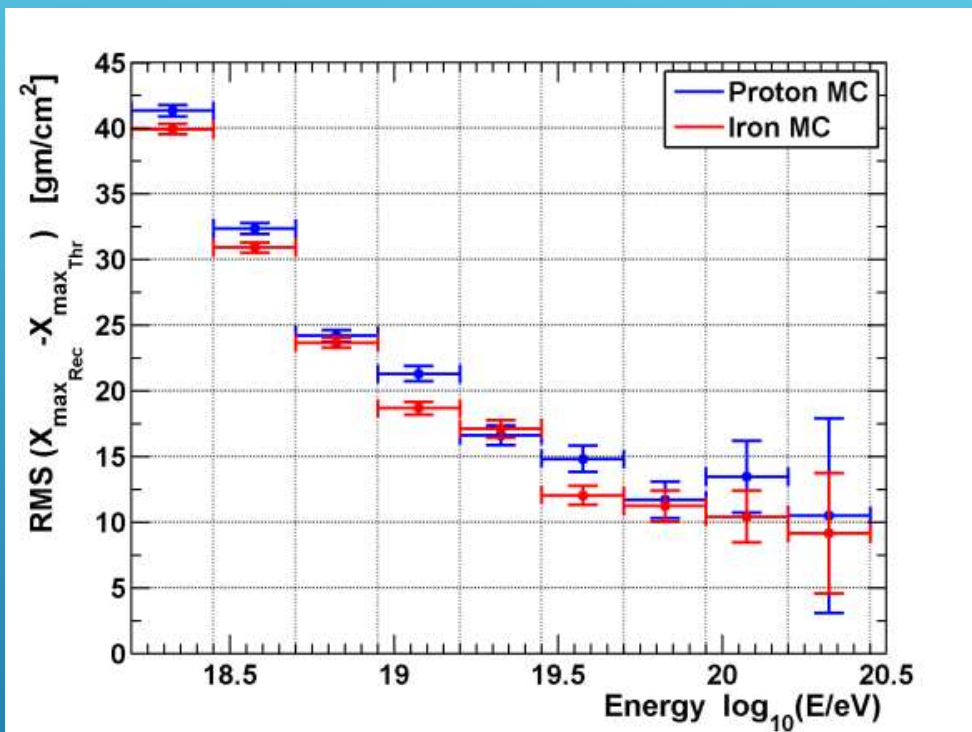
Discrepancy is ~2 times the separation between means of Iron and proton primaries.



$$X_{max_{Reconstructed}} - X_{max_{Thrown}} = -130 \frac{gm}{cm^2}$$

$E = 10^{18.3} eV, \theta = 40.2 deg, R_p = 17 m, SD/FD \text{ Core Diff} = 511,$
 Boundary Dist. = 2883 m, Tracklength = 13.4

PRA RESOLUTION IMPROVEMENT

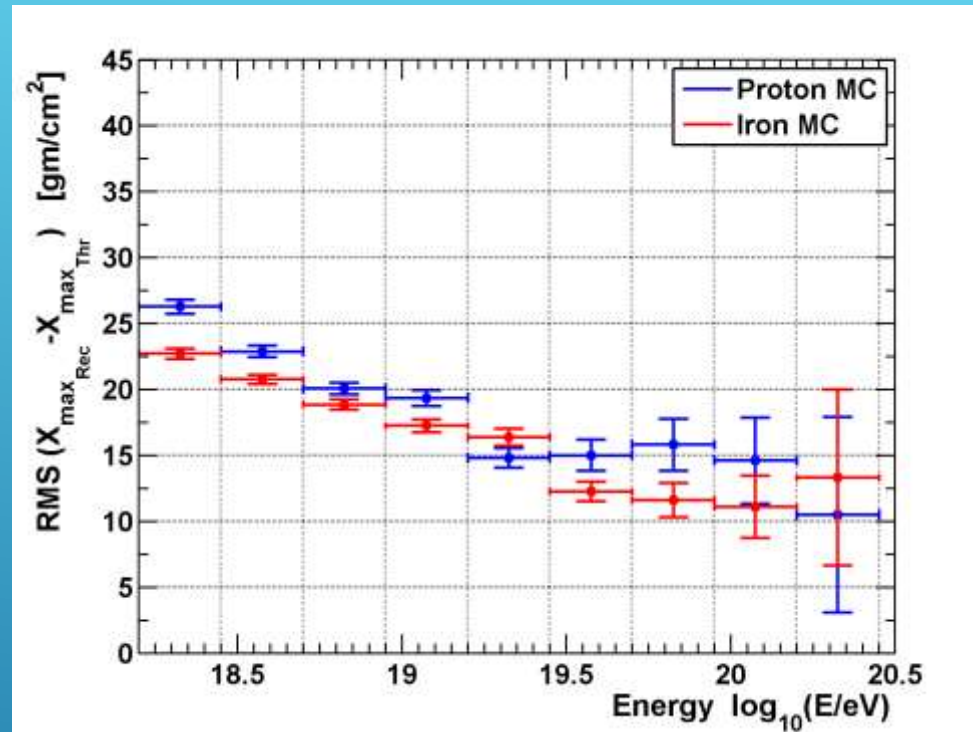


Tight Geometry Cuts

Composition Results Published in: R. U. Abbasi, et al., Study of Ultra-High Energy Cosmic Ray composition using Telescope Arrays Middle Drum detector and surface array in hybrid mode, *Astropart. Phys.* 64 (2014) 49–62. arXiv:1408.1726

Also used for:

- R. U. Abbasi, et al., Measurement of the proton-air cross section with Telescope Arrays Middle Drum detector and surface array in hybrid mode, *Phys.Rev. D* 92 (3) (2015) 032007. arXiv:1505.01860
- T. Stroman, Y. Tameda, Telescope Array measurement of UHECR composition from stereoscopic fluorescence detection, *PoS ICRC2015* (2016) 361.



Loose Geometry Cuts and PRA

BINARY PRA TO QUALITY FACTOR ANALYSIS (QFA)

- ▶ A good start. How do you make it better? **MORE EVENTS**
 - ▶ Maybe, we can lower our standards (or make the computer smarter than us) without compromising resolutions, resolution slopes, and biases.
- ▶ Instead of a yes/no answer a scale of event quality.



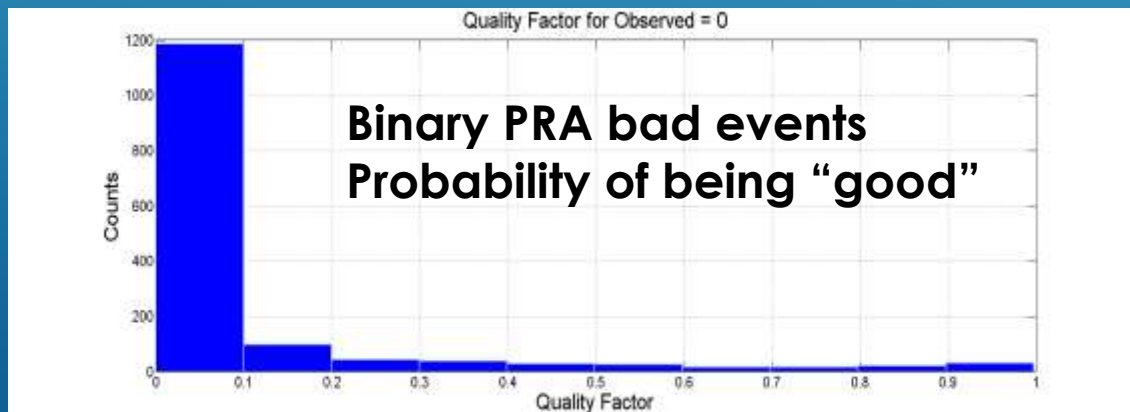
LOGISTIC REGRESSION

Finds weights, β_j , for prediction from features

$$\min_{\beta} J(\beta) = \sum_{j=1}^N [y_j \log p(\vec{x}_j) + (1 - y_j) \log(1 - p(\vec{x}_j))]$$

$$p_j(\vec{x}_j) = \frac{1}{1 + e^{-(\beta_0 + \vec{\beta} \cdot \vec{x}_j)}}$$

y_j (Binary PRA) (1 or 0) and \vec{x}_j vector of triangle feature values for that event.



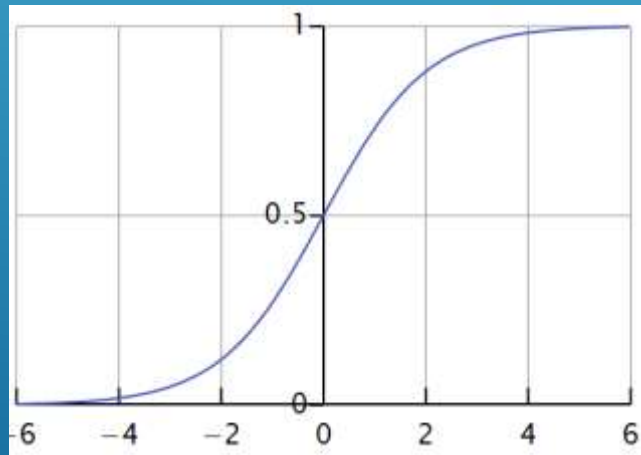
LOGISTIC REGRESSION

$$t_j = \beta_0 + \sum_i^{10} \beta_i \cdot x_{ji}$$

Found weights β_i

Result is $p_j(t_j)$ the **probability** that the vector \vec{x}_j comes from an event that is a 'success'

$$p_j(t_j) = \frac{1}{1 + e^{-t_j}}$$



Logistic Function maps the range $(-\infty, \infty)$ to $[0, 1]$

EXAMPLE EVENT

Triangle Attributes

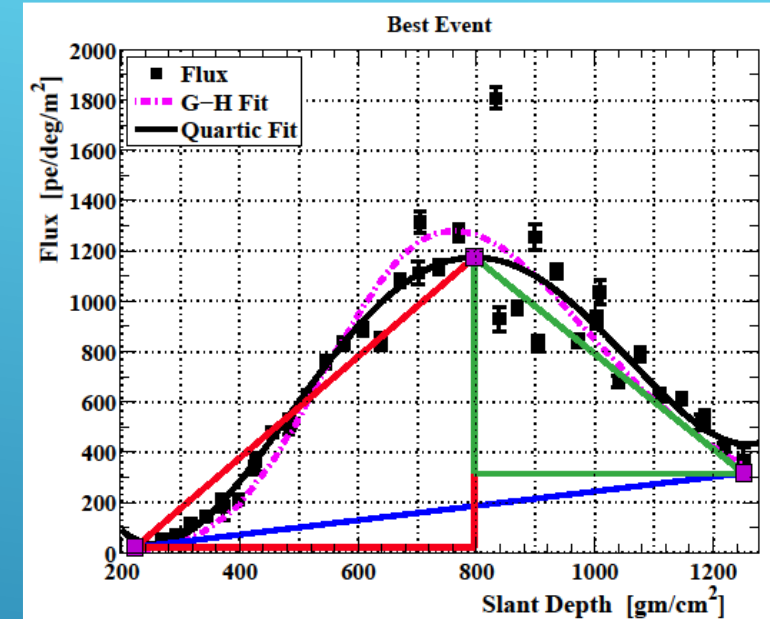
\vec{x}_j

1. Apex highest point = 1
2. Bins before apex = 0.315
3. Cubic term = 0.021
4. Max. Sig. Diff. = 2.471
5. Midsize length = 3.271
6. Signal Mean = 3.524
7. Norm. Missing = -1.721
8. Apex angle/Hyp. = -1.665
9. Left Oblique. = -3.292
10. Large under right = -0.179

Fitted Weights

β_j

0. -7.969
1. 3.474
2. 7.456
3. 42.286
4. 0.570
5. -0.054
6. 0.391
7. -0.242
8. 0.632
9. -3.351
10. 2.068

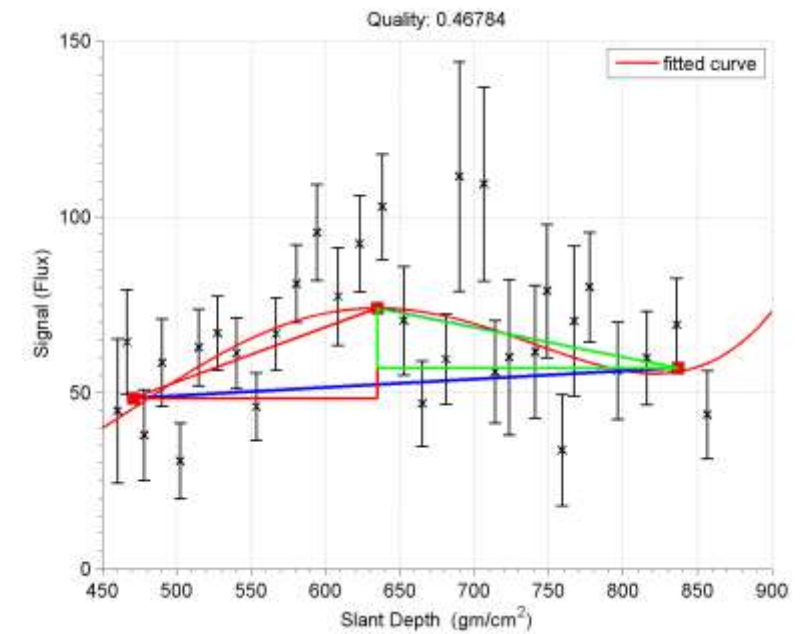
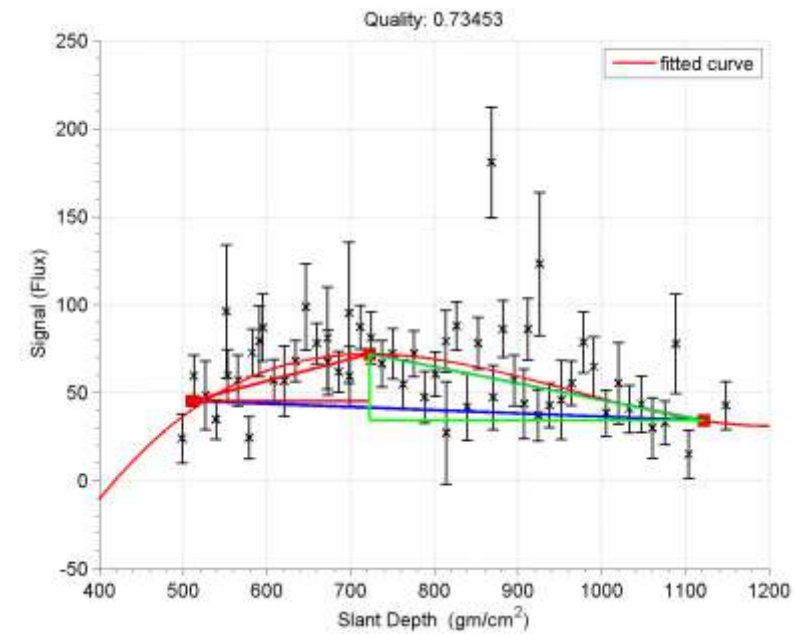
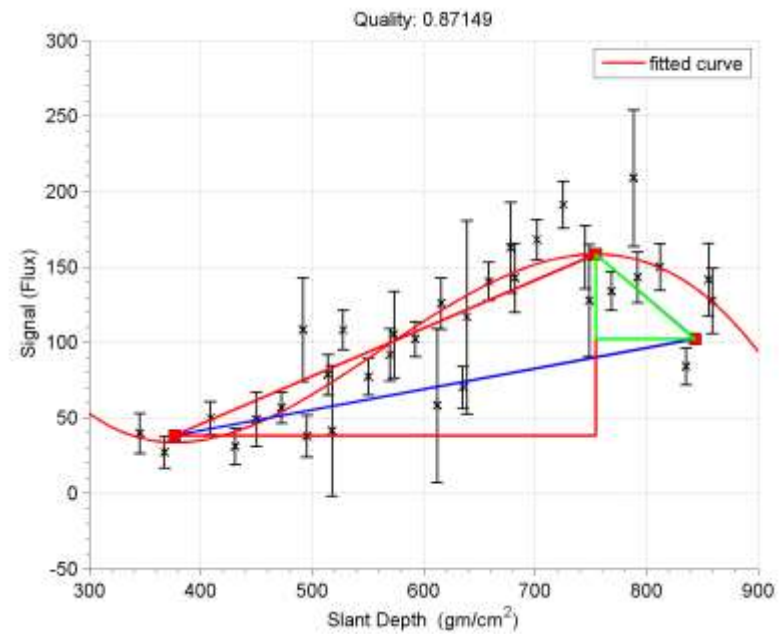
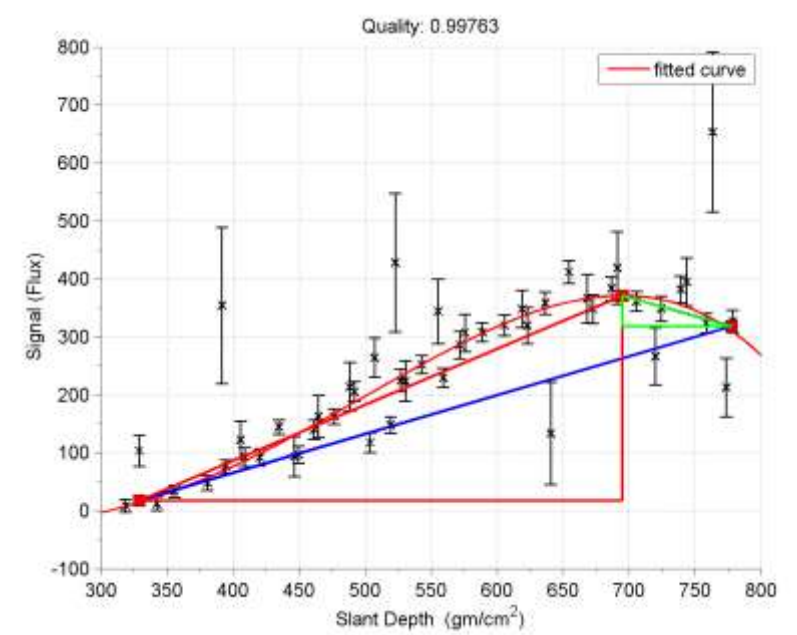
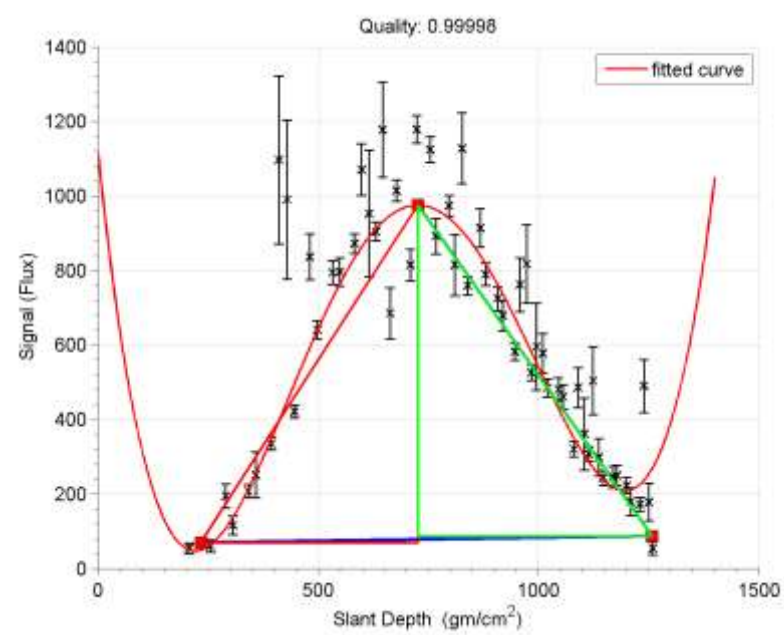
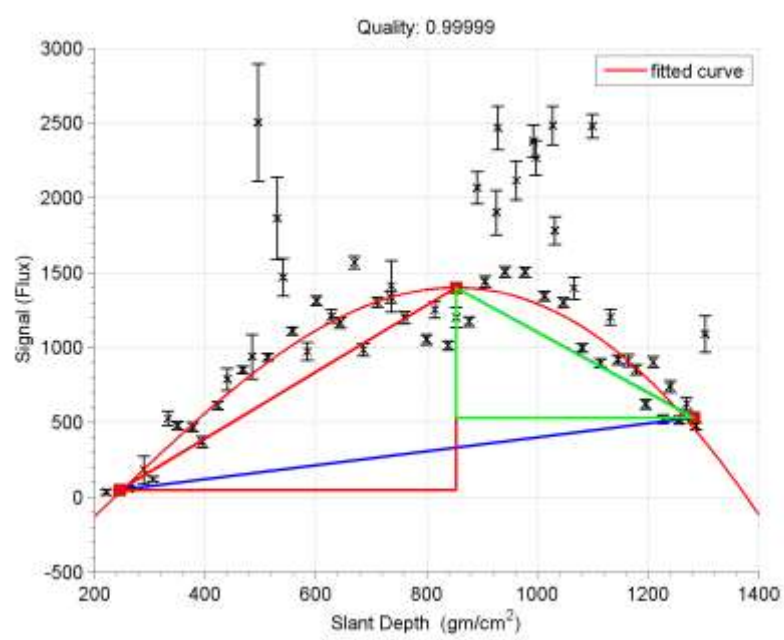


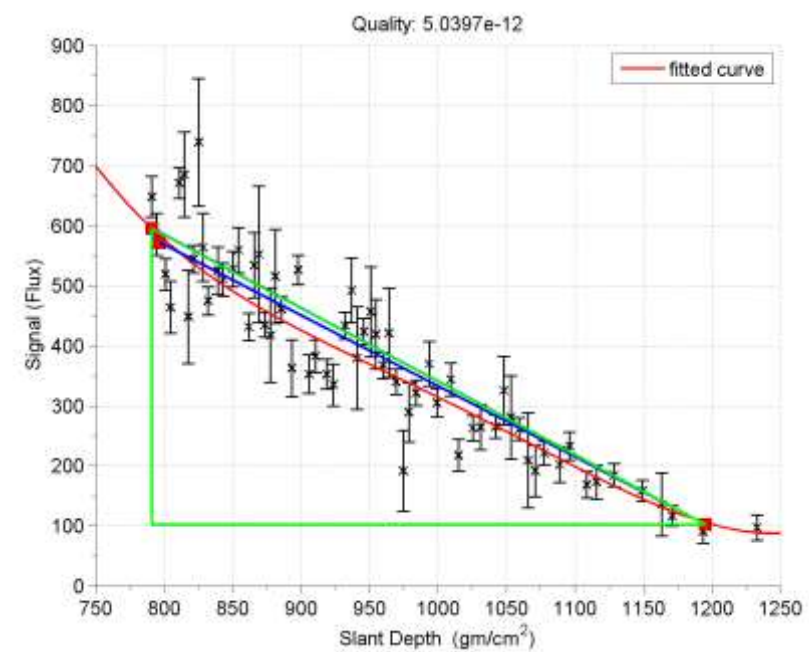
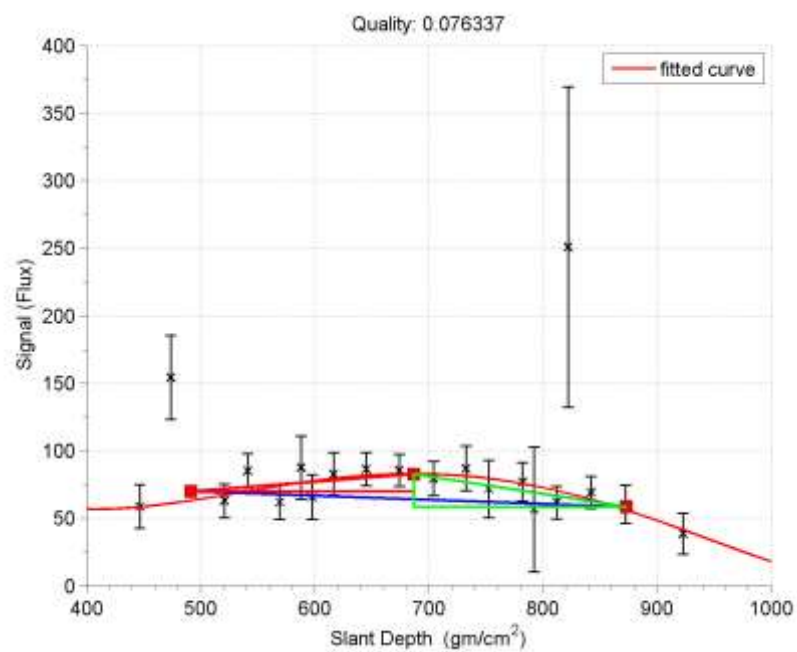
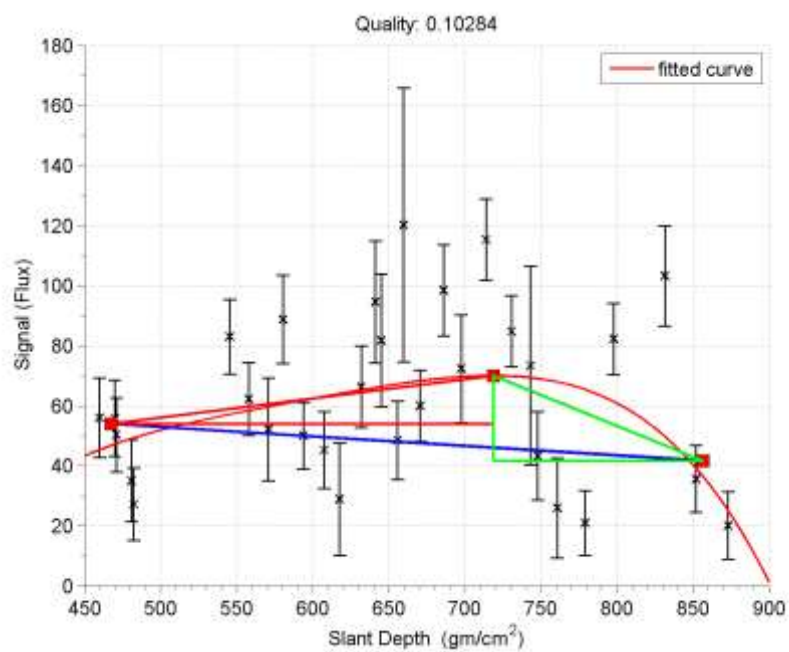
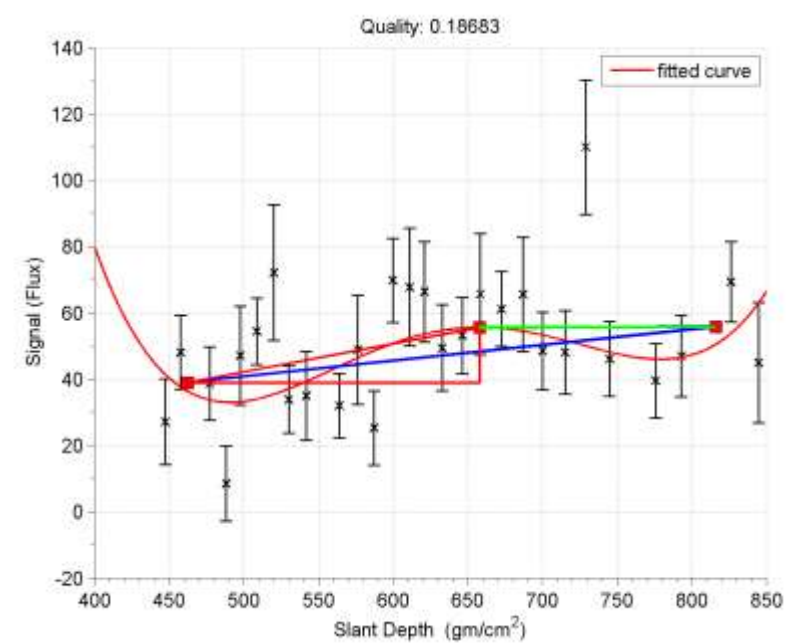
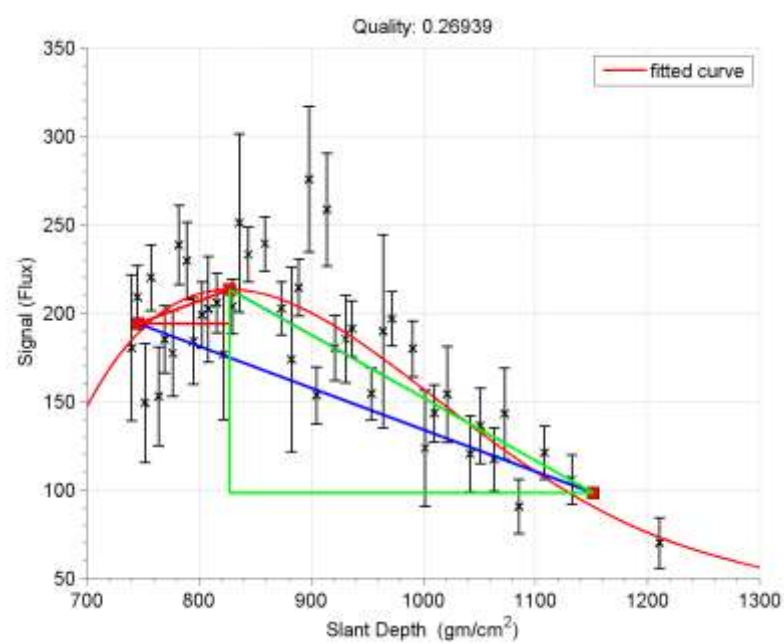
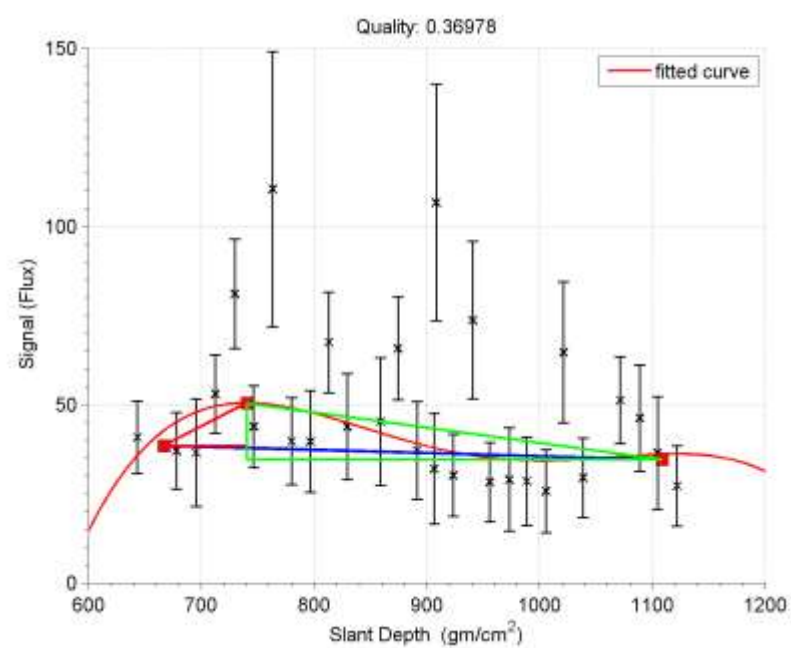
- Highest energy event in data set.
- Has 5th highest quality factor at 0.99999

$$t_j = \beta_0 + \sum_i^{10} \beta_i \cdot x_{ji} = 11.391$$



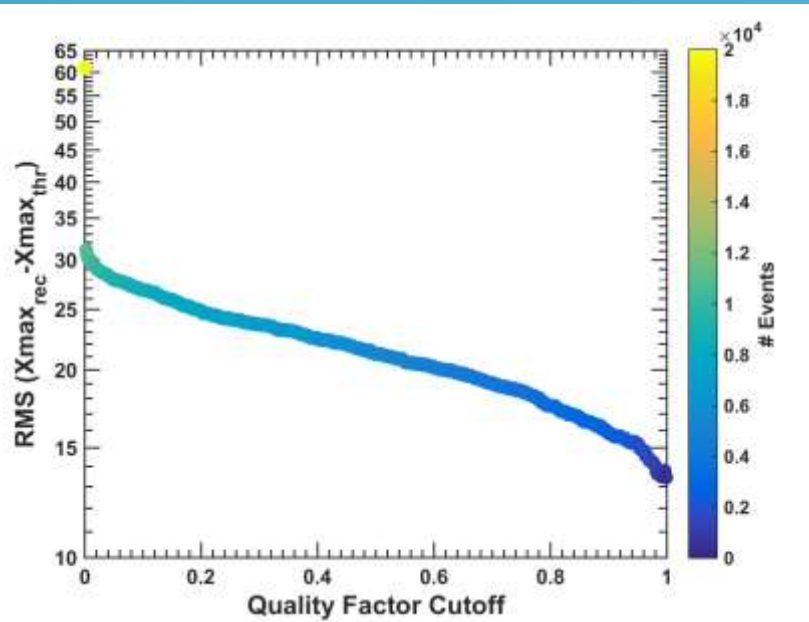
$$p_j(\vec{x}_j) = \frac{1}{1 + e^{-(11.391)}} = 0.99999$$



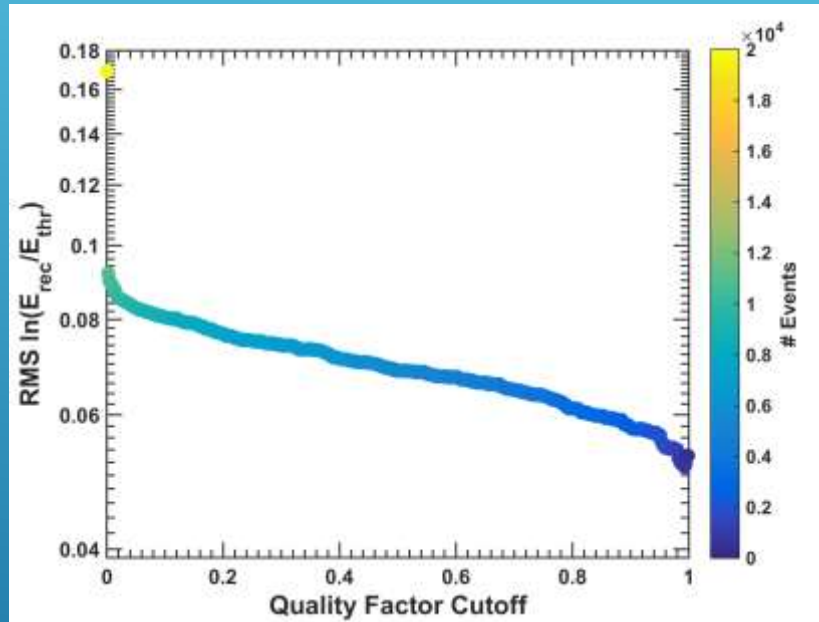


RESOLUTION CORRELATIONS WITH QUALITY FACTOR

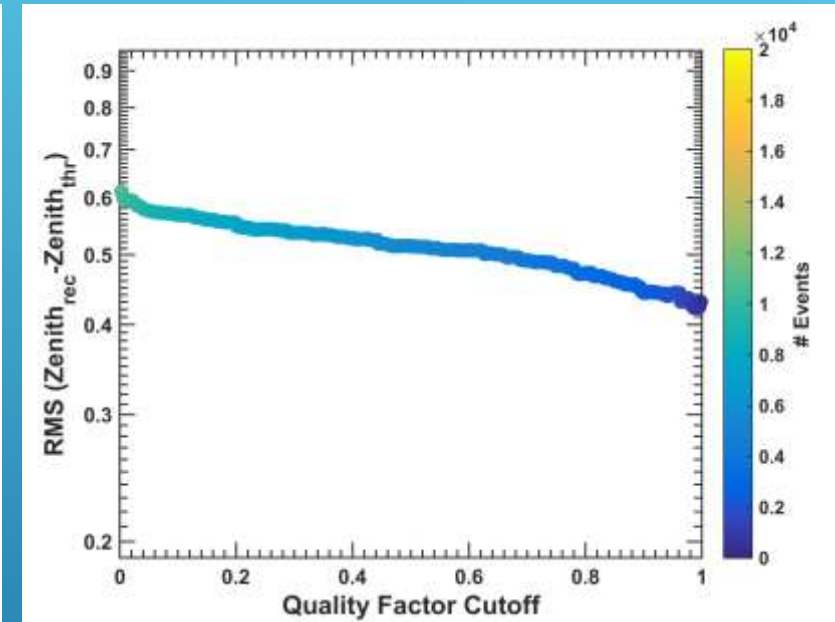
RMS of difference between thrown and reconstructed values for proton MC



Xmax



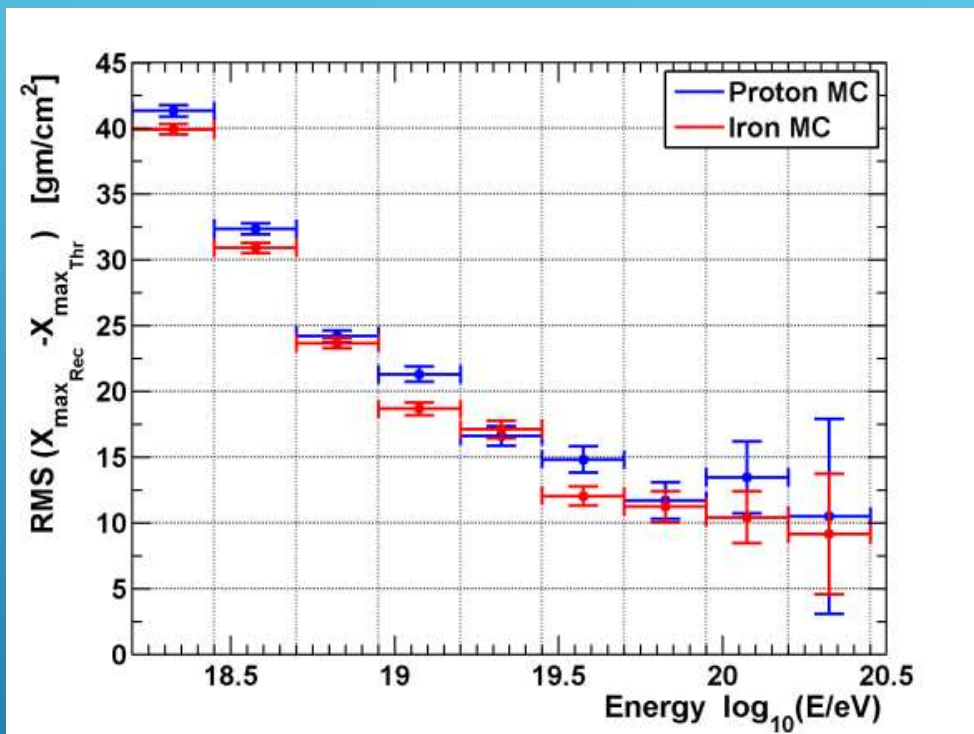
Energy



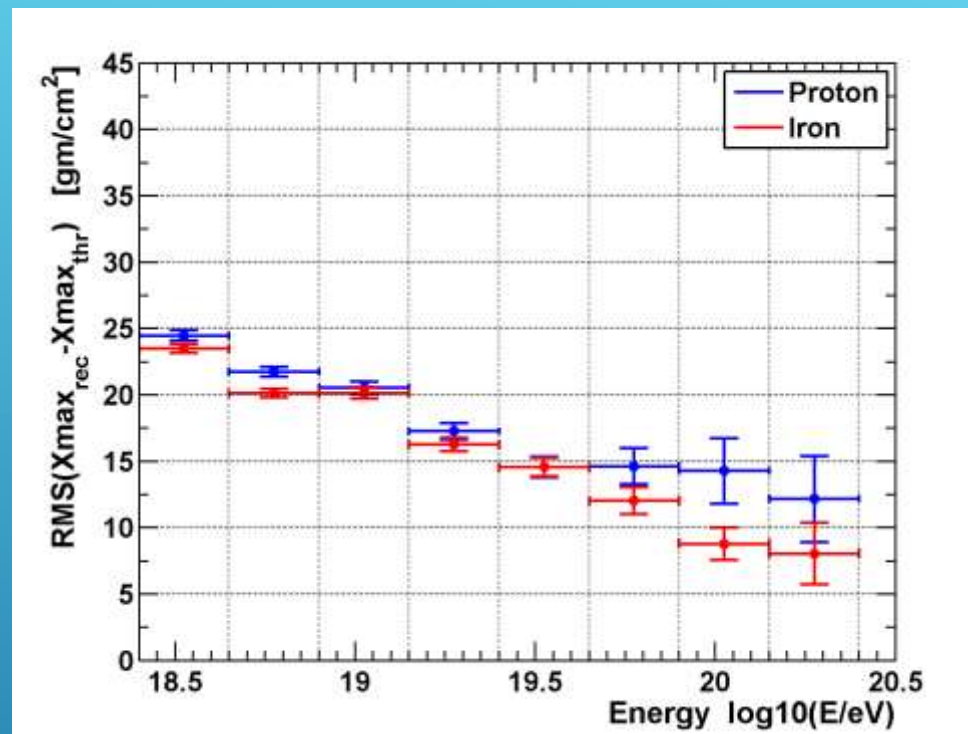
Zenith Angle

*Very loose geometry cuts

QFA RESOLUTION IMPROVEMENT



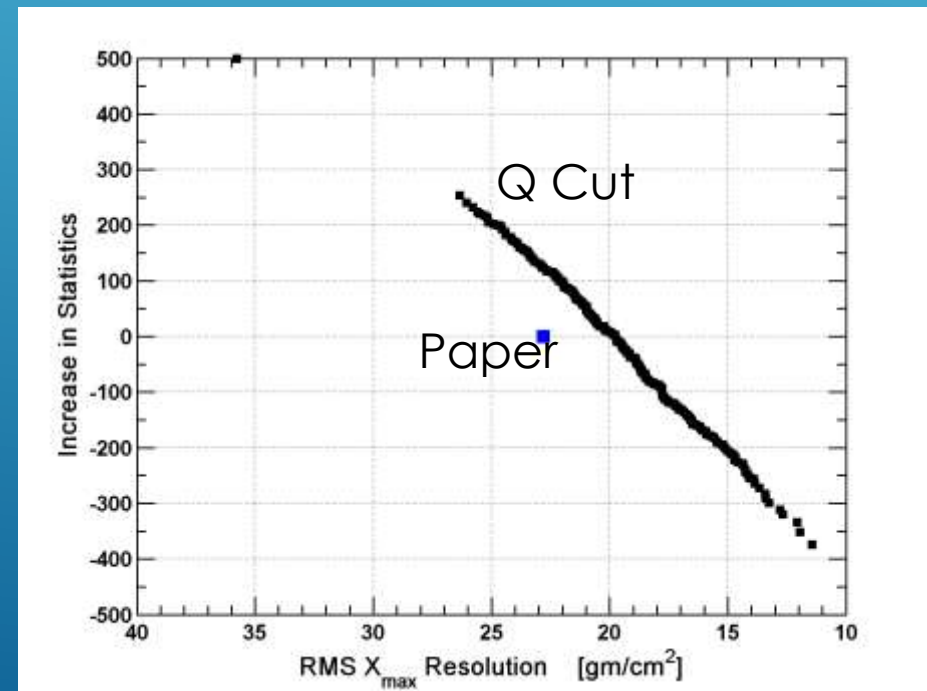
Tight Geometry Cuts



Loose Geometry Cuts and PRA

QFA CONCLUSION

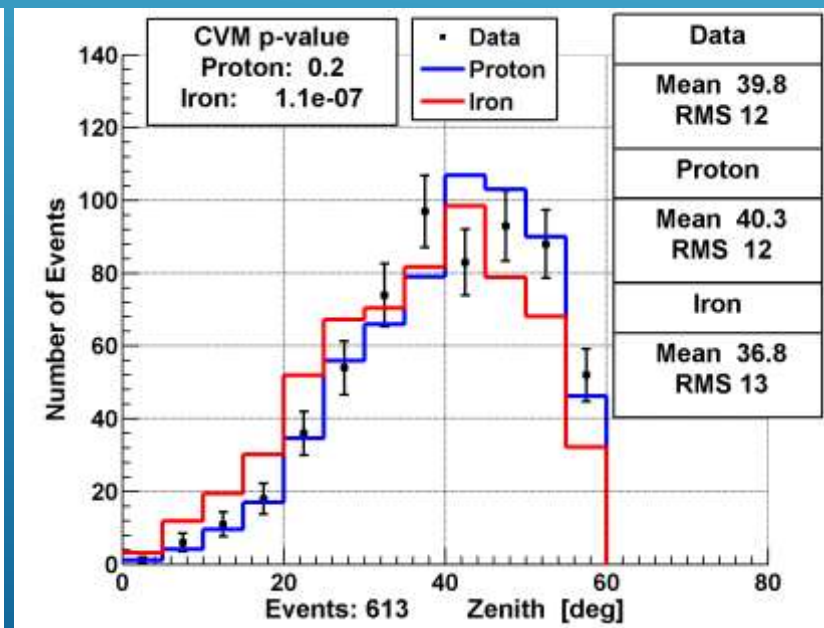
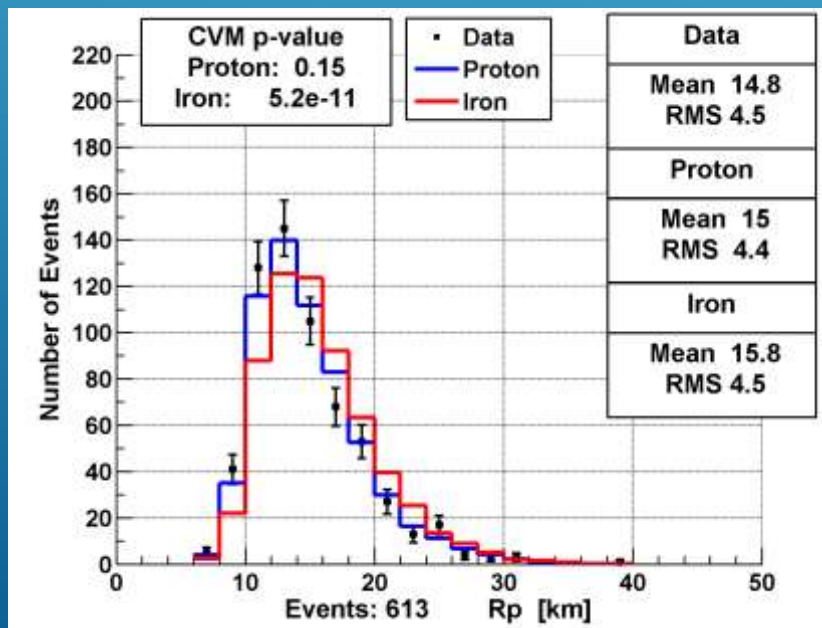
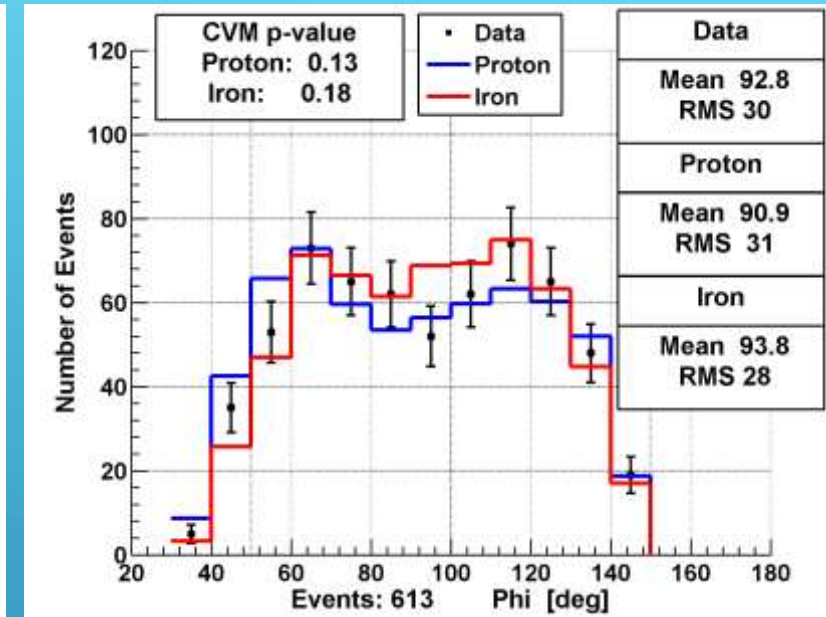
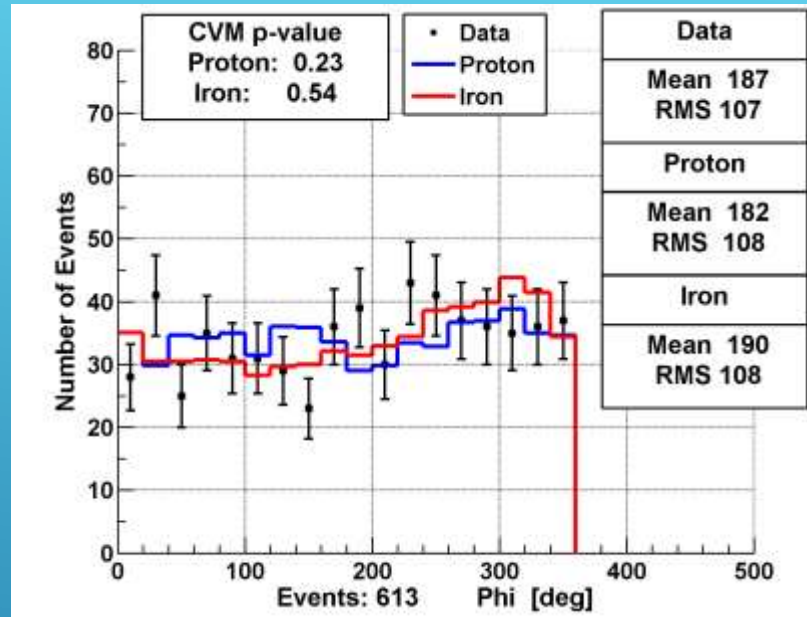
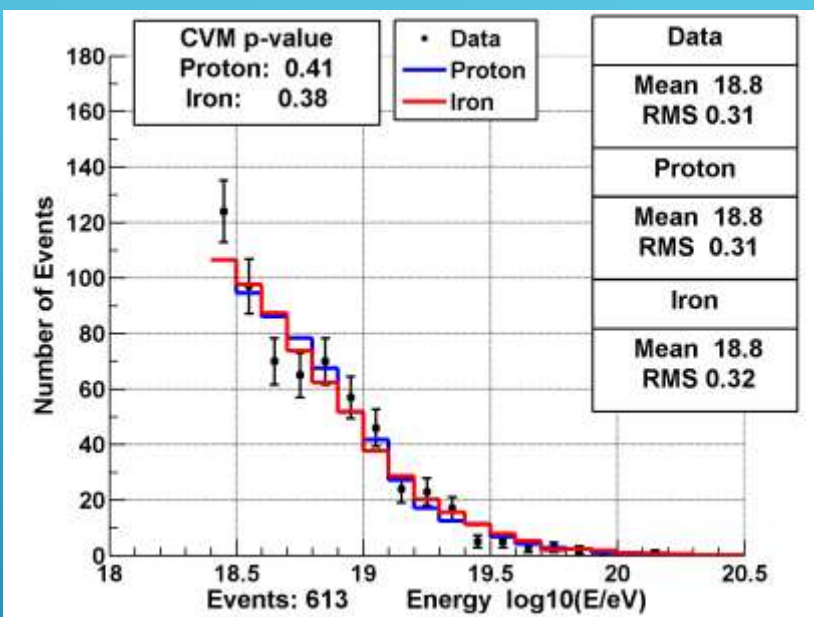
- ▶ Quality Factor describes how well events are seen by the FD
- ▶ Fairly linear correlation between Quality and RMS resolutions (and biases).
- ▶ Setting a QF threshold instead Binary PRA improves statistics.



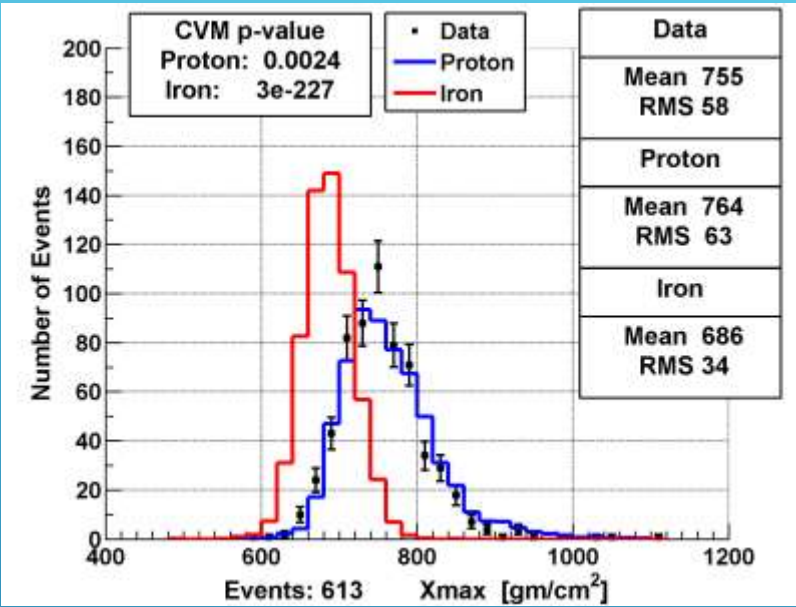
7 YEAR GDAS(3-HOUR) DATA 4 YEAR QGSJETII-03 FLOATED $X_0 = -60$, $LAMBDA = 70$

Quality Factor > 0.2 (for ~ 22 gm/cm² resolution), Energy > 18.4 , Boundary Dist. > -500 m
SD/FD Core Difference < 1600 m, Zenith < 58 , Geometry Fit $\chi^2/\text{DOF} < 5$, and Xmax Bracketed.

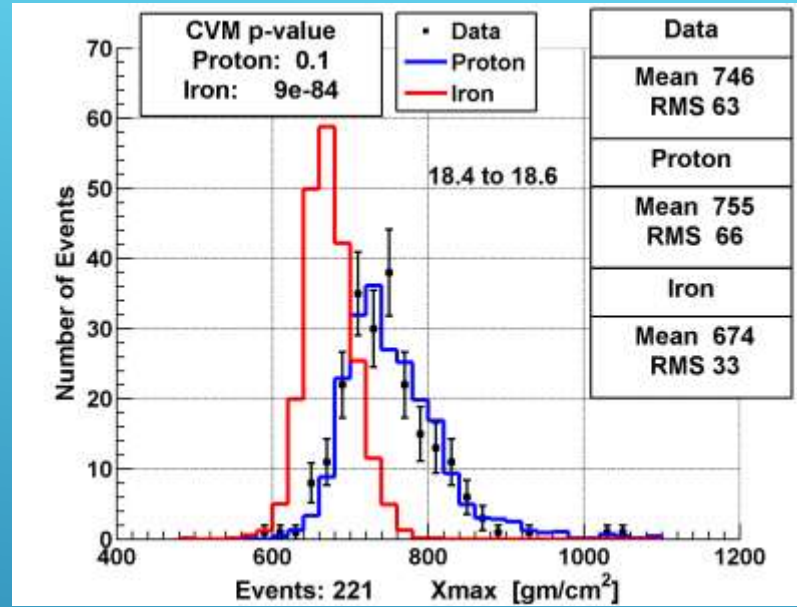
DATA/MC COMPARISONS



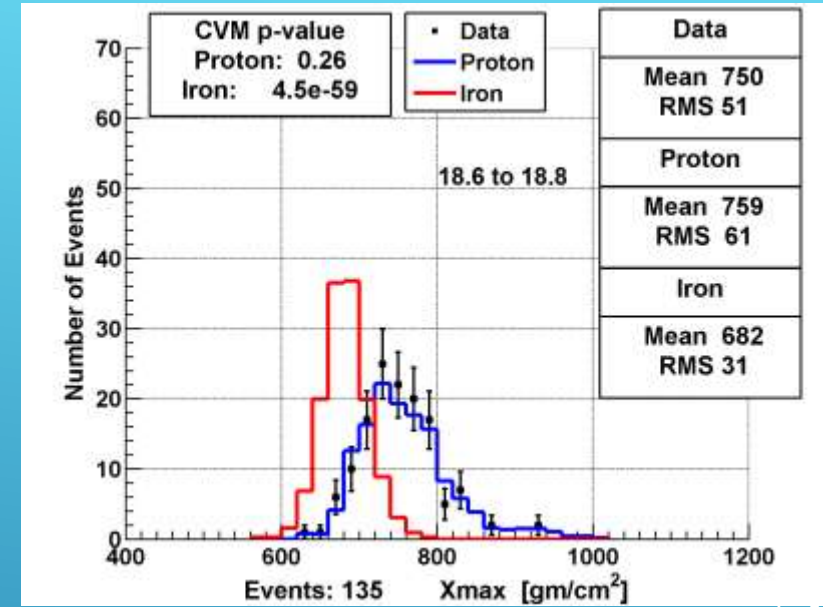
XMAX DISTRIBUTIONS



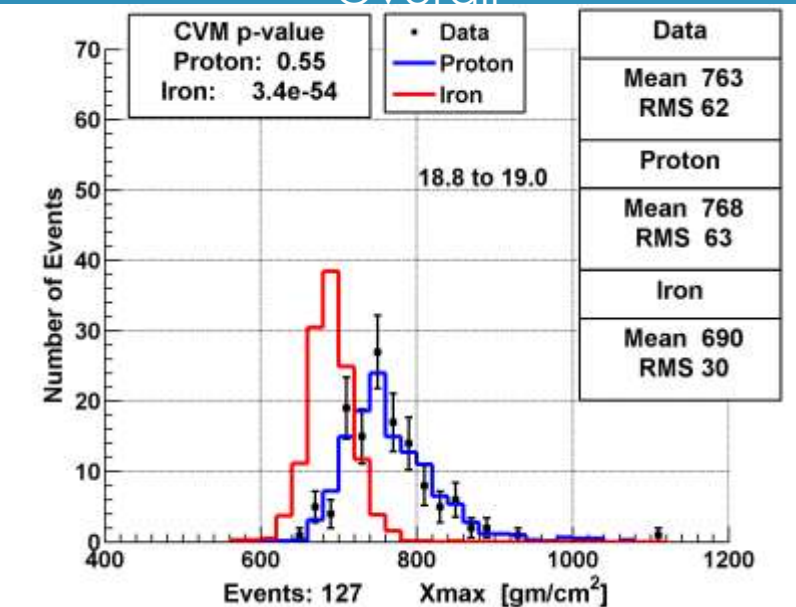
Overall



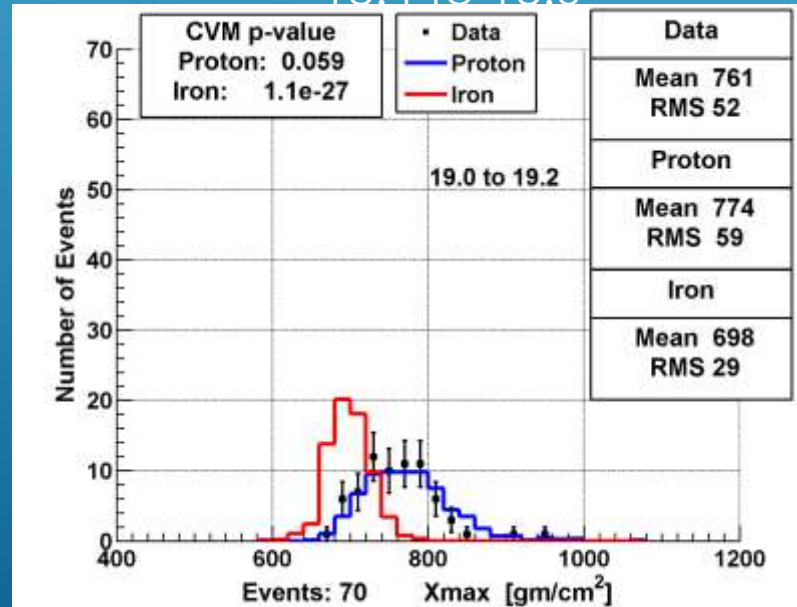
18.4 to 18.6



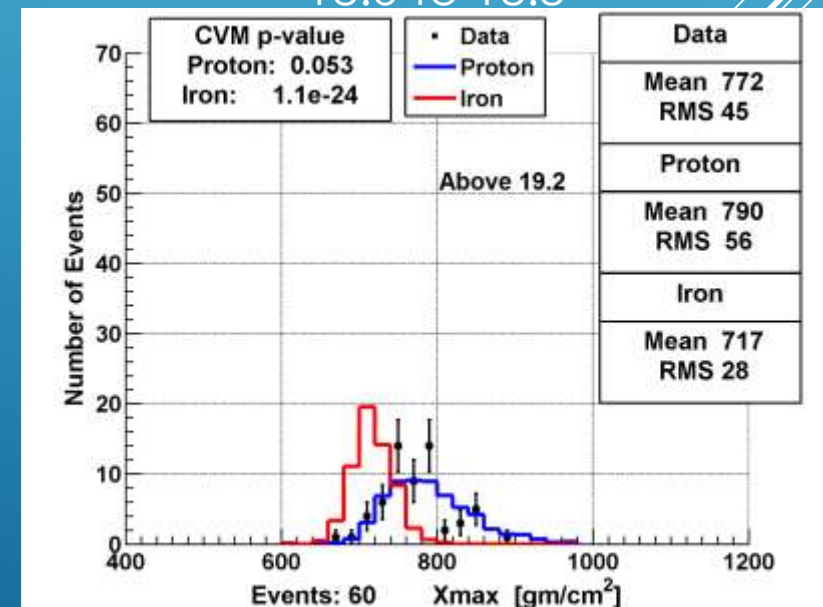
18.6 to 18.8



18.8 to 19



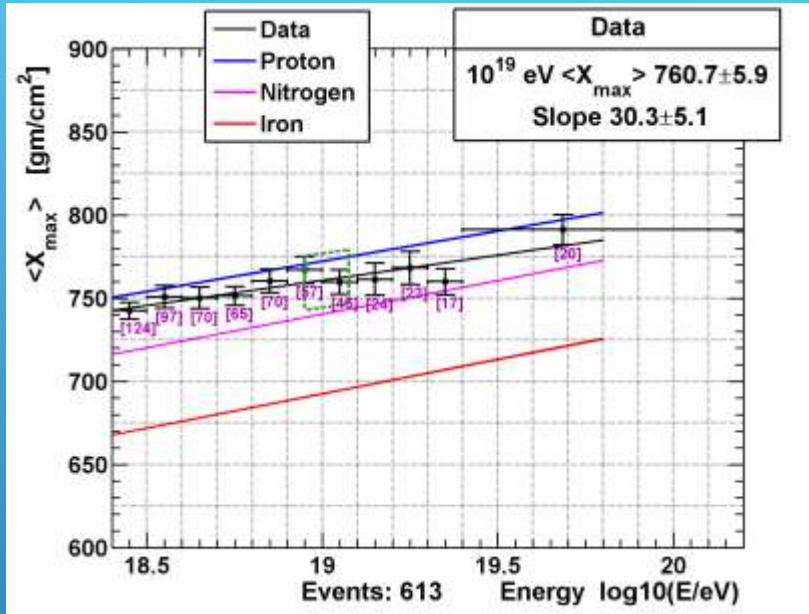
19 to 19.2



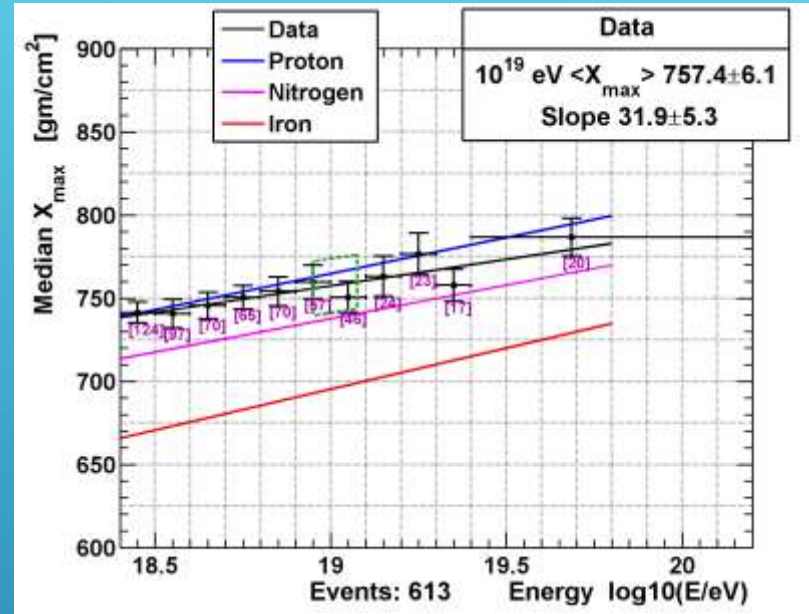
Greater than 19.2

MOMENTS

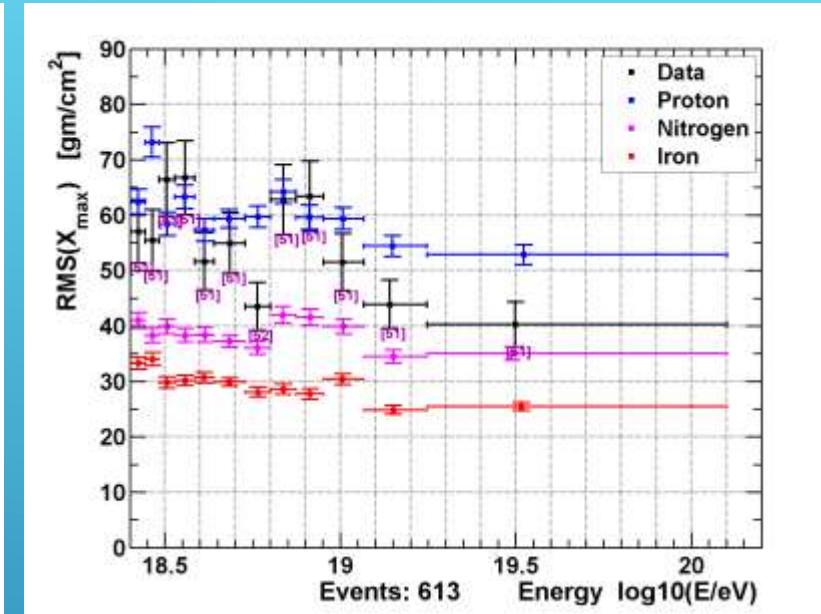
QGSJETII-03



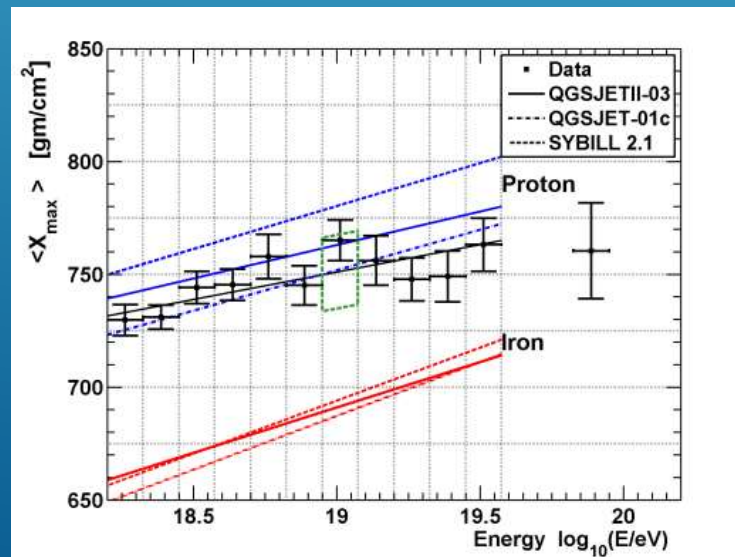
Mean



Median



RMS



Various models

COMPOSITION WITHOUT $\langle X_{max} \rangle$

A decorative graphic consisting of several parallel white lines of varying thicknesses, extending diagonally from the bottom-left towards the top-right of the slide.

MOTIVATION

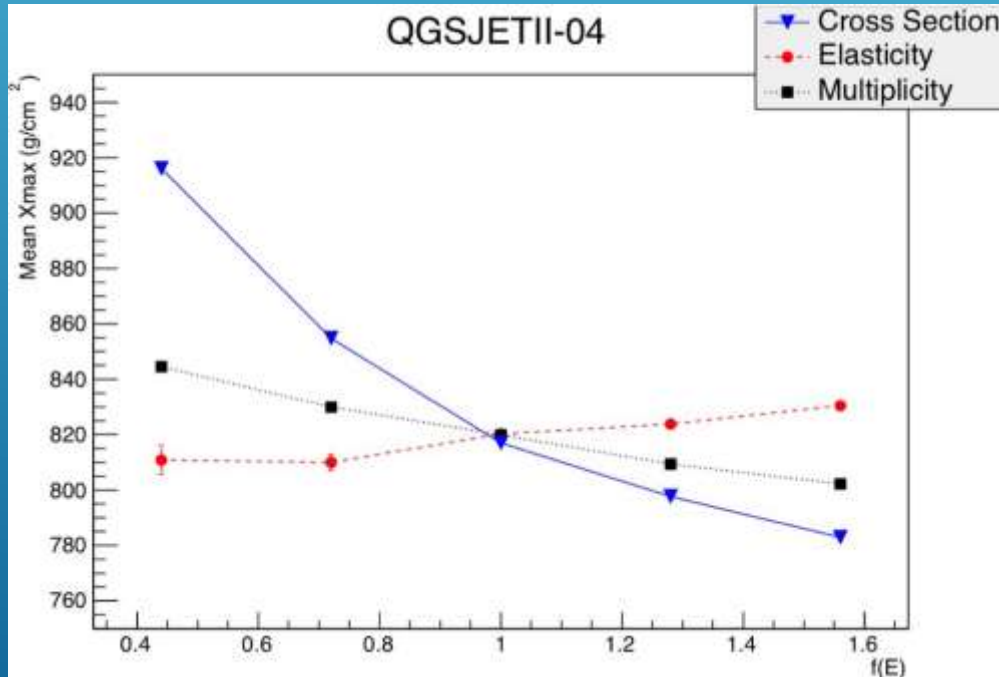
- ▶ Results show *model parameter* uncertainty within a model results in $\langle X_{max} \rangle$ uncertainty as large as difference between models.

Model	$\langle X_{max} \rangle$ uncertainty at 10^{17} eV	$\langle X_{max} \rangle$ uncertainty at $10^{19.5}$ eV
SIBYLL	7 gm/cm ²	36 gm/cm ²
QGSJET01	6 gm/cm ²	32 gm/cm ²
QGSJETII4	6 gm/cm ²	36 gm/cm ²
EPOS-LHC	6 gm/cm ²	36 gm/cm ²

+/- ~15 g/cm²

TABLE I: Results of extrapolations of accelerator measurements.

Abbasi and Thompson



Variation between models: +/- ~15g/cm²

Data uncertainties:

- ~17 g/cm² systematic
- ~5 g/cm² statistical



Combined: ~30 g/cm² (23 without model var.)

Conclusion:

Uncertainties on X_{max} distribution locations complicate the usual statistical inferences about composition

Dependence of $\langle X_{max} \rangle$ on cross section, elasticity, and multiplicity at an energy of $10^{19.5}$ eV.

MOTIVATION

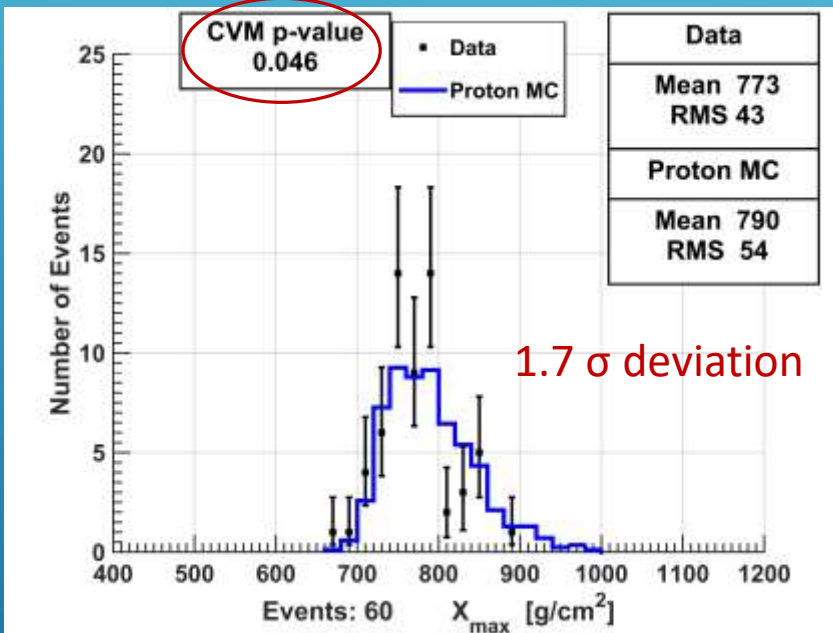
Variation between models: +/- ~15g/cm²

Data uncertainties:

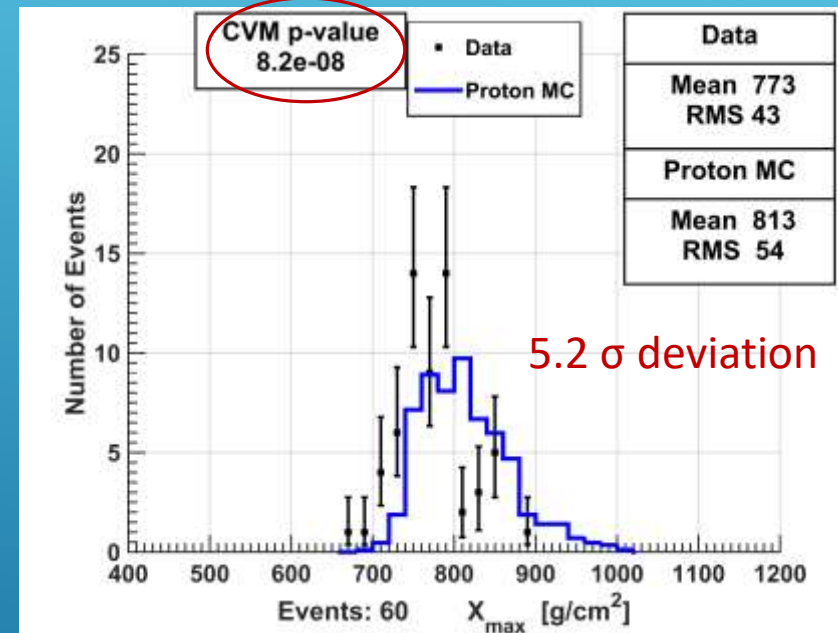
- ~17 g/cm² systematic
- ~5 g/cm² statistical



Combined: ~30 g/cm² (23 without model var.)



7 year data, QGSJETII-03 proton
No shift



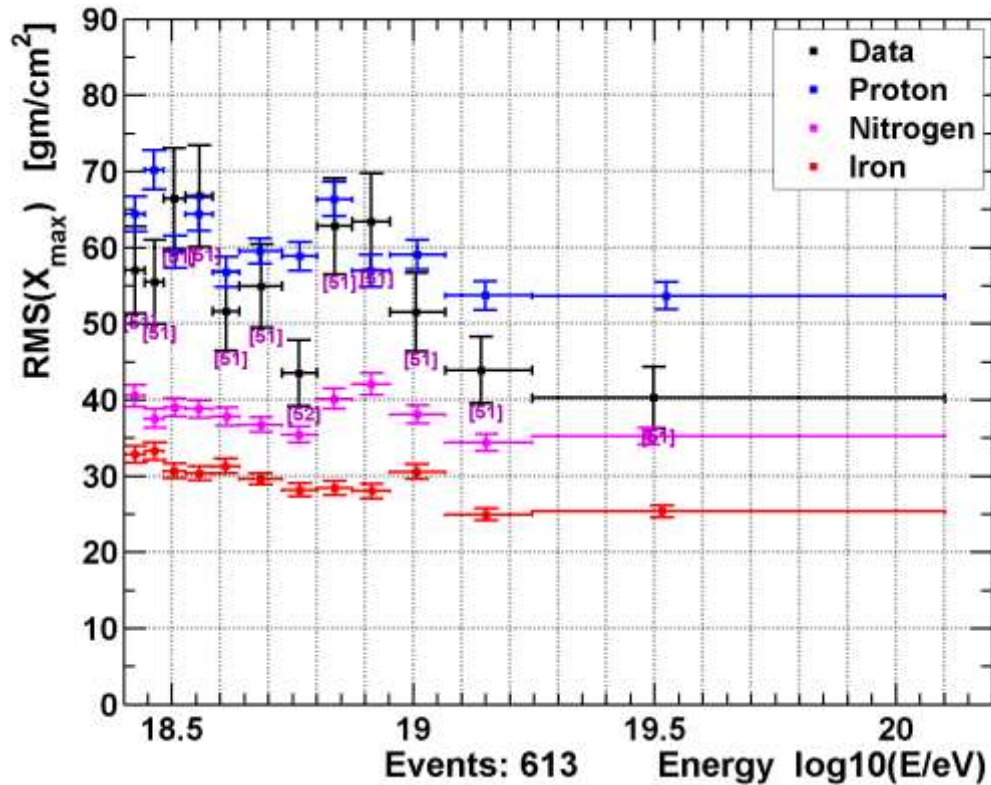
7 year data, QGSJETII-03 proton
+23 g/cm² to MC

Conclusion:

Uncertainties on X_{max} distribution locations complicate the usual statistical inferences about composition

VARIANCE - NARROWING

Compare data to models



- $RMS(X_{max})$ of data and QGSJETII-03
 - Sampling issue or actual change?

- Question: Significantly different variance?

$$H_0: \sigma_1^2 = \sigma_2^2$$

$$H_a: \sigma_i^2 \neq \sigma_j^2$$

- Method: O'Brien's Test for Homogeneity of Variance

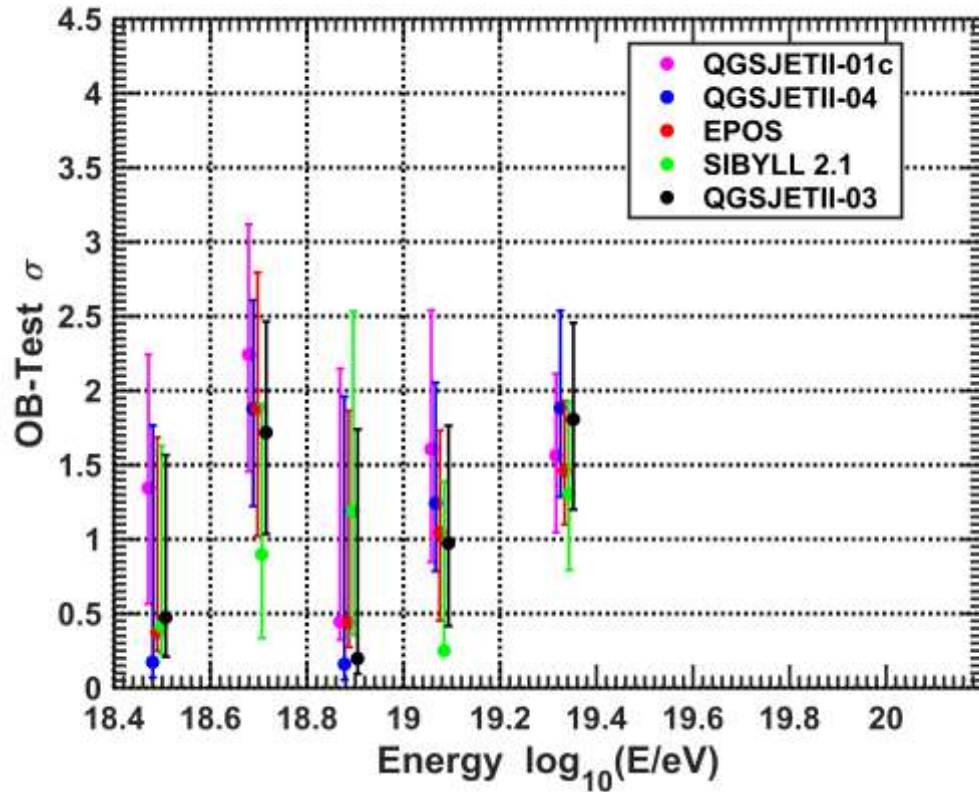
$$W = \frac{(N - k) \sum_{i=1}^k N_i (\bar{Z}_i - \bar{Z}_{..})^2}{(k - 1) \sum_{i=1}^k \sum_{j=1}^{N_i} (Z_{ij} - \bar{Z}_i)^2},$$

$$Z_{ij} = \frac{N_i(N_i - 1.5)(y_{ij} - \bar{y}_i)^2 - 0.5\sigma_i^2(N_i - 1)}{(N_i - 1)(N_i - 2)}$$

P-value is calculated from $F_{k-1, N-k}$ the F distribution with $k-1$ and $N-k$ degrees of freedom.

VARIANCE - NARROWING

Compare data to models



- Significance of p-value that variance is the same
 - All models are in good agreement
 - No evidence for “narrowing” or change in composition
 - Statistically compatible with pure proton for any model at any energy

Compare data to data: test if $\sigma_1^2 = \sigma_2^2 = \dots = \sigma_5^2$ for the 5 energy bins of data
Result: Significance of deviation is **0.97σ or 33%** probability they are the same.
Again, no statistical evidence for narrowed distribution

MOMENTS ≥ 2

Developed for this thesis work

- Question: Do two samples belong to the same location-family distribution?

H_0 : $G(x)$ is sample CDF from $F(z-a)$ & $H(y)$ is sample CDF from $F(z-b)$, for any a and b
($x \in G(x) \sim F(z-a)$ & $y \in H(y) \sim F(z-b)$)

- Method: **L-test**. This is a more stringent test.

$$L = \log \left\{ \min_{a \leq s \leq b} \frac{N_1 N_2}{(N_1 + N_2)^2} \sum_{k=1}^{N_1 + N_2} [\hat{H}(s)_k - \hat{G}(s)_k]^2 \right\},$$

$$\hat{F}(s)_k = \frac{1}{N_1} \sum_{j=1}^{N_1} I[(x_j - s) \leq z(s)_k], \quad \hat{G}(s)_k = \frac{1}{N_2} \sum_{j=1}^{N_2} I[y_j \leq z(s)_k], \quad z(s) = (x - s, y)$$

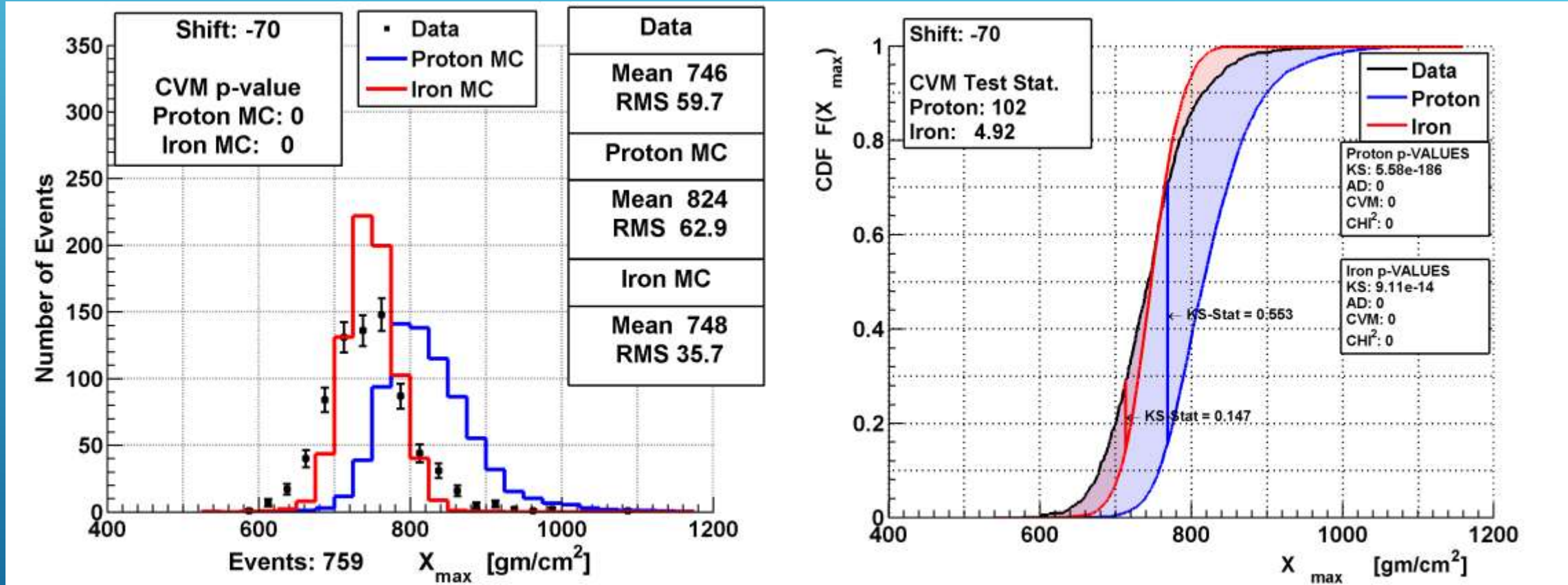
In words:

Log of the minimum, by shifting, of the sum difference squared of two empirical CDF's

Distribution of L is the Generalized Maximum Likelihood distribution

MOMENTS ≥ 2

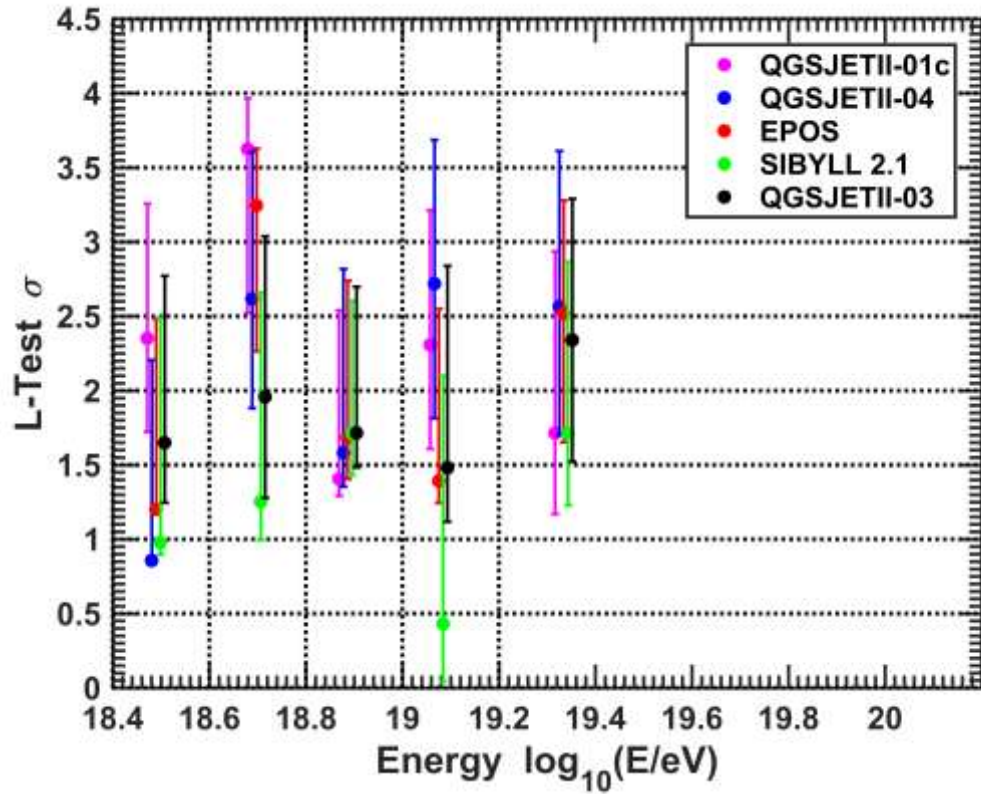
Tight geometry cuts and all energies



QGSJETII-03 distribution histograms and CDF's shifted for best agreements

MOMENTS ≥ 2

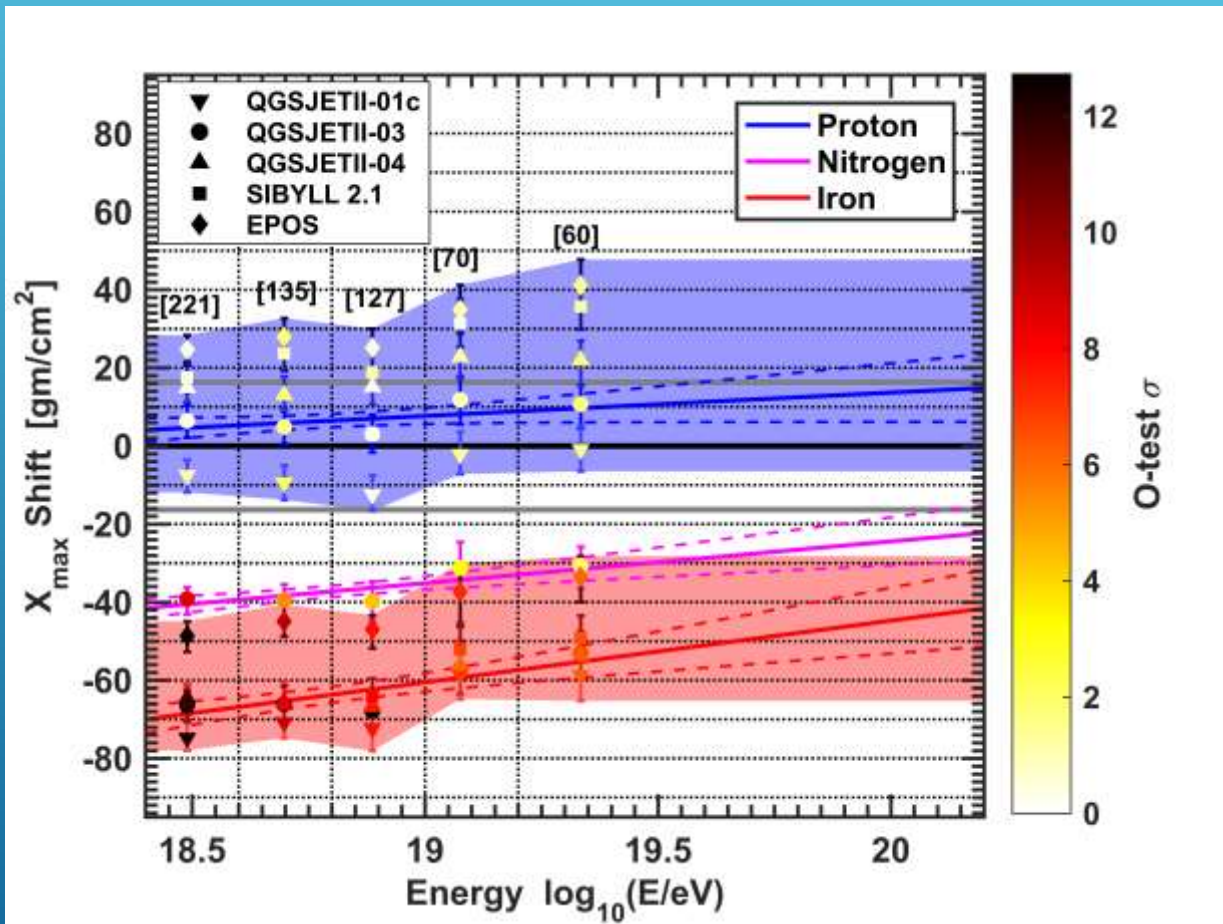
Compare data to models



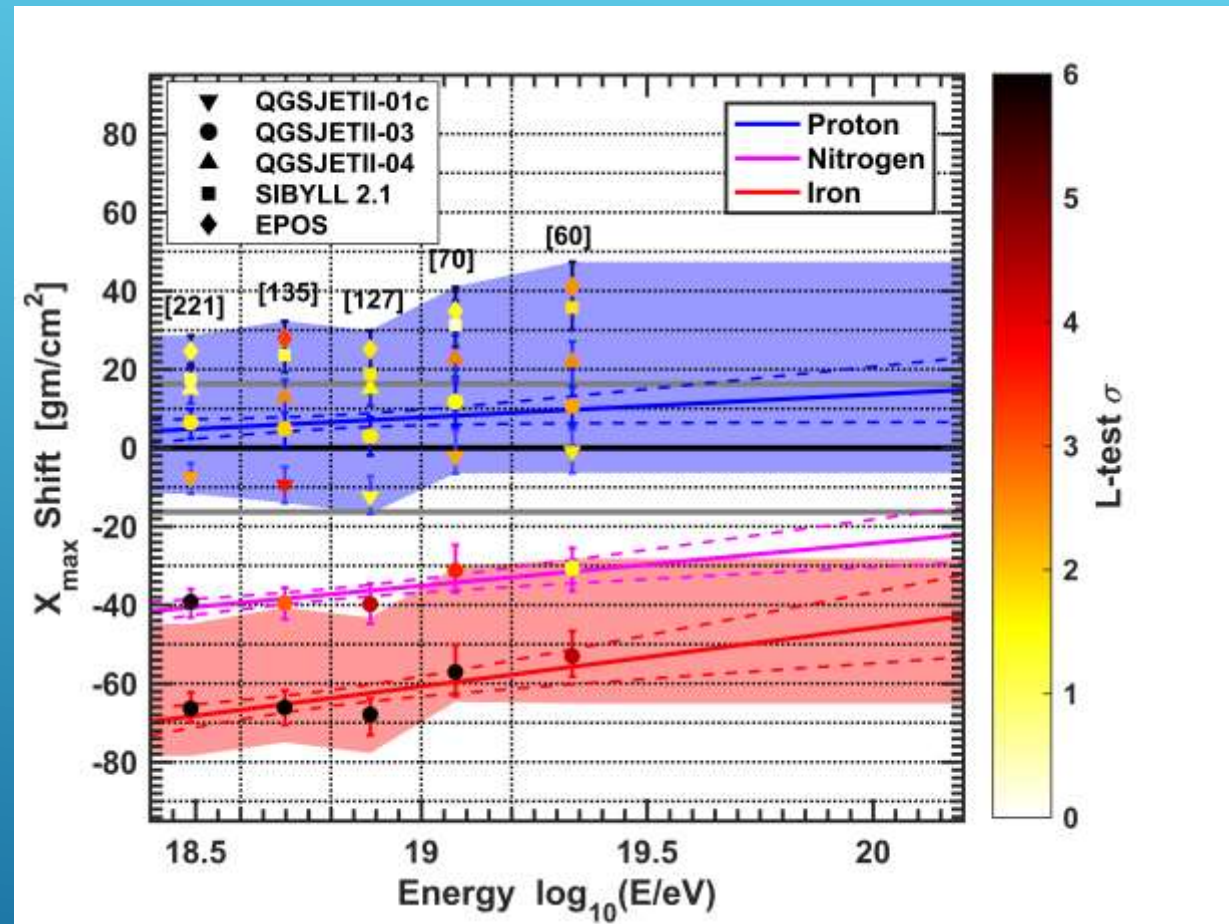
- Significance of p-value that distributions are location family related
 - All models are in good agreement
 - No evidence for “narrowing” or change in composition
 - Statistically compatible with pure proton for any model at any energy

SHIFT PLOT

Shift plot using L-test by combining robust measure of bias and location family test



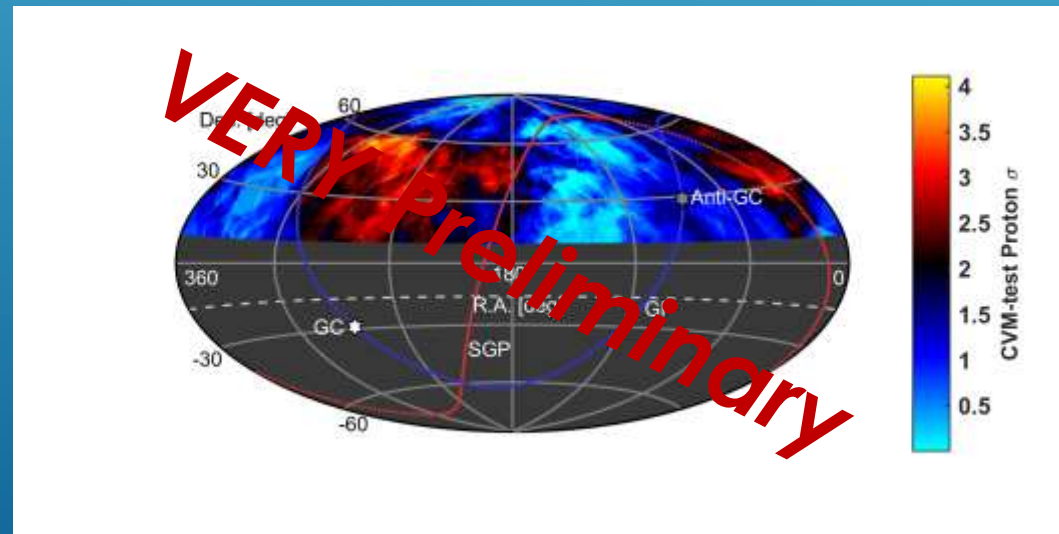
L-test shifts with O'Brien's σ



L-test shifts with L-test σ
(stopped calculating at 6σ)

COMPOSITION CONCLUSIONS

- Statistical tests using distribution locations are inconclusive:
 - Stat. error, sys. error, model parameter uncertainty, model variation
- Higher moments agree between all models
 - *Data is statistically compatible with pure proton, at all energies, for all models*
 - Not compatible with iron.
- Significance of data being “narrowed” in RMS is 0.97σ .



Next to do?
Composition
Anisotropy
Using L-test?

THESIS CONCLUSIONS

- Hot/Coldspot Event Density Asymmetry Observed with **5.4 σ** significance
 - Energy Spectrum Anisotropy with **3.74 σ**
 - Energy-Distance Correlation Anisotropy with **3.4 σ**
 - *Suggests magnetic deflection of source by possible supergalactic fields*
- Higher moments of Xmax distributions agree between all models
 - *Data is statistically compatible with pure proton, at all energies, for all models*
 - Not compatible with iron.
- Significance of data being “narrowed” in RMS is **0.97 σ** .

$$E < \frac{E_{max}}{10^{18} \text{ eV}} \cong \frac{1}{2} \beta \cdot Z \cdot \frac{B}{\mu G} \cdot \frac{L}{kpc}$$



This information should be useful for informing future models of magnetic fields and sources

$$\delta = \frac{s}{R_{Larmor}} = 0.5^\circ Z \frac{L}{kpc} \frac{B}{\mu G} \frac{10^{20}}{E}$$

***Kernel Density Estimation Hotspot: 3.65 σ**

PART ONE
ADDITIONAL MATERIAL



SIMULATION - LONGITUDINAL

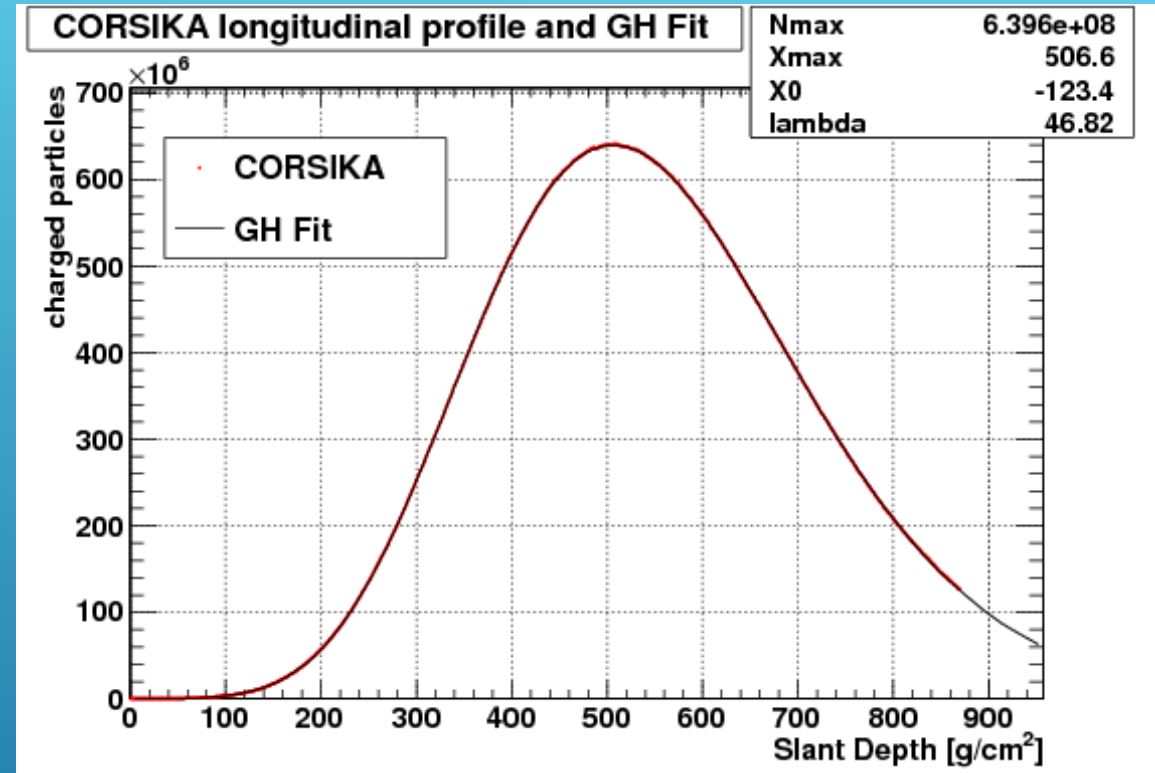


CORSIKA Simulated Air Shower 10^{15} eV 45° inclination

Red – $e^{+/-}, \gamma$

Green – $\mu^{+/-}$

Blue – Hadrons ($\pi^{0/+/-}, K^{0/+/-}, p, n$)



Gaisser-Hillas Parameterization

$$N(X) = N_{\max} \left(\frac{X - X_0}{X_{\max} - X_0} \right)^{\frac{X_{\max} - X_0}{\lambda}} \exp\left(-\frac{X_{\max} - X}{\lambda} \right)$$

- Match fit to real event data.

SIMULATION - LATERAL

Largely from coulomb multiple scattering of electrons

Nishimura-Kamata-Geisen (NKG) formula.

Lateral density of electrons as function of shower age

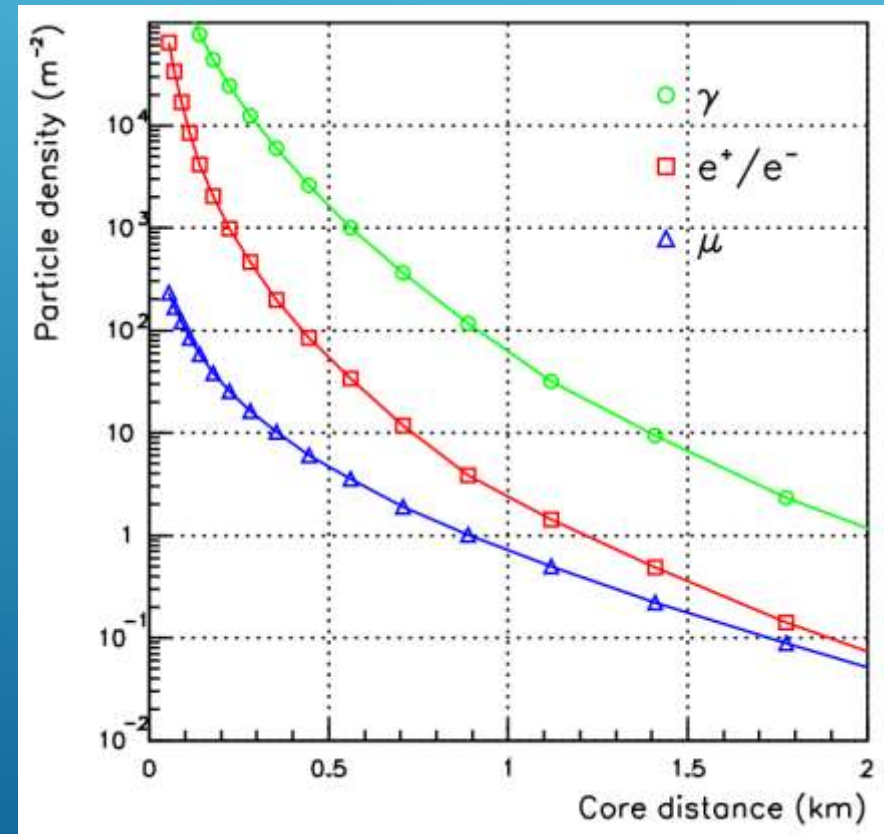
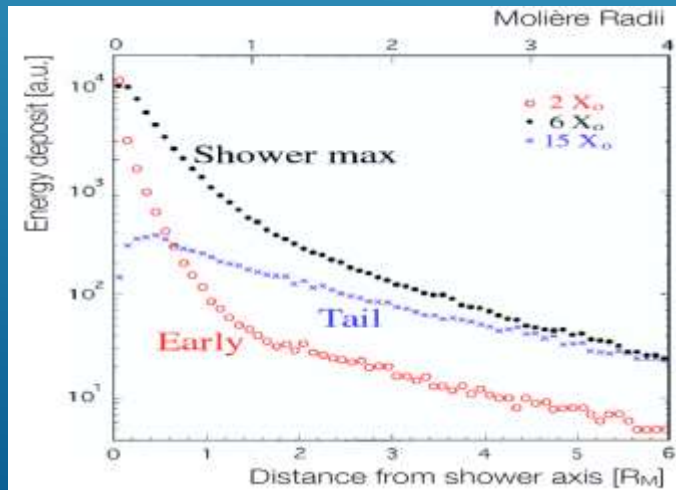
$$\rho(r) = \frac{N}{r^2} f\left(s, \frac{r}{r_M}\right)$$

$$f\left(s, \frac{r}{r_M}\right) = \left(\frac{r}{r_M}\right)^{s-2} \left(1 + \frac{r}{r_M}\right)^{s-4.5} \frac{\Gamma(4.5 - s)}{2\pi\Gamma(s)\Gamma(4.5 - 2s)}$$

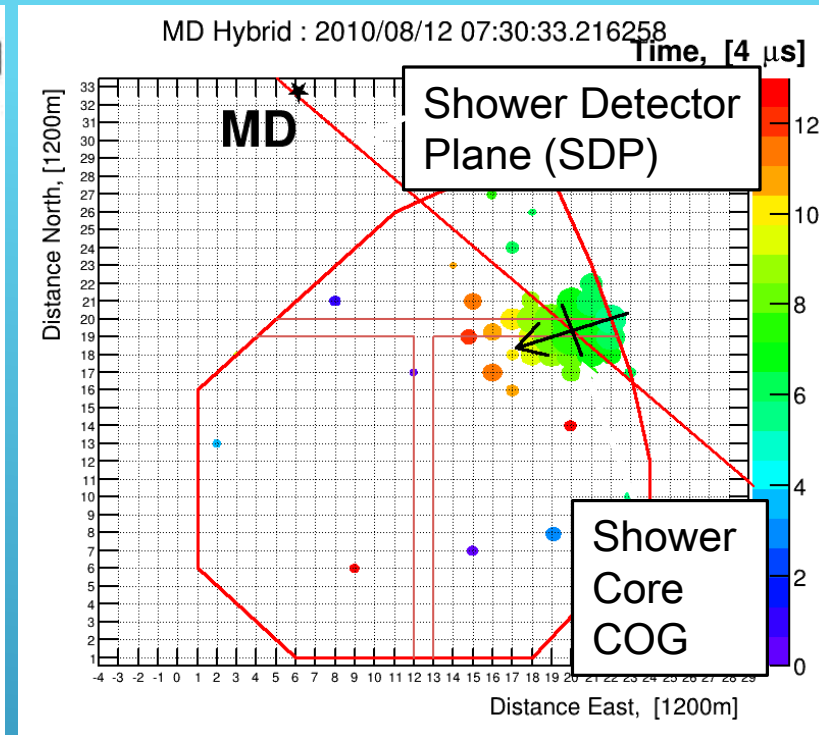
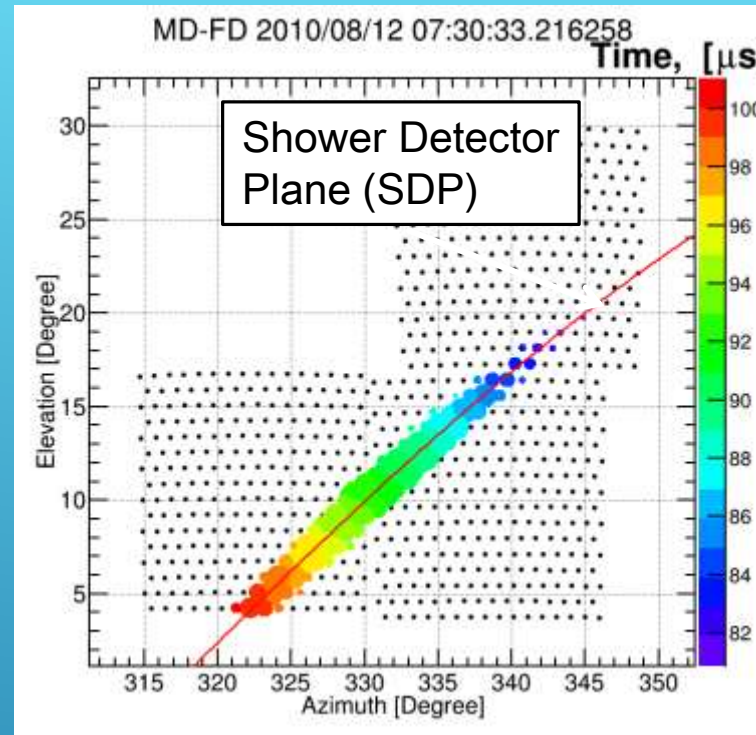
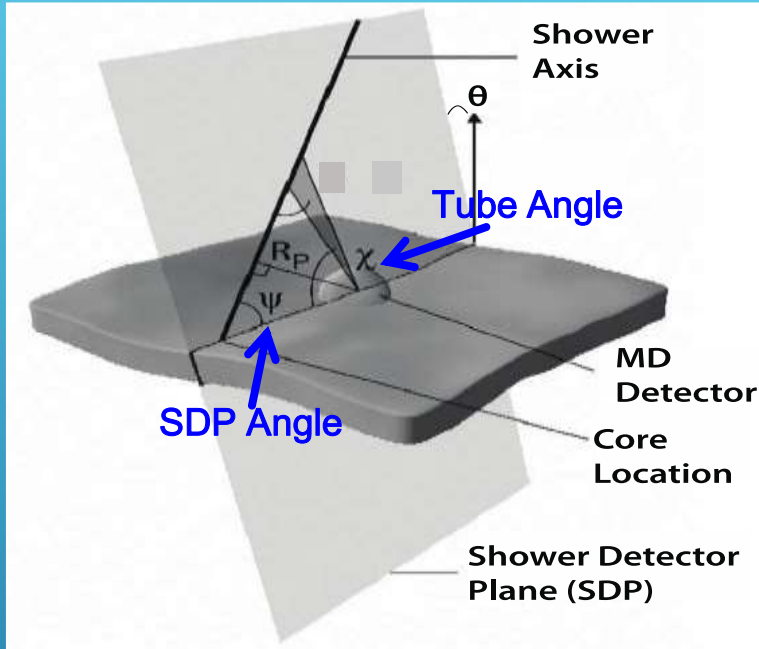
$$s = \frac{3X}{2X + X_{max}}$$

Shower Age: 1 is Xmax

$$R_M = \frac{21 \text{ MeV}}{E_c} \lambda \approx 9 \text{ gm/cm}^2 \quad \text{Moliere radius}$$



RECONSTRUCTION



First find SDP: $\chi^2 = \sum_i \frac{(\hat{n} \cdot \hat{n}_i)^2 \cdot w_i}{\sigma_i^2}$

Labels: SDP Normal (points to \hat{n}), Tube Direction (points to \hat{n}_i), Charge SD Virtual Tube Timing (points to w_i)

$$t_{SD} = t_{SD_{Trig}} + \frac{SD_{Dist}}{c}$$

Timing to Minimize:

$$t_i = T_{Rp} + \frac{R_P}{c} \tan \left(\frac{\pi - \psi - \chi_i}{2} \right)$$

Chi-Square Minimization of Parameters: $\psi, \theta, R_P, R_x, R_y$

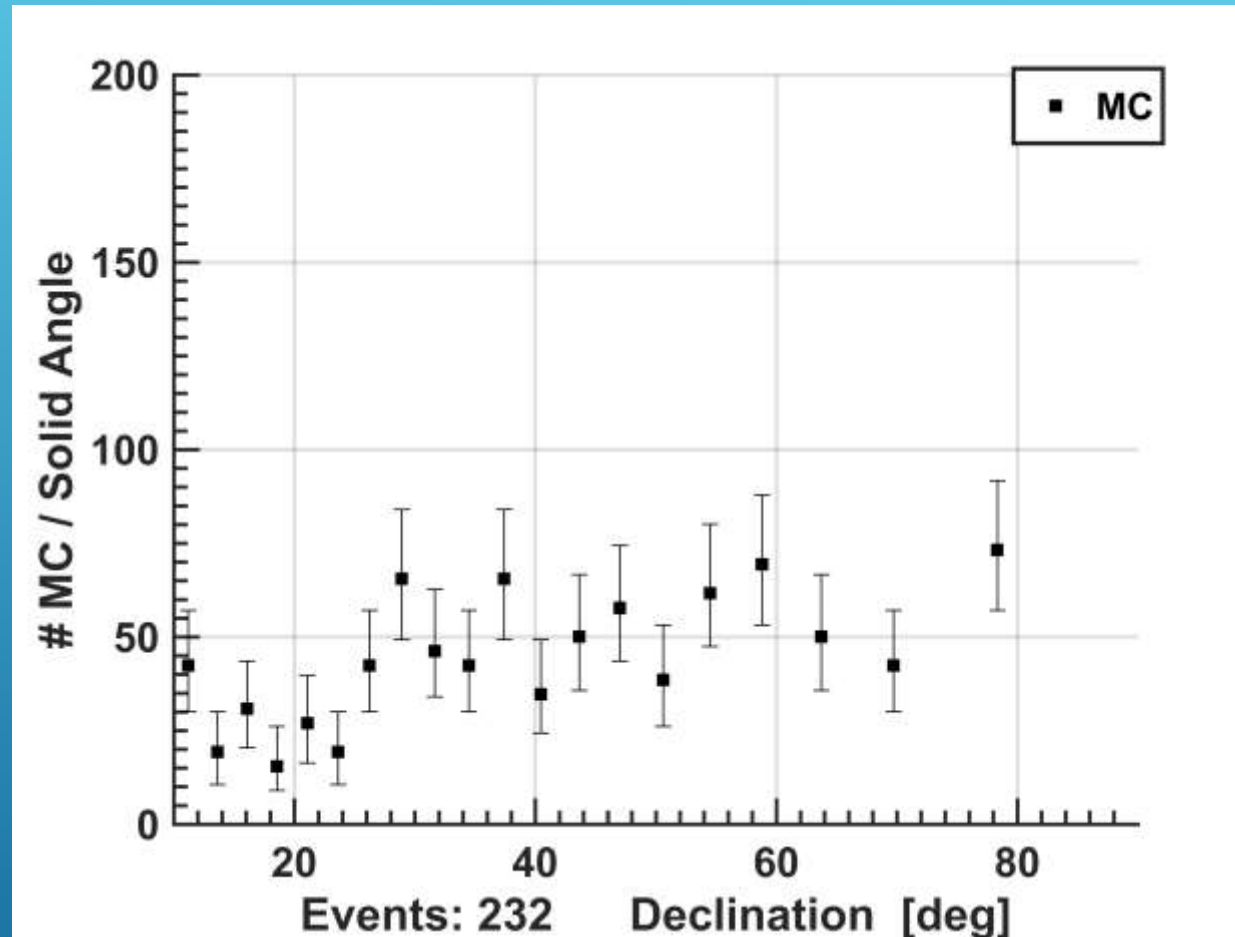
$$\chi^2 = \chi_{MD_{Timing}}^2 + \chi_{SD_{Timing}}^2 + \chi_{SD_{Core}}^2$$

$$\chi_{Core}^2 = \sum_1^2 \frac{\|\mathbf{R}_i - \mathbf{R}_{COG}\|^2}{\sigma_{\mathbf{R}_{COG}}^2}$$

ENERGY SPECTRUM ANISOTROPY ADDITIONAL MATERIAL

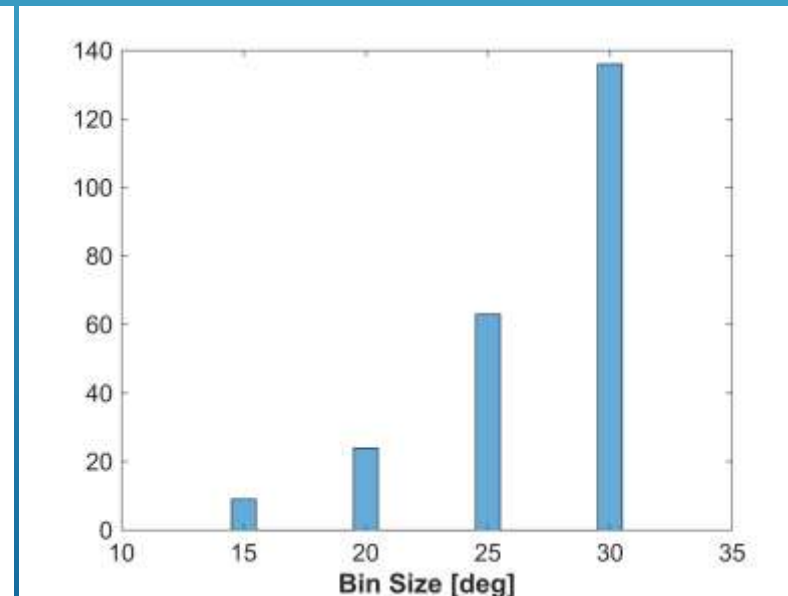
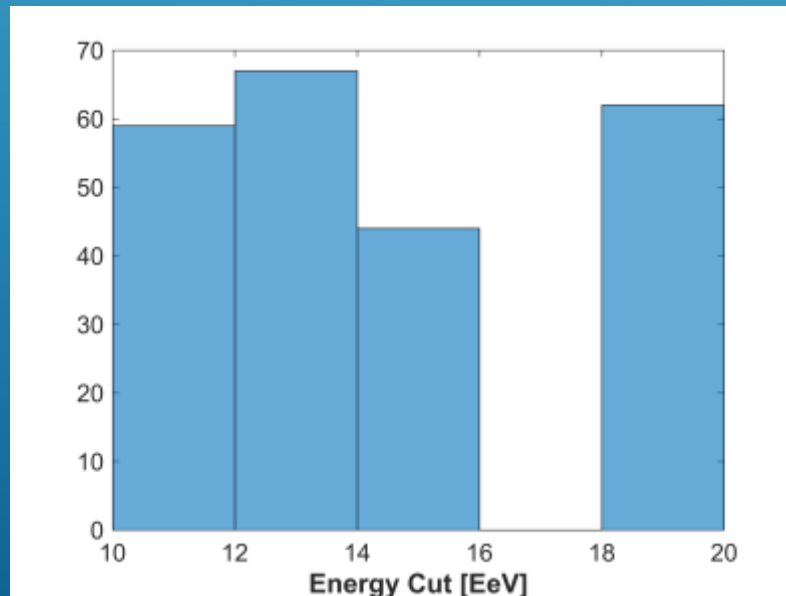
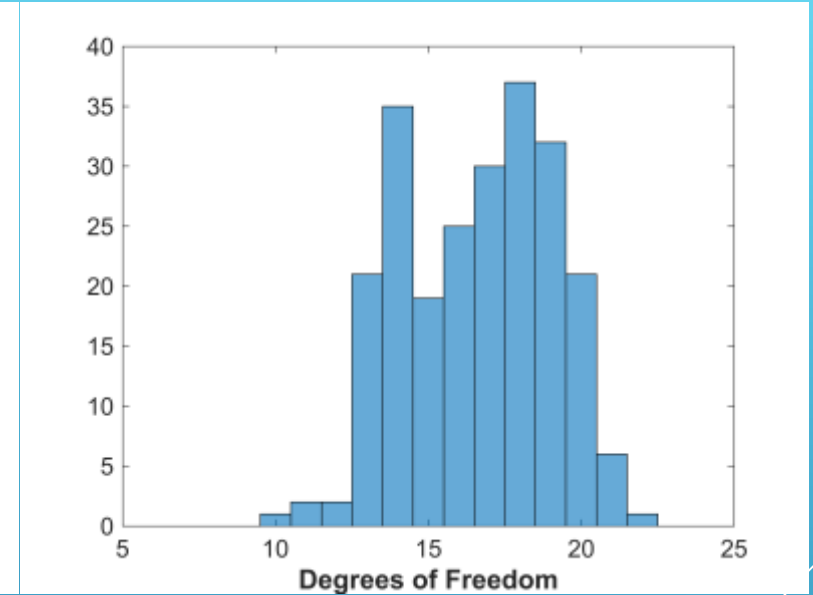
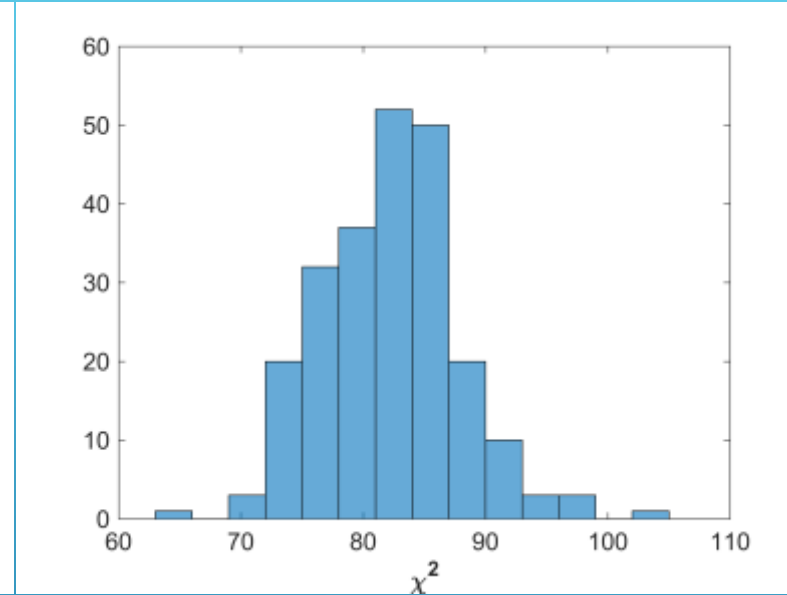
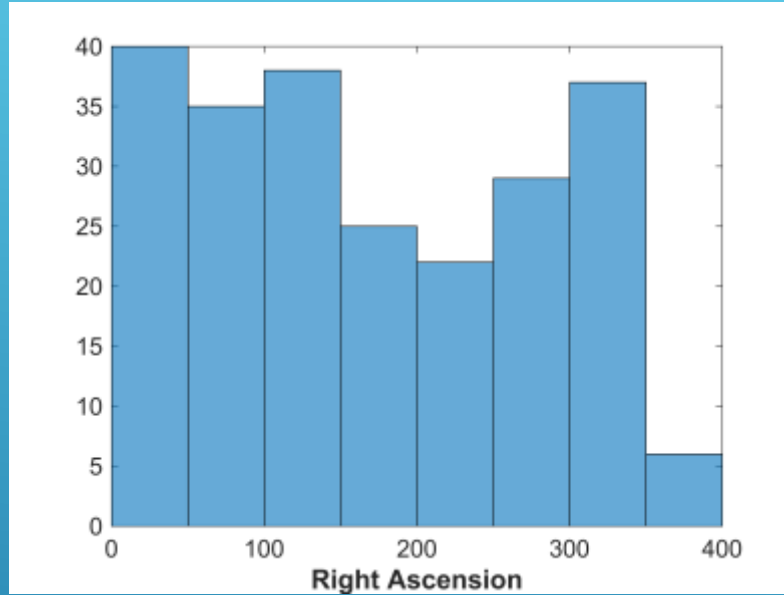


MC DISTRIBUTION OF HITS



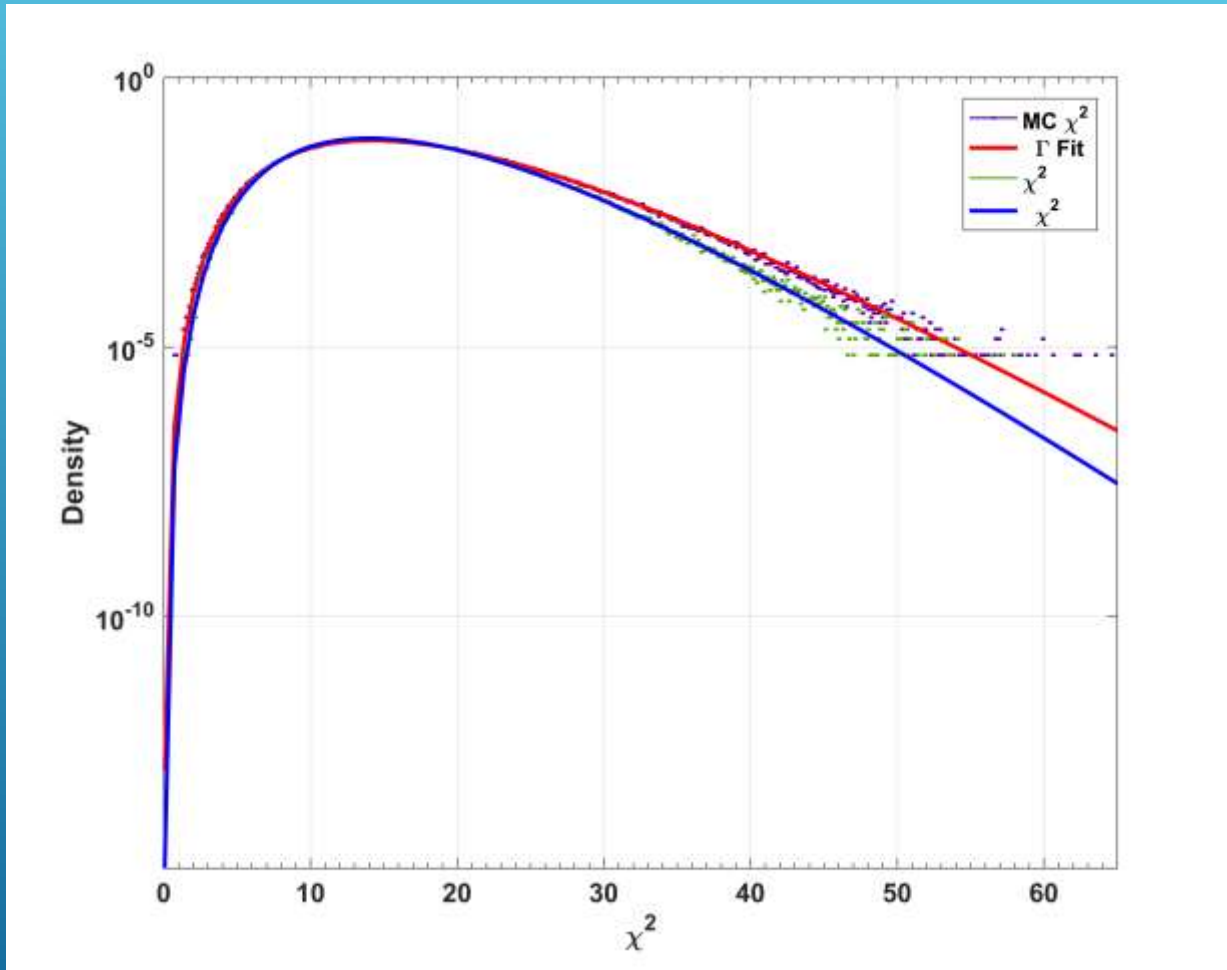
Shows small amount of declination bias in the analysis

MC DISTRIBUTION OF HITS



MC CHI² DISTRIBUTION AT DATA MAX SIGMA POINT

138.8 R.A. 44.8 Dec.
19.2 energy cut
30 deg binning



“Chi square” distribution of MC sets

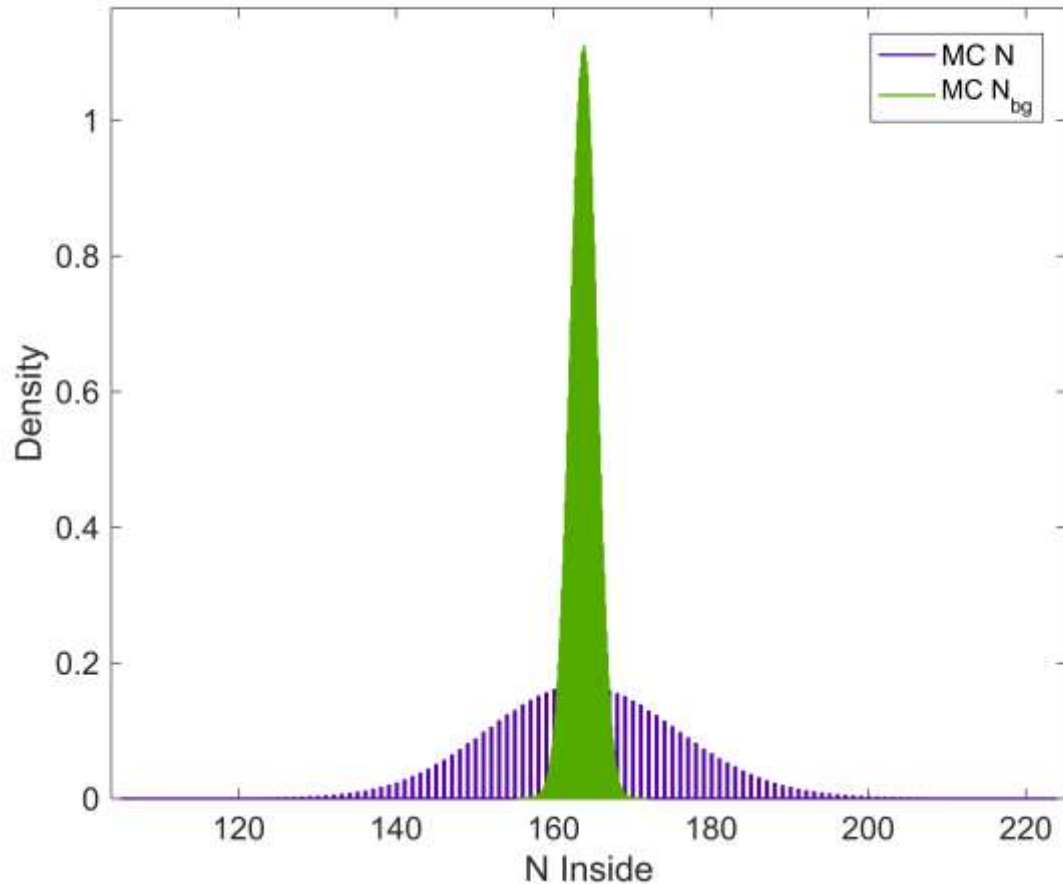
Data chi square: 78.3 for 14 energy bins

- There are two additional degrees of freedom:
 - Background Fluctuation
 - Rebinning

MC sets with 14 energy bins
Closest to chi² with 16 degrees of freedom

MC DISTRIBUTIONS AT DATA MAX SIGMA POINT

138.8 R.A. 44.8 Dec.
19.2 energy cut
30 deg binning



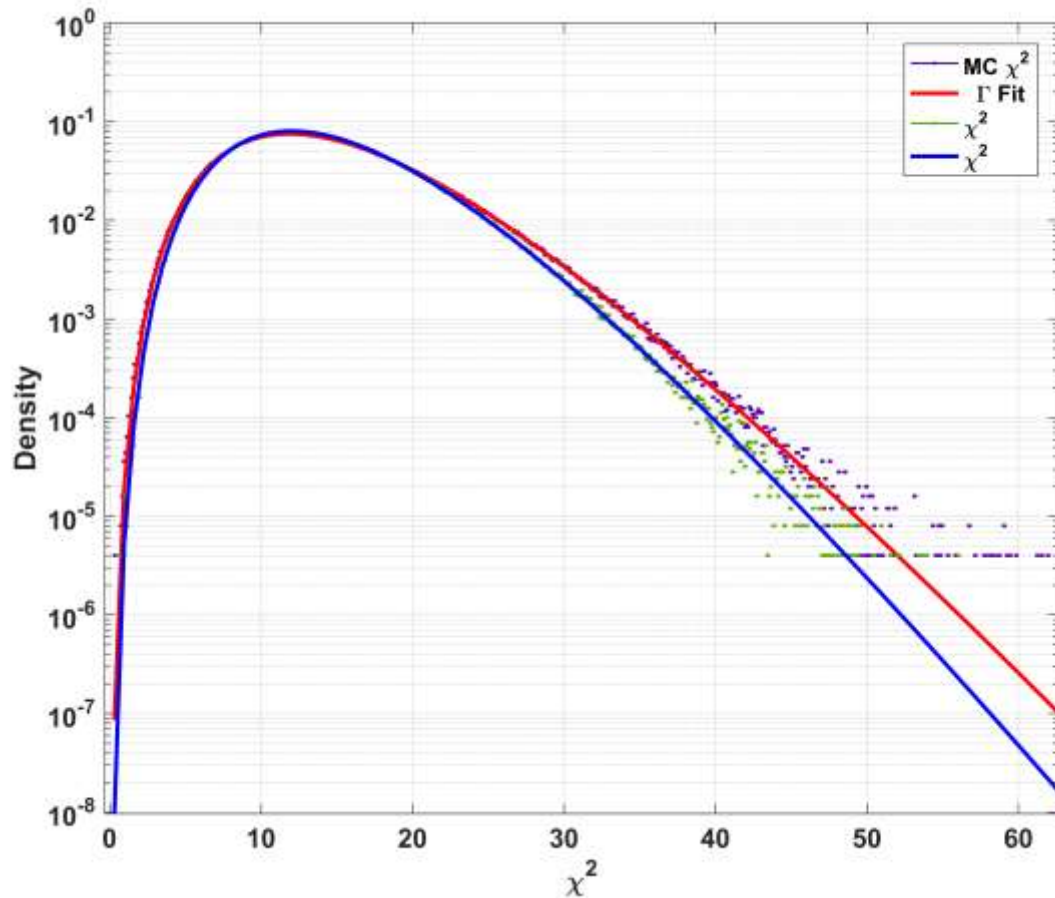
MC N inside is Poisson: 163.8 ± 12.0
($\sqrt{163.8} = 12.8$)

MC N_{bg} background is not Poisson: 163.8 ± 1.7
Fluctuation is $\sqrt{N} \cdot 0.14$ exposure ratio exactly

*This is the same background fluctuation
Li-Ma uses*

MC CHI² DISTRIBUTION AT DATA MAX SIGMA POINT

138.8 R.A. 44.8 Dec.
19.2 energy cut
30 deg binning

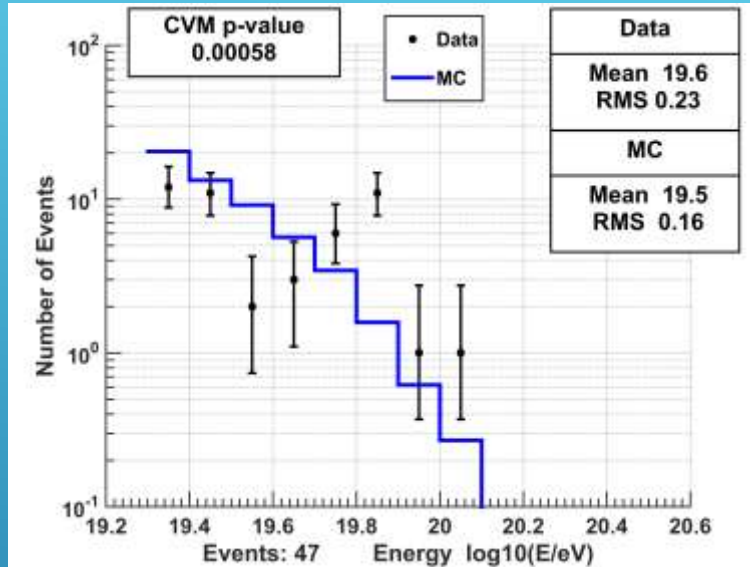


“Chi square” distribution of MC sets
with no background fluctuation or rebinning

547 MC have infinite chi² due to no rebinning

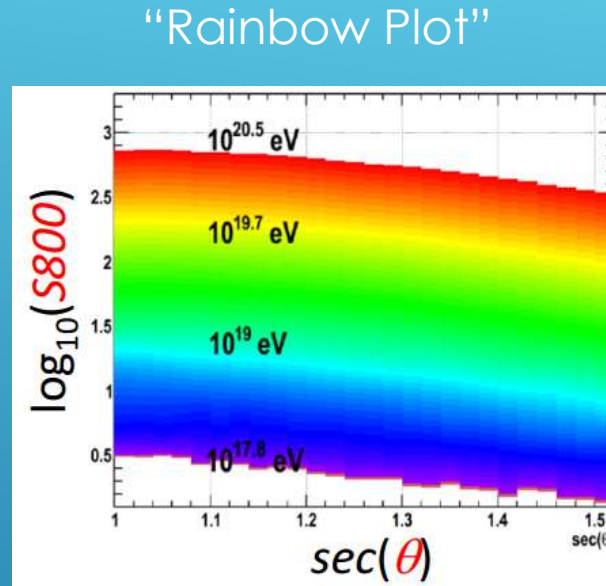
MC sets with 14 energy bins
Closest to chi² with 14 degrees of freedom

ENERGY SYSTEMATICS – INSIDE VS OUTSIDE

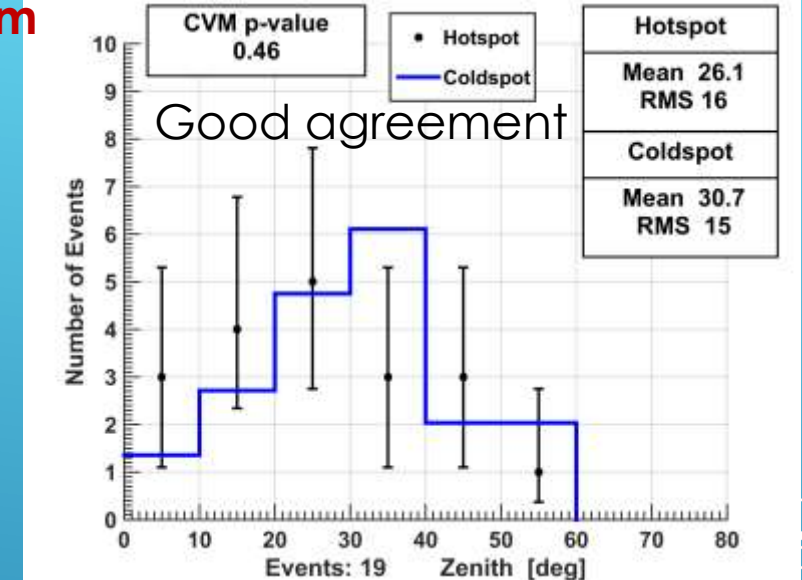


Data Vs MC comparison
(normalized to data/MC outside spot)
3.44 σ different.

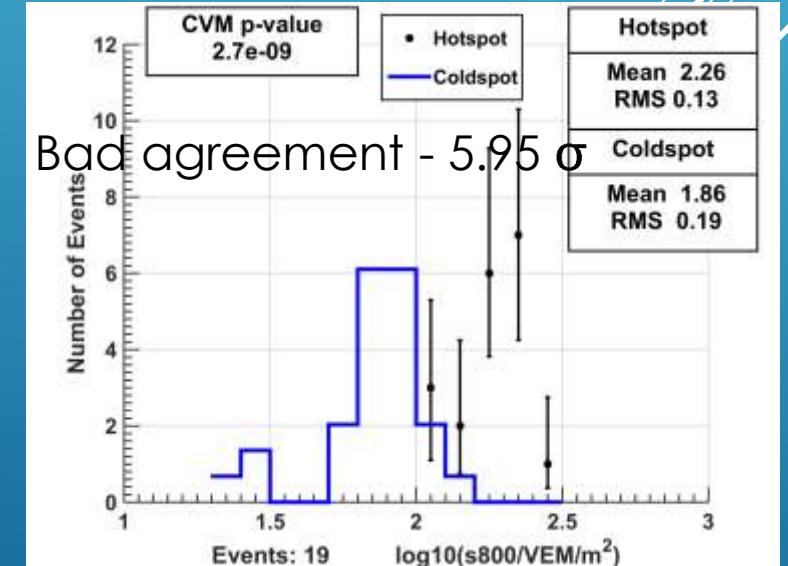
At location of Li-Ma hot/cold maximum



Data Vs Data comparison



Coldspot events normalized to hotspot



Data Vs Data comparison

Could systematics cause events to migrate from Coldspot to Hotspot?

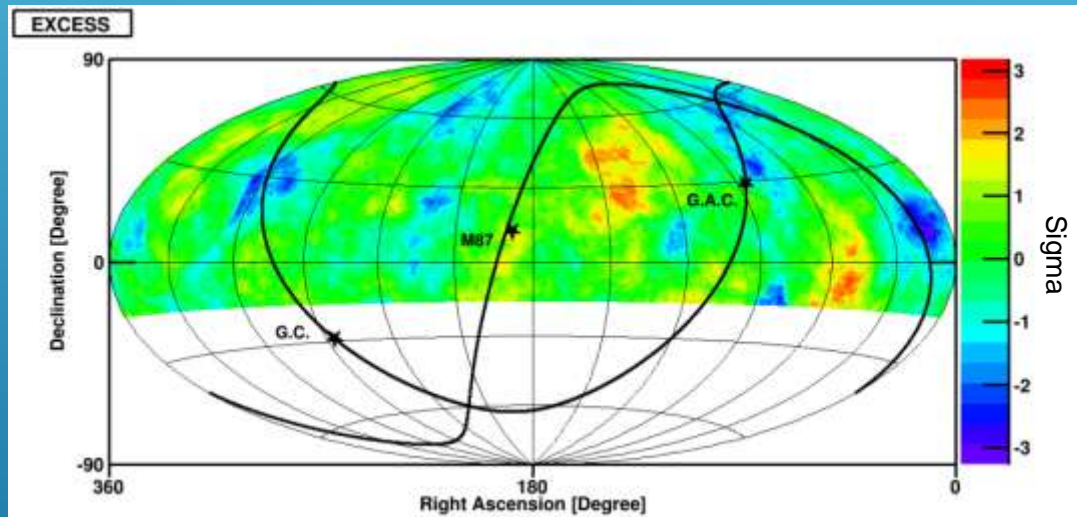
Energy is reconstructed by Zenith angle and s800 signal

- Zenith agrees very well. Systematic must come from s800
- **s800 would have to be increased by 139% for hotspot to be systematic from the coldspot**

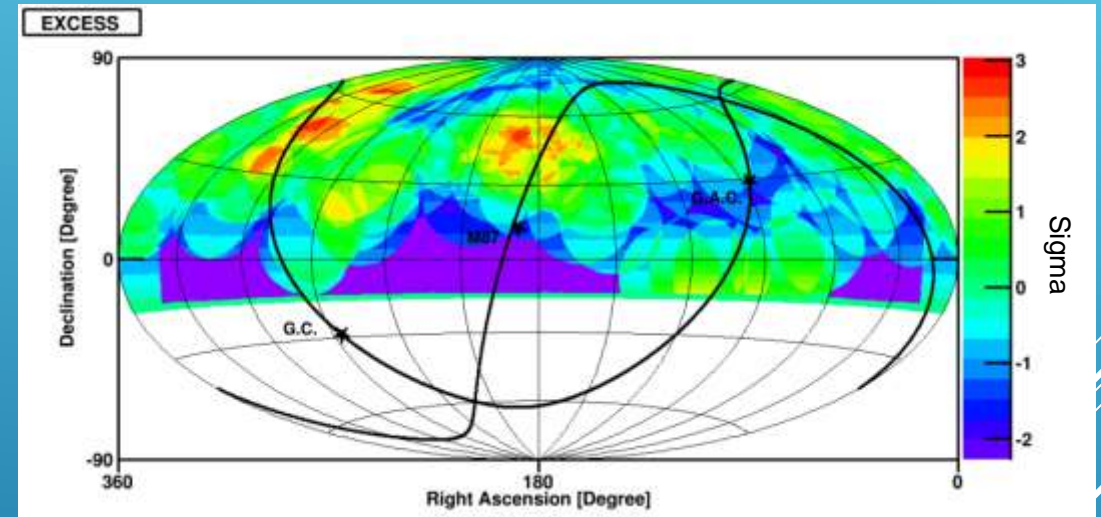
$E \geq 57$ EeV events: ~ 14 over N_{bg} or $3.6N_{bg}$
 $20 \leq E < 57$ EeV events: ~ 21 under N_{bg} or $0.57N_{bg}$

OTHER SYSTEMATIC CHECKS

- Seasonal and hourly energy corrections result in little change to joint significance
- Anti-Sidereal time results in no significant excesses, deficits or combinations

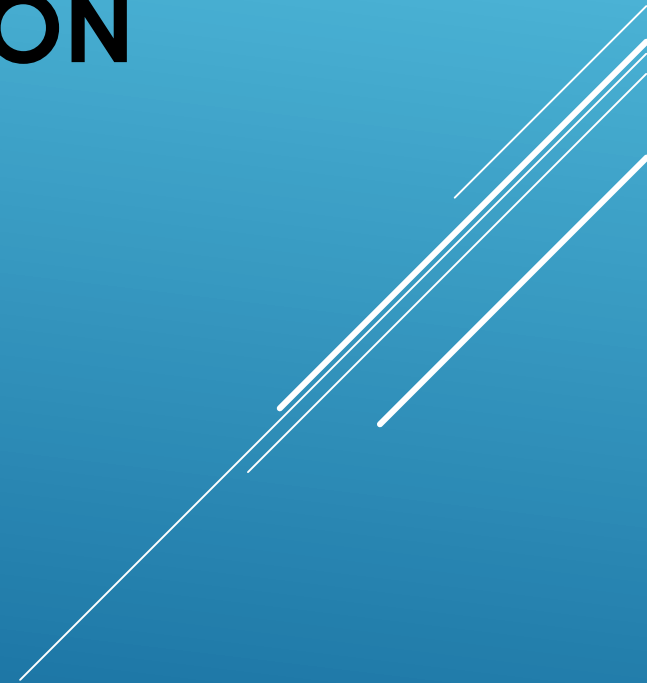


$20 \leq E < 57$ EeV Anti-Sidereal



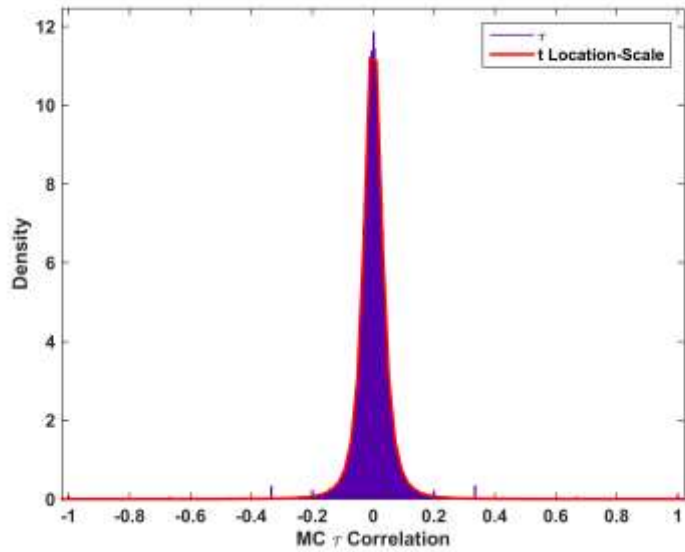
$E \geq 57$ EeV Anti-Sidereal

ENERGY-DISTANCE CORRELATION ADDITIONAL MATERIAL

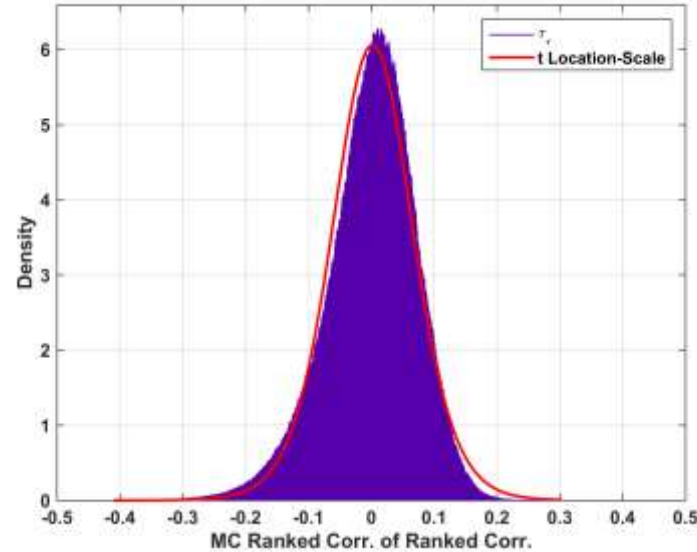


CHECK FOR GOOD BEHAVIOR

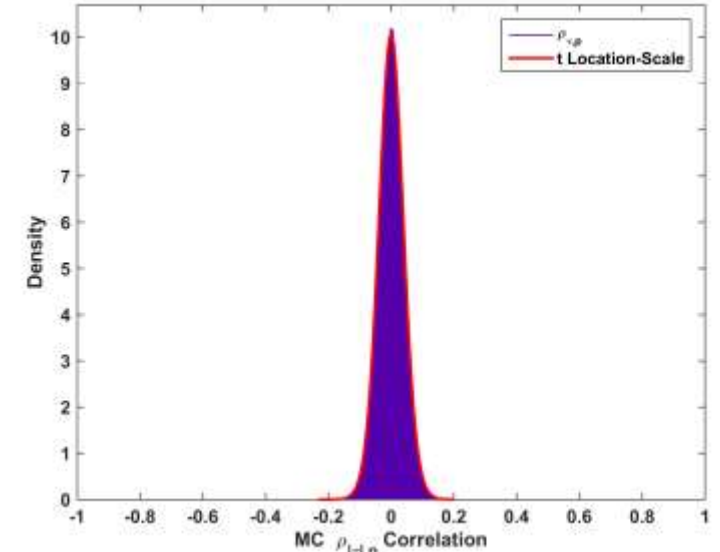
- Correlation coefficients follow the t Location-Scale distribution
 - Literature states correlations of correlations should have a wider distribution
- p -values should be Uniform (Null – single correlation)
or a Beta distribution (prior information – second correlation)



Ranked correlation τ
Fits well



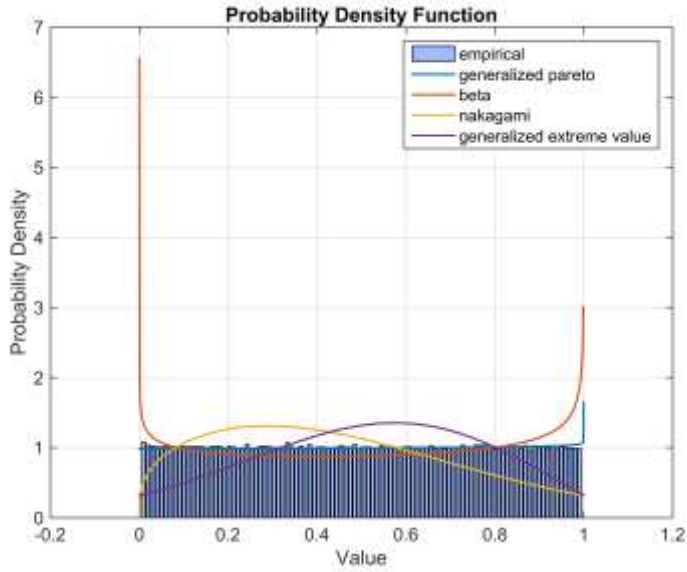
Double Ranked Correlations $\tau_{|\tau|}$
Doesn't behave properly
Not Used



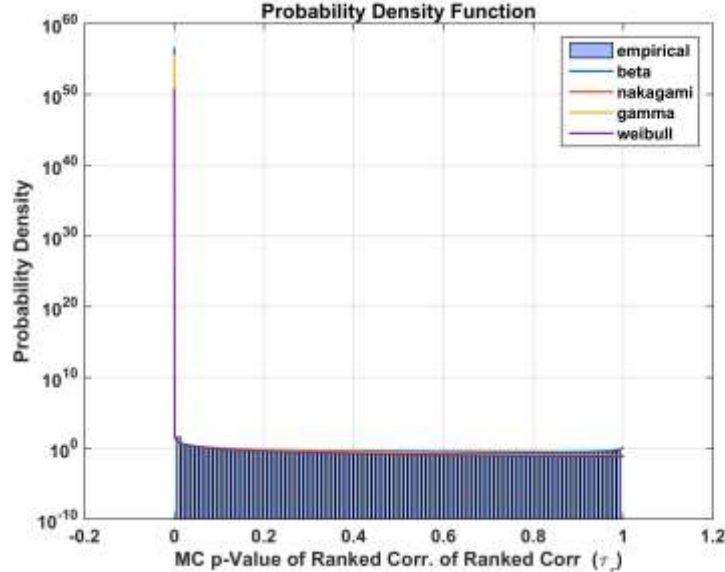
$\rho_{|\tau|,p}$
Fits distribution well
Used for significance test

CHECK FOR GOOD BEHAVIOR

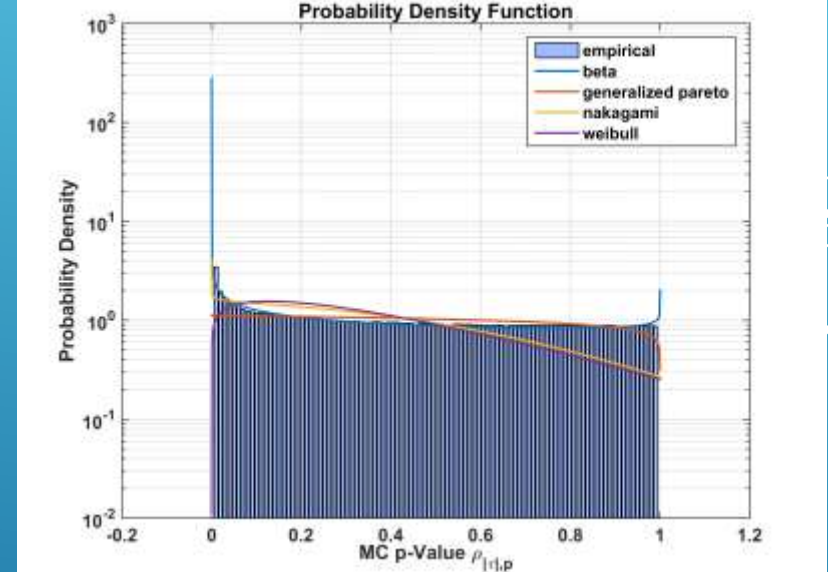
- Correlation coefficients follow the t Location-Scale distribution
 - Literature states correlations of correlations should have a wider distribution
- p-values should be Uniform (Null – single correlation) or a Beta distribution (prior information – second correlation)



Ranked correlation p-Value
Uniform Distribution



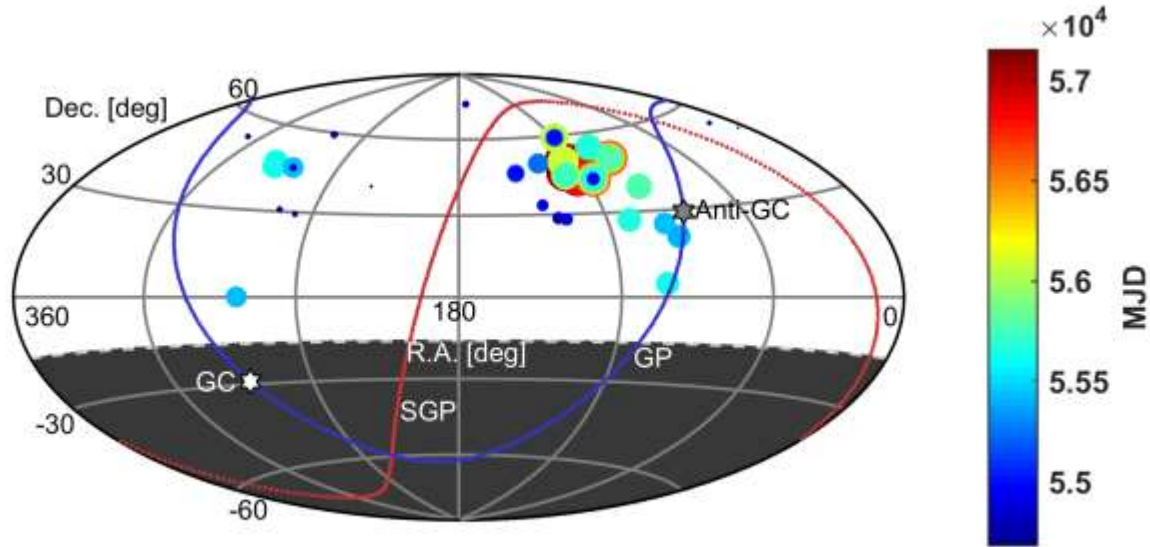
Double Ranked Correlations p-Value
Beta Distribution
Not Used



$\rho_{|\tau|,p}$'s p-Value
Fits Beta Distribution Better
Used for significance test

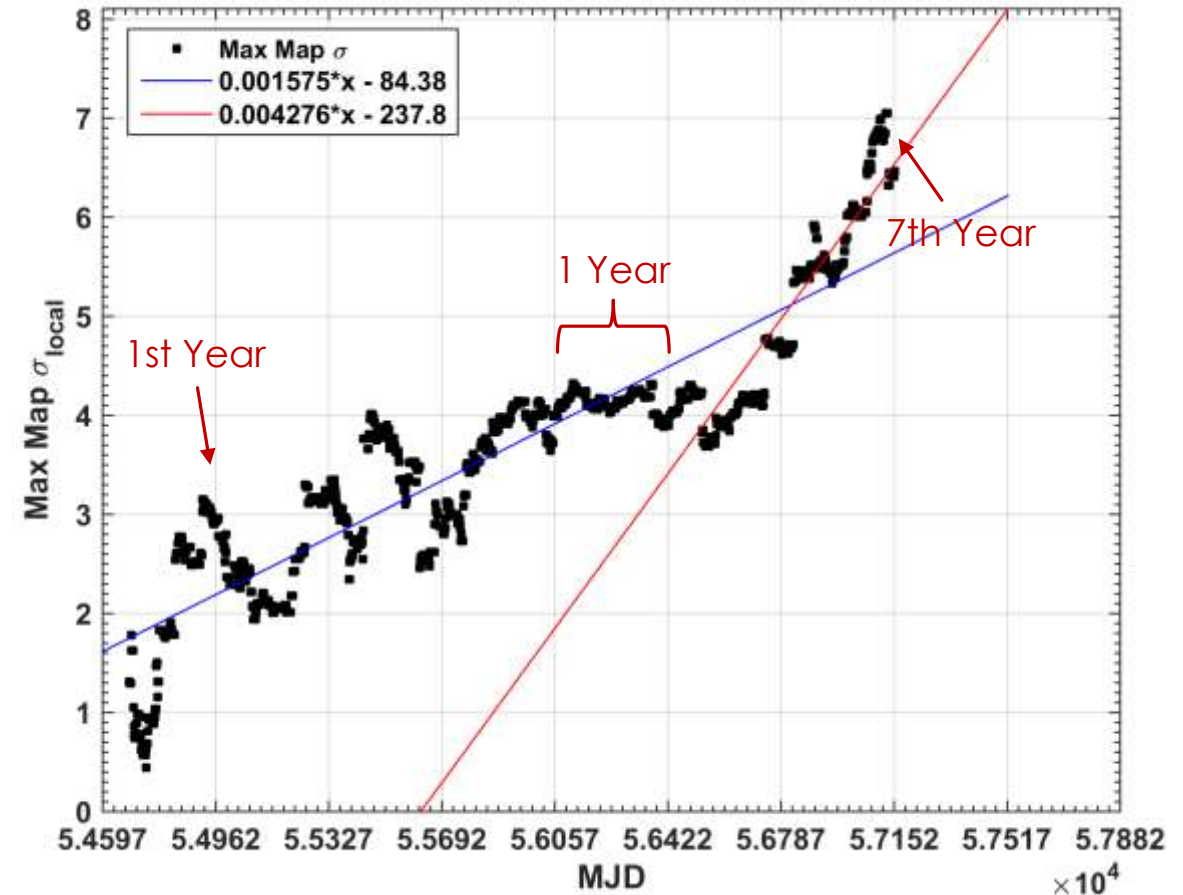
INTEGRAL DAY SIGNIFICANCE

- Blue line is linear fit — 0 to 7 years
- Red line is linear fit — 5th to 7 years



- Location of maximum colored/sized by MJD
 - General location is found within ~3 years

8 year estimate $\sim 4\sigma_{global}$

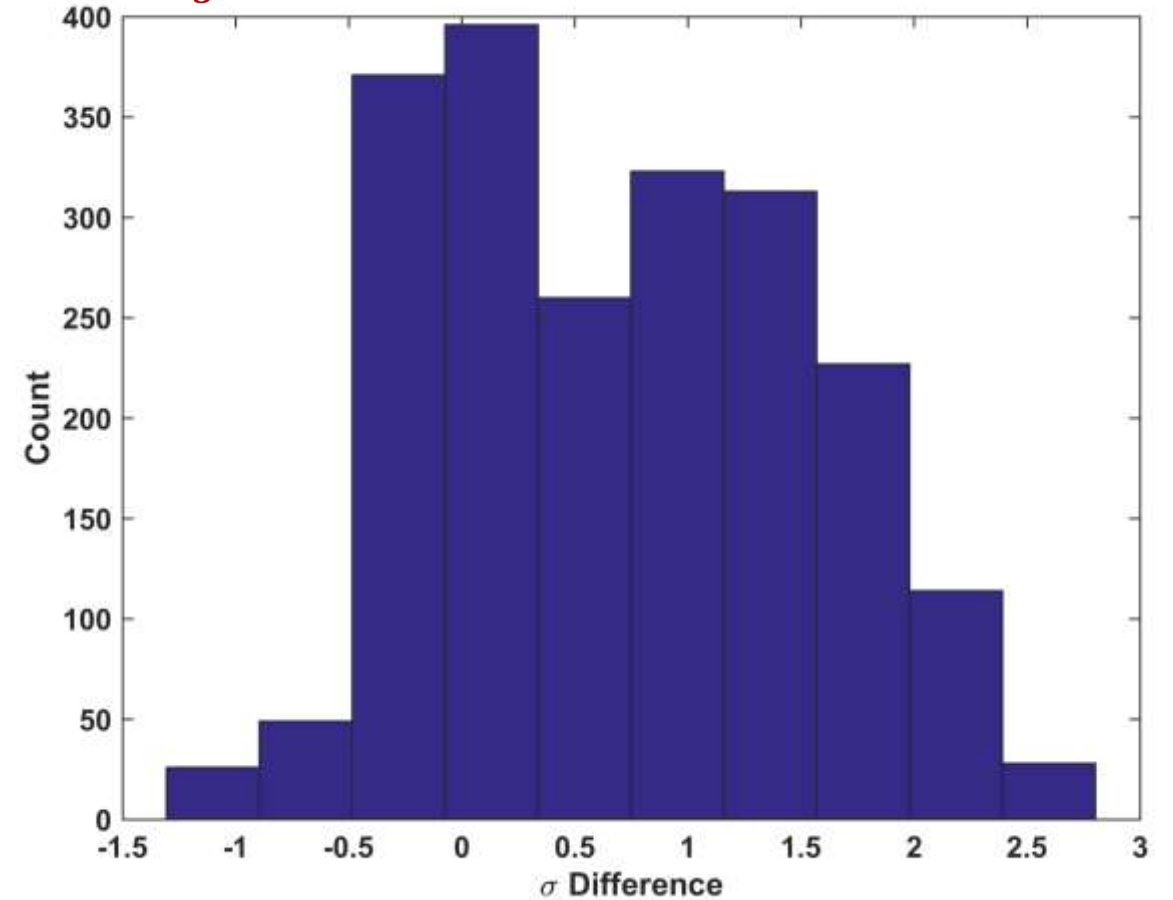


- Maximum σ_{local} on map
- Linear correlation 0.905 (0.935 after 5th year)

YEAR BY YEAR TREND

We only use integral year data

8 year estimate $\sim 4\sigma_{global}$



- Median sliding 1 year change
 - 0 to 7 years — $+0.7 \sigma/\text{year}$
 - 5 to 7 years — $+1.8 \sigma/\text{year}$
- 2,107 sliding 1 year σ differences (0 to 7 years)
 - 1554 σ increases
 - 553 σ decreases

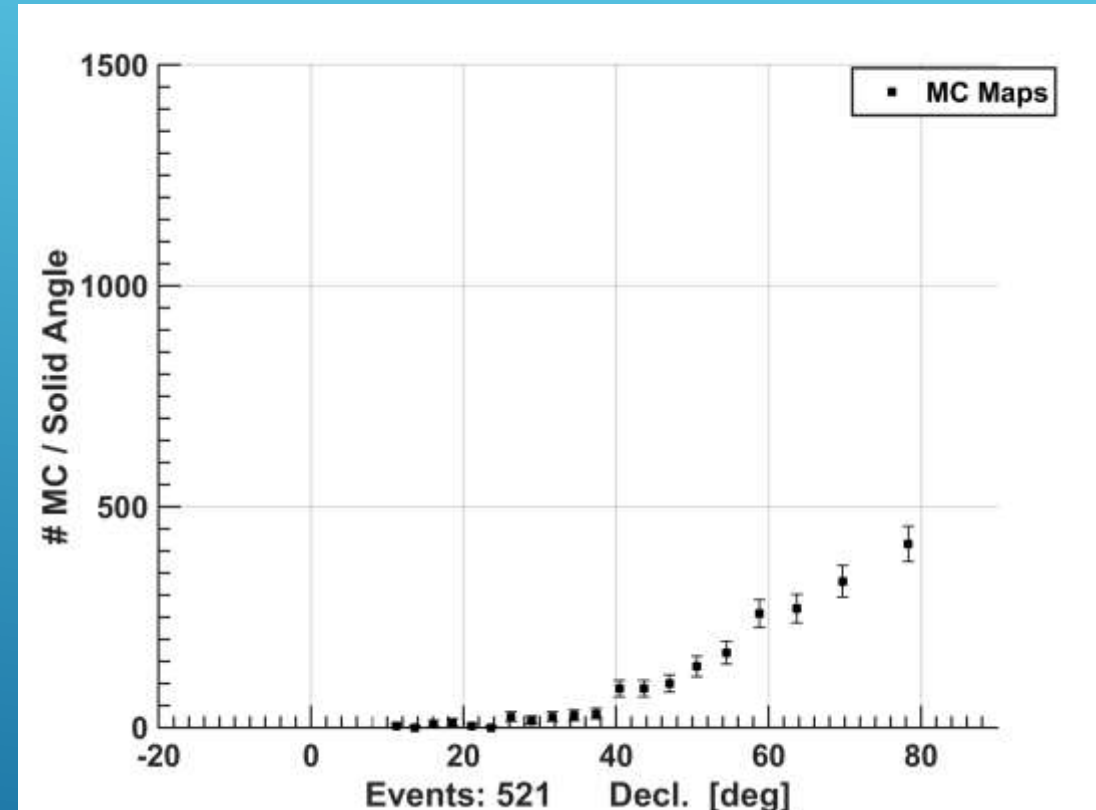
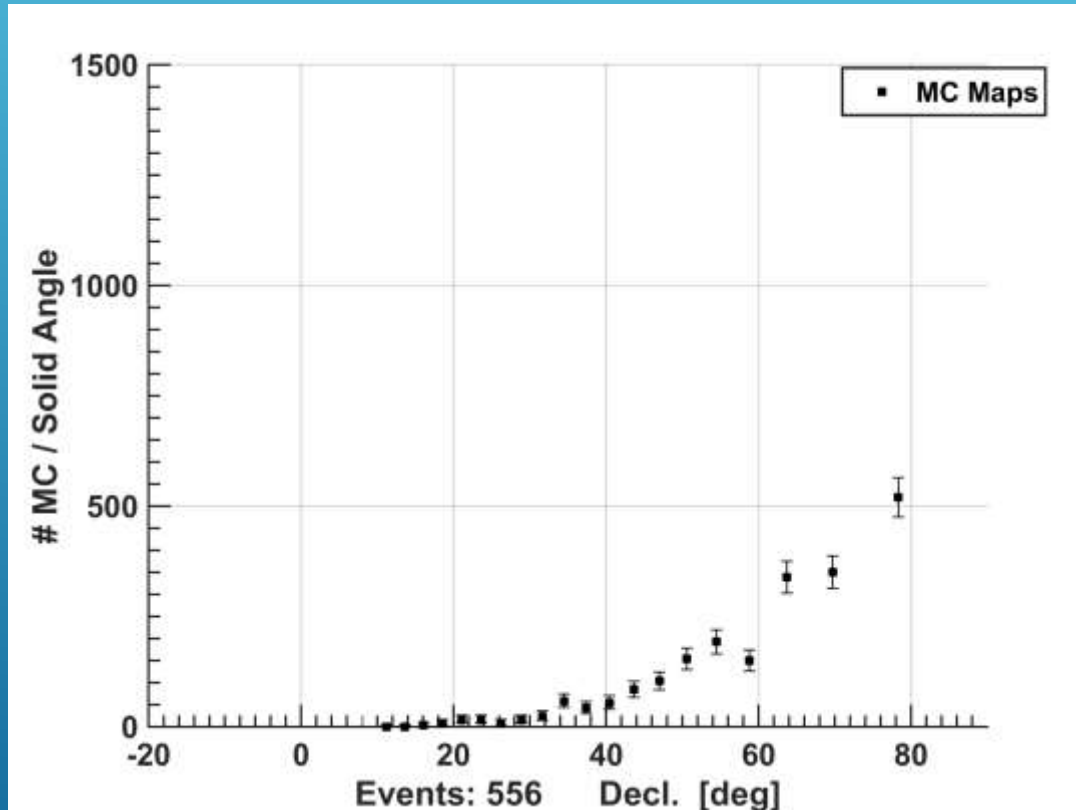
DECLINATION COUNT DISTRIBUTION

This is for *negative* $\rho_{|\tau|,p}$ only. The data was negative

MC

Equal Solid Angle bins

Energy Scrambled Data



Position is dependent on over/under-density but significance is not
Position is also more sensitive to energy anisotropy as shown by integral day data figures

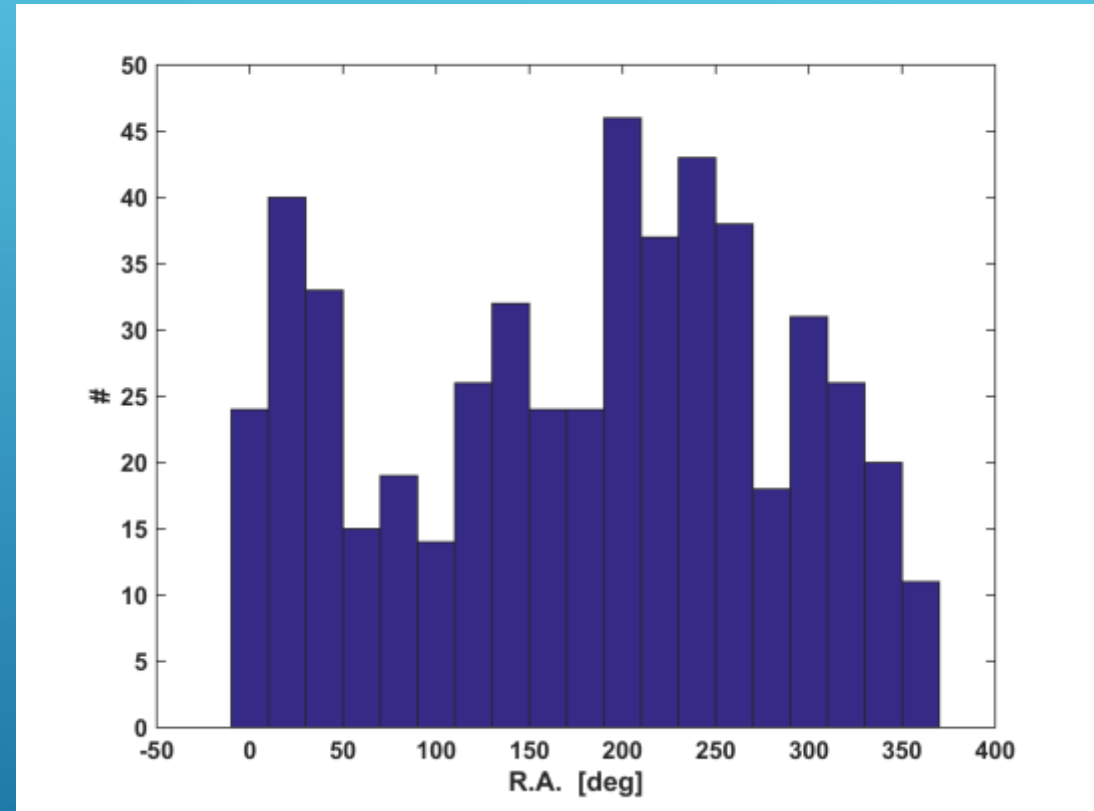
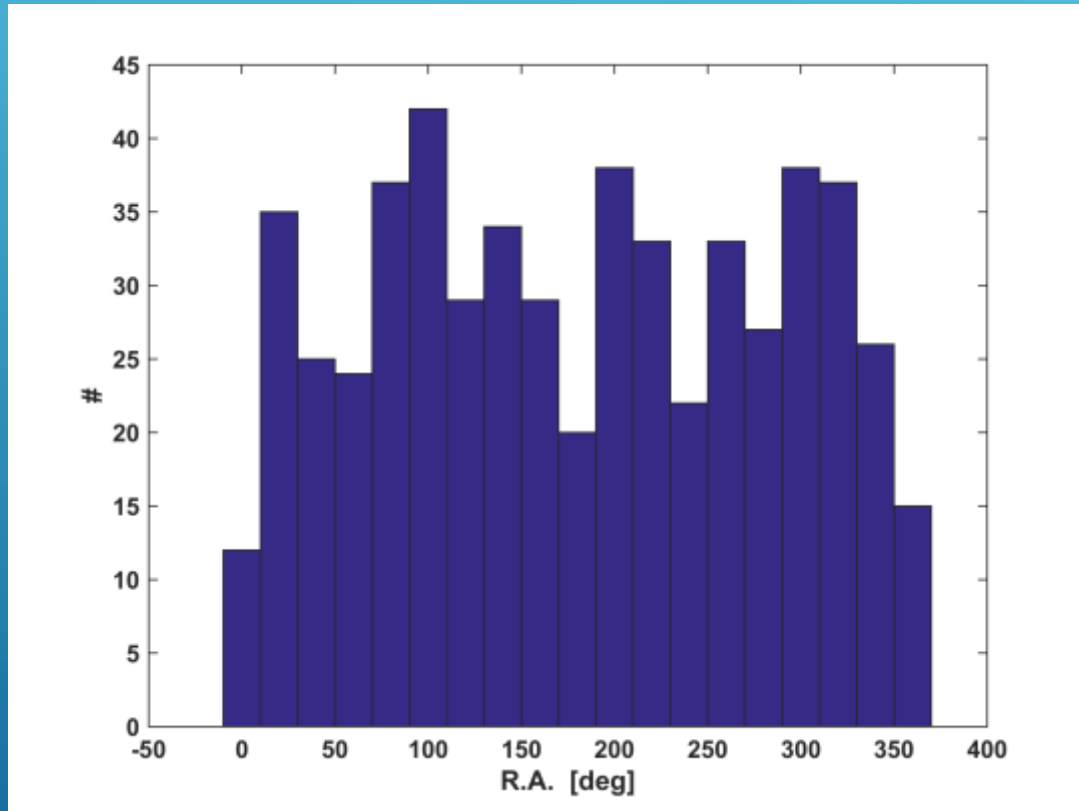
RIGHT ASCENSION COUNT DISTRIBUTION

This is for **negative** $\rho_{|\tau|,p}$ only. The data was negative

MC

Equal Solid Angle bins

Energy Scrambled Data



Position is dependent on over/under-density but significance is not
Position is also more sensitive to energy anisotropy as shown by integral day data figures

SEASONAL CORRECTION TEST

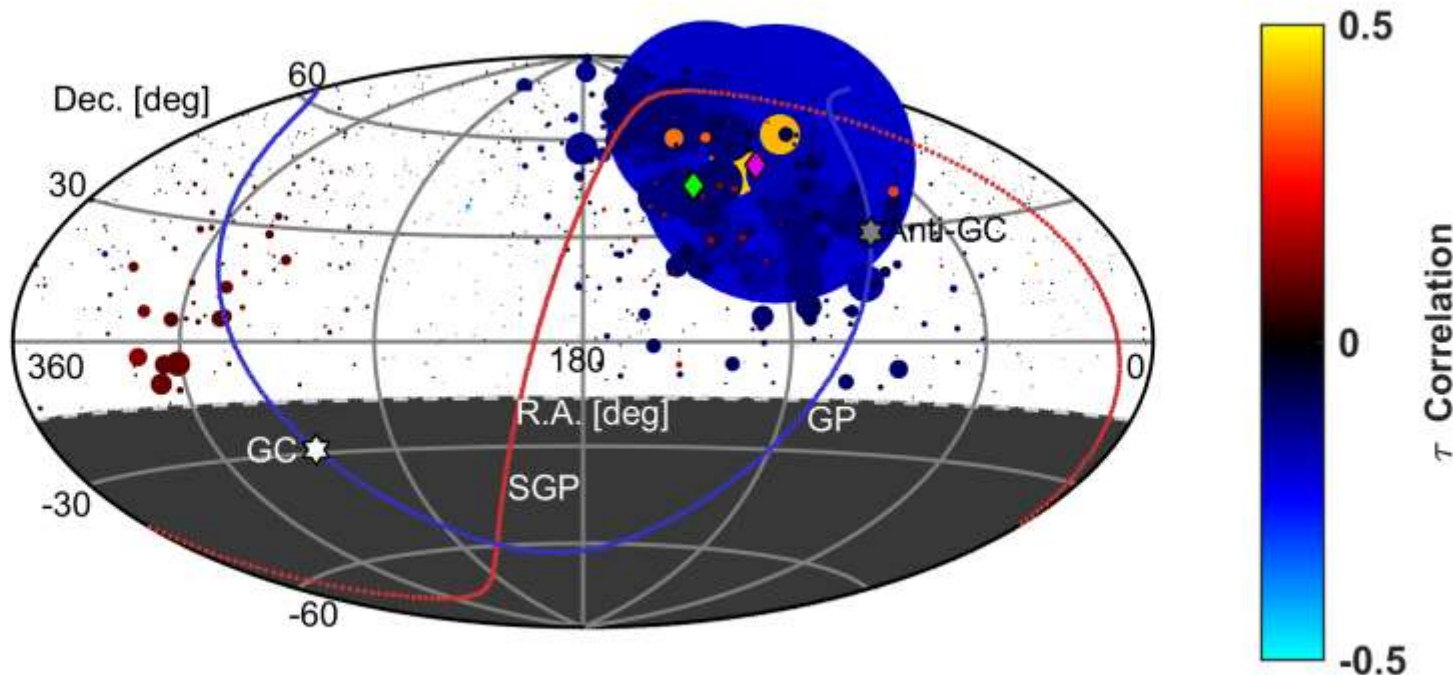
DATA RESULT

- ▶ Each test point (i) calculate Kendall's τ correlation $F_i[E_j(E_j > E_i), \theta_{ij}(E_j > E_i)]$
Choosing events with Energy > test point energy - removes adjacent double counting.

- Negative Correlation: Energy Increases \rightarrow Angle decreases
- Positive Correlation: Energy Increases \rightarrow Angle Increases

- Size proportional to **1/p-Value**
- Color is **Opening angle/Energy correlation**

Data: 833 events
E > 20 EeV after adjustment

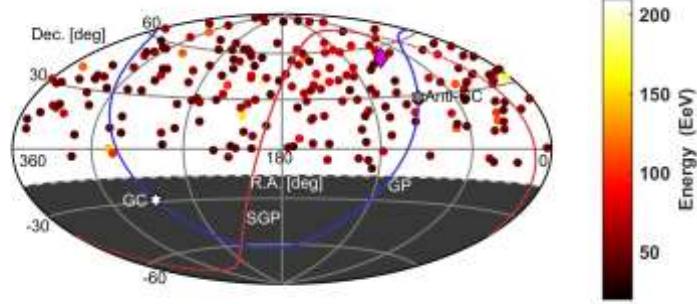
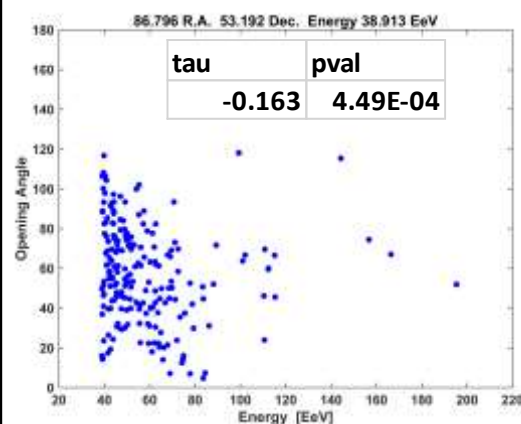
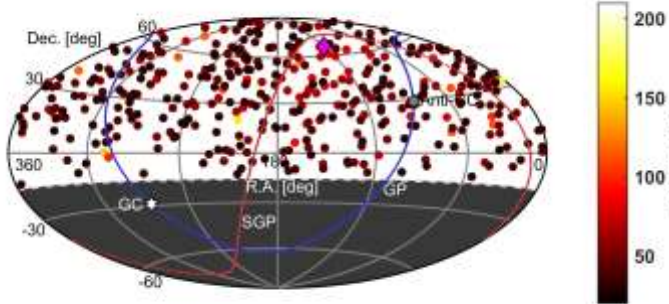
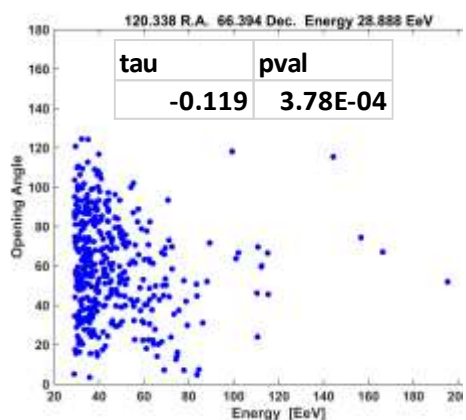
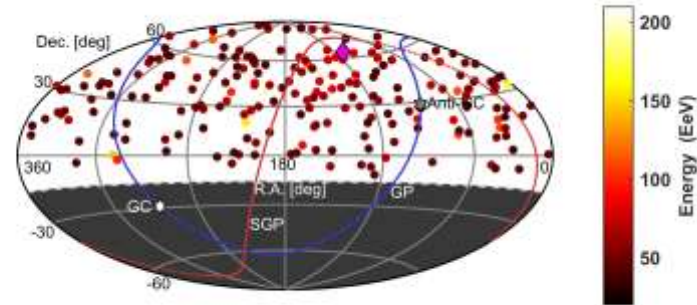
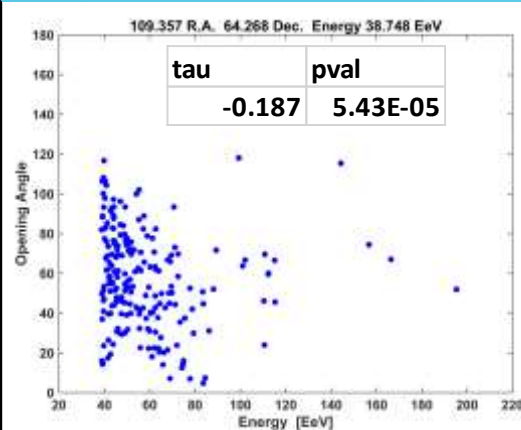
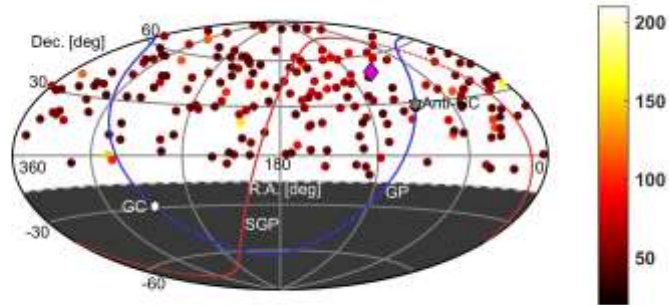
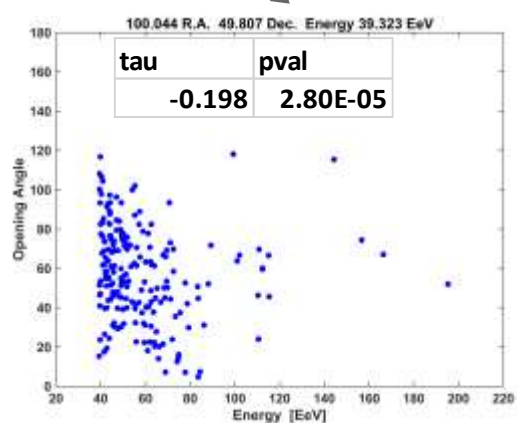


Each Test Point sample size is different

- Spectrum Anisotropy center:
138.8° R.A., 44.8° Dec.
- Correlation Weighted
(1/p-val) Average:
109.0° R.A. , 49.7° Dec.

4 MOST SIGNIFICANT POINTS

Test Point location and Energy Cut



Energy Vs Distance

$$E \geq E_i$$

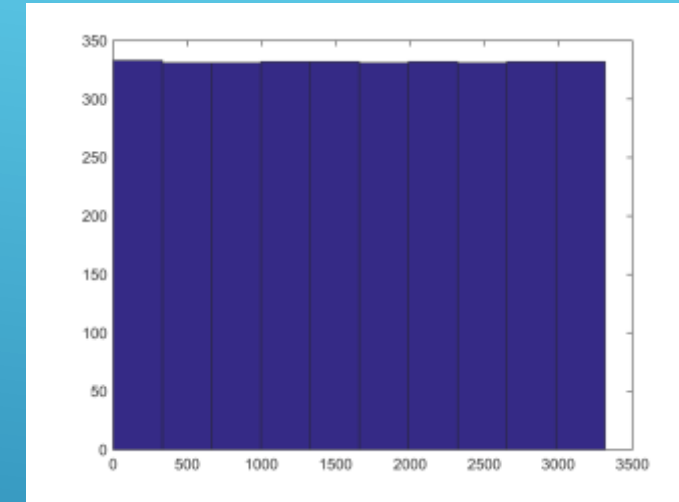
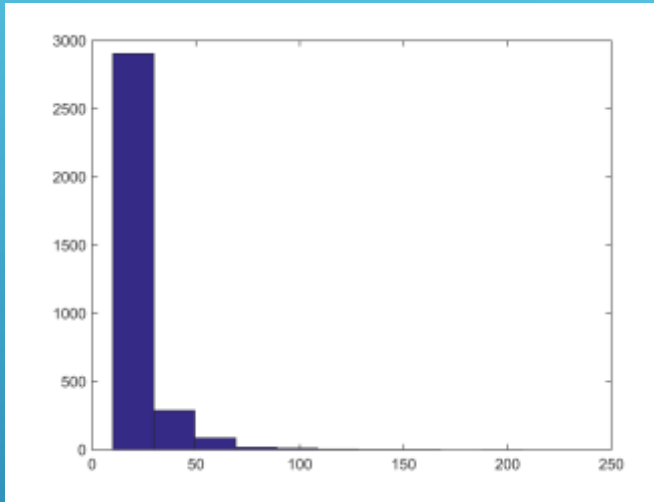
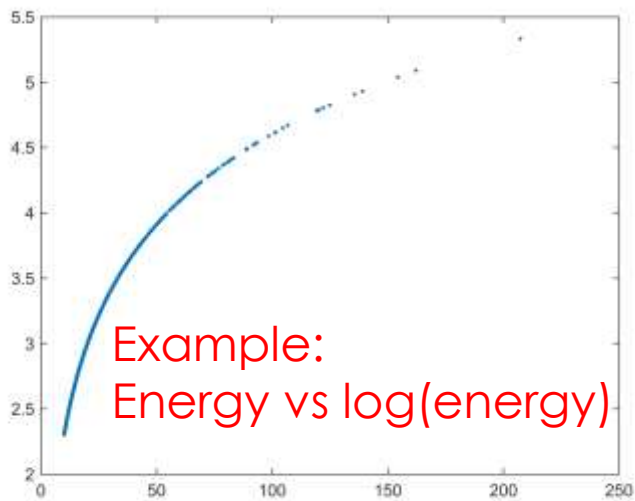
Energy Vs Distance

$$E \geq E_i$$

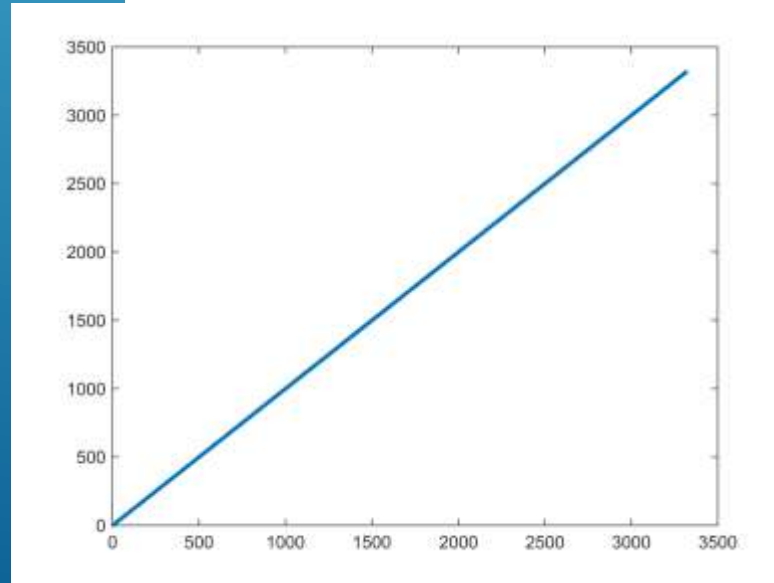
RANKING

- An ordered list of magnitude.
- Ranking removes functional form of dependence.
- Lowest variable value = 1.
- Highest variable value = N events.

Linear Correlation: 0.92



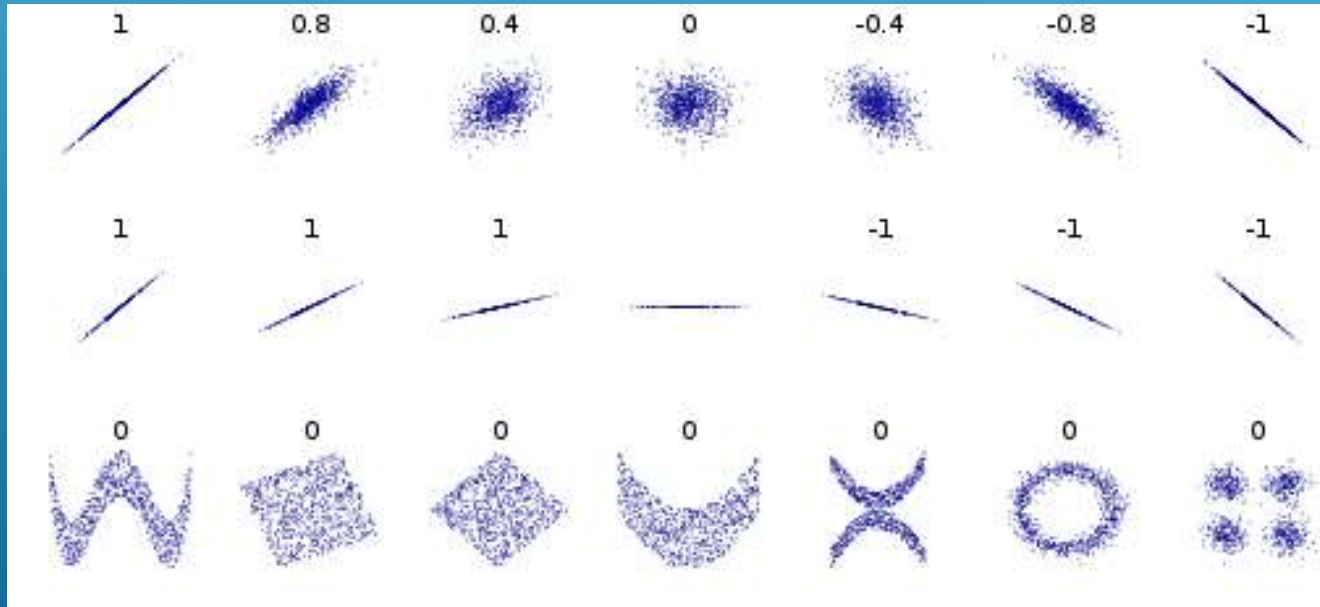
Rank Correlation: 1



LINEAR CORRELATION (PEARSONS)

$$\rho_{X,Y} = \frac{\text{cov}(X, Y)}{\sigma_X \sigma_Y}$$

$$r = r_{xy} = \frac{\sum_{i=1}^n (x_i - \bar{x})(y_i - \bar{y})}{\sqrt{\sum_{i=1}^n (x_i - \bar{x})^2} \sqrt{\sum_{i=1}^n (y_i - \bar{y})^2}}$$



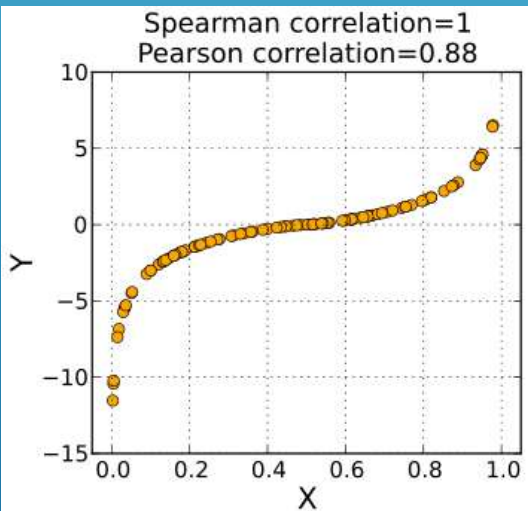
Measurement of linear dependence

RANK CORRELATION

- ▶ All values are ranked. Kendall's correlation is used.

$$\tau = \frac{(\text{number of concordant pairs}) - (\text{number of discordant pairs})}{\frac{1}{2}n(n-1)}$$

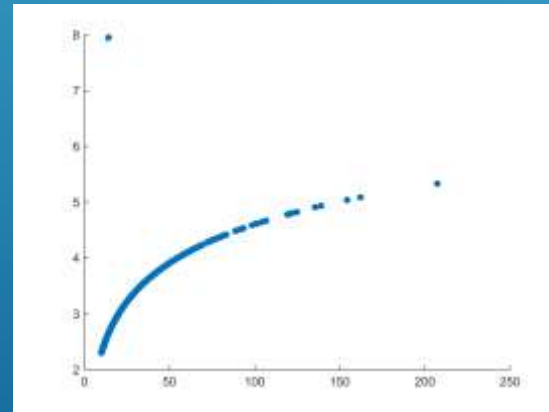
- ▶ Ranked correlations are permissive: any perfectly monotonic function $F(x,y)$ results in correlation = 1. Removes model assumption



Source: wikipedia

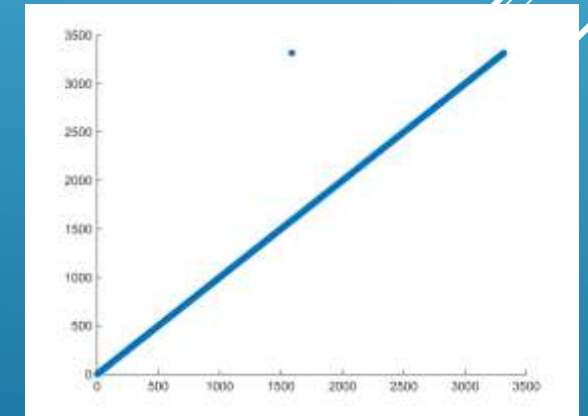
- p-Values

- calculated by permutation
- null hypothesis is zero correlation.
- p-Value is probability correlation is zero.



Linear Corr: 0.903
Outlier decreases
corr: ~0.02

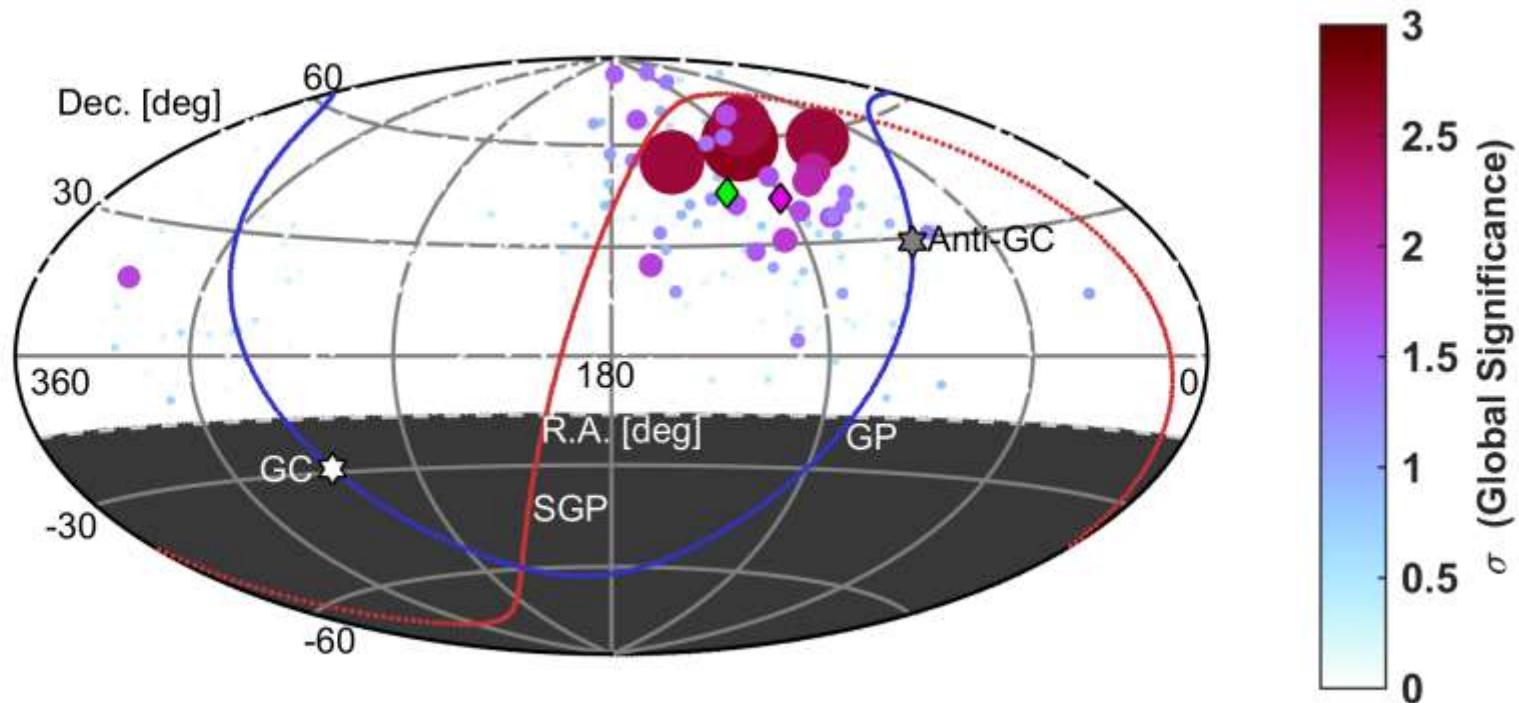
Robust
against
outliers



Rank Corr: 0.9994
Outlier decreases
corr: 0.0006

GLOBAL POINT SIGNIFICANCE

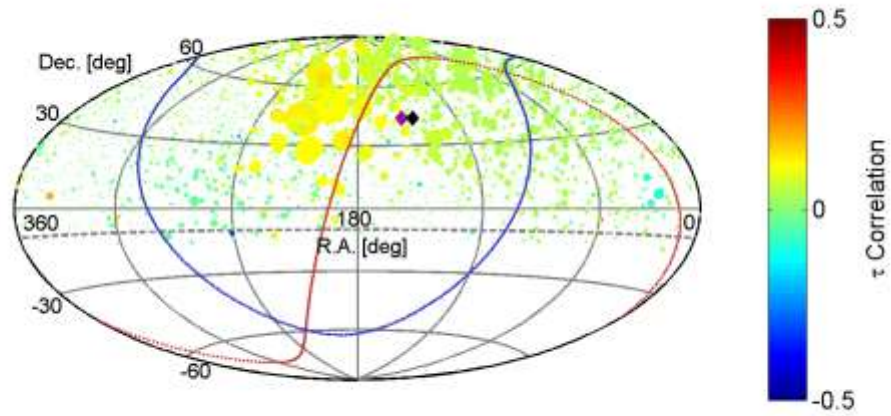
- 1,000,000 Isotropic MC maps the size of data
 - Count maps with at least one test point with:
 - $|\tau| \geq |\tau_{data}|$ & $sign(\tau) = sign(\tau_{data})$ & $p \leq p_{data}$
(At least as ordered change in same direction, with greater or equal samples)
- Size proportional to **1/p_global**
- Color is **Global Significance**
- Highest Significant test point: **2.7 σ**



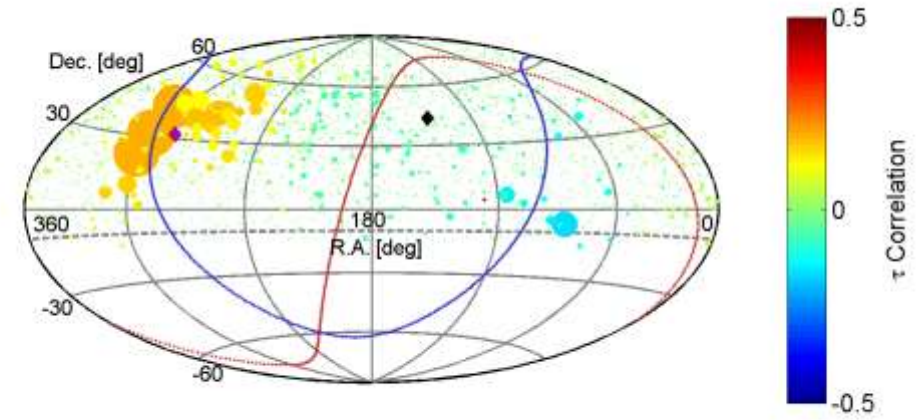
Sigma	tau
4.571	-0.1747
4.643	-0.1879
4.643	0.4302
4.736	0.4523

Individual correlations clearly don't tell the whole story

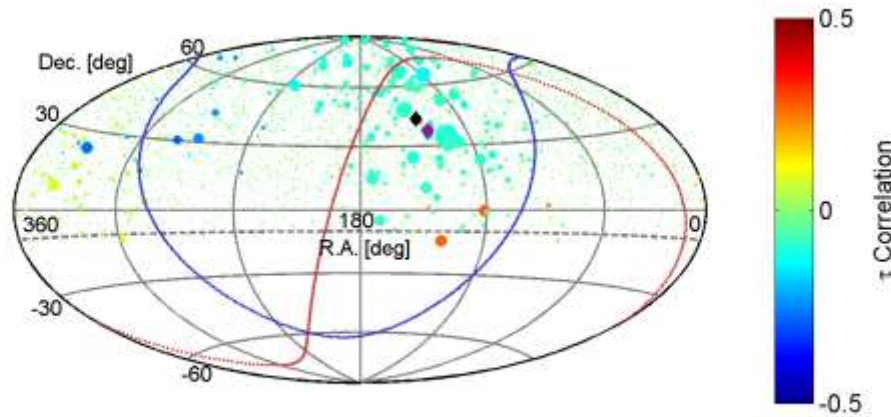
EXAMPLE MC MAPS



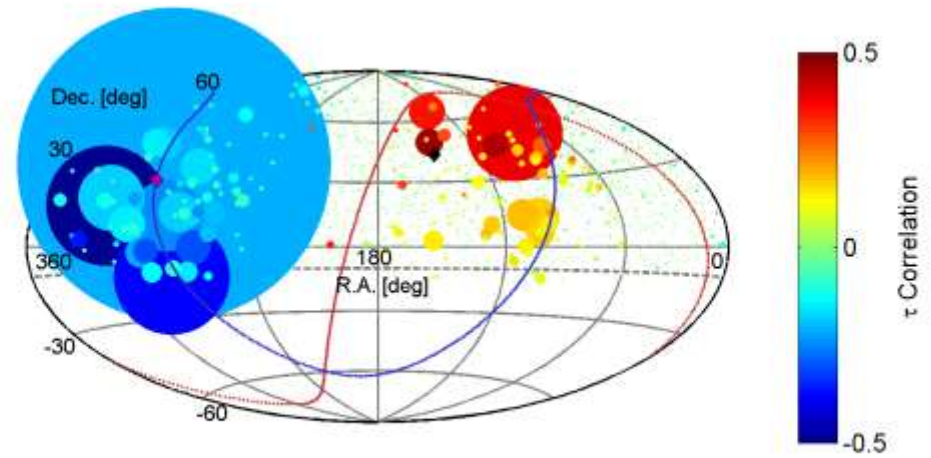
Distribution of p-val and tau least like data



Distribution of p-val most like data

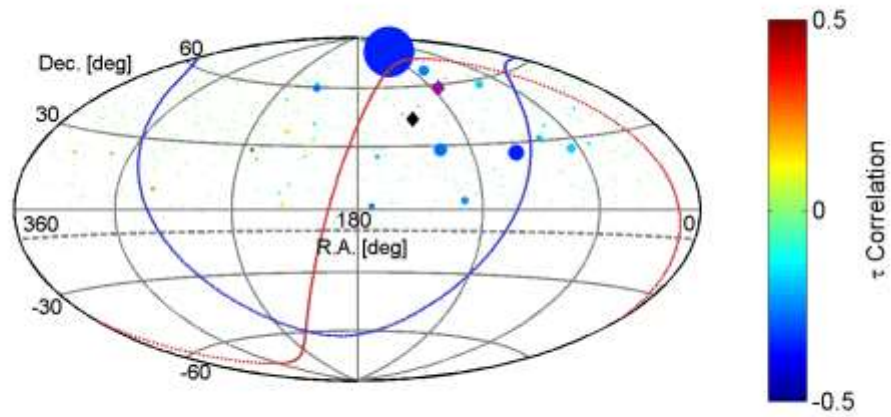


Distribution of tau most like data

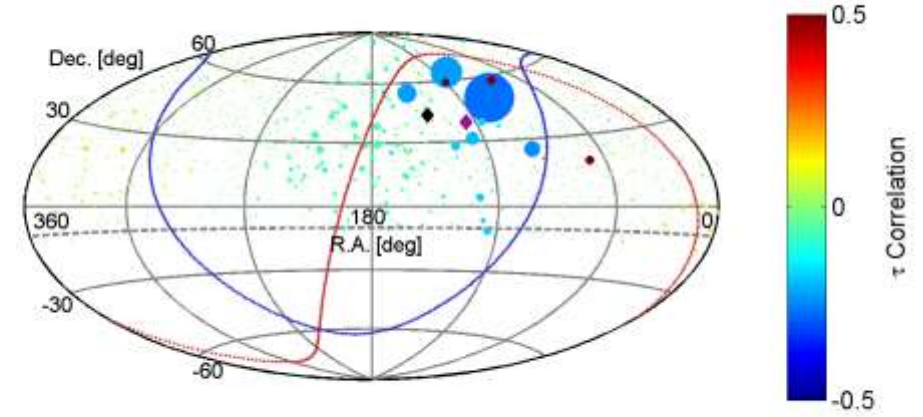


Most points like best p-val point from data. (2 points)

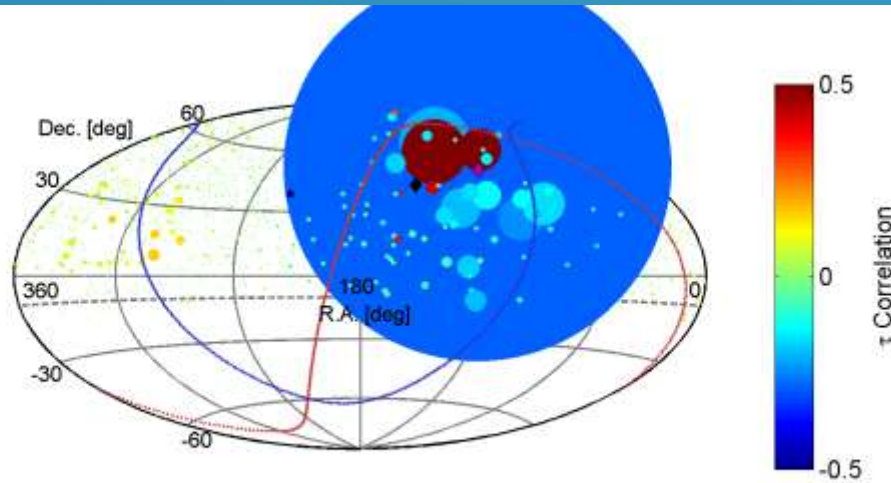
DATA CUMULATIVE TIME QUANTILES



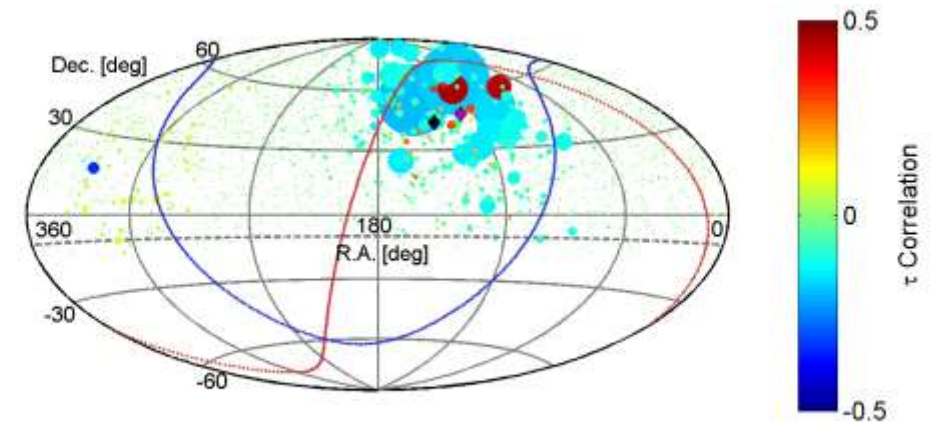
Quartile 1



Quartiles 1 and 2

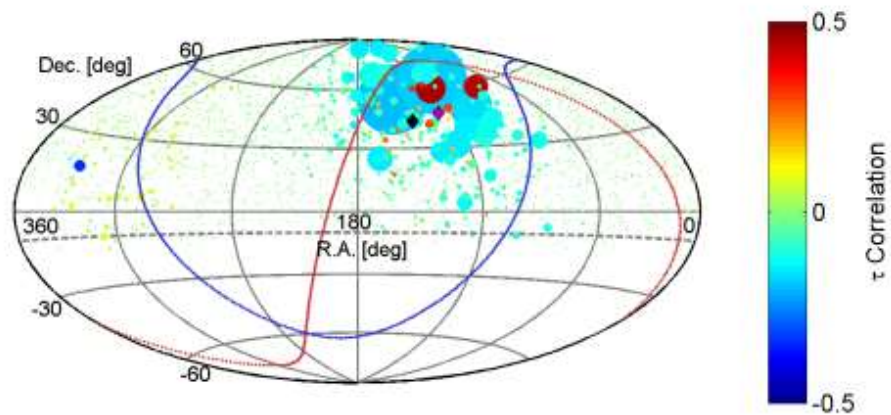


Quartiles 1 to 3

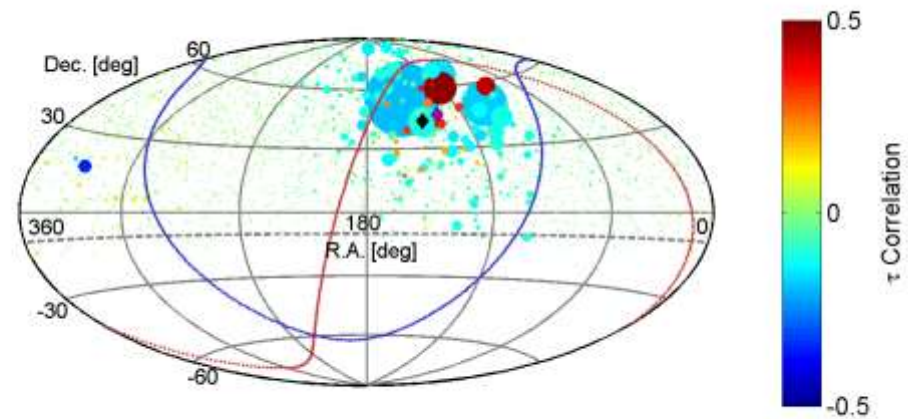


All

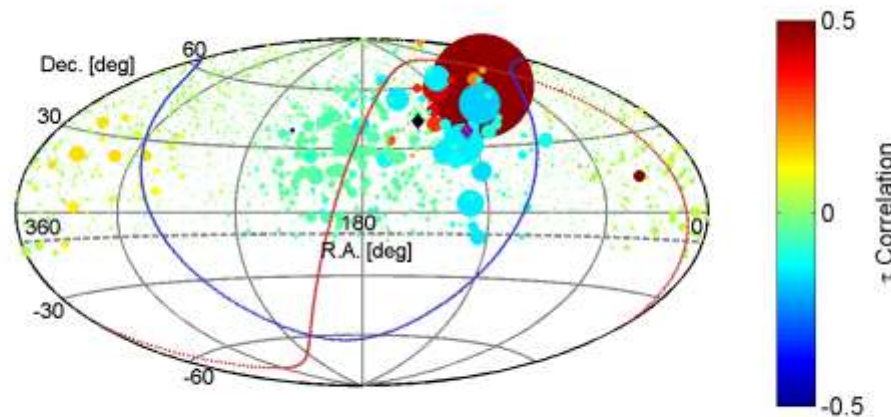
DIFFERENT DATA SUBSETS



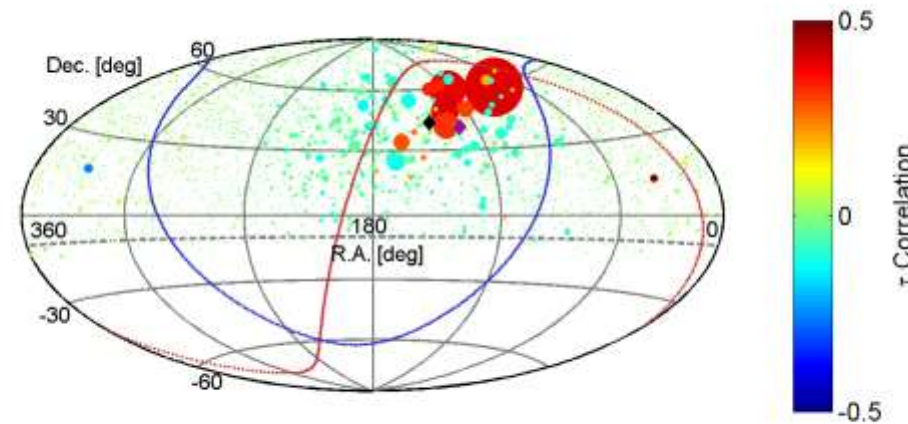
7 Year Kawata-san data with additional cuts



7 Year Dmitri's data (tighter cuts)

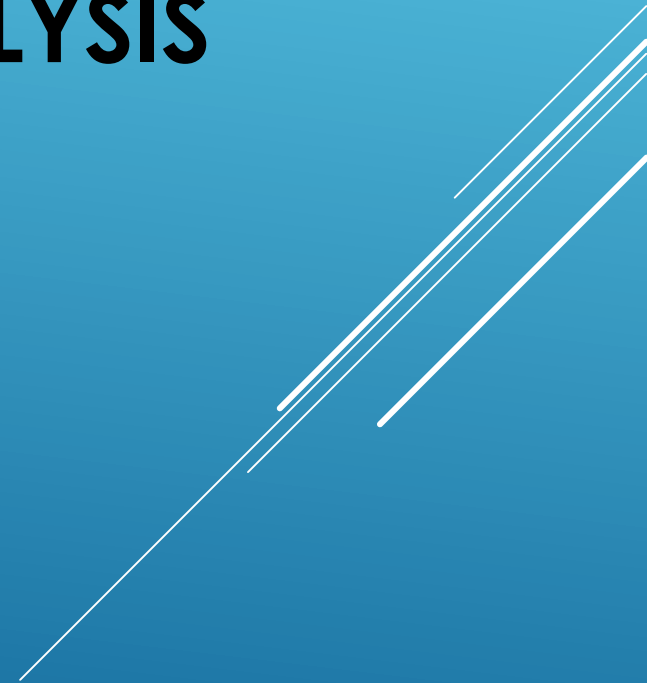


5 Year Kawata-san hotspot paper data



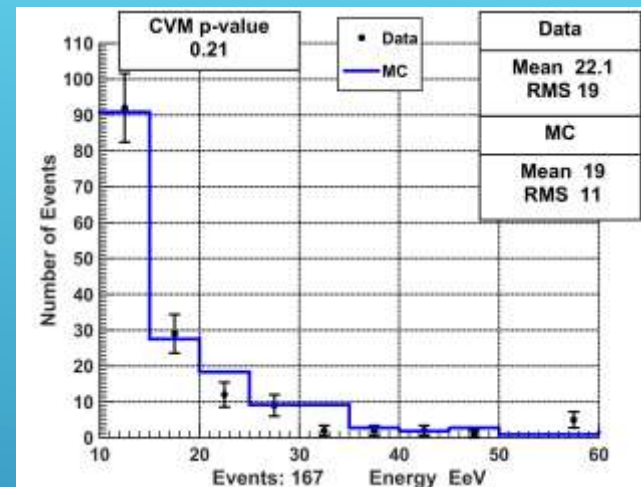
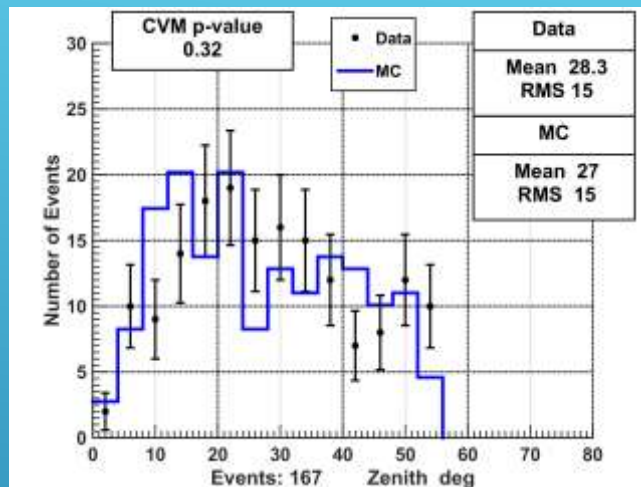
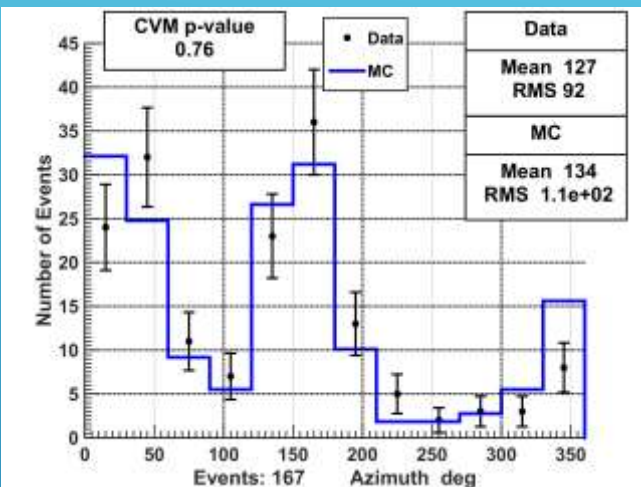
7 Year Kawata-san ICRC data

HOT/COLDSPOT SUMMARY ANALYSIS ADDITIONAL MATERIAL

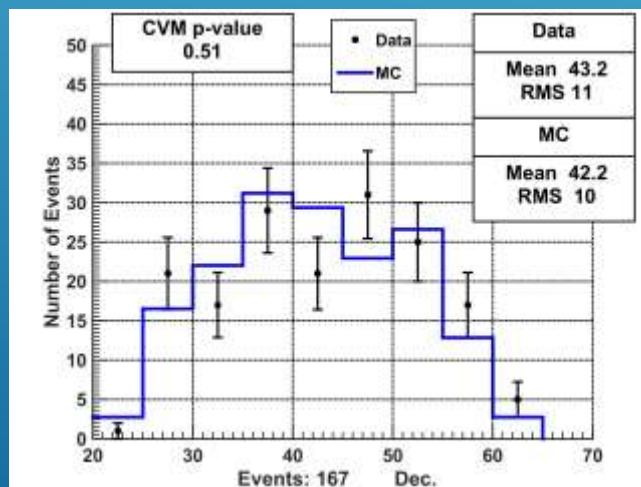
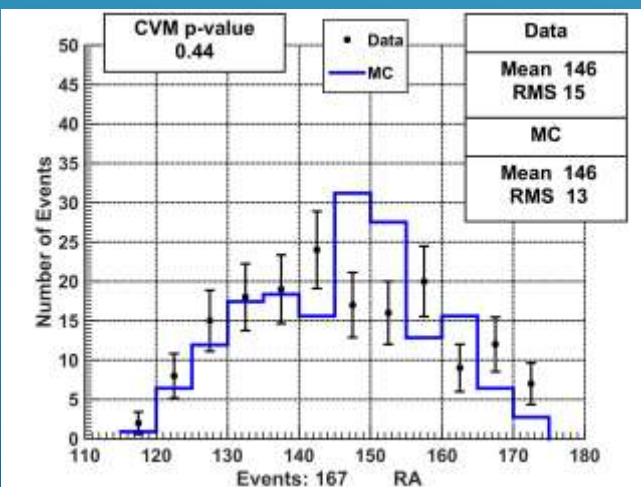


ISOTROPIC MC VS DATA IN HOTSPOT – ALL ENERGIES

10 EeV cut – 20 degree radius spherical cap

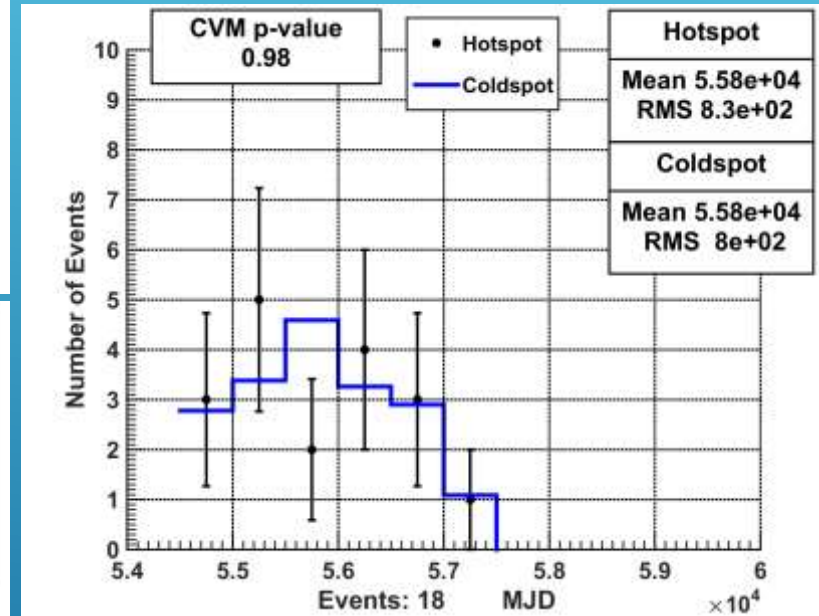
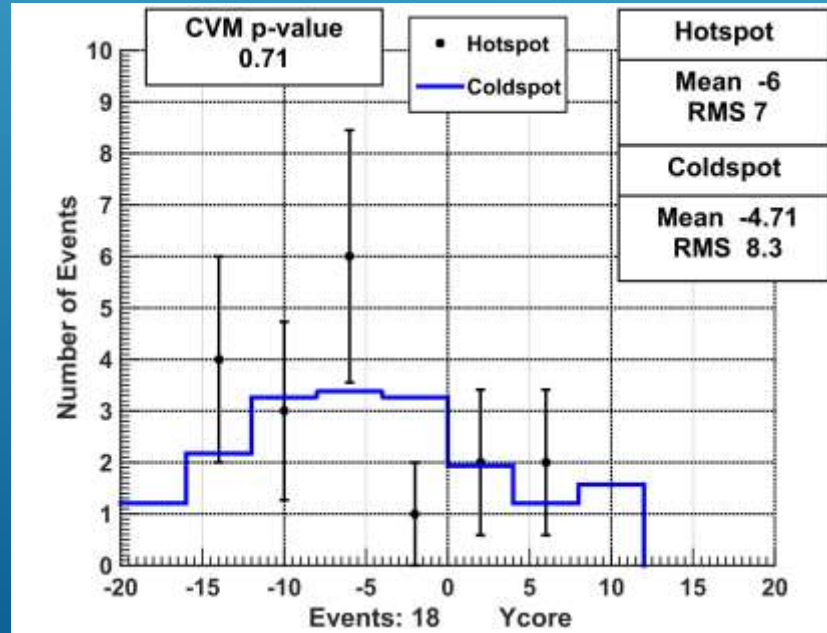
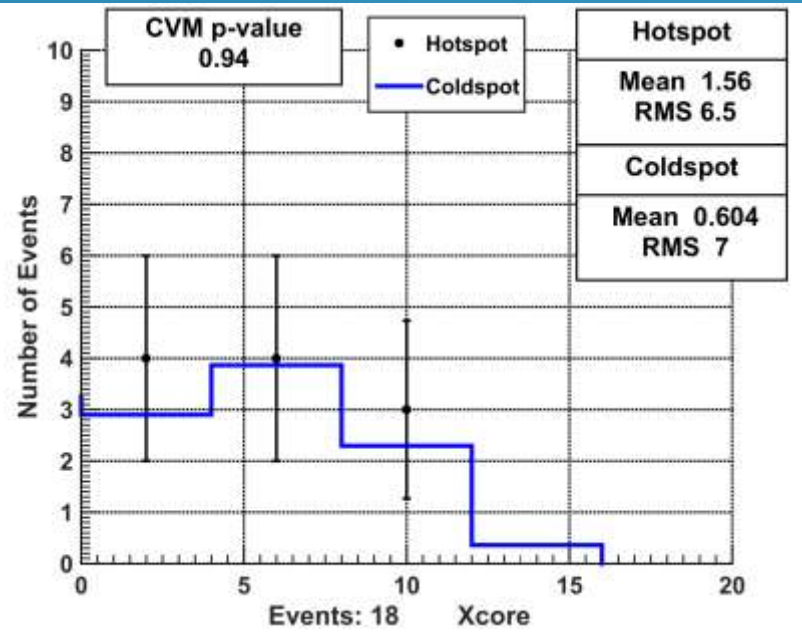
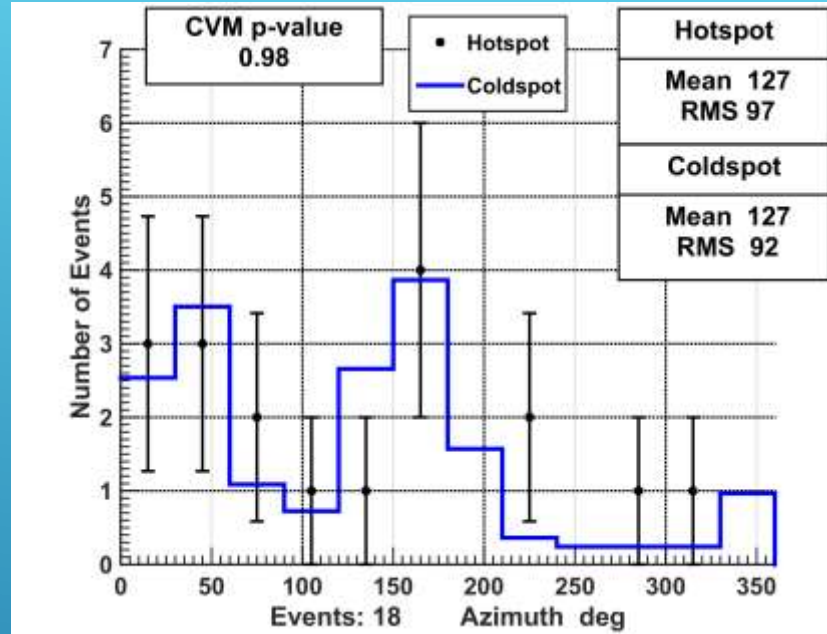
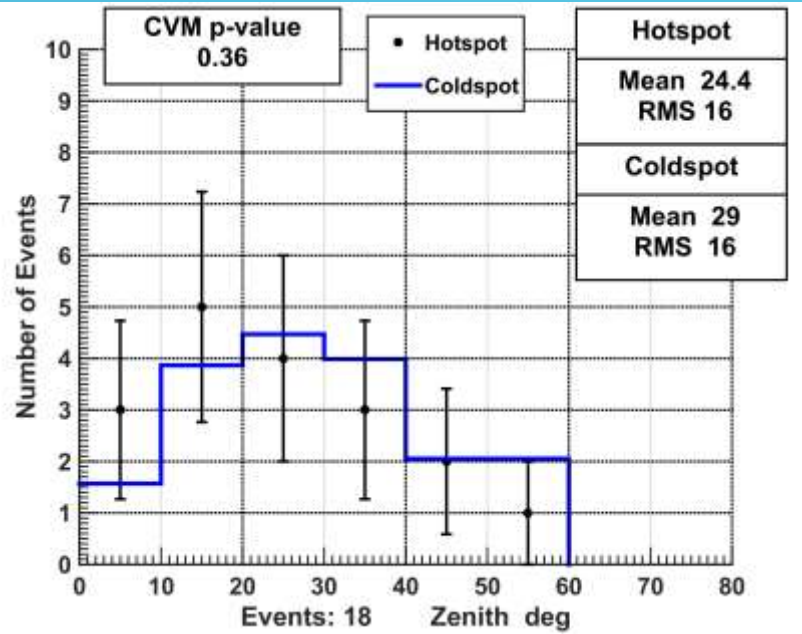


One random isotropic MC map the size of the data

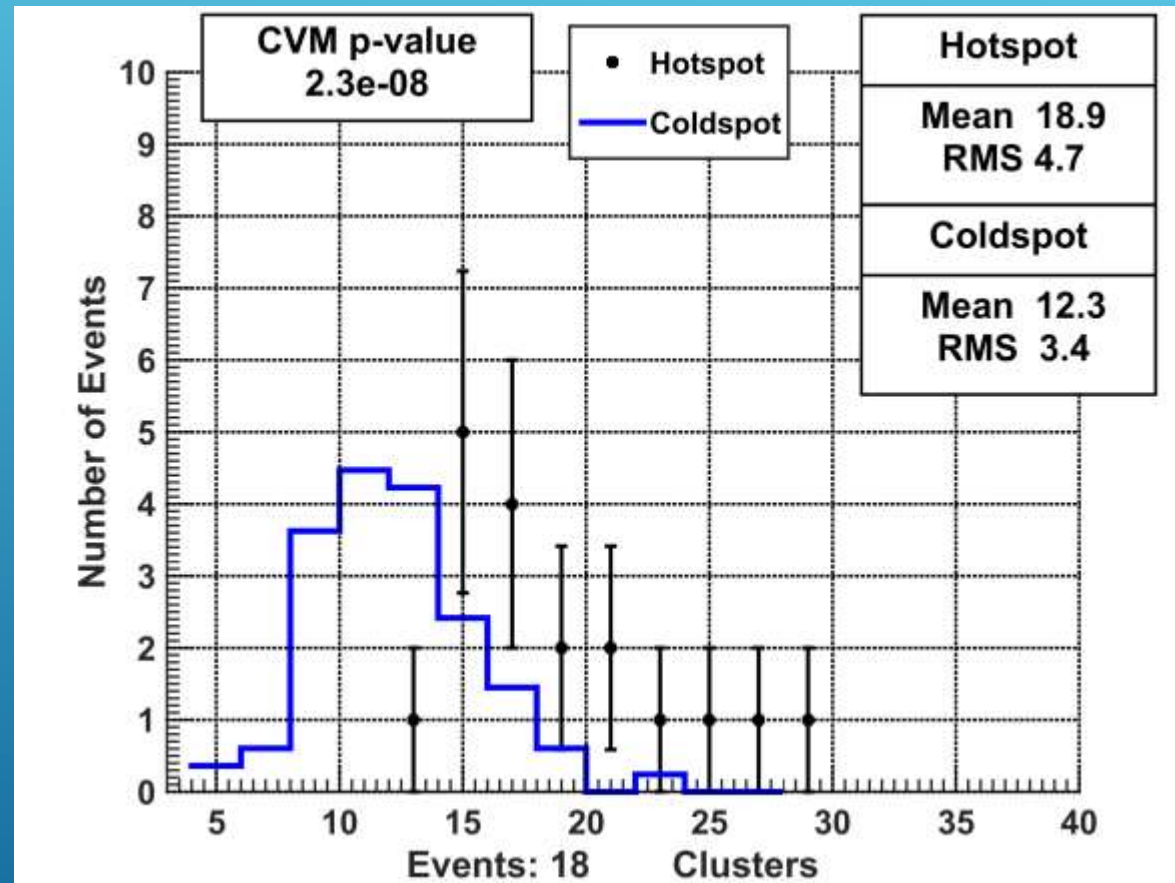
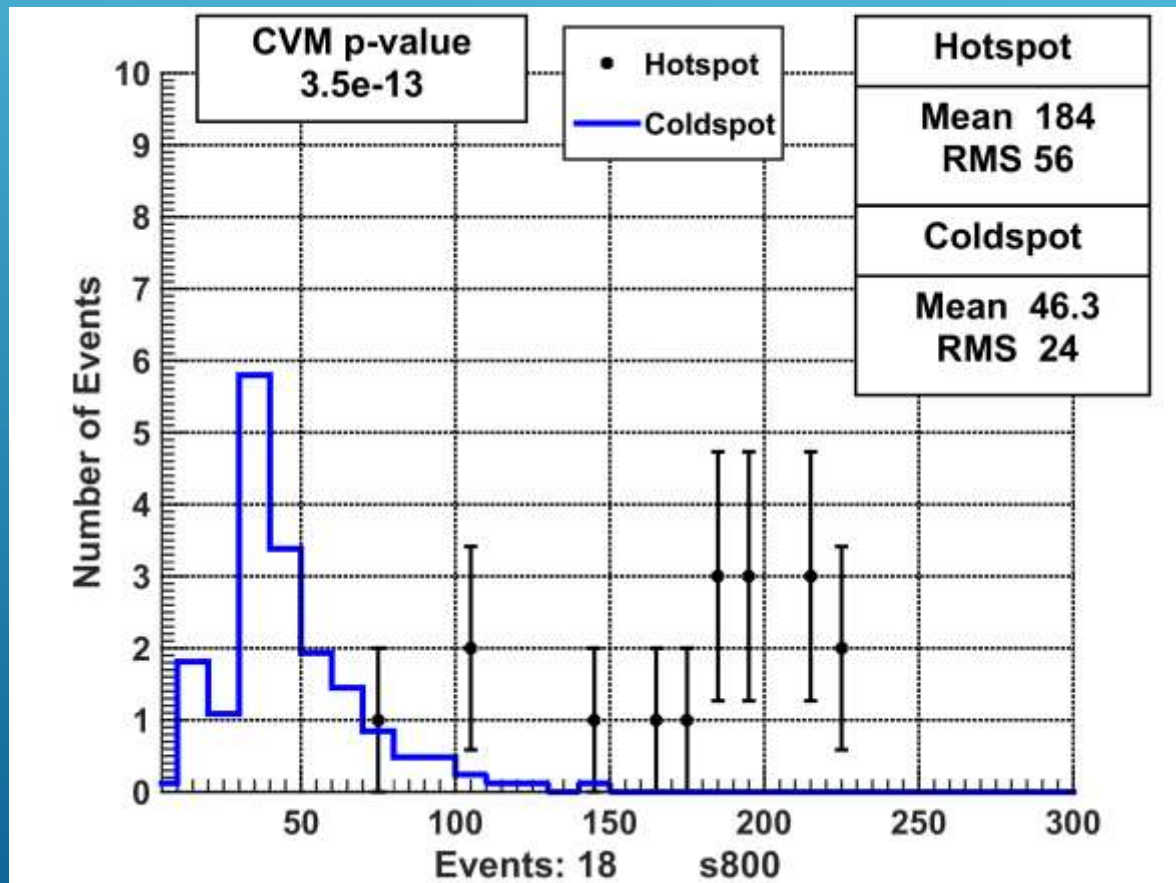


Inside hotspot there is possibly something Different with zenith, energy, and RA.

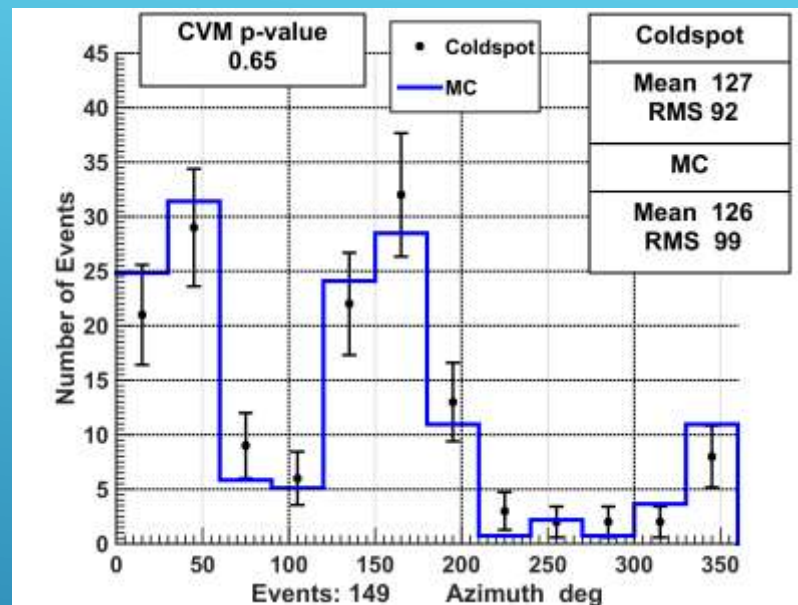
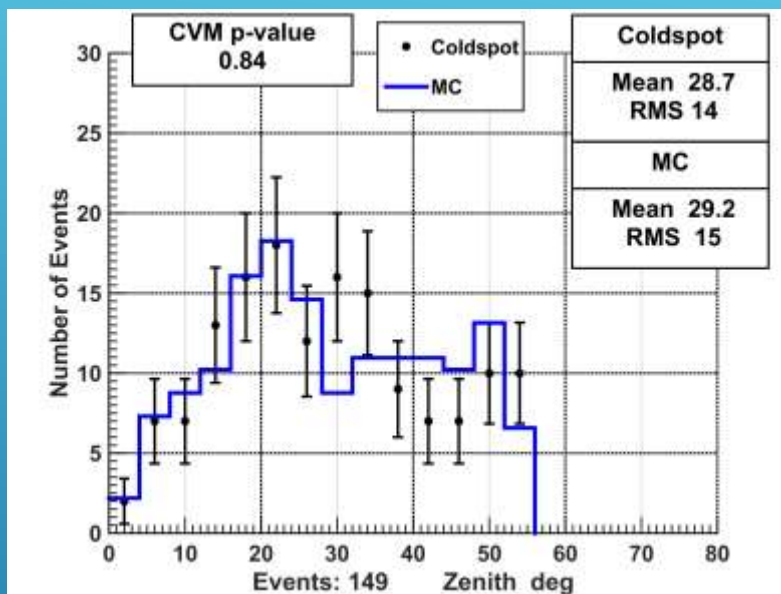
COMPARISON WITHIN HOT/COLD SPOT – $E > 57$ VS $E < 57$



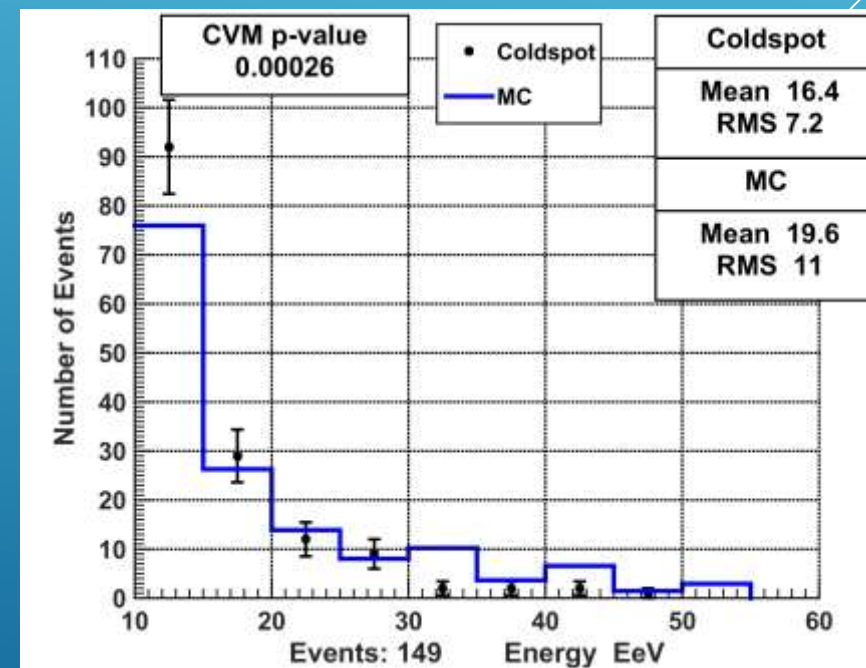
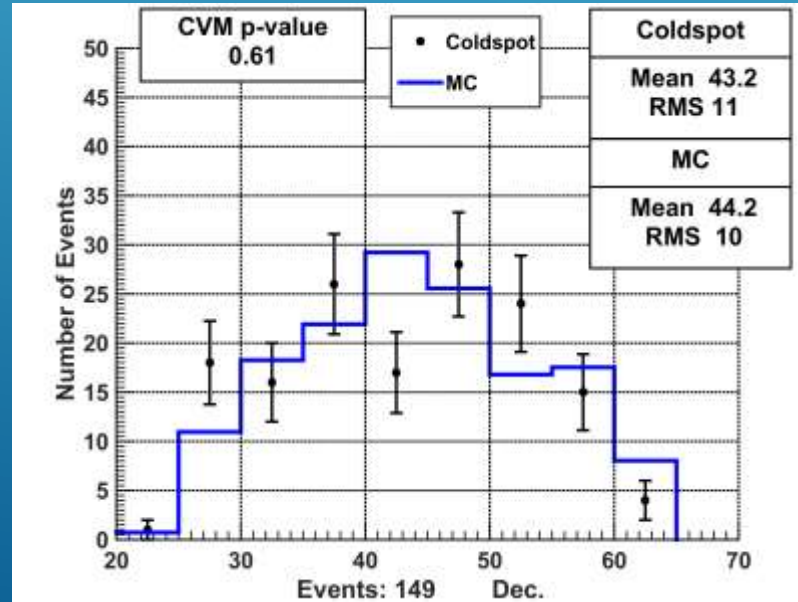
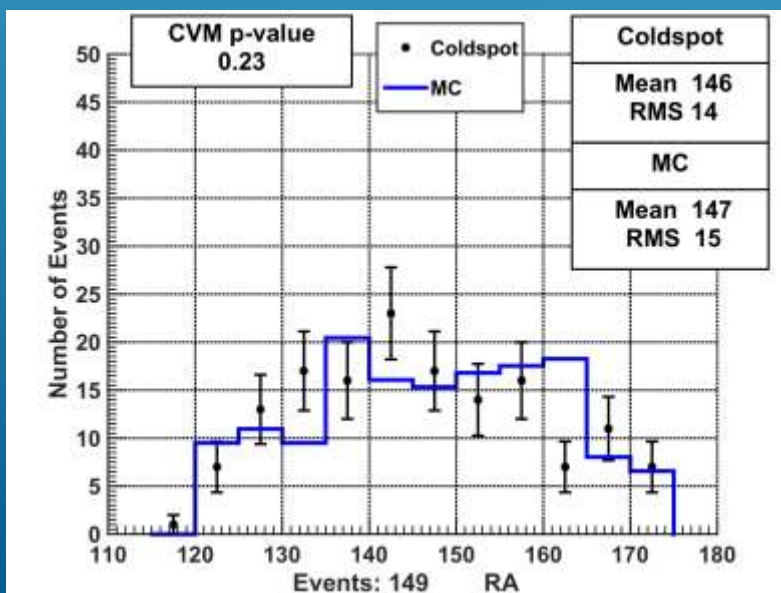
S800 AND CLUSTERS – SHOULD NOT BE THE SAME



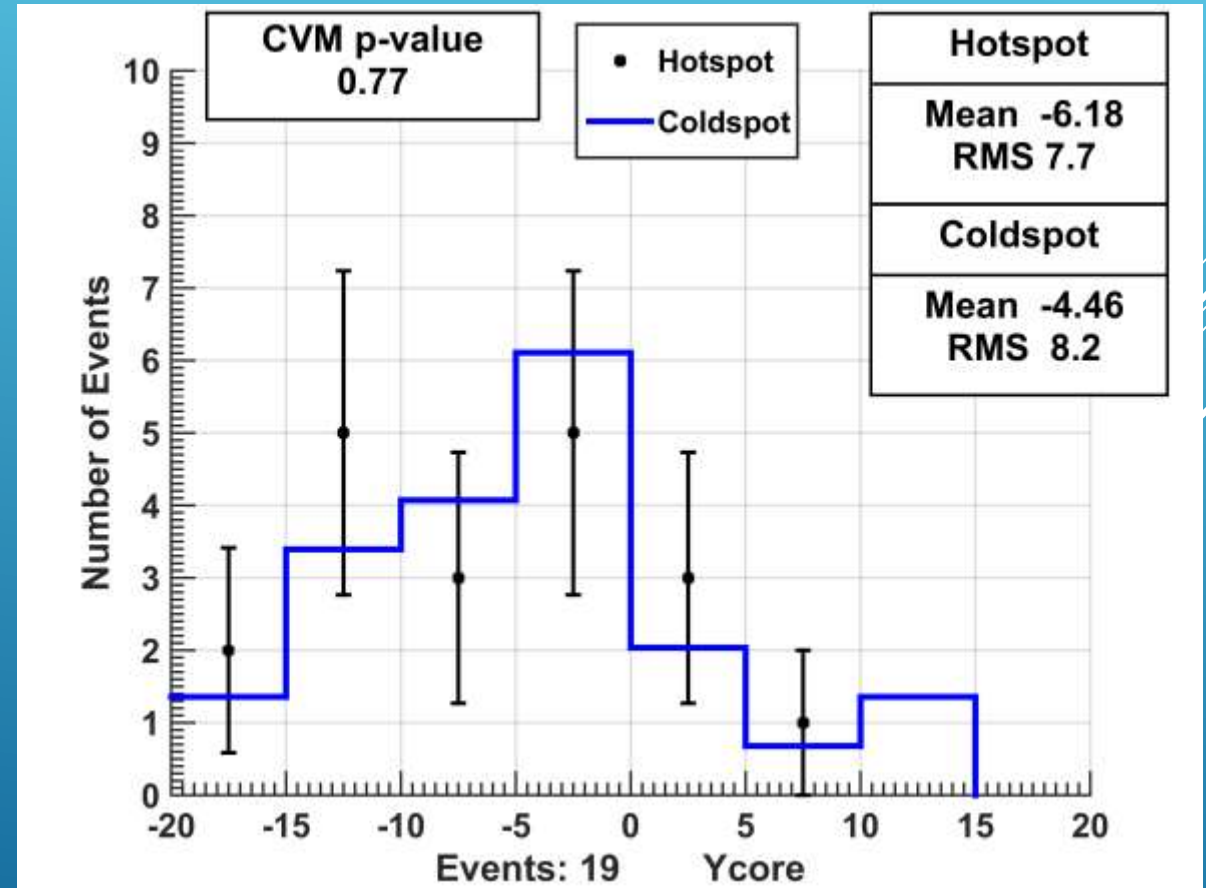
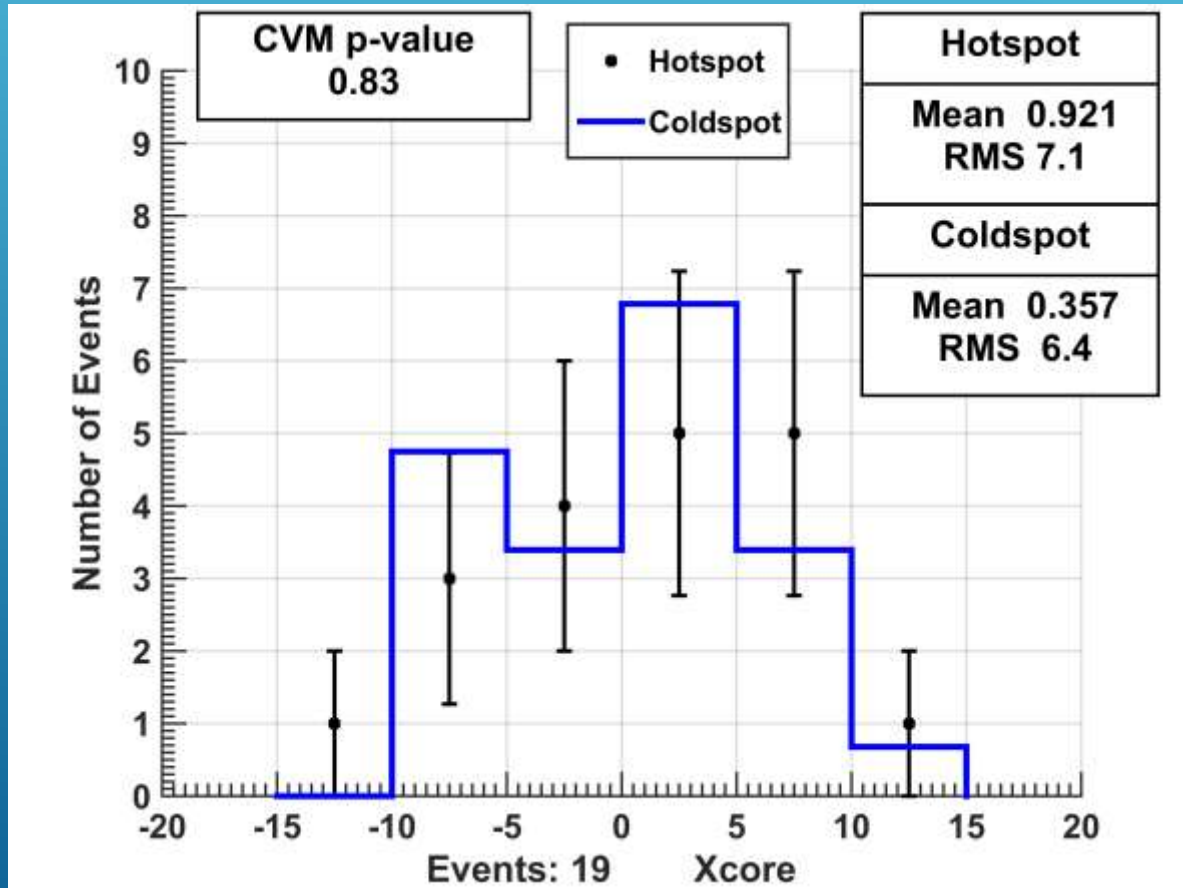
COMPARE COLDSPOT TO ISOTROPIC MC



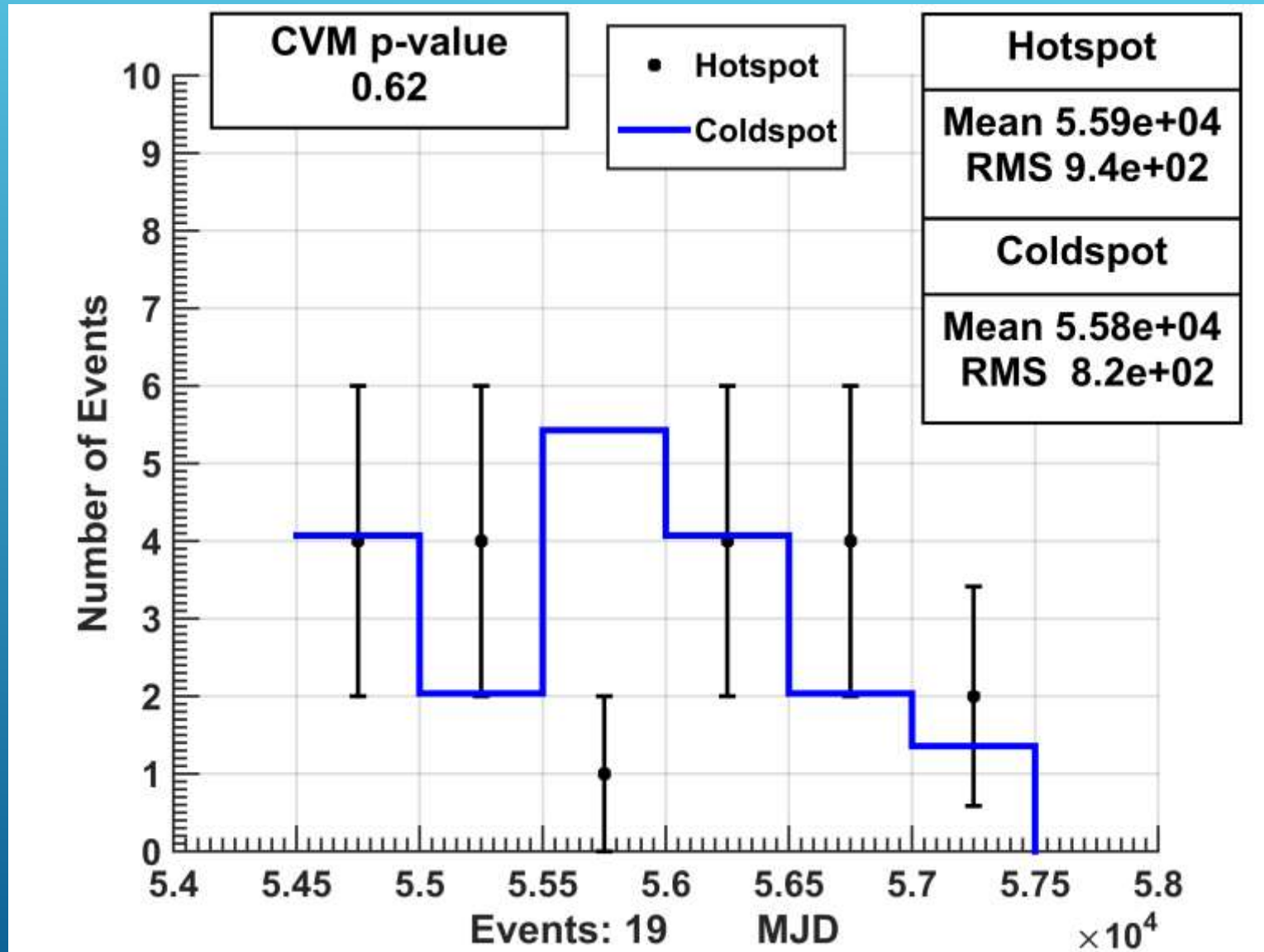
Energy and RA are a bit different.



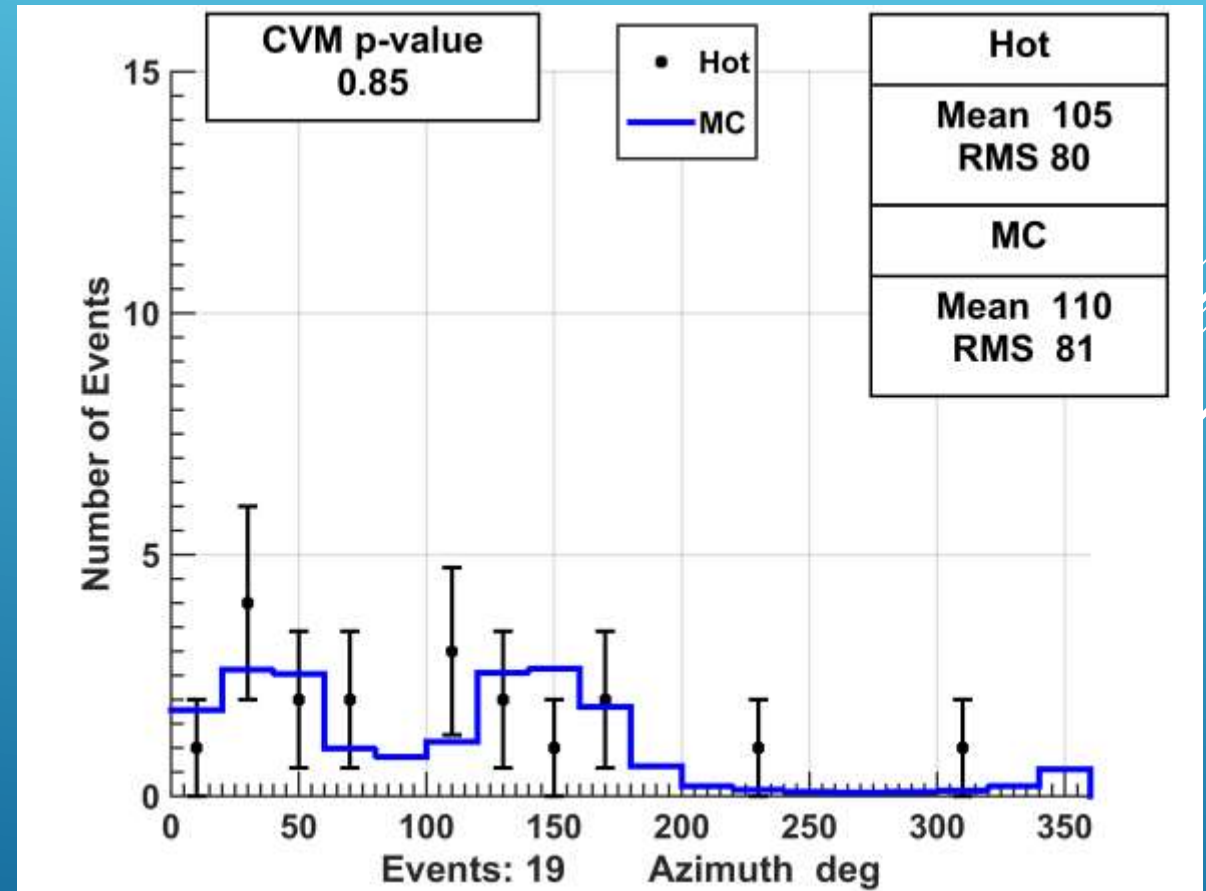
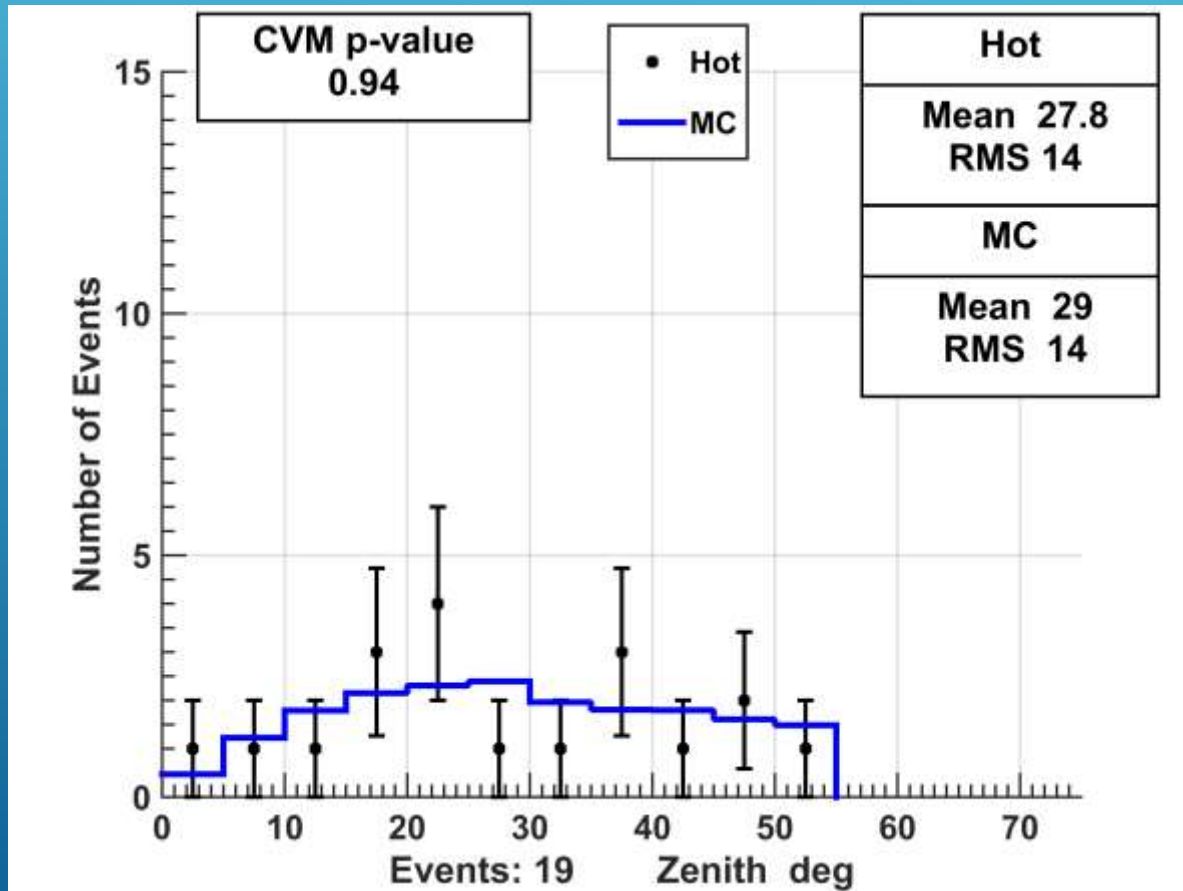
CORE



DATE

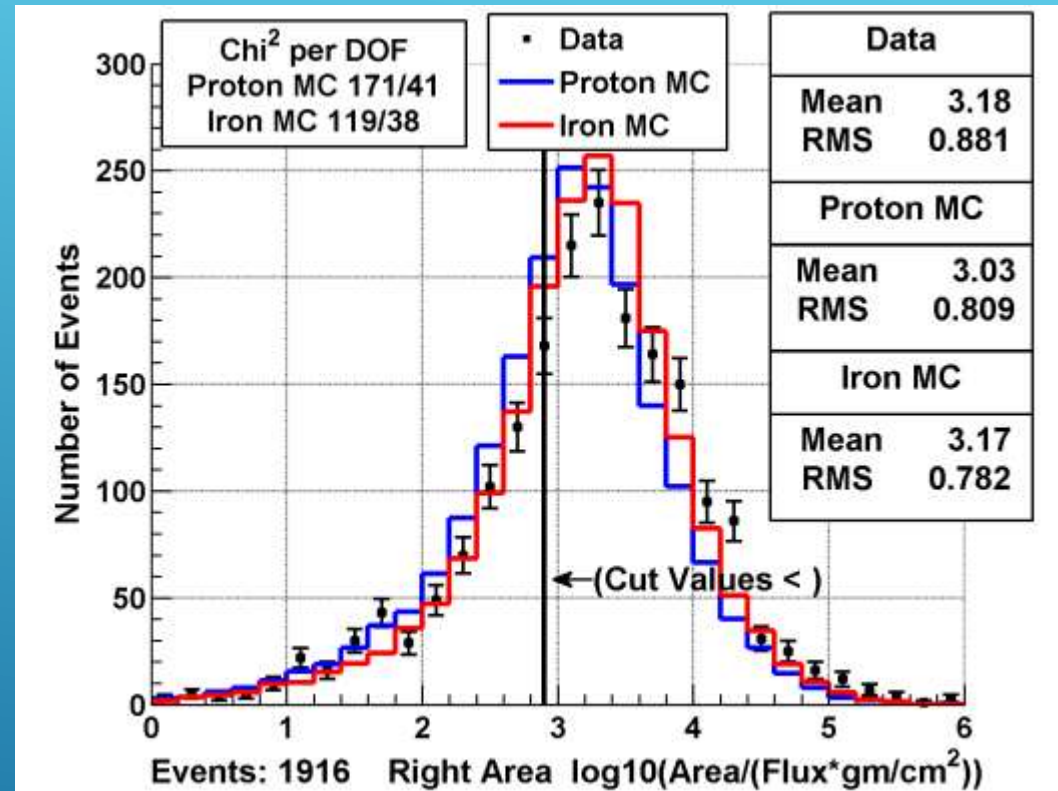
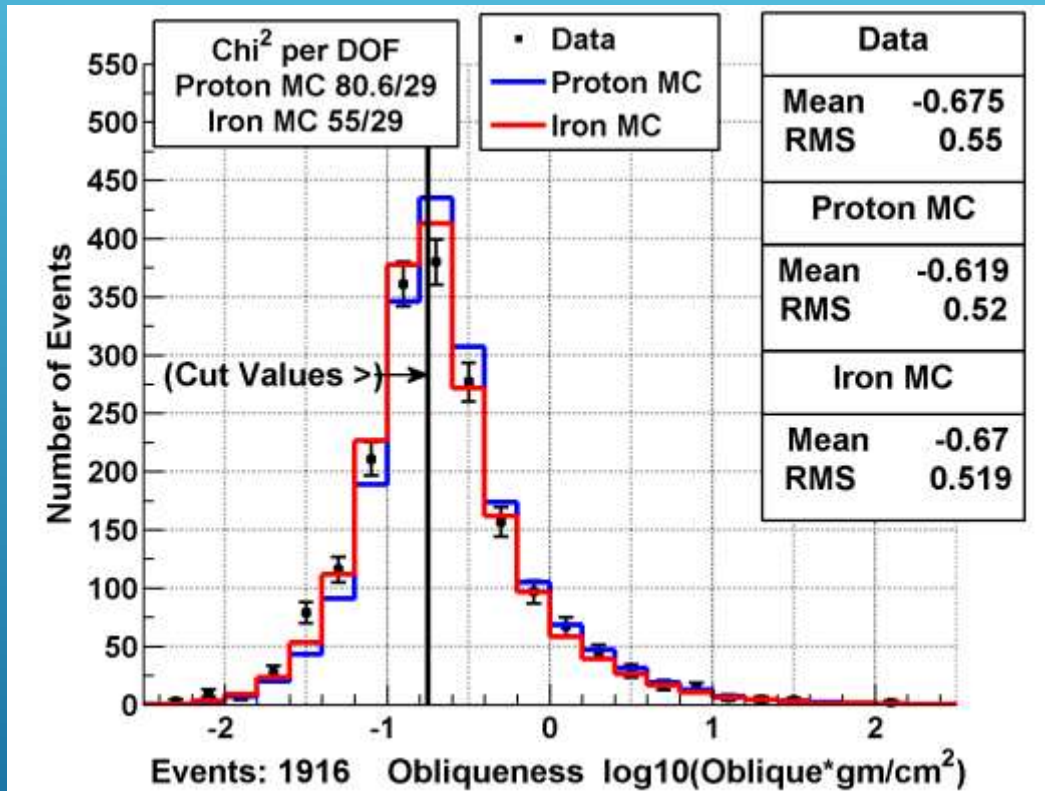


COMPARE HOTSPOT TO ISOTROPIC MC



COMPOSITION ADDITIONAL MATERIAL





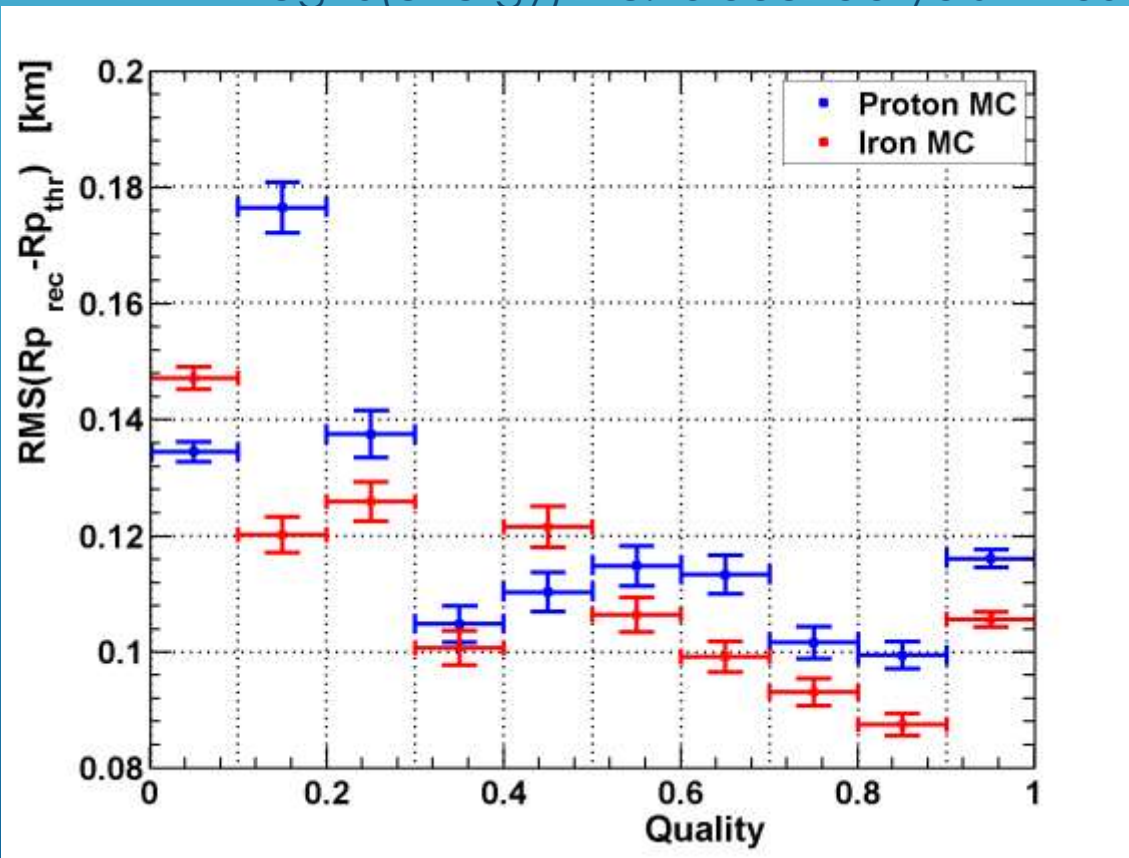
COMPUTER OBSERVER (YES/NO PRA) CUTS

Examples of attributes

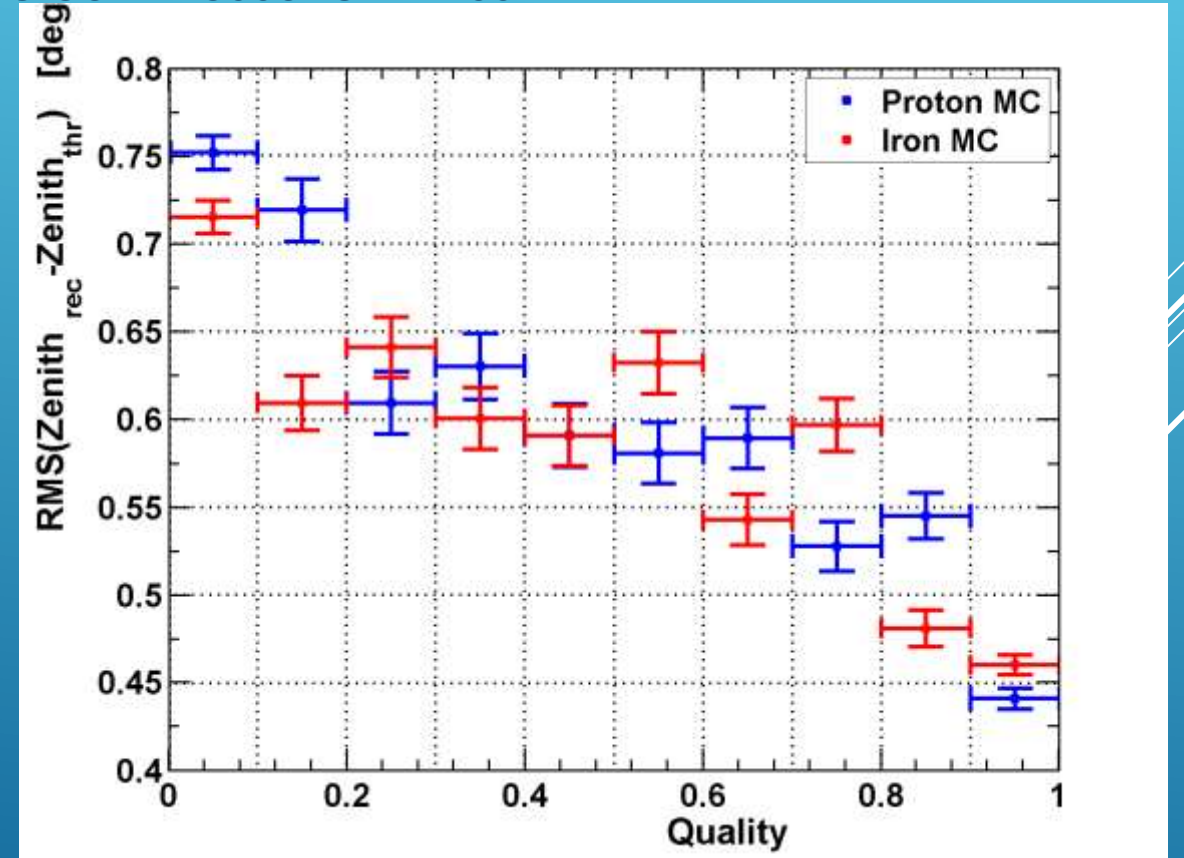
- ▶ At least 2 bins before apex and either end.
- ▶ Cubic term of quadratic fit used to find triangle apex.
- ▶ Size of small side of large triangle.
- ▶ Standard deviation of signal flux.
- ▶ Normalized maximum missing slant depth in profile.
- ▶ Obliqueness (perimeter/area) of large triangle.
- ▶ Allowed missing area between bins.
- ▶ Normalized Largest side of under right triangle.
- ▶ Ratio of normalized largest side of large triangle to apex angle.

RECONSTRUCTED VS. THROWN

- ▶ (Reconstructed – Thrown) Vs. Quality
- ▶ Minimum cuts applied to make limits of MC and data the same:
 - ▶ $\log_{10}(\text{energy}) > 18.2 \& \text{boundarydist} > -1500 \& \text{corediff} < 2500 \& \text{zenith} < 60$



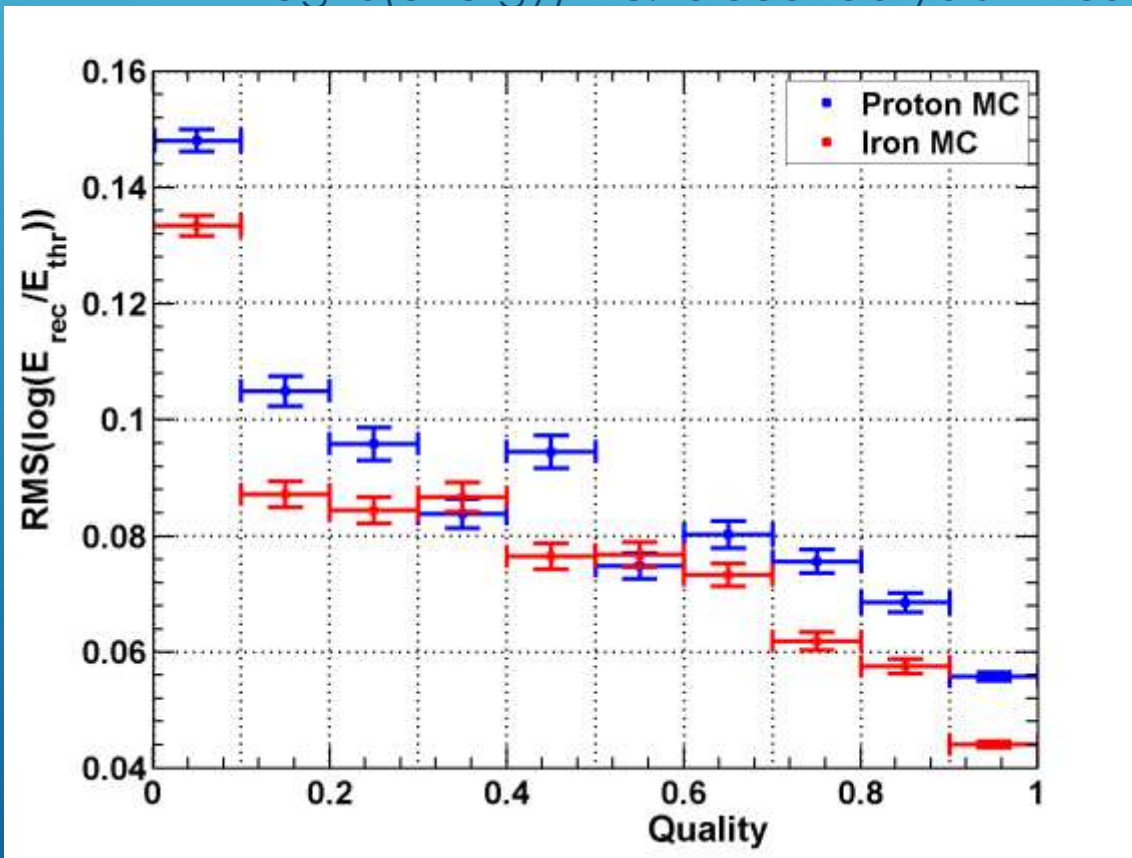
R_p



Zenith

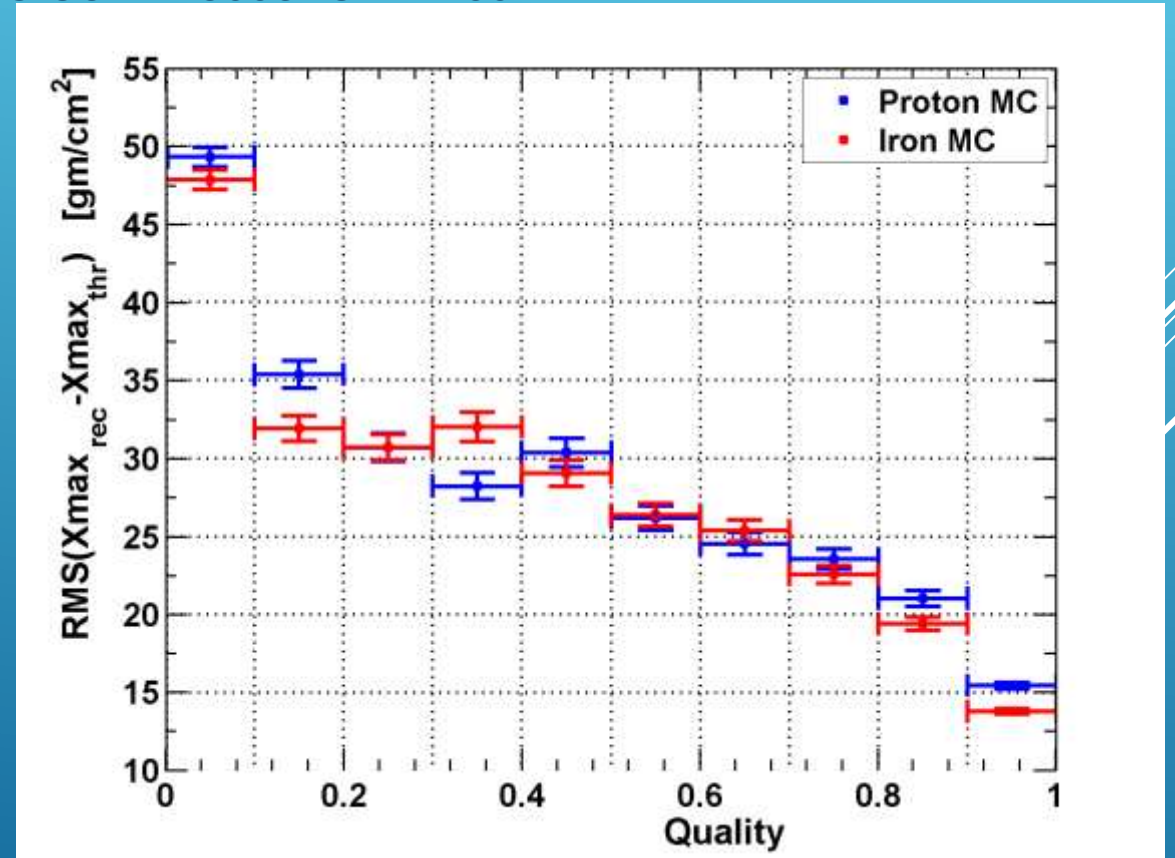
RECONSTRUCTED VS. THROWN

- ▶ (Reconstructed – Thrown) Vs. Quality
- ▶ Minimum cuts applied to make limits of MC and data the same:
 - ▶ $\log_{10}(\text{energy}) > 18.2$ & $\text{boundarydist} > -1500$ & $\text{corediff} < 2500$ & $\text{zenith} < 60$



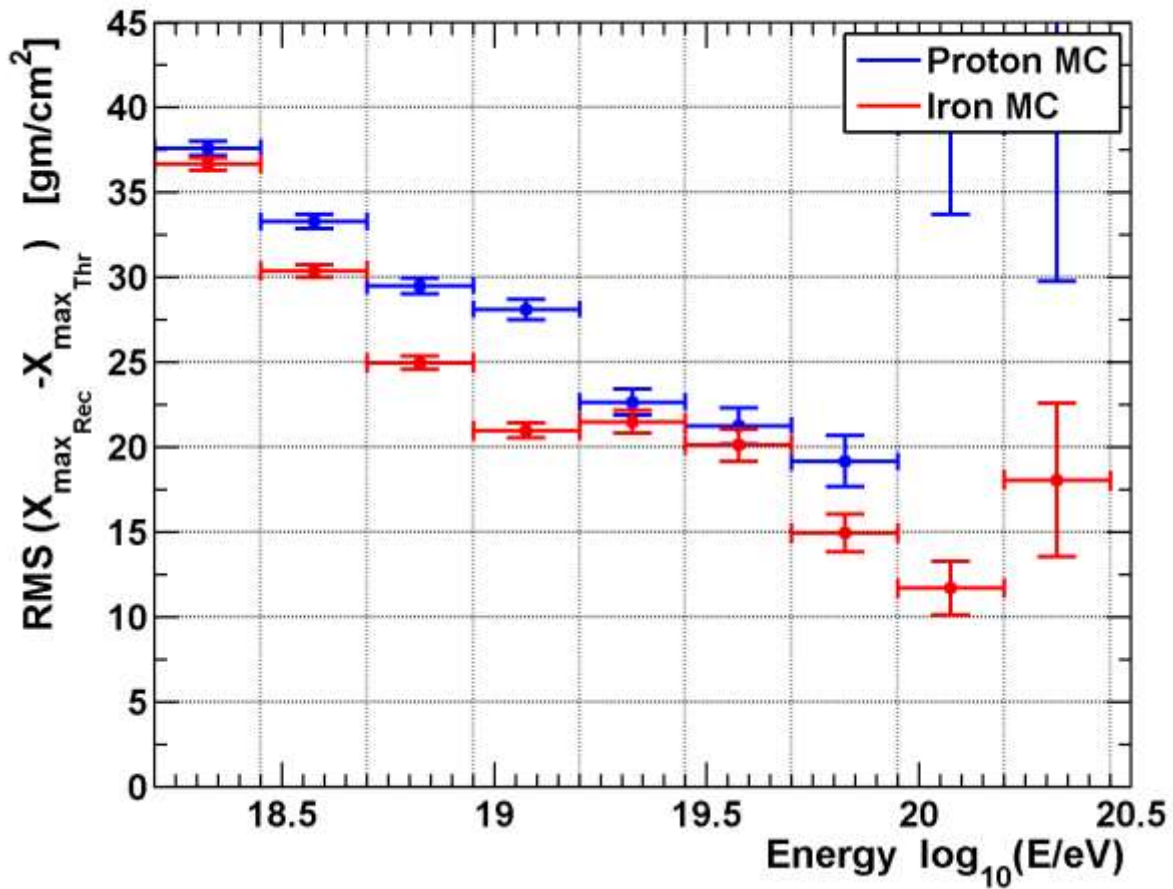
Energy

Less spread at higher quality.

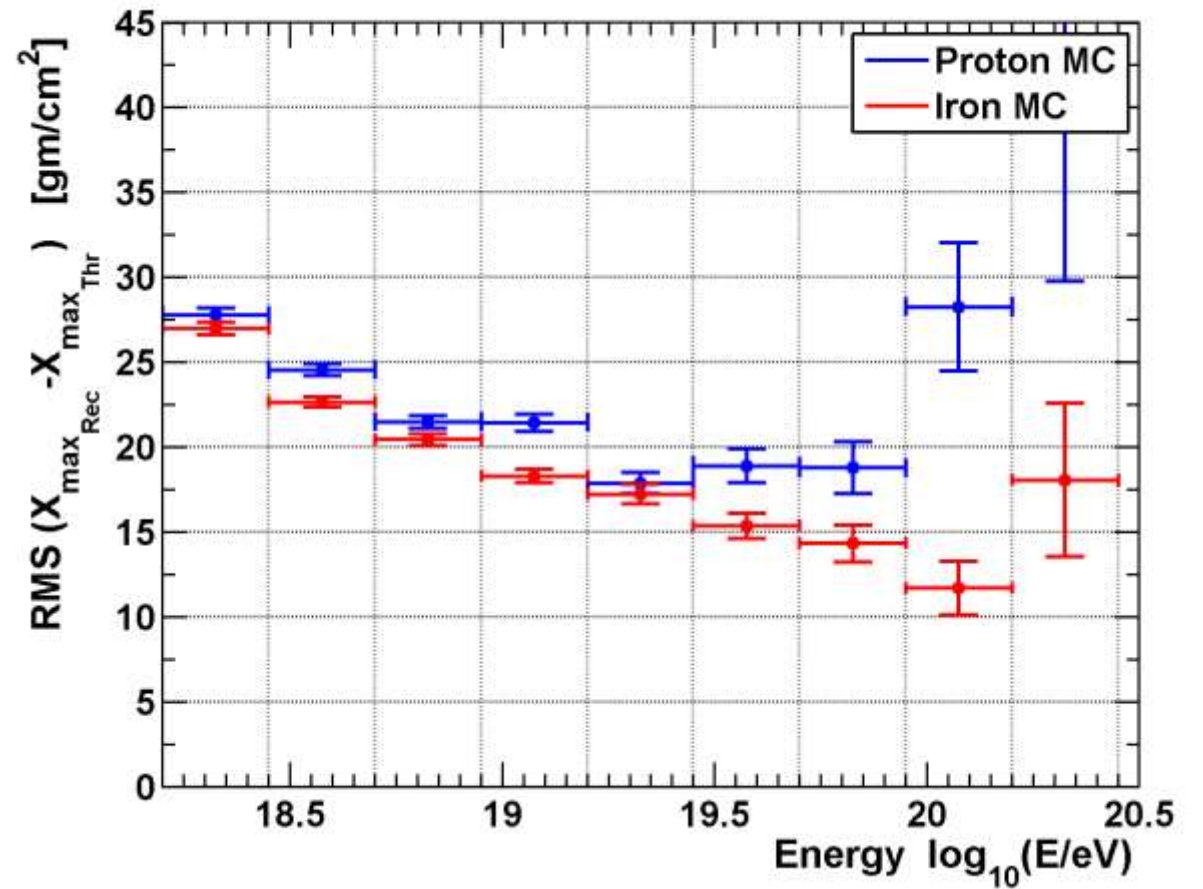


Xmax

RESOLUTION VS. ENERGY VS. Q THRESHOLD

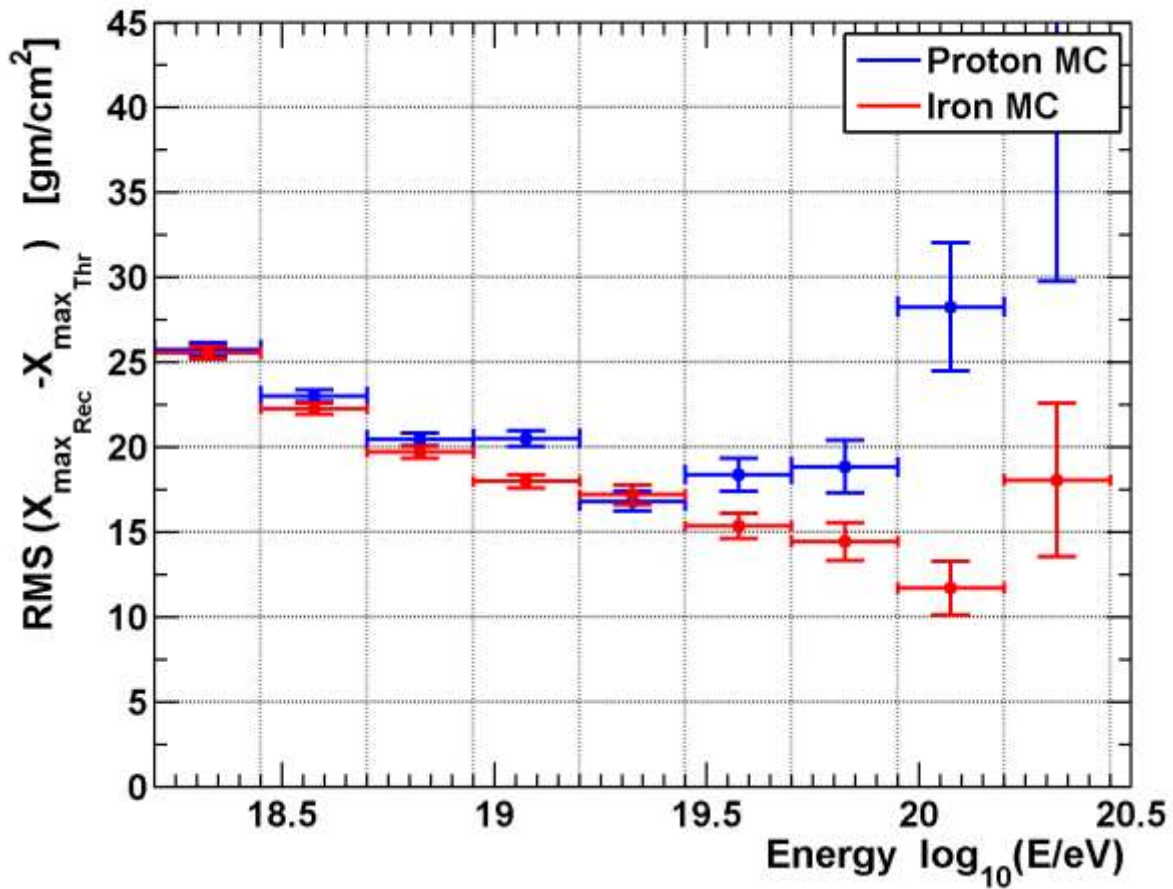


Q > 0

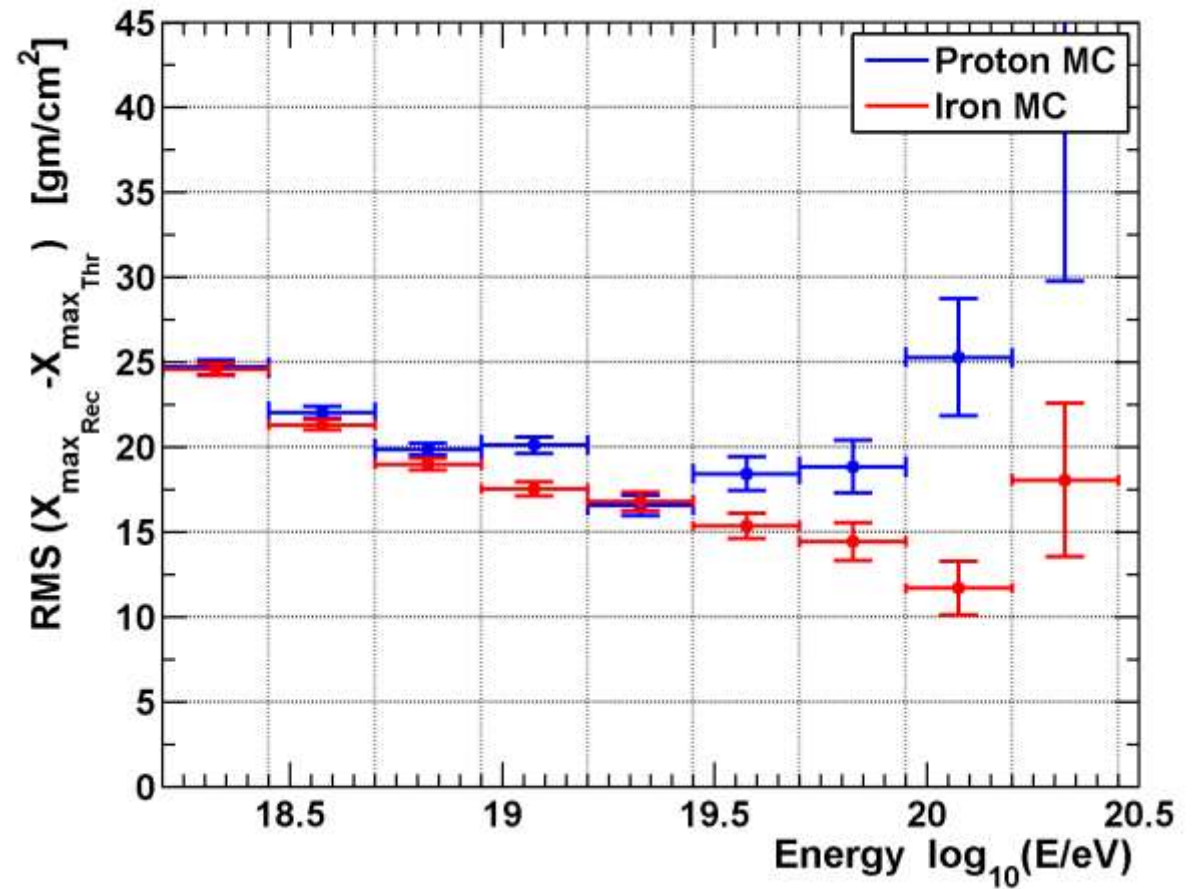


Q ≥ 0.1

RESOLUTION VS. ENERGY VS. Q THRESHOLD

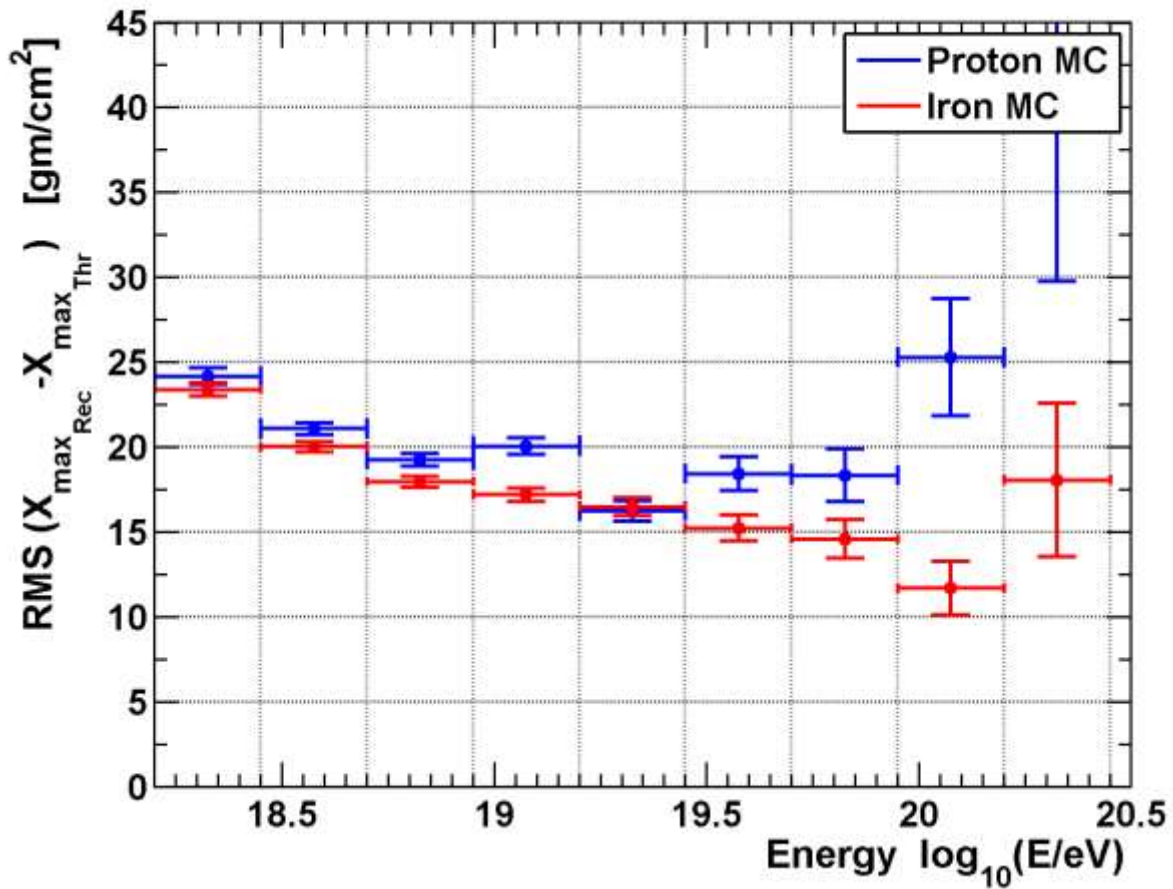


$Q \geq 0.2$

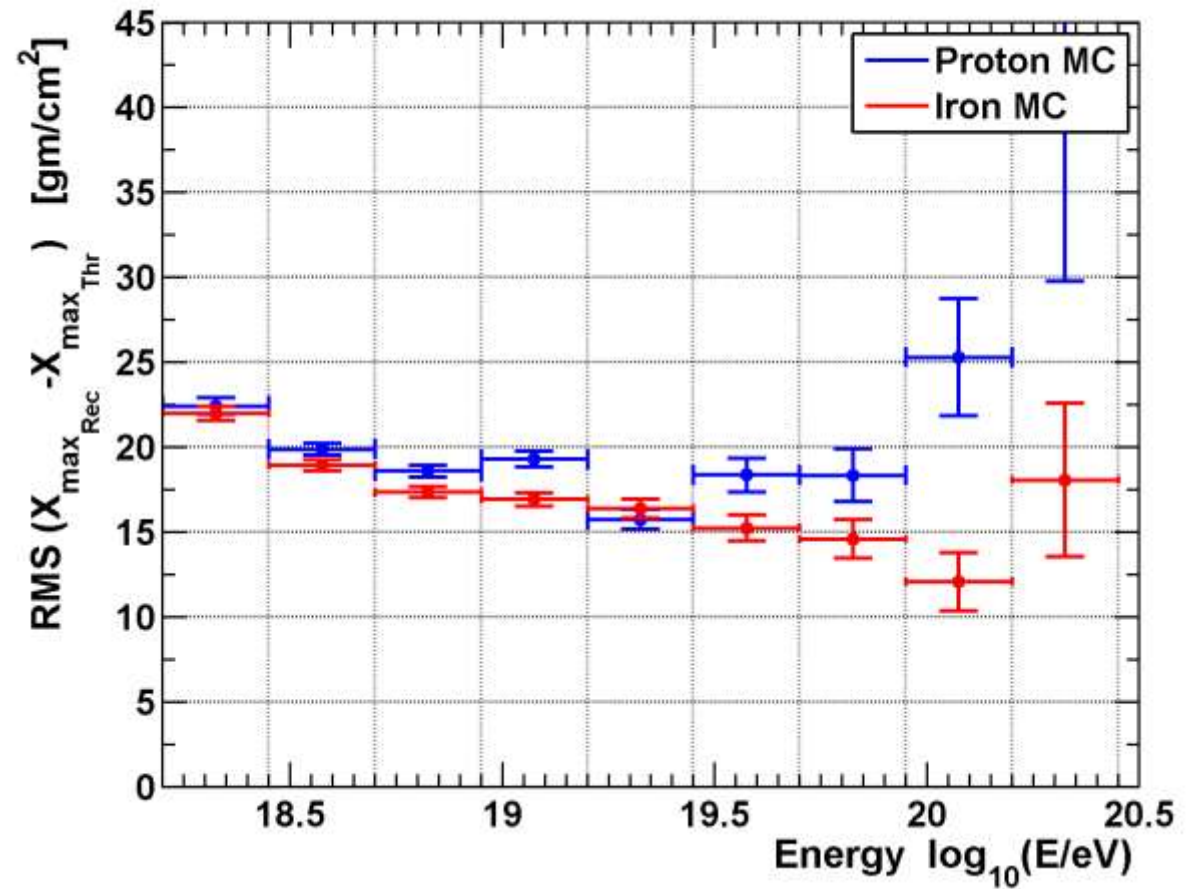


$Q \geq 0.3$

RESOLUTION VS. ENERGY VS. Q THRESHOLD

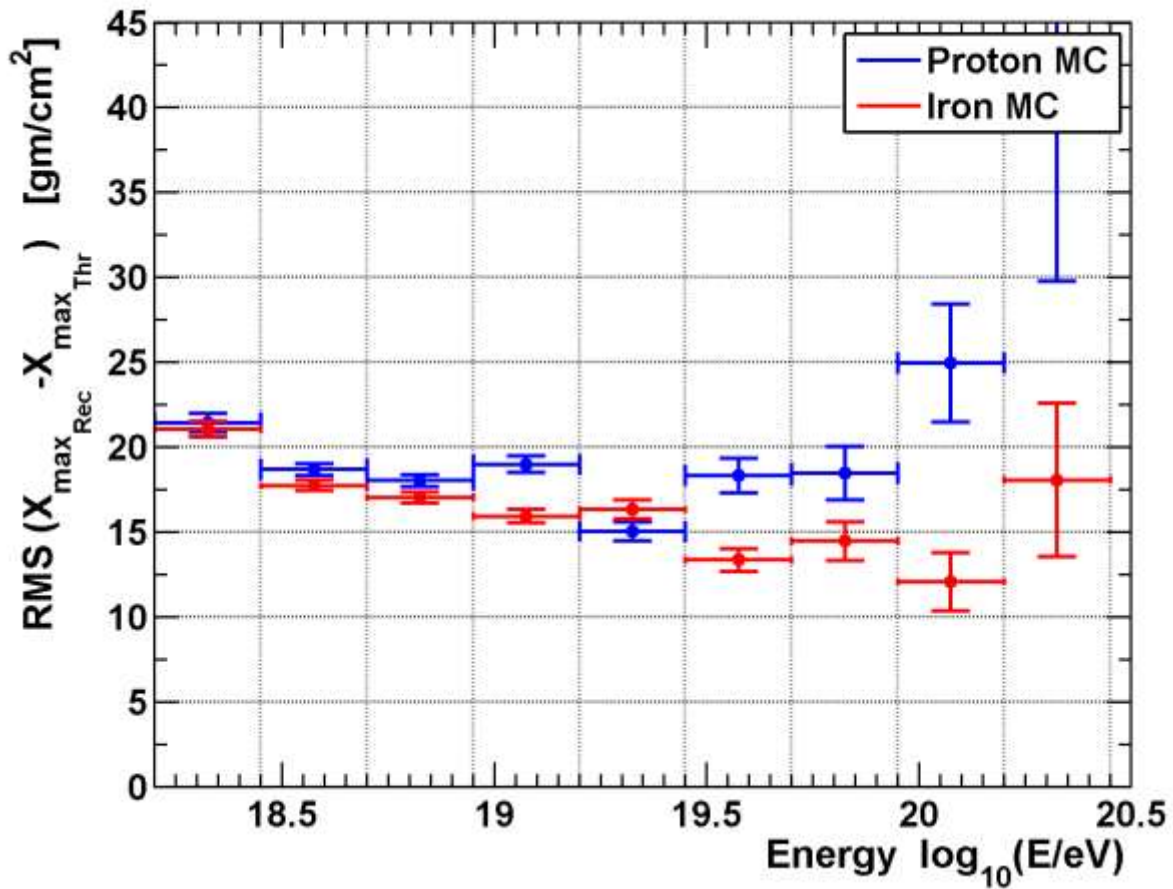


$Q \geq 0.4$

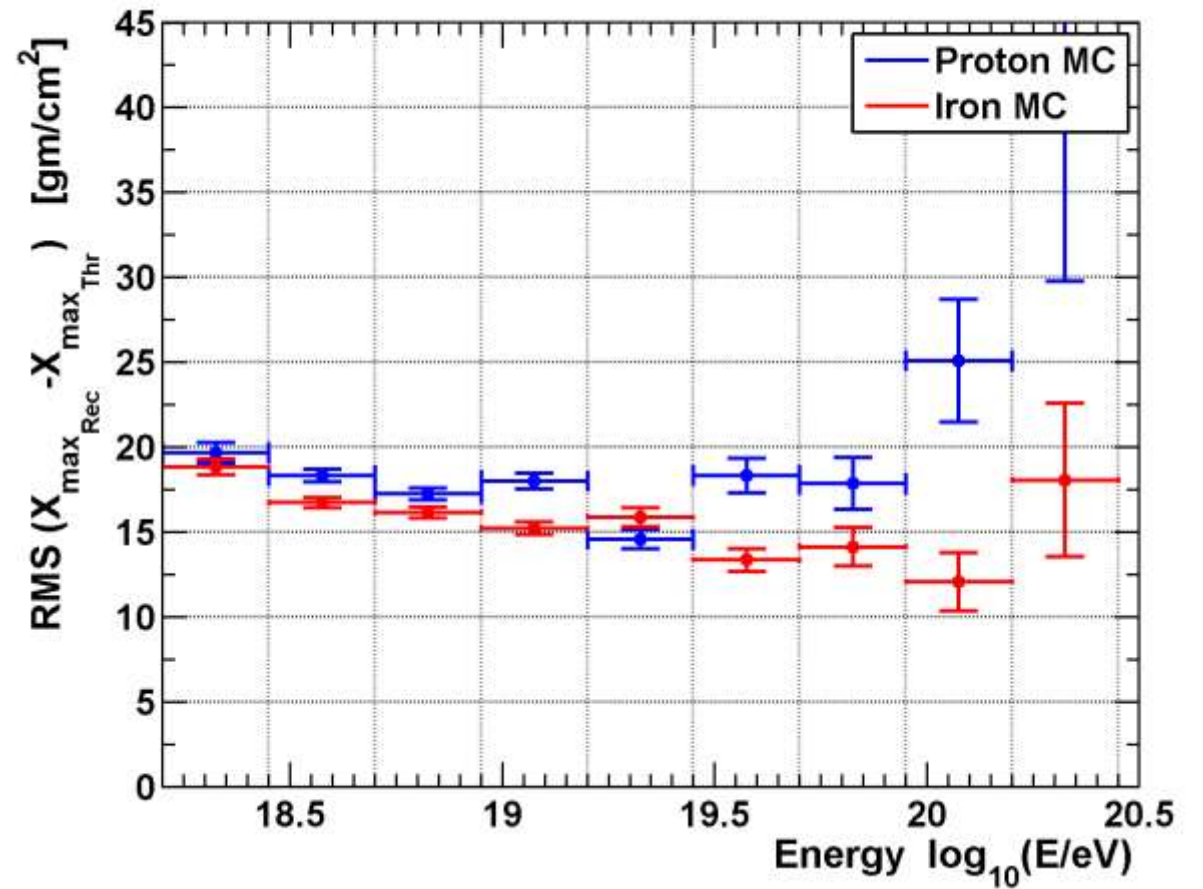


$Q \geq 0.5$

RESOLUTION VS. ENERGY VS. Q THRESHOLD



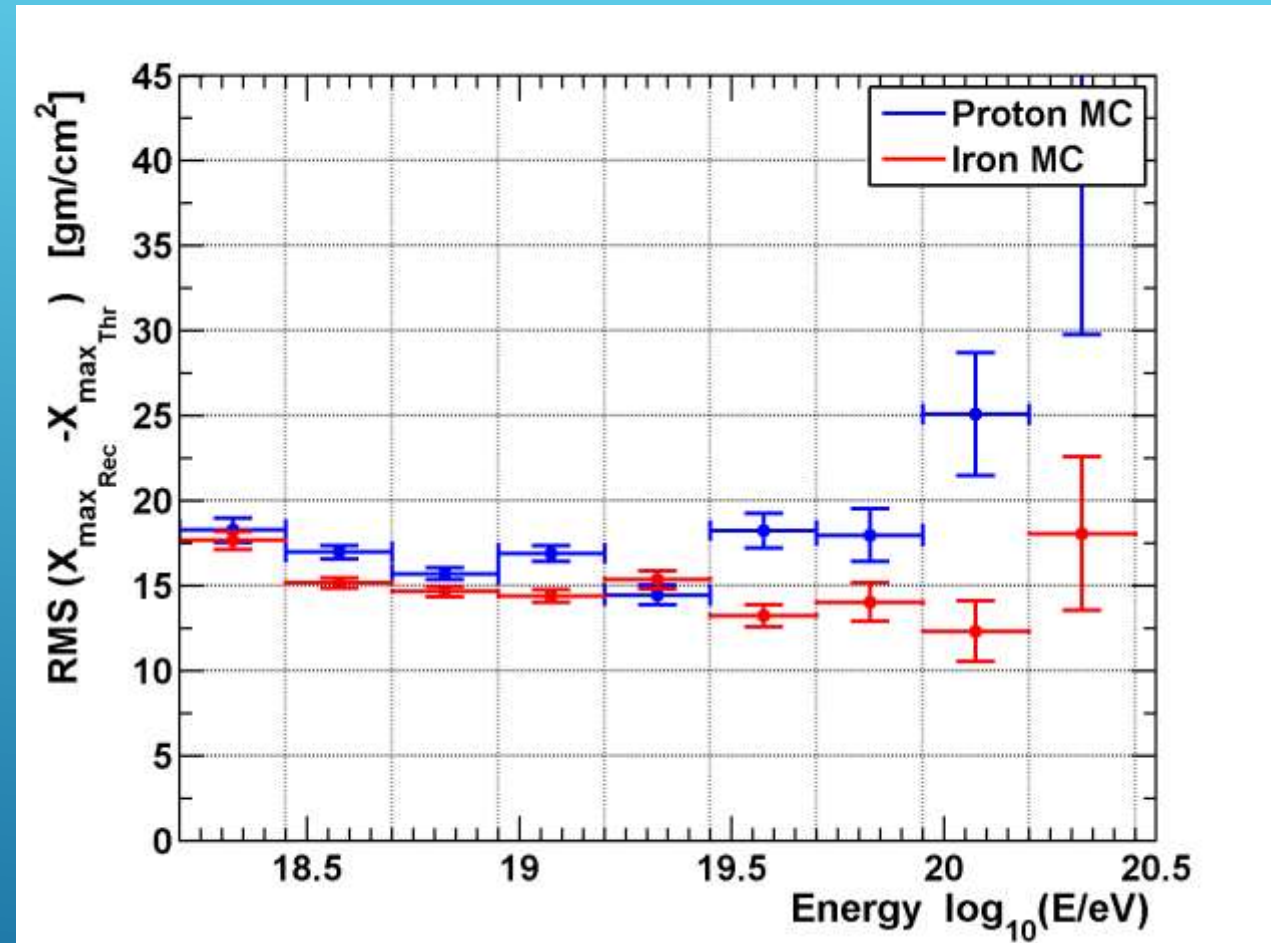
$Q \geq 0.6$



$Q \geq 0.7$

RESOLUTION VS. ENERGY VS. Q THRESHOLD

Resolution with respect to energy flattens with increasing Quality



$Q \geq 0.8$

SYSTEMATIC ERRORS

$$\langle X_{max} \rangle = 751 \pm 16.3 \text{ sys.} \pm 9.4 \text{ stat. } gm/cm^2 \text{ at } \log_{10}(E) = 19$$

$\langle X_{max} \rangle$ Systematic errors include:

Mirror alignment (known to $\pm 0.05^\circ$): $\pm 2.6 gm/cm^2$

Atmosphere Density (US 1976 Standard Vs. Yearly Ave. Radiosonde): $\pm 11.7 gm/cm^2$

Vertical Aerosol Optical Depth (VAOD) Nightly Variation: $\pm 2 gm/cm^2$

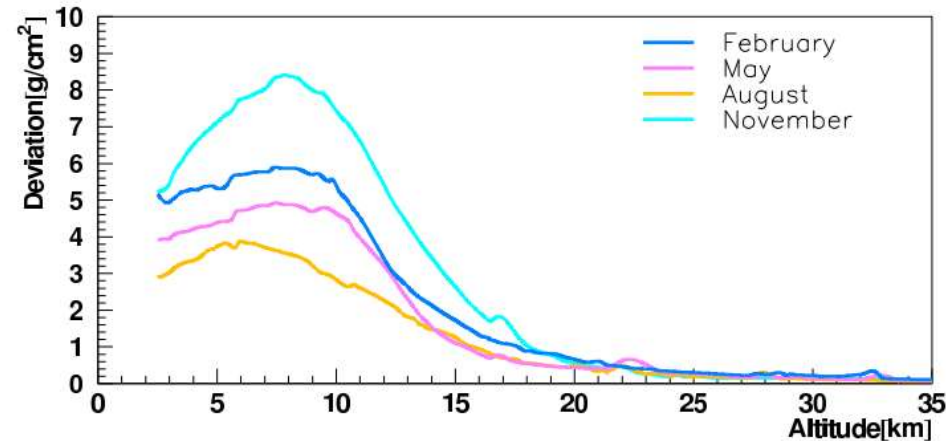
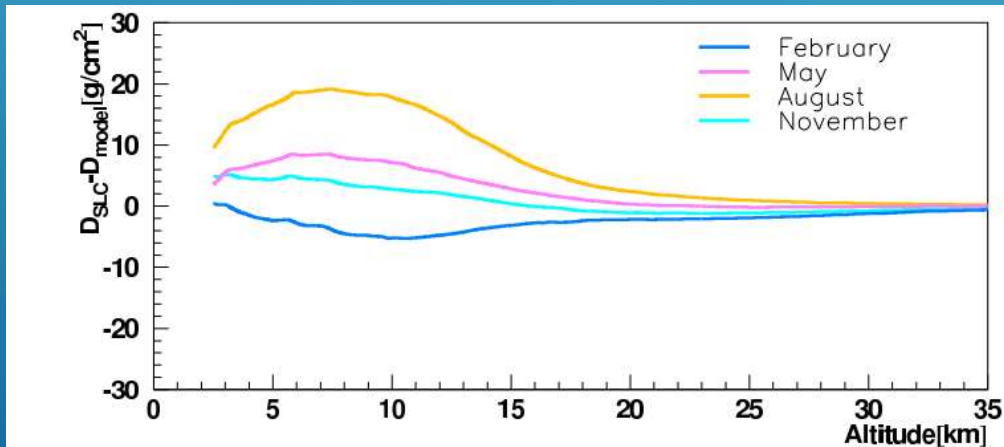
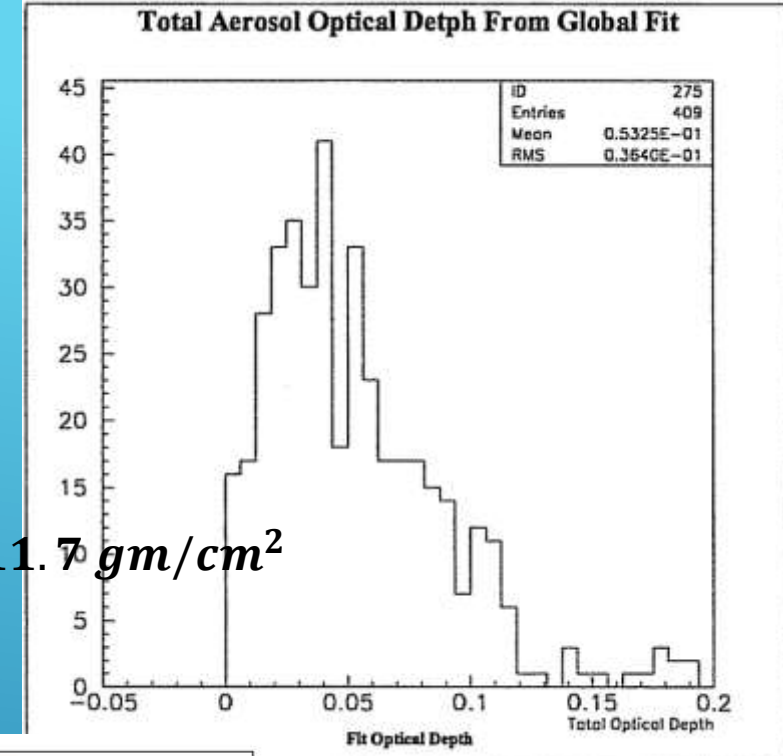
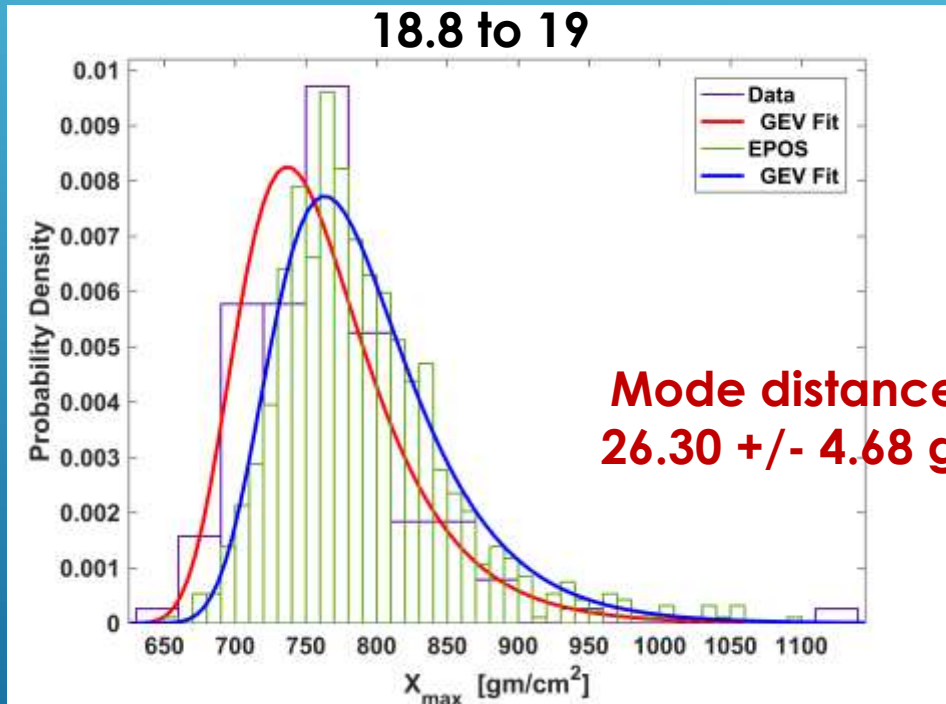


Figure 1. Differences of atmospheric depth from the US-SA model (left: average, right: standard deviation)

ROBUST MEASURE OF BIAS

L-test shift - robust bias measure for skewed distributions
(Distance between population modes/locations)

EPOS PROTON
18.8 to 19



Mode distance of GEV fit distributions
26.30 +/- 4.68 g/cm² (fit uncertainty)

Procedure: **5000 random number sets from fitted distributions and measure distances**

Test: Measure L-test Shifts, Difference of sample modes
Difference of medians, and Difference of Means

Data Set

#data = 127, #MC = 937

- **Shift: 25.2 g/cm²**
- **Mode: 95.5 g/cm²**
- **Median: 28.2 g/cm²**
- **Mean: 22.2 g/cm²**

Distances of 5000 MC

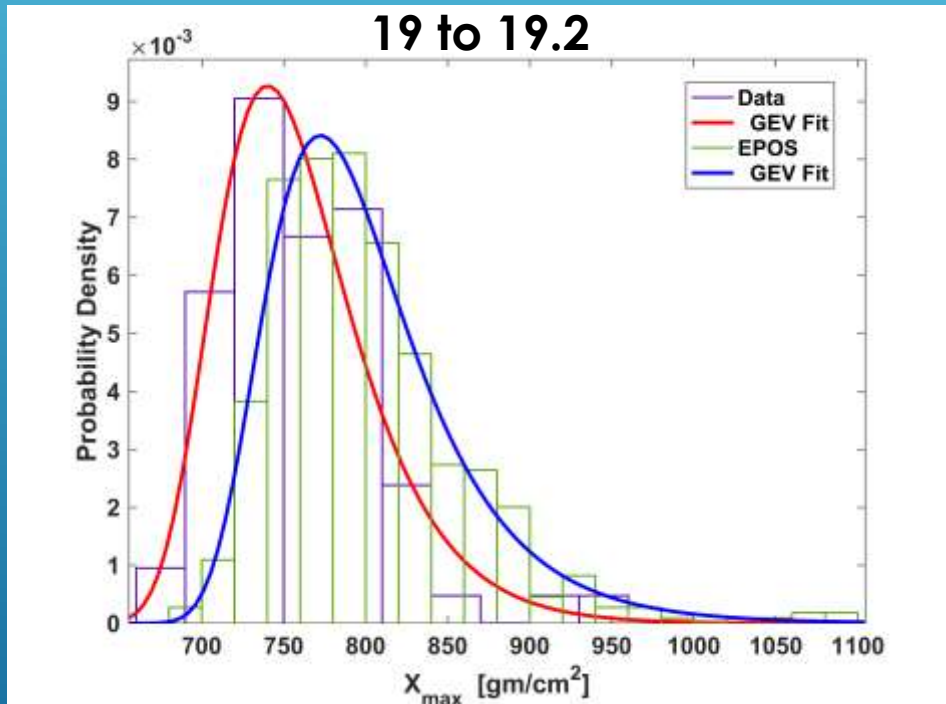
- **Shift: 26.7 RMS 4.8 g/cm²**
- **Mode: 5.9 RMS 12.3 g/cm²**
- **Median: 27.3 RMS 6.1 g/cm²**
- **Mean: 27.9 RMS 5.6 g/cm²**

ROBUST MEASURE OF BIAS

L-test shift - robust bias measure for skewed distributions
(Distance between population modes /locations)

EPOS PROTON

19 to 19.2



Mode distance of GEV fit distributions
 $34.78 \pm 5.68 \text{ g/cm}^2$

Procedure: 5000 random number sets from fitted distributions
and measure distances

Distances of 5000 MC

Data Set

#data = 70, #MC = 549

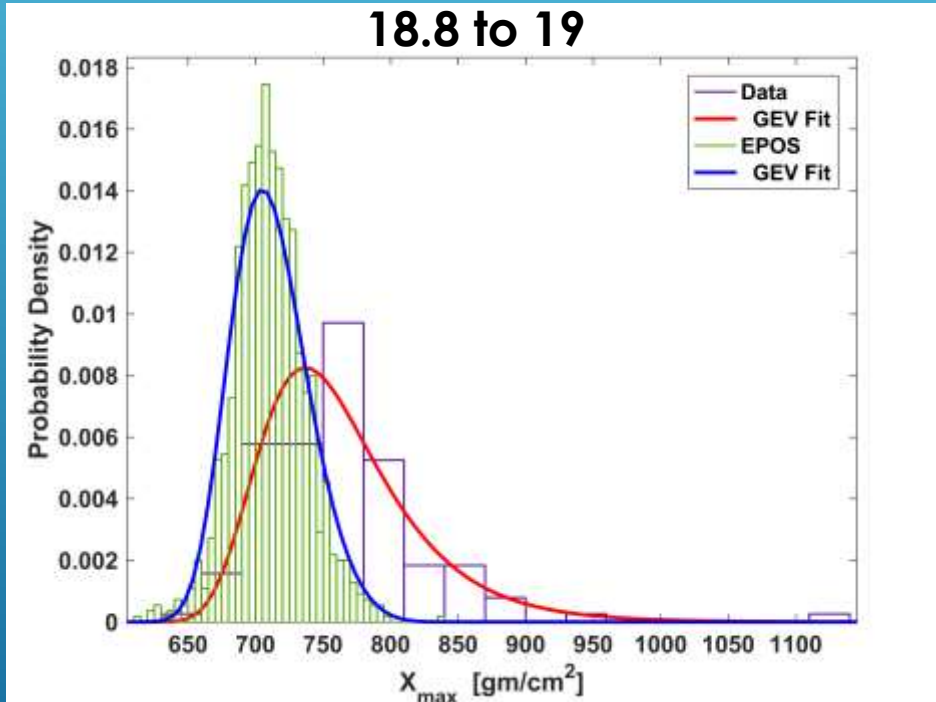
- Shift: 34.83 g/cm²
- Mode: 114.87 g/cm²
- Median: 30.45 g/cm²
- Mean: 39.77 g/cm²

- Shift: 36.1 RMS 5.8 g/cm²
- Mode: 16.4 RMS 12.7 g/cm²
- Median: 36.4 RMS 7.3 g/cm²
- Mean: 39.8 RMS 6.4 g/cm²

ROBUST MEASURE OF BIAS

L-test shift - robust bias measure for skewed distributions
(Distance between population modes /locations)

EPOS IRON
18.8 to 19



Mode distance of GEV fit distributions
-37.4 +/- 4.4 g/cm²

Data Set

#data = 127, #MC = 1100

- **Shift: -46.9 g/cm²**
- **Mode: +36.5 g/cm²**
- **Median: -48.0 g/cm²**
- **Mean: -52.5 g/cm²**

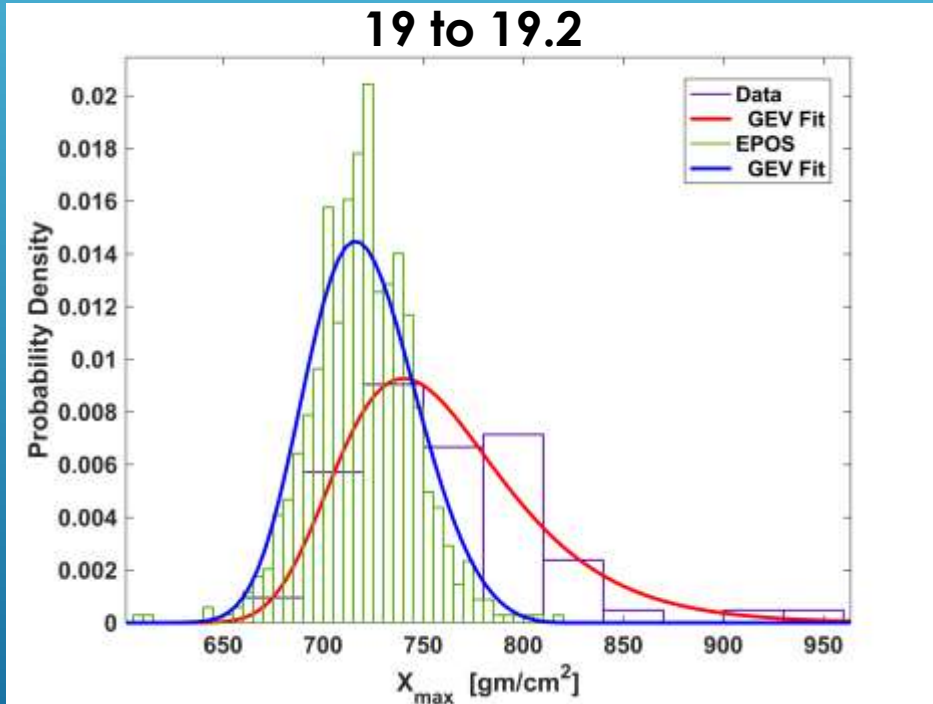
Distances of 5000 MC

- **Shift: -43.1 RMS 5.2 g/cm²**
- **Mode: -28.6 RMS 11.6 g/cm²**
- **Median: -44.3 RMS 5.8 g/cm²**
- **Mean: -52.3 RMS 5.2 g/cm²**

ROBUST MEASURE OF BIAS

L-test shift - robust bias measure for skewed distributions
(Distance between population modes /locations)

EPOS IRON 19 to 19.2



#data = 70, #MC = 685

Data Set

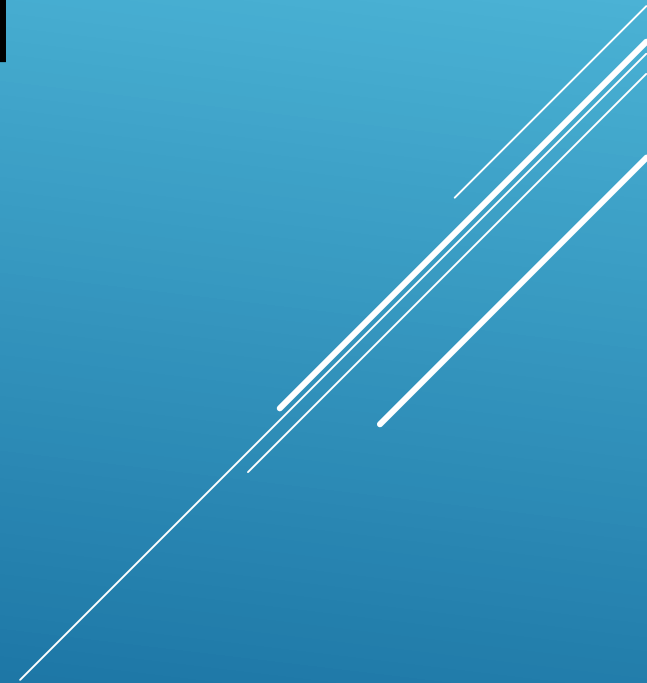
- **Shift:** -37.3 g/cm²
- **Mode:** +16.8 g/cm²
- **Median:** -39.9 g/cm²
- **Mean:** -40.7 g/cm²

Mode distance of GEV fit distributions
-28.92 +/- 5.39 g/cm²

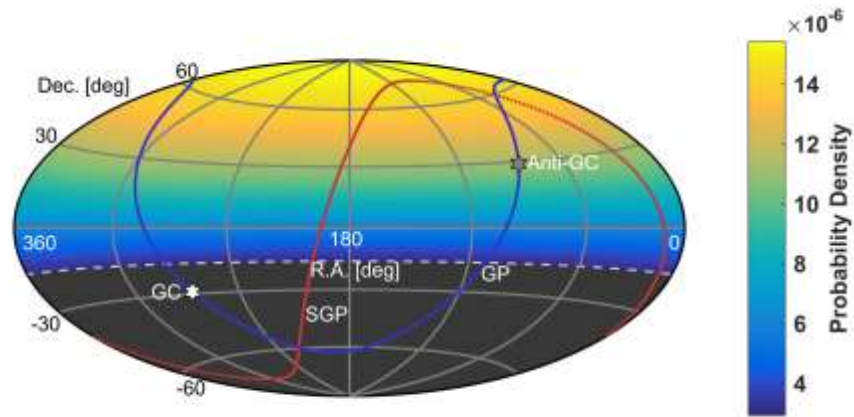
Distances of 5000 MC

- **Shift:** -33.87 RMS 6.16 g/cm²
- **Mode:** -29.3 RMS 12.6 g/cm²
- **Median:** -34.26 RMS 6.86 g/cm²
- **Mean:** -40.22 RMS 5.98 g/cm²

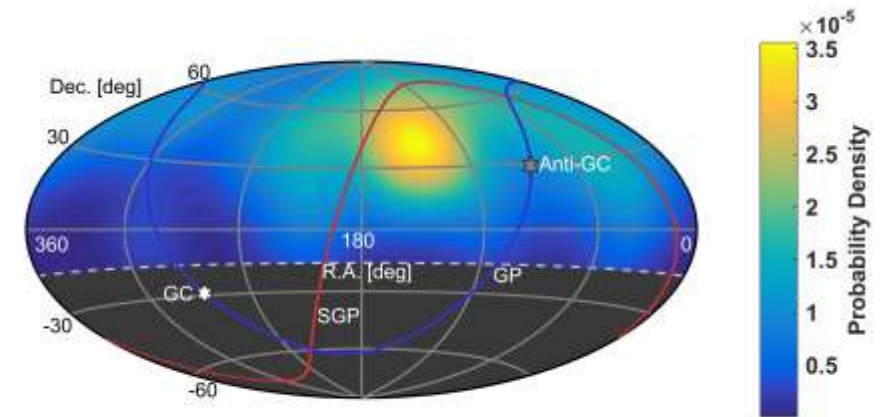
KERNEL DENSITY ESTIMATION ADDITIONAL MATERIAL



KERNEL DENSITY ESTIMATION



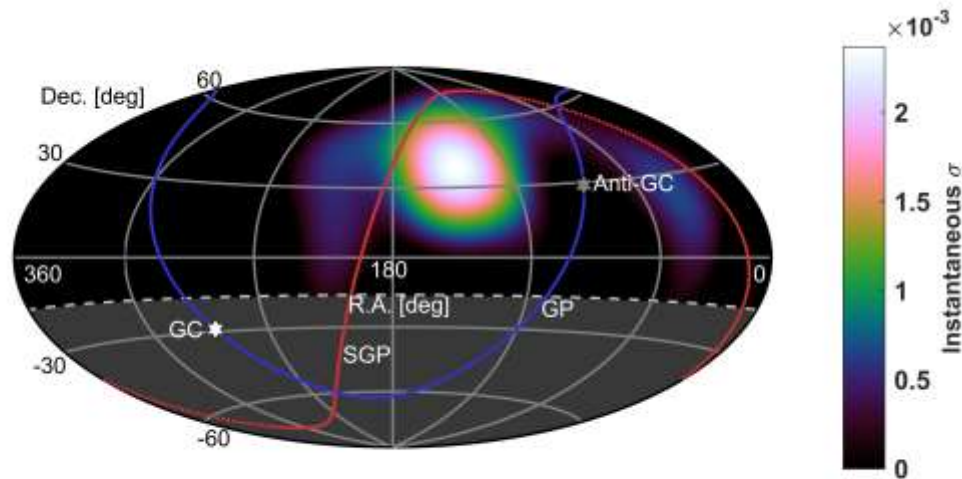
5 year
tight cuts
shown



Test statistic: Wald's Proportion test

$$Z = \frac{\hat{p} - p_{bg}}{\sqrt{\hat{p}(1-\hat{p})}} \text{ Flattest Dec. Response}$$

Optimal von-Mises-Fisher kernel concentration for PDF
found automatically for data and MC

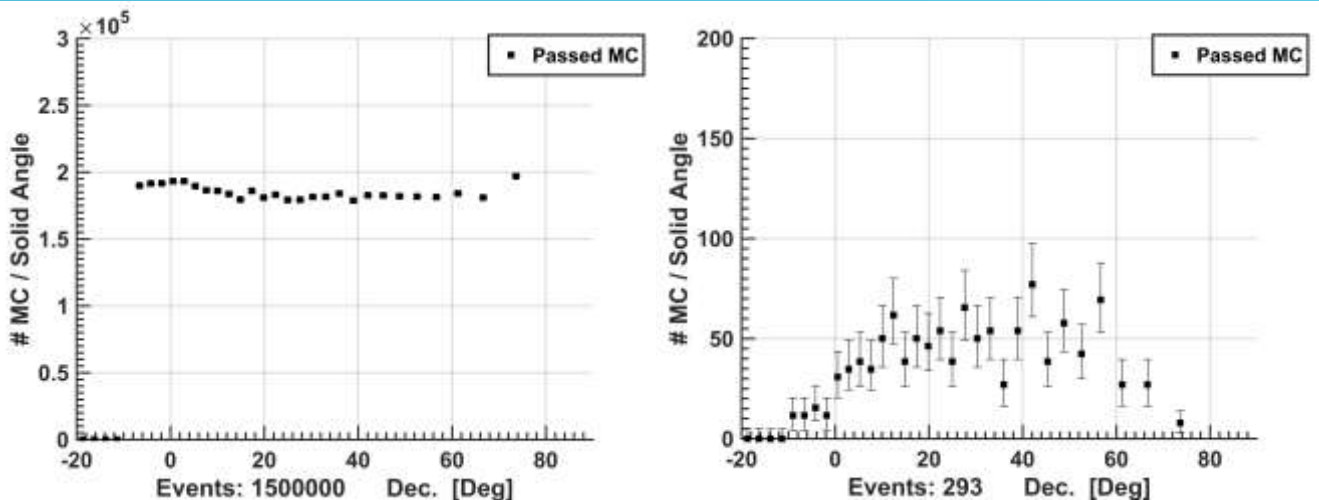


Post-trial sigmas
5 to 9 year

Loose cuts: 3.89, 4.36, 3.84, 2.92, 2.78

Tight cuts: 3.72, 4.39, 3.81, 3.06, 2.98

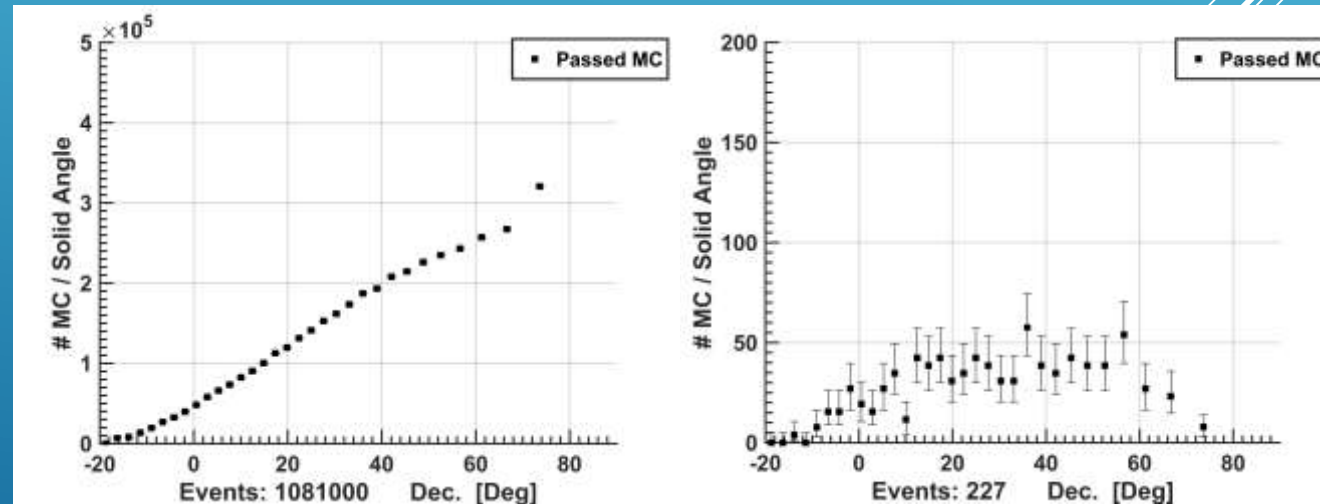
KDE DECLINATION RESPONSE



5 year simulation
Wald Test Statistic
All maximums

5 year simulation
Wald Test Statistic
Passed maximums

Next best statistic: $p/\sqrt{p_{bg}}$

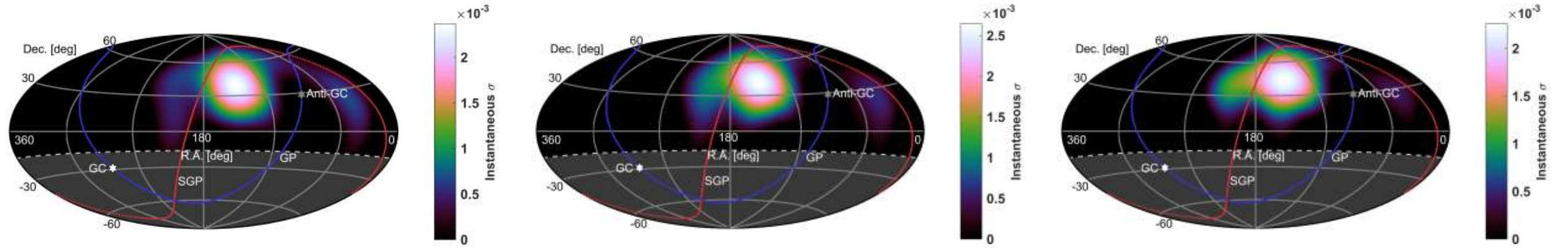


5 year simulation
All maximums

5 year simulation
Passed maximums

Equal opening angle grid. p_{bg} calculated with trigger times for each year.

KDE PDF TIGHT CUTS

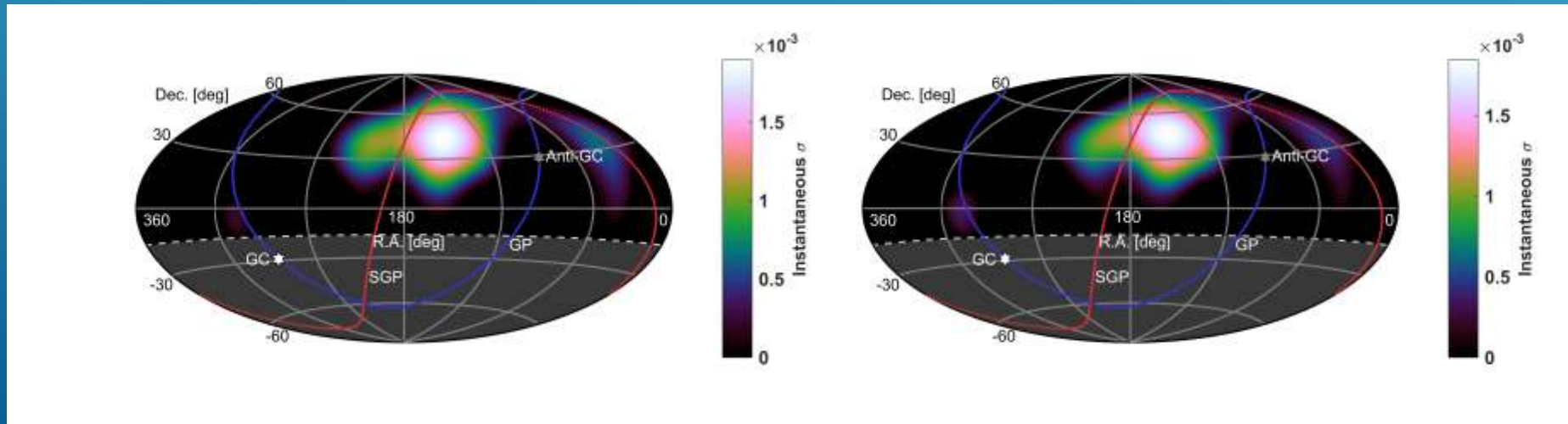


5 year

6 year

7 year

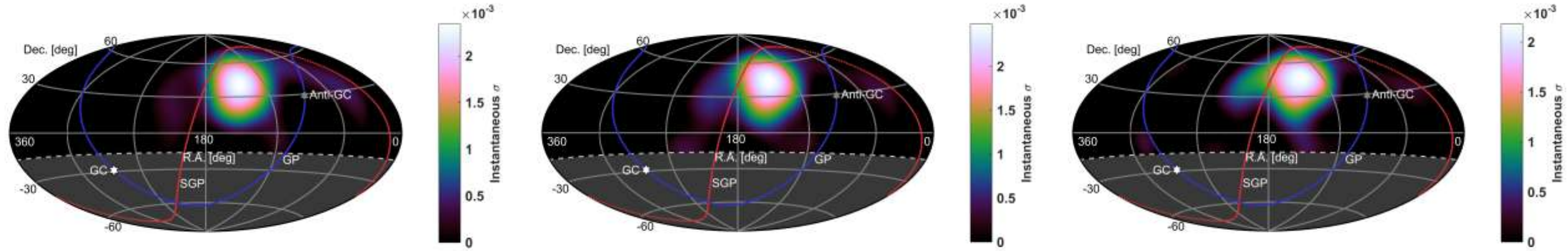
8 year



9 year

Equal opening angle grid. p_{bg} calculated with trigger times for each year.

KDE PDF LOOSE CUTS

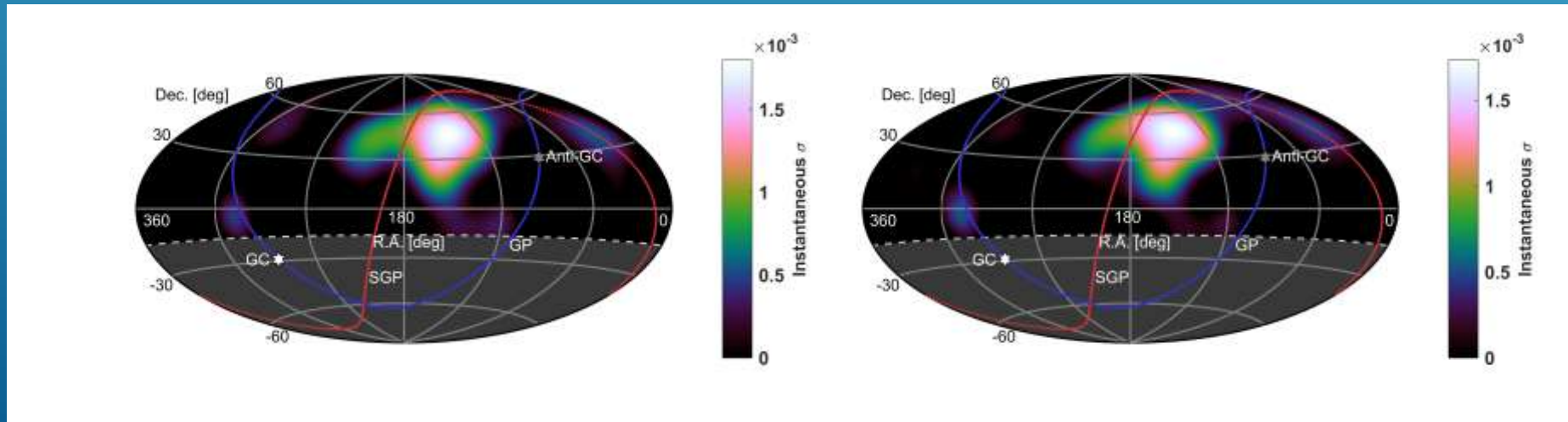


5 year

6 year

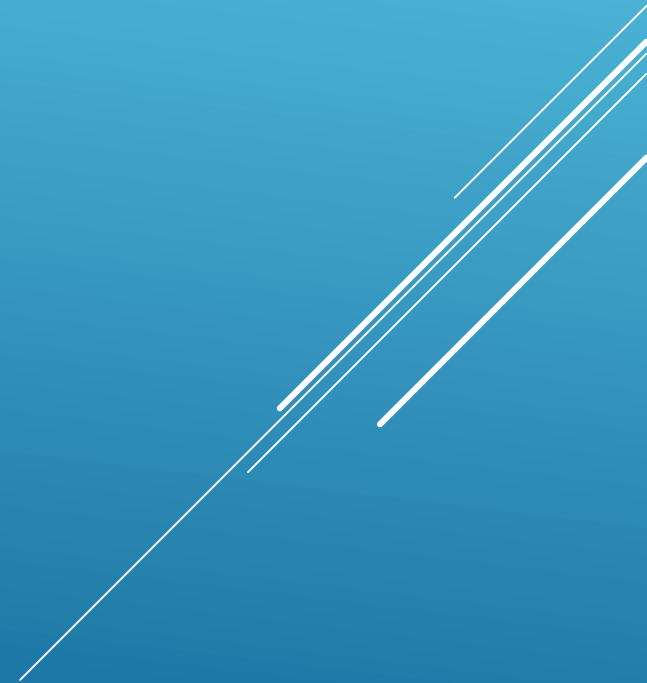
7 year

8 year



9 year

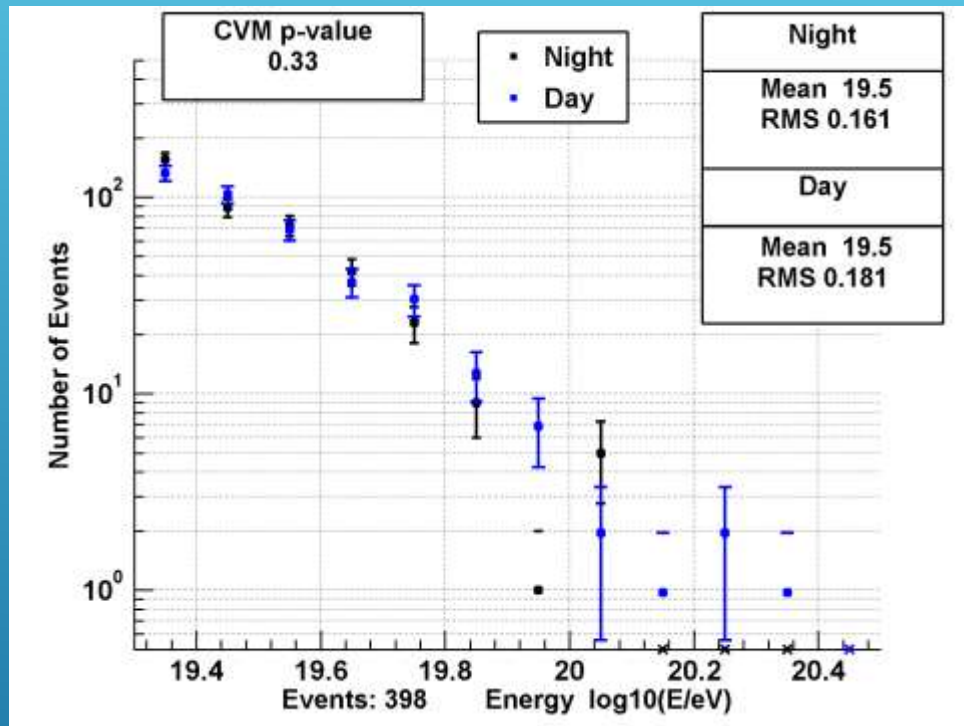
**EVEN MORE HOT/COLD
ADDITIONAL MATERIAL**



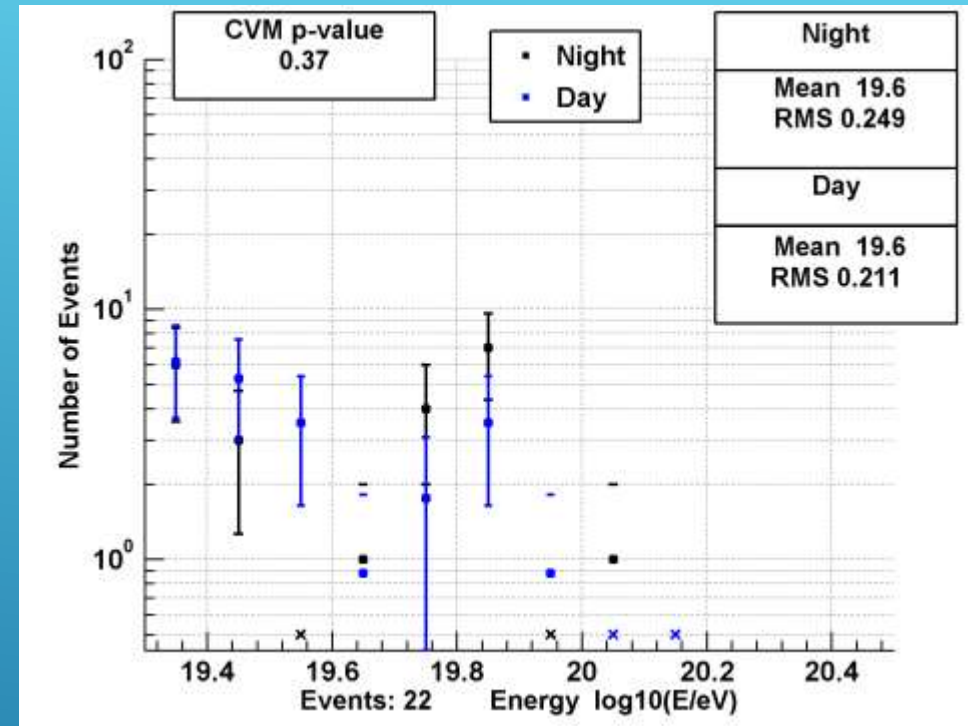
HOT/COLD SPOT -SUMMER/WINTER AND NIGHT/DAY

Jon Paul Lundquist

DAY/NIGHT ENERGY DISTRIBUTION COMPARISON



Outside hot/cold spot



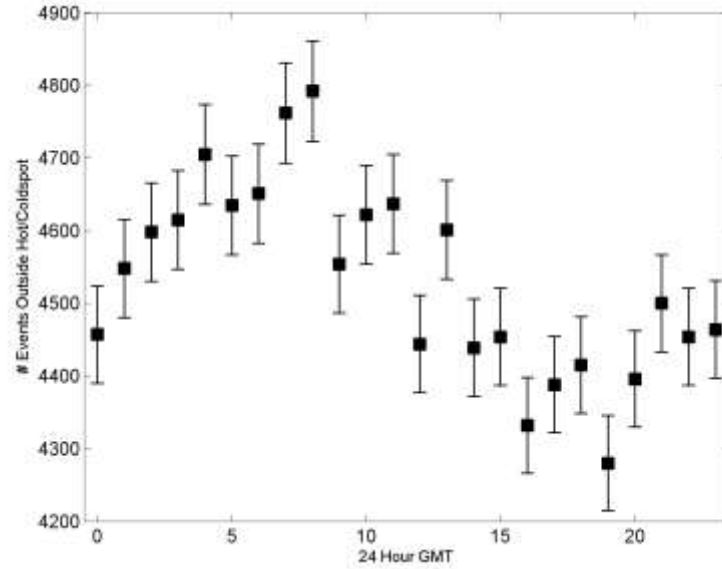
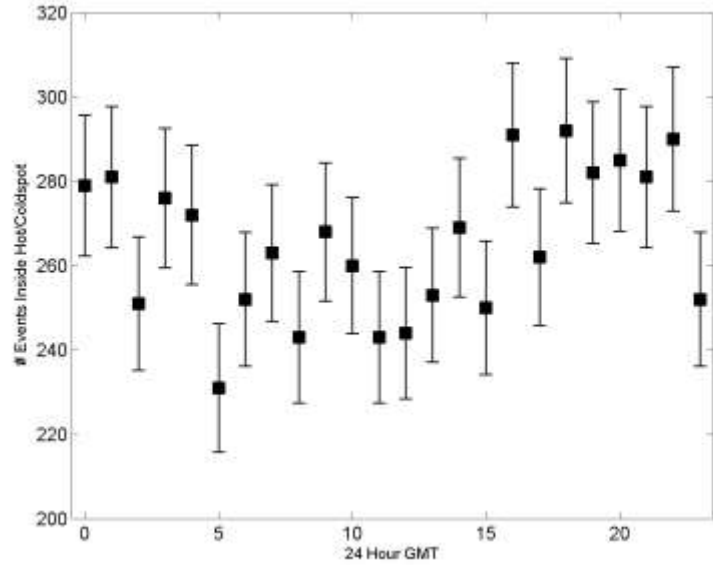
Inside hot/cold spot

Energy distributions agree within statistics

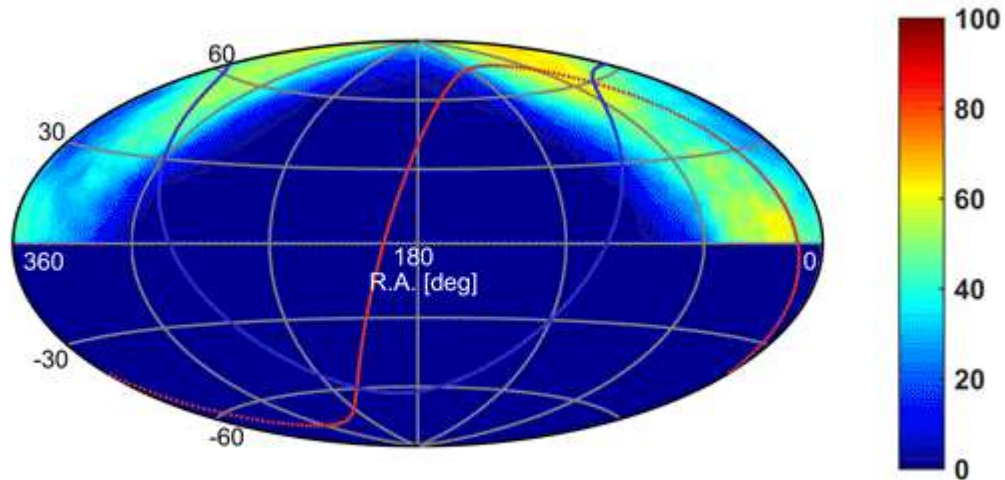
FIELD OF VIEW PROBLEM

INSIDE

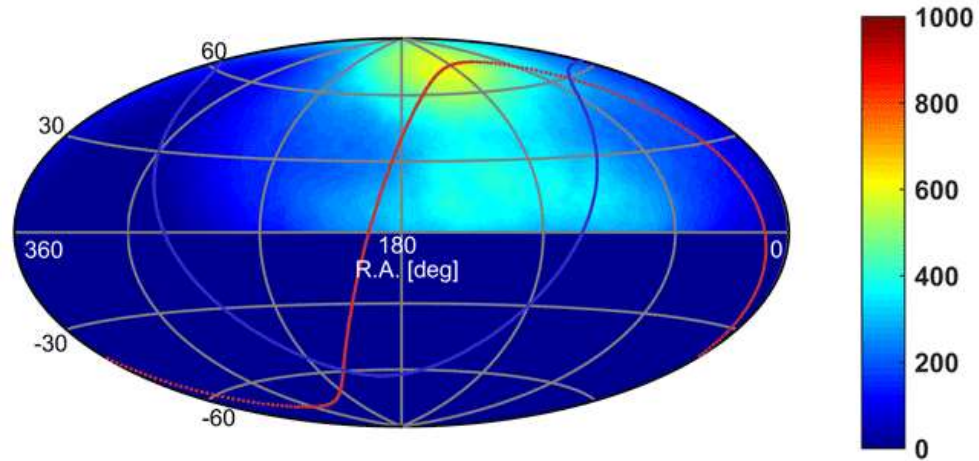
OUTSIDE



Inside hot/cold spot number of Events per hour is different than overall sky due to TA decl. = 40

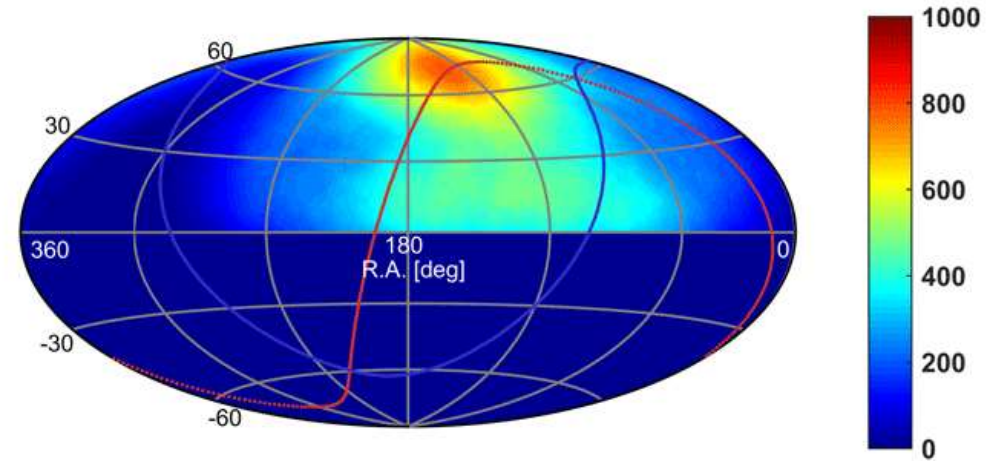


FIELD OF VIEW PROBLEM



Night – January to December

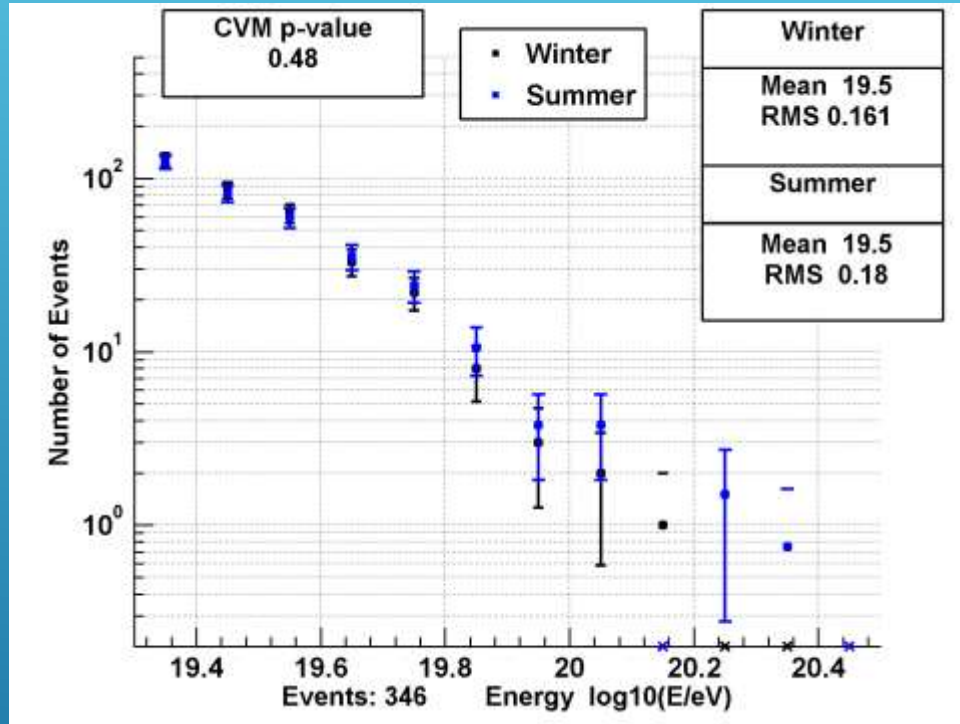
Uneven in RA



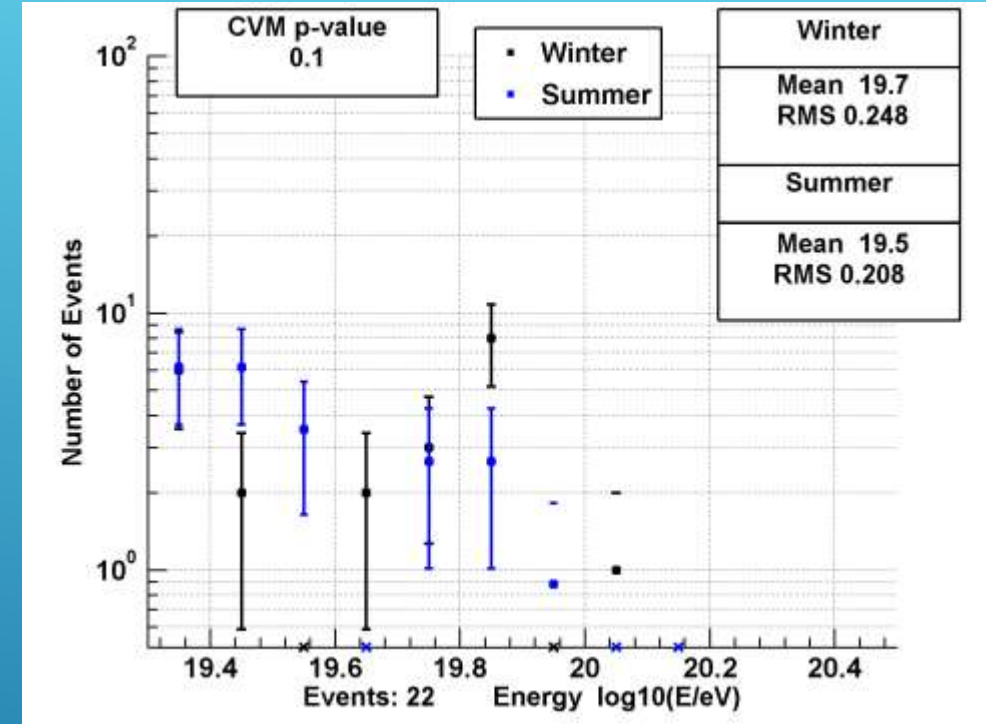
Day – July to June (6 months offset)

Uneven in Declination

SUMMER/WINTER ENERGY DISTRIBUTION COMPARISON



Outside hot/cold spot



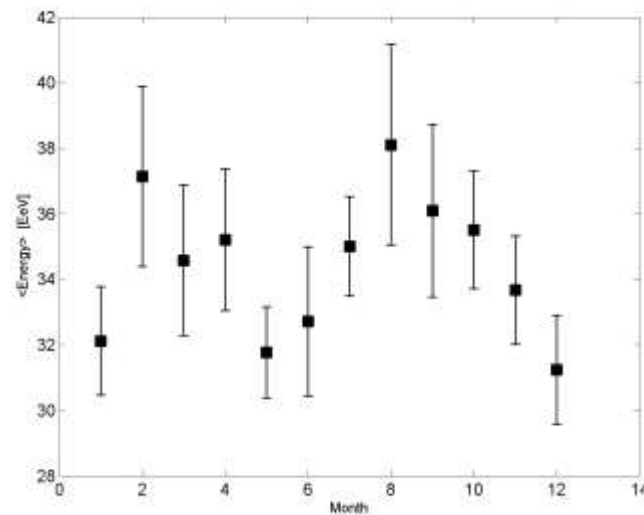
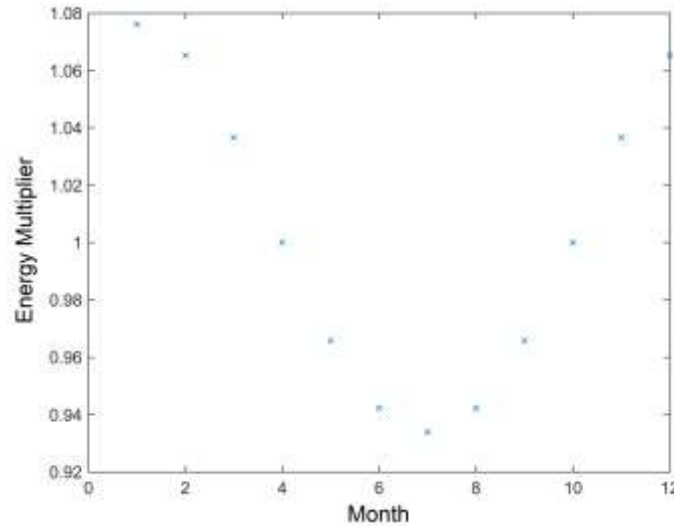
Inside hot/cold spot

Energy distributions agree within statistics

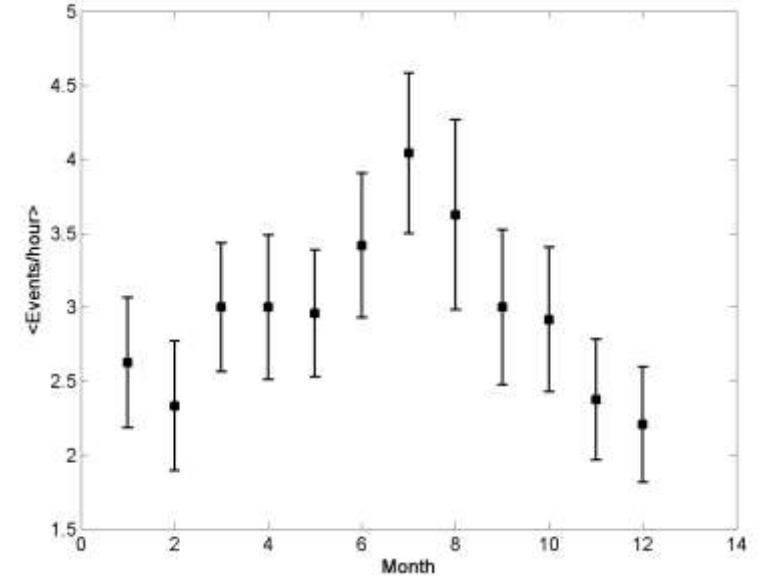
SEASONAL ENERGY CORRECTION

- Energy correction found from reconstructed MC using Elko radiosonde data (D.Ivanov)
- Lateral dist. change from atmos. temperature changes

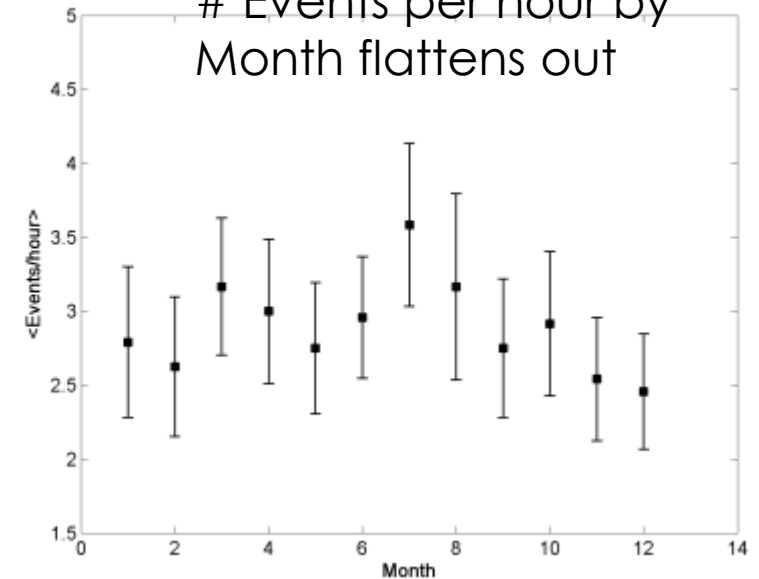
Correction +/- 7%



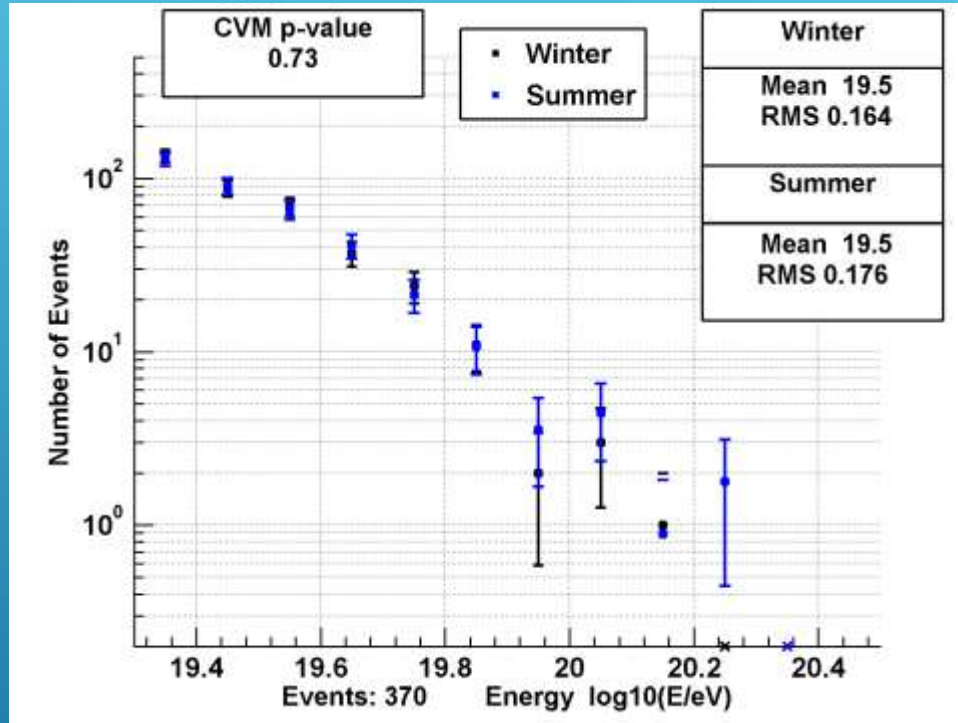
Energy Vs Month



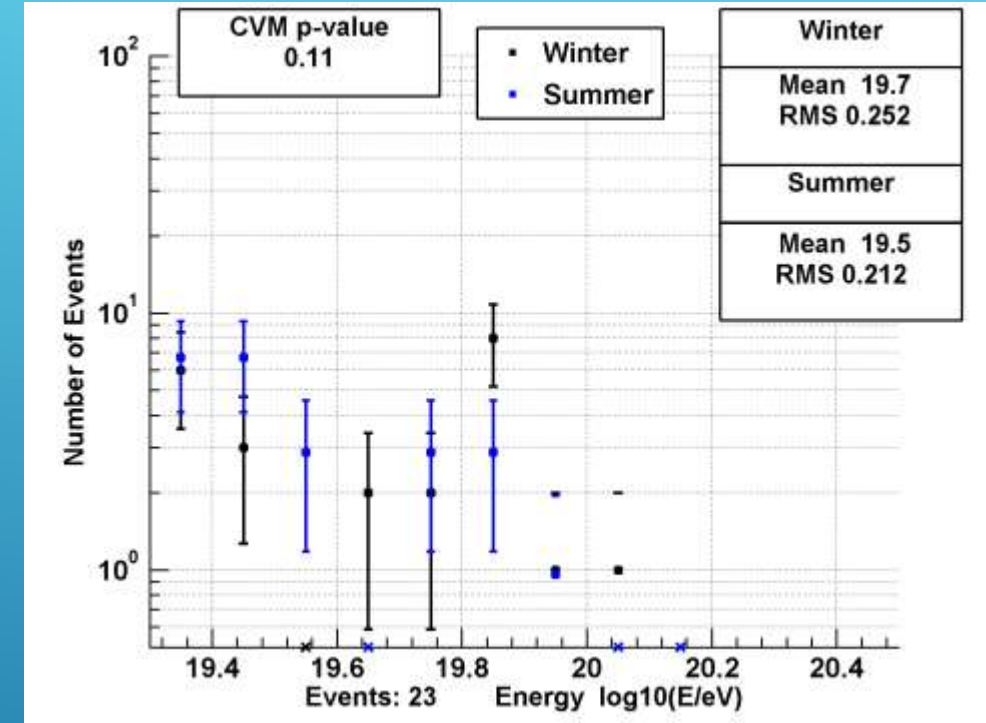
Events per hour by Month flattens out



SUMMER/WINTER ENERGY AFTER CORRECTION



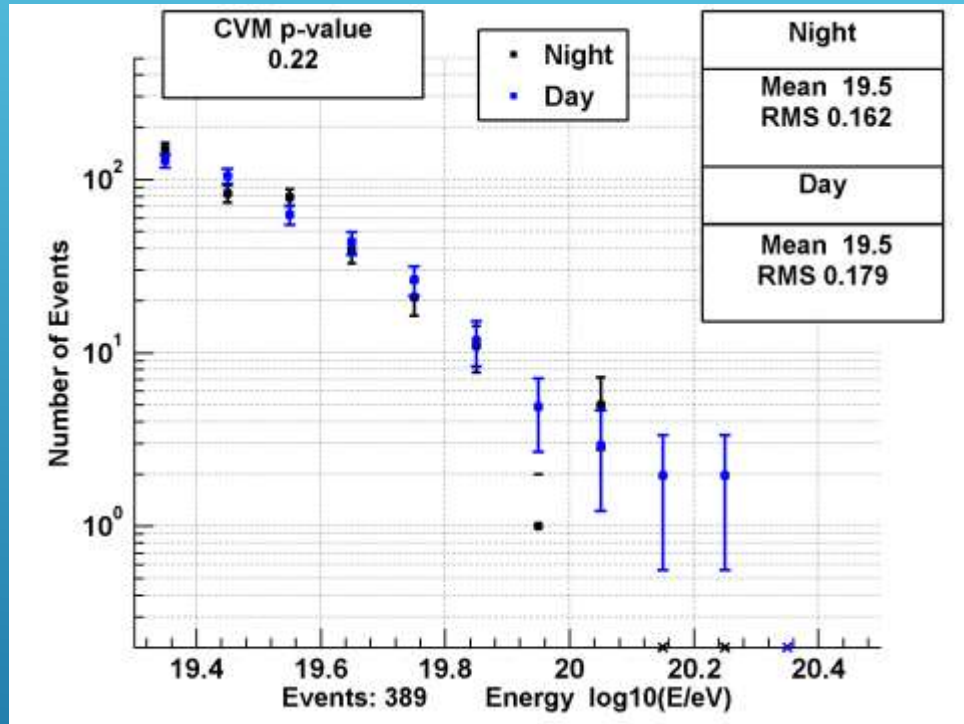
Outside hot/cold spot
Agreement improved



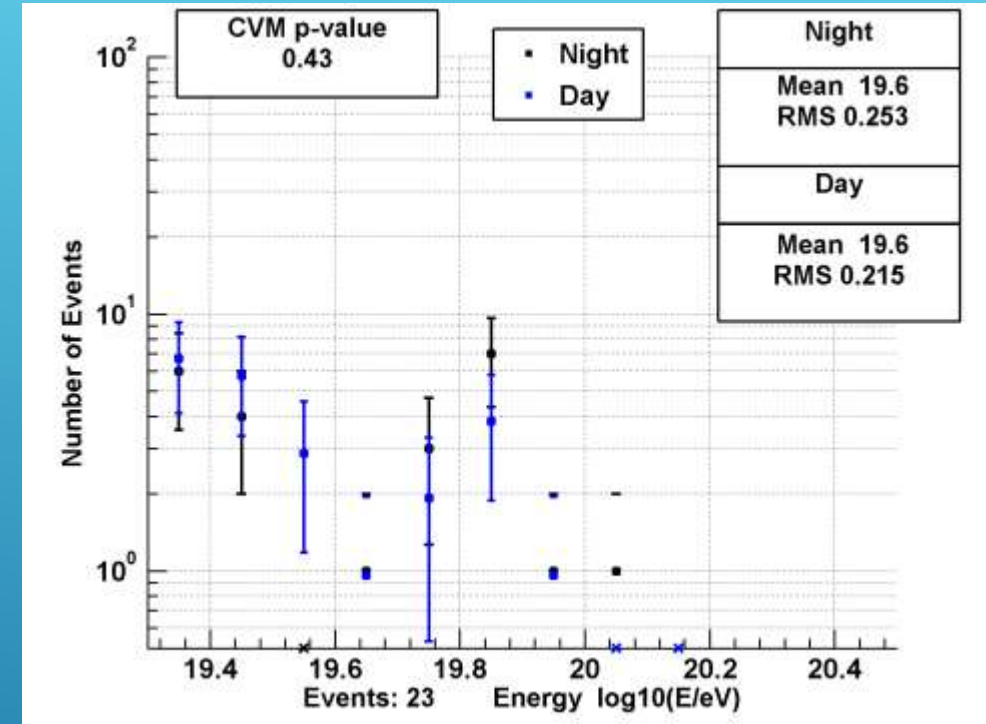
Inside hot/cold spot
Agreement improved

Energy distributions agree within statistics

DAY/NIGHT ENERGY AFTER CORRECTION



Outside hot/cold spot



Inside hot/cold spot

Agreement improved

Energy distributions agree within statistics

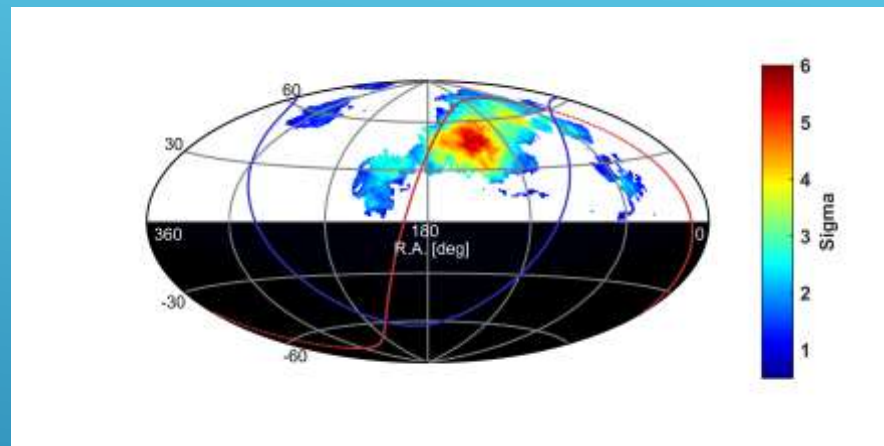
SEASONAL ENERGY CORRECTION

852 events

Original σ Combined

Max: 5.92

At max:
R.A. = 139
decl. = 48
Cold = -3.25
Hot = 4.54

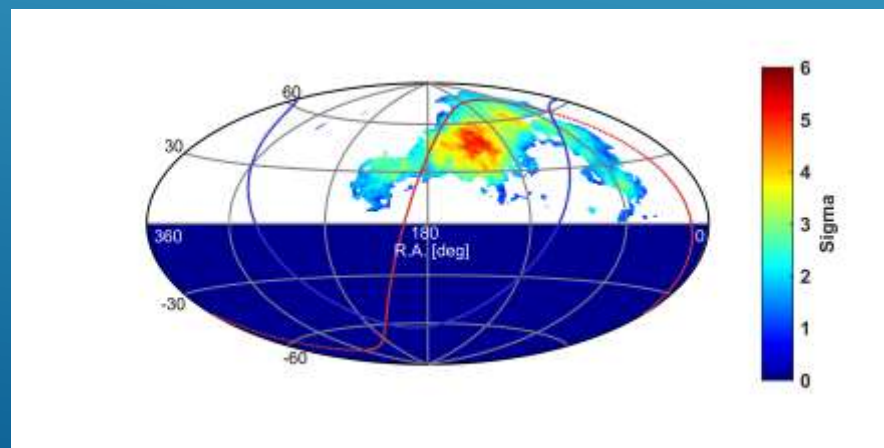


833 events

Seasonal Energy Corrected σ Combined

Max: 5.36

At max:
R.A. = 137
decl. = 48
Cold = -2.80
Hot = 4.16



5000 random samples of 833 events:
Combined Median: $5.90 - 0.14 + 0.12$

Corrected Combined
is 3.86 error bars from median.

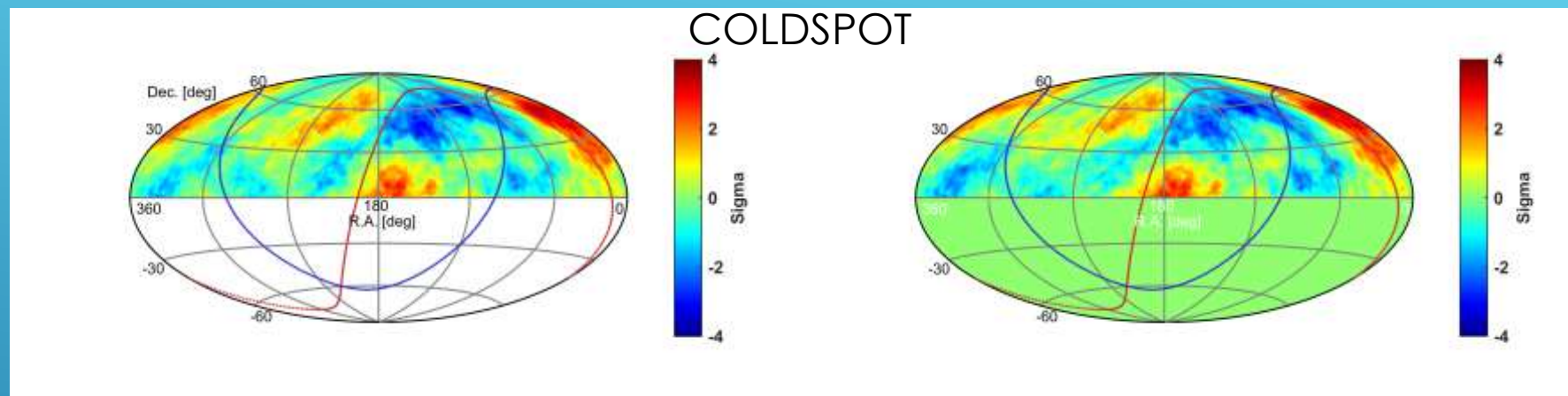
SEASONAL ENERGY CORRECTION

852 events

Original $\sigma E < 57$ EeV

833 events

Seasonal Corrected $\sigma E < 57$ EeV

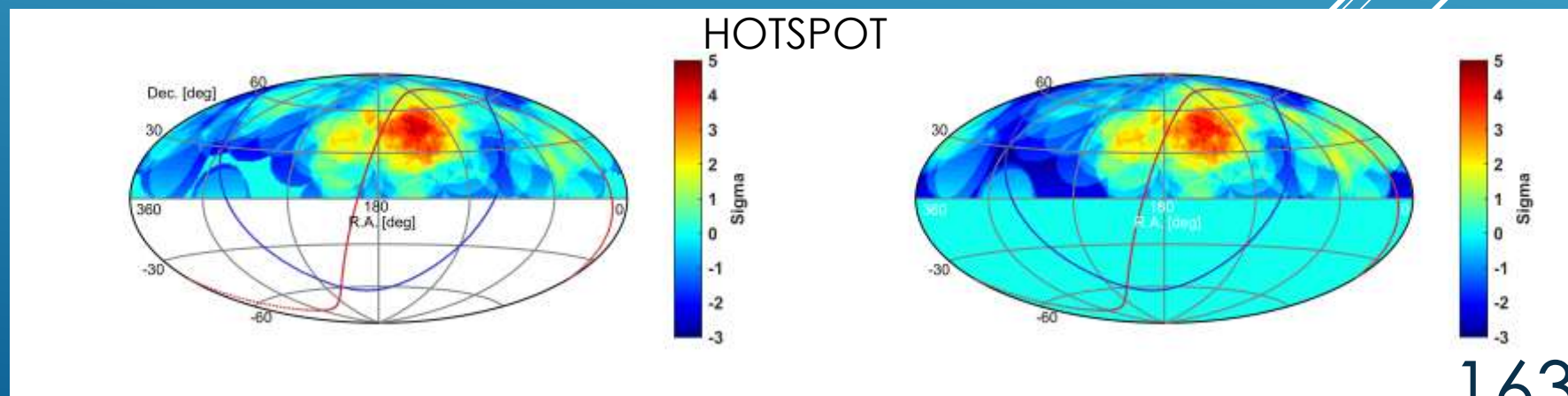


Original $\sigma E > 57$ EeV

Max: 4.61

Seasonal Corrected $\sigma E > 57$ EeV

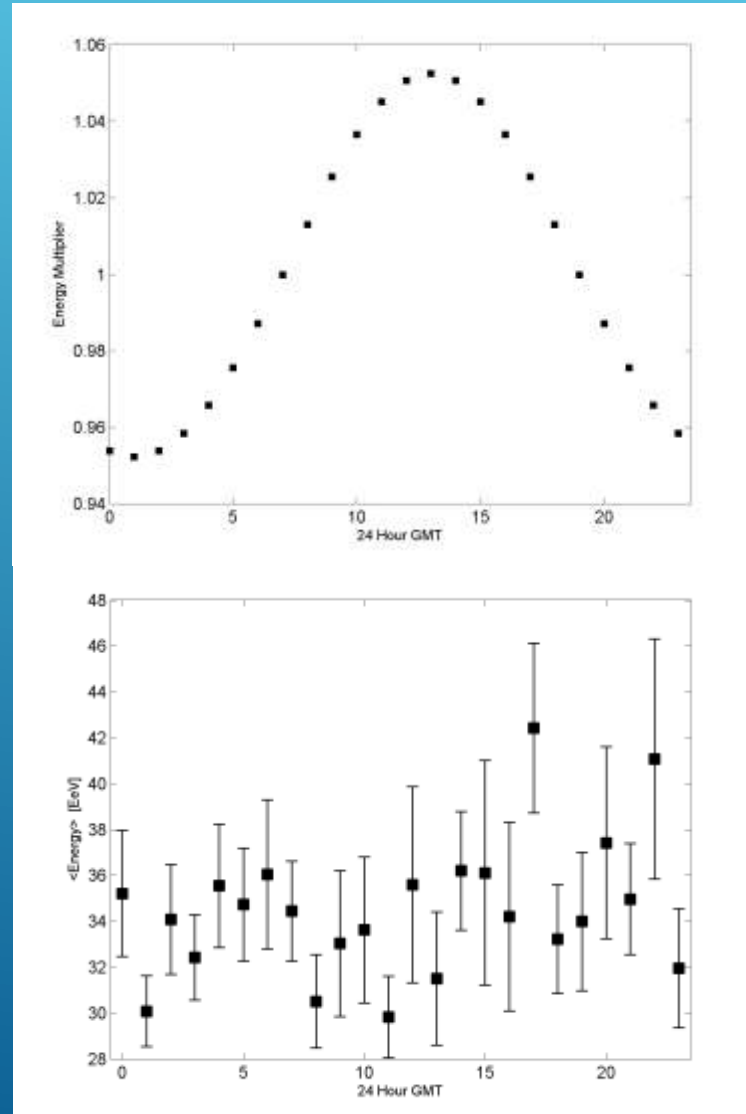
Max: 4.22



HOURLY ENERGY CORRECTION

- Energy correction found from hourly events rates (D.Ivanov)
- Lateral dist. change from atmos. temperature changes

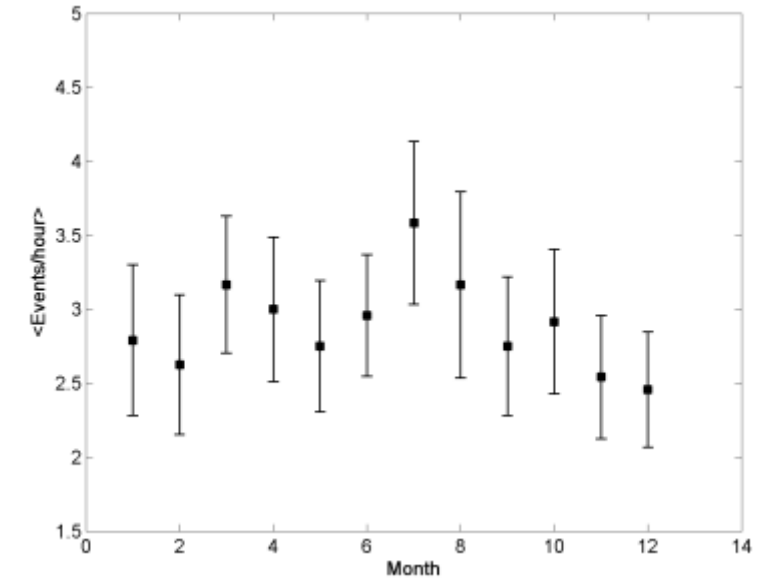
Correction +/- 5%
after seasonal correction



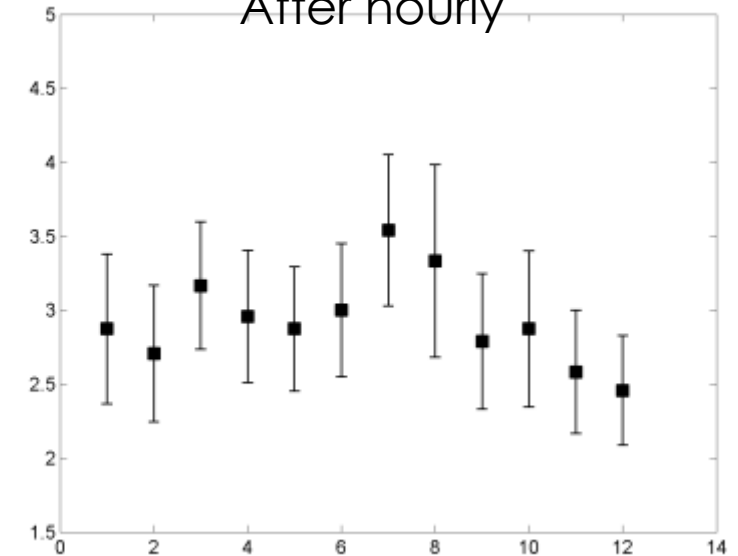
Affects 20 EeV cut and 57 EeV
energy split

Energy Vs Hour

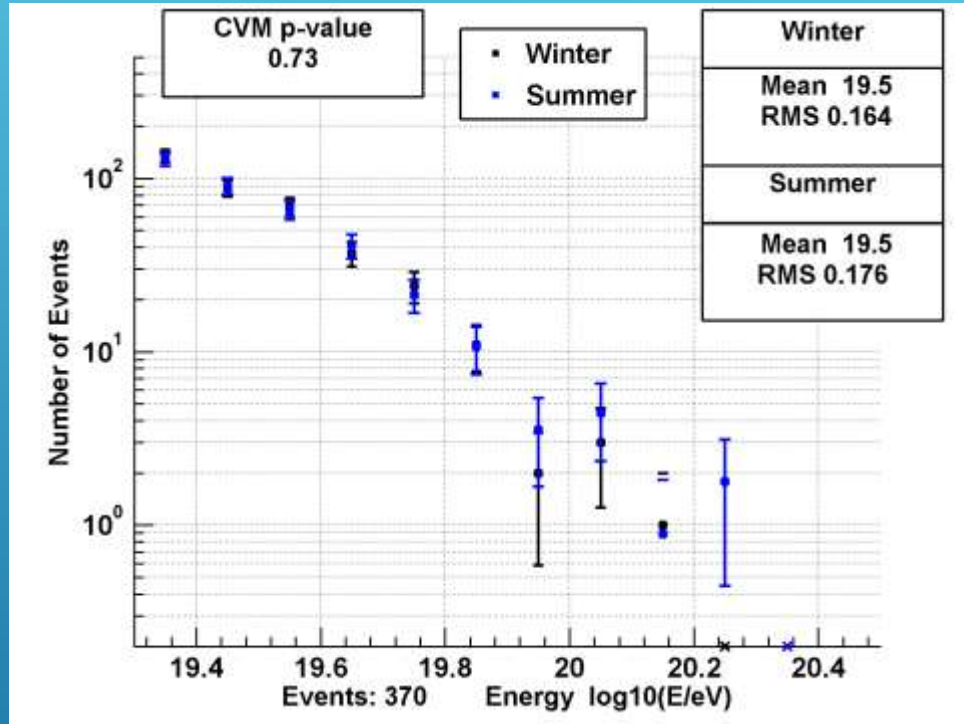
After seasonal



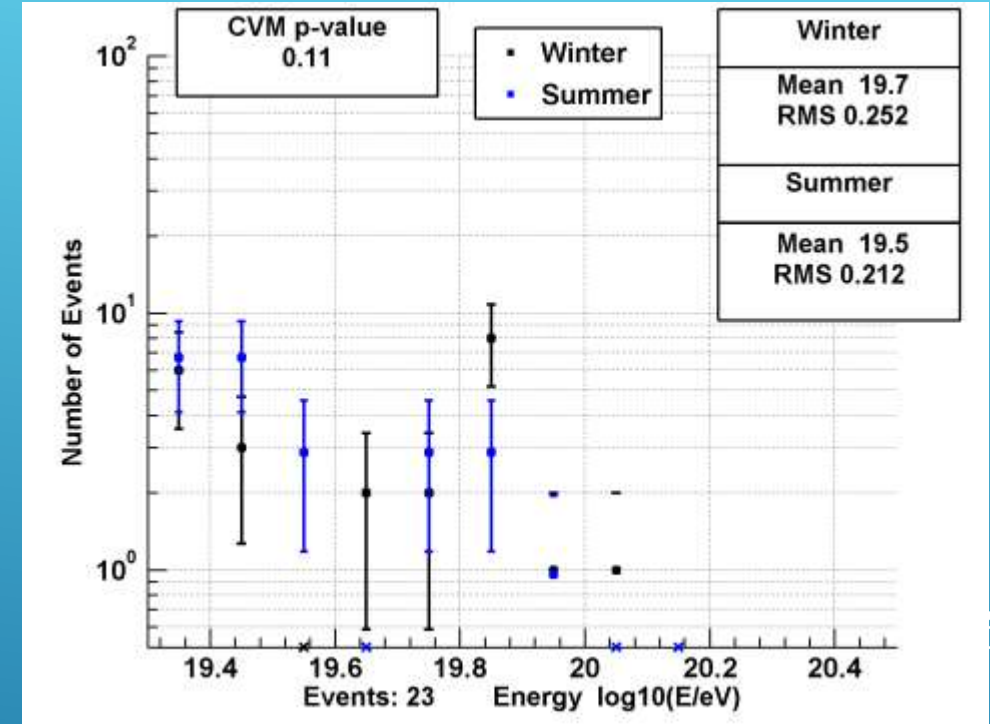
After hourly



SUMMER/WINTER ENERGY AFTER HOURLY CORRECTION



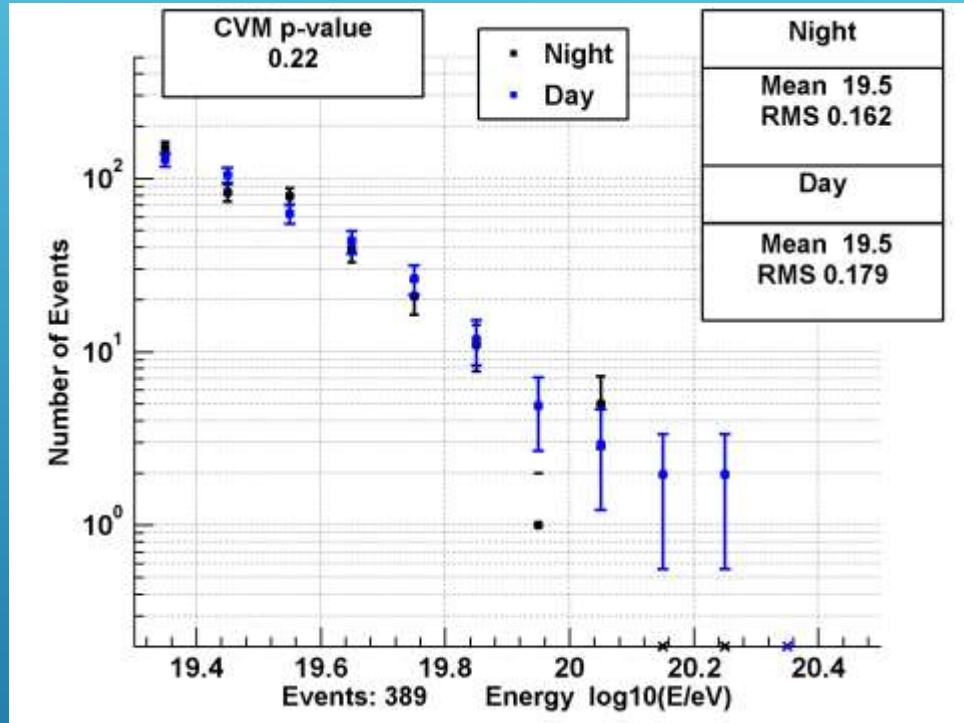
Outside hot/cold spot
Agreement improved



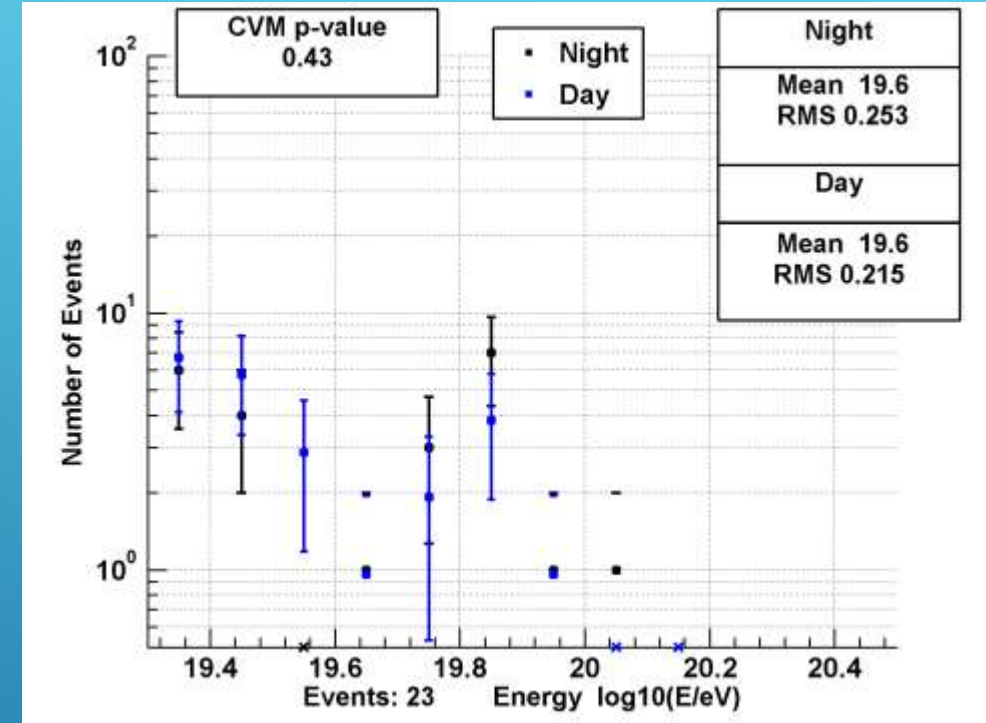
Inside hot/cold spot
Agreement improved

Energy distributions agree within statistics

DAY/NIGHT ENERGY AFTER HOURLY CORRECTION



Outside hot/cold spot



Inside hot/cold spot

Agreement improved

Energy distributions agree within statistics

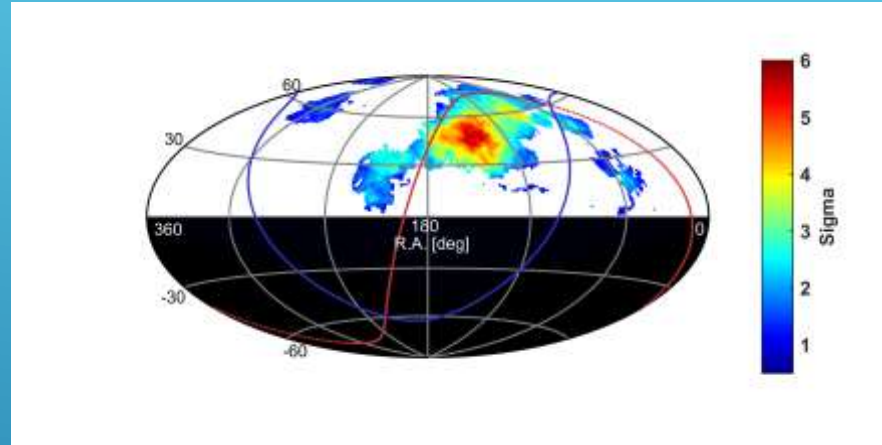
HOURLY ENERGY CORRECTION

852 events

Original σ Combined

Max: 5.92

At max:
R.A. = 139
decl. = 48
Cold = -3.25
Hot = 4.54

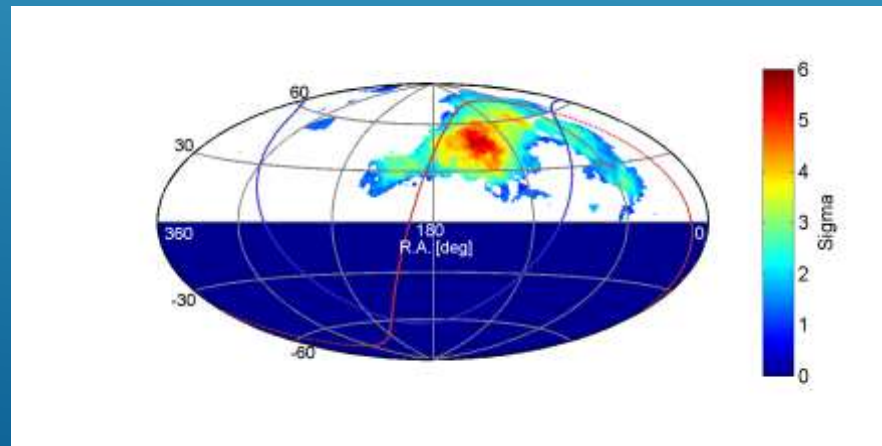


844 events

Hourly Energy Corrected σ Combined

Max: 5.86

At max:
R.A. = 139
decl. = 48
Cold = -3.23
Hot = 4.48



5000 random samples of 844 events:
Combined Median: 5.90 - 0.07 + 0

Corrected Combined
is 1.7 error bars from median.

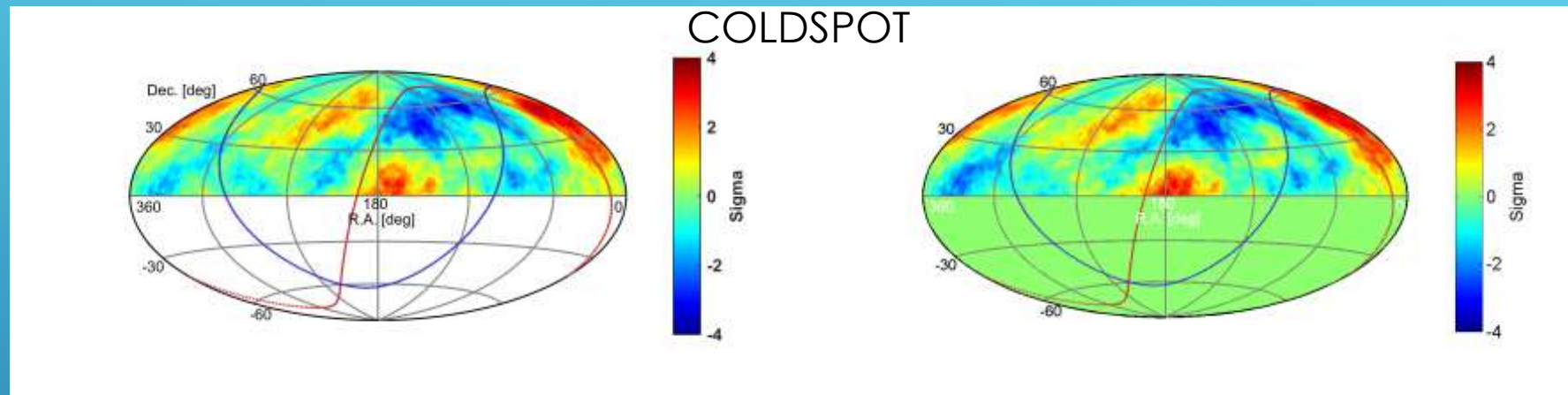
HOURLY ENERGY CORRECTION

852 events

Original $\sigma E < 57$ EeV

844 events

Hourly Corrected $\sigma E < 57$ EeV

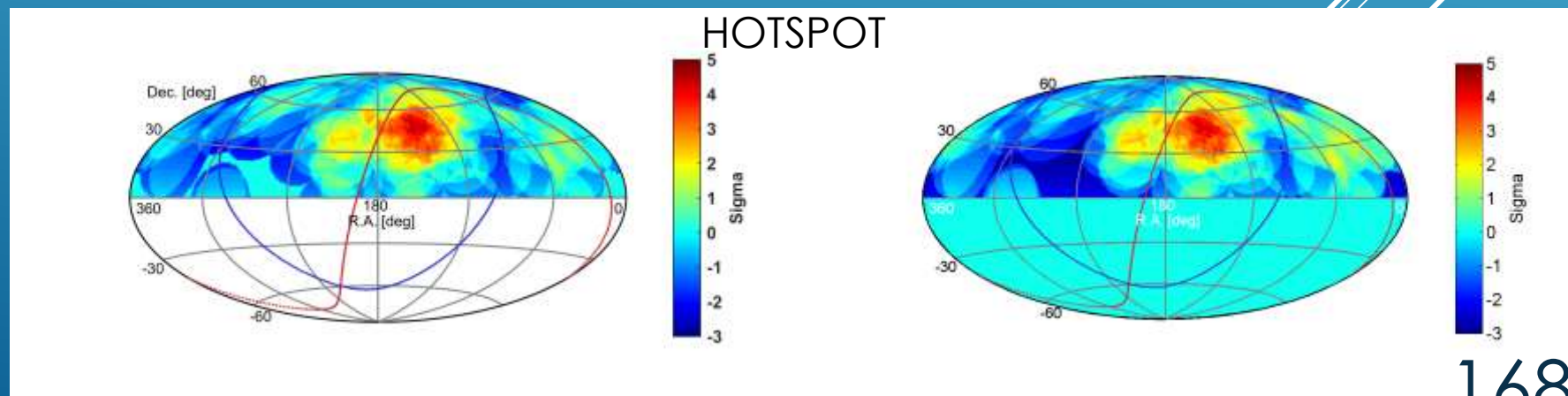


Original $\sigma E > 57$ EeV

Max: 4.61

Hourly Corrected $\sigma E > 57$ EeV

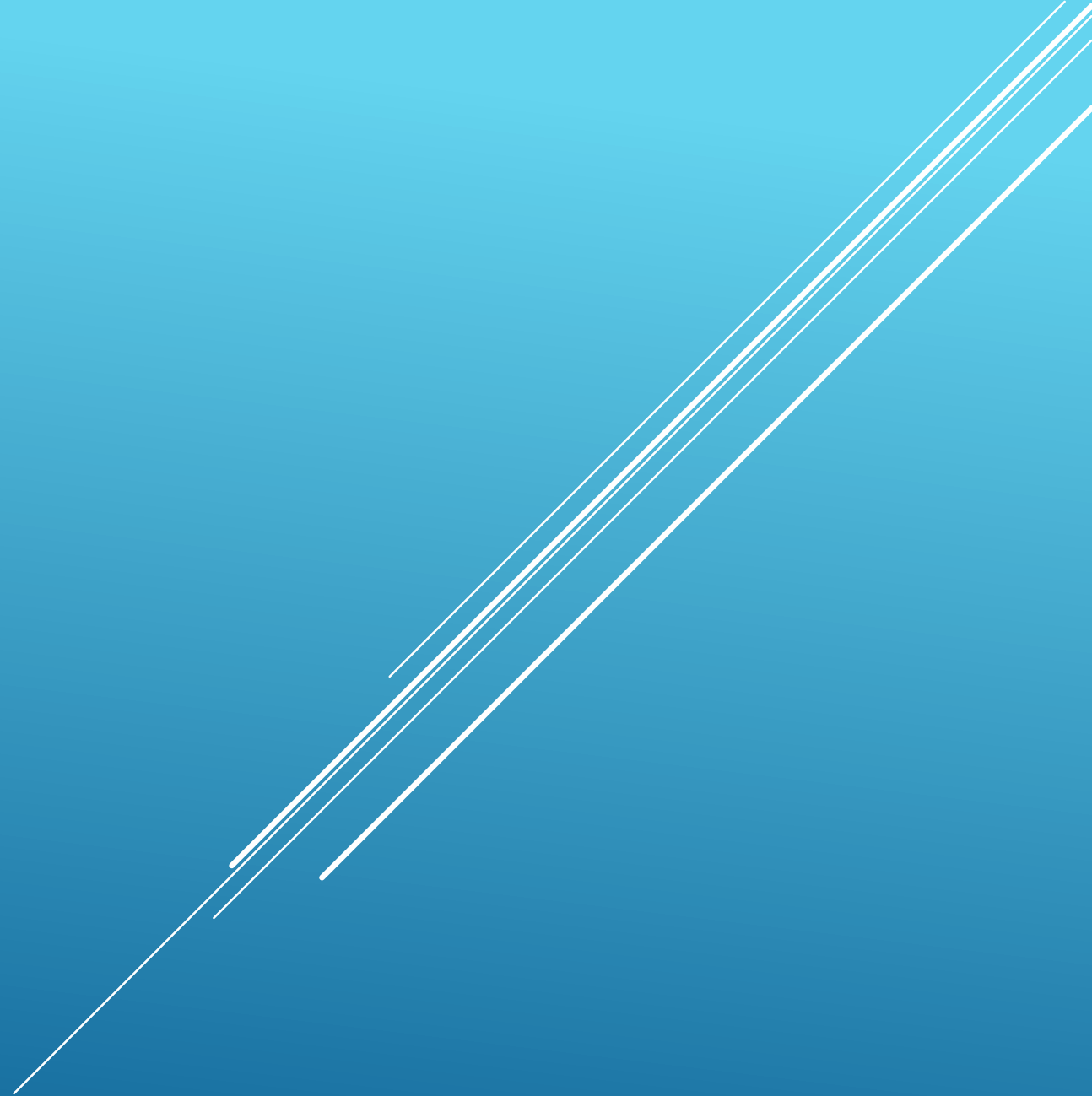
Max: 4.52



CONCLUSION

- Energy distributions between day/night and summer/winter agree within statistics.
- After MC derived energy correction energy distributions still agree.
- Hot/Coldspot is stable after energy correction. Affects both hotspot and coldspot almost equally.

APPENDIX



SPLIT CONCLUSION

No statistically significant difference from full data set is found by splitting data in half.

SUMMER-WINTER SPLIT

A decorative graphic consisting of several parallel white lines of varying lengths, all slanted diagonally from the bottom-left towards the top-right, located in the lower right quadrant of the image.

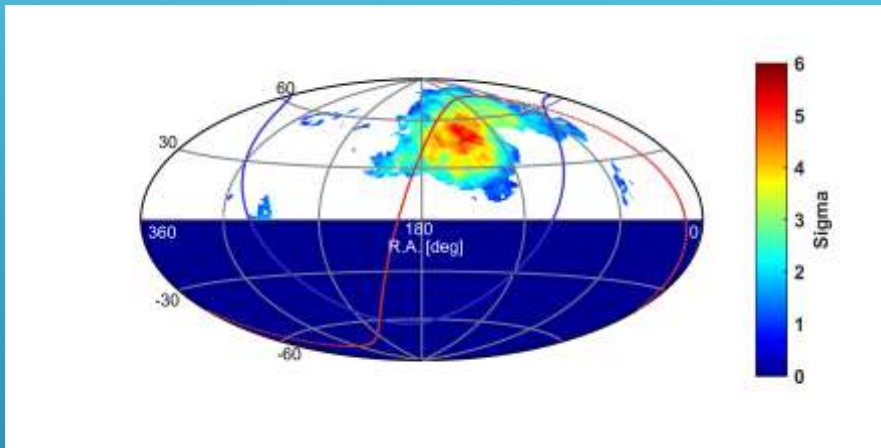
SPLIT SUMMER – WINTER

368 events

Winter σ Combined

Max: 5.52

At max:
R.A. = 139
decl. = 48
Cold = -3.90
Hot = 3.89



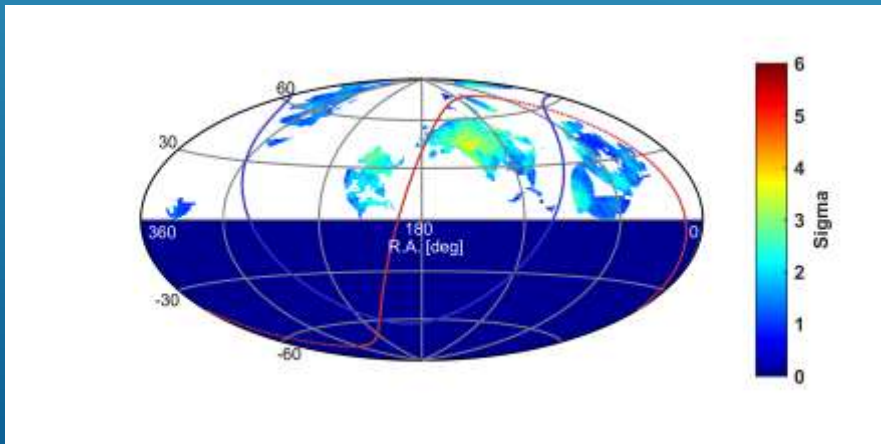
Rand data (same #) σ , Combined
Hot/Cold Median: 4.64 – 0.55 + 0.63

Significance higher than random sampling
by 1.4 sigma.

484 events
Summer σ Combined

Max: 4.08

At max:
R.A. = 146
decl. = 42
Cold = -1.78
Hot = 3.24



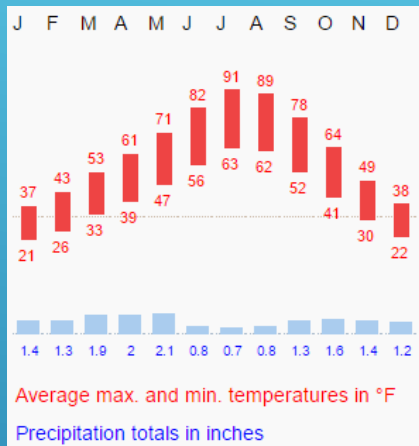
Random data (same # events) σ , Combined
Hot/Cold Median: 5.01 – 0.56 + 0.55

Significance lower than random sampling
by 1.7 sigma.

SPLIT SUMMER – WINTER

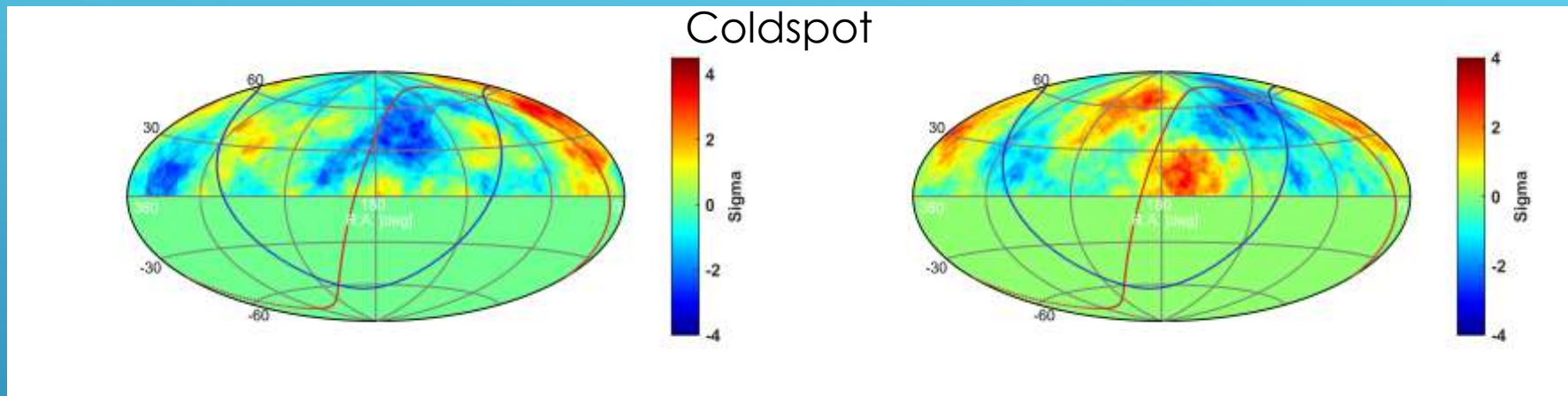
368 events

Winter $\sigma E < 57$ EeV



494 events

Summer $\sigma E < 57$ EeV

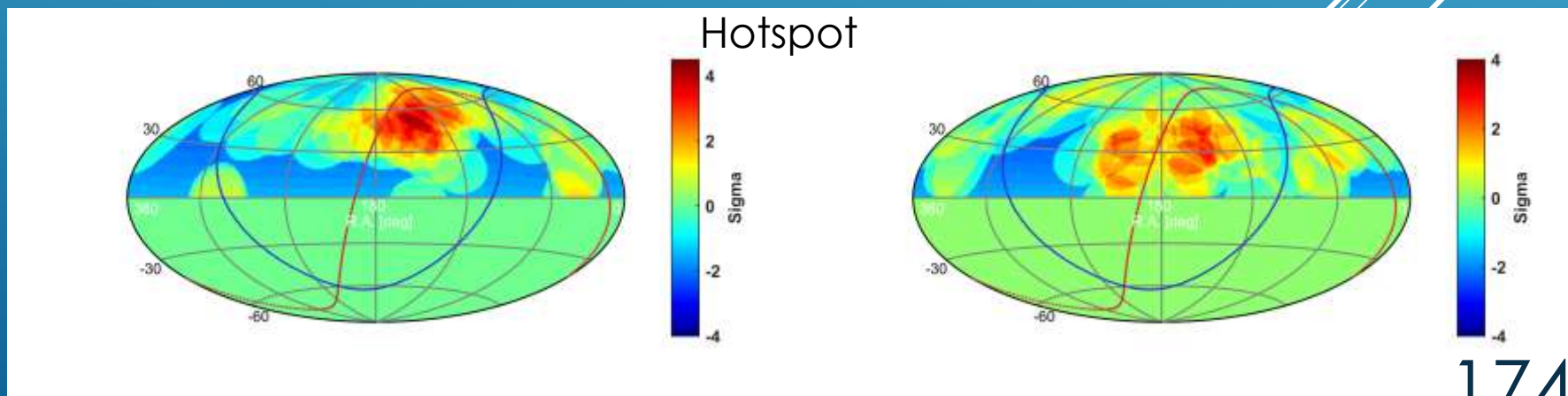


Winter $\sigma E > 57$ EeV

Max. Hot: 4.43

Summer $\sigma E > 57$ EeV

Max. Hot: 3.24



HOT/COLD SOURCE SIGNIFICANCE – SUMMER ONLY

437 events

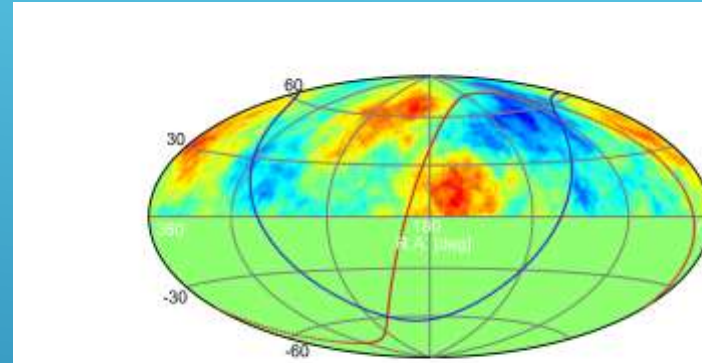
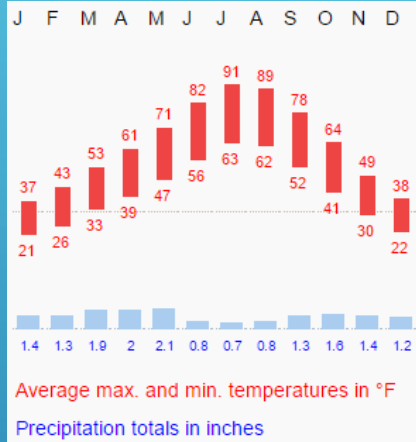
$\sigma E < 57 \text{ EeV}$

Min Cold: -3.46

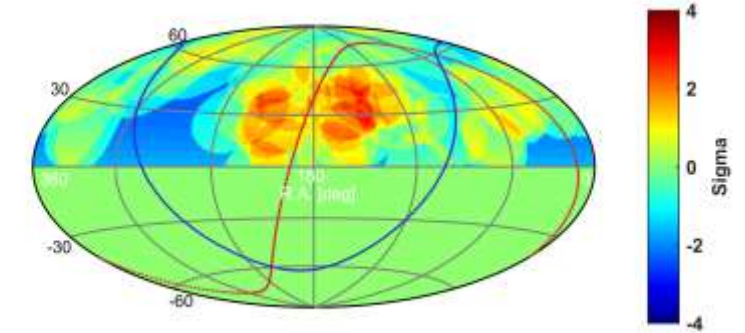
47 events

$\sigma E > 57 \text{ EeV}$

Max Hot: 3.24



Coldspot



Hotspot

- ▶ Summer – April, 15th to October, 15th.

At Hot/Cold Spot: -1.99

At Hot/Cold Spot: 1.95

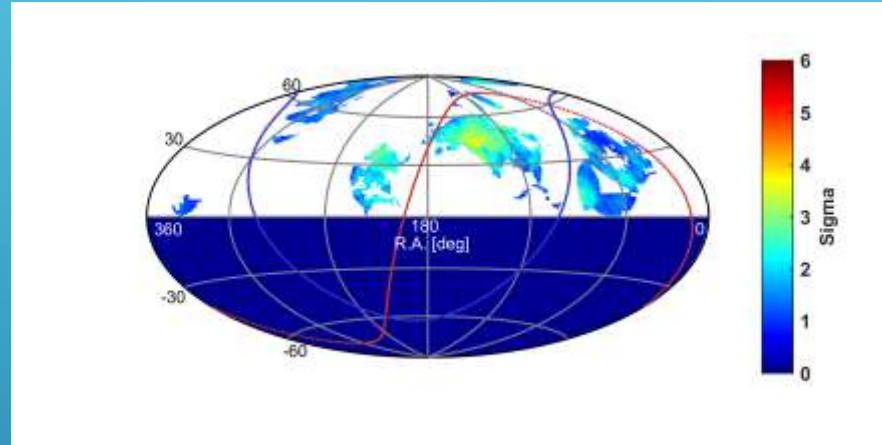
5000 random selections
of 494 events

HOT/COLD SOURCE SIGNIFICANCE – SUMMER ONLY

494 events

Summer σ Combined

Max Hot/Cold: 4.08



- ▶ Summer – April, 15th to October, 15th.

Random data (same # events) σ , Combined

Hot/Cold Median: 5.01 – 0.56 + 0.55

Significance lower than random sampling by 1.7 sigma.
Change not significantly different from random sampling

HOT/COLD SOURCE SIGNIFICANCE – WINTER ONLY

331 events

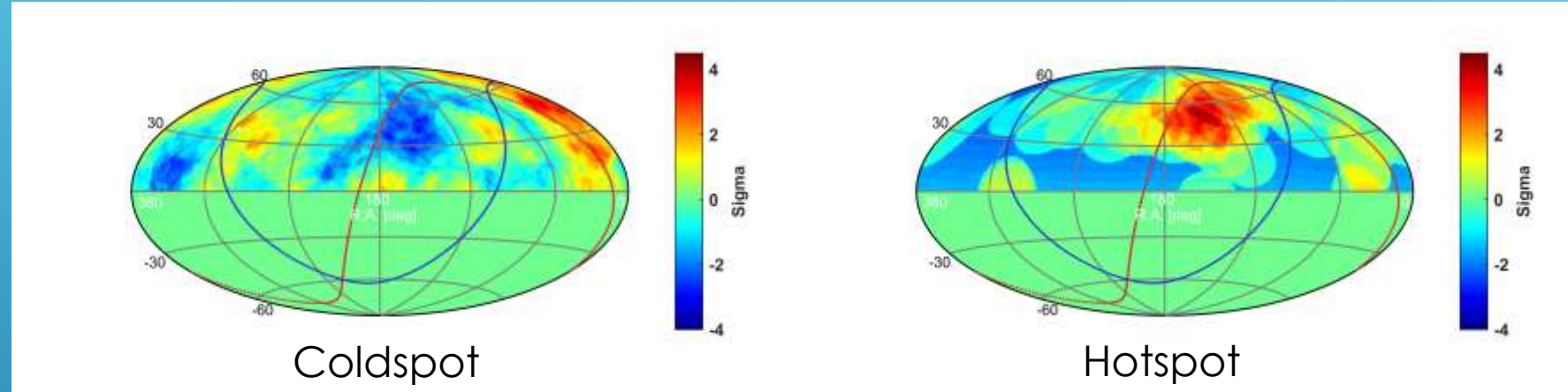
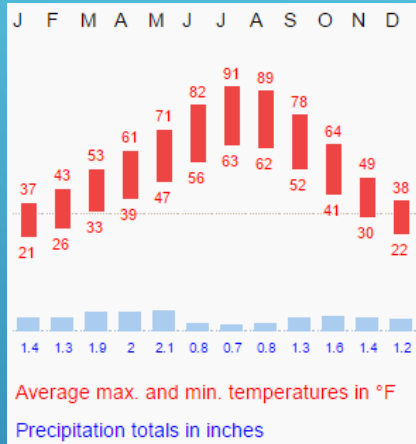
$\sigma E < 57$ EeV

Min Cold: -3.3

37 events

$\sigma E > 57$ EeV

Max. Hot: 4.43



- ▶ Winter – October 16th to April, 14th

At Hot/Cold Spot -2.69

At Hot/Cold Spot 4.42

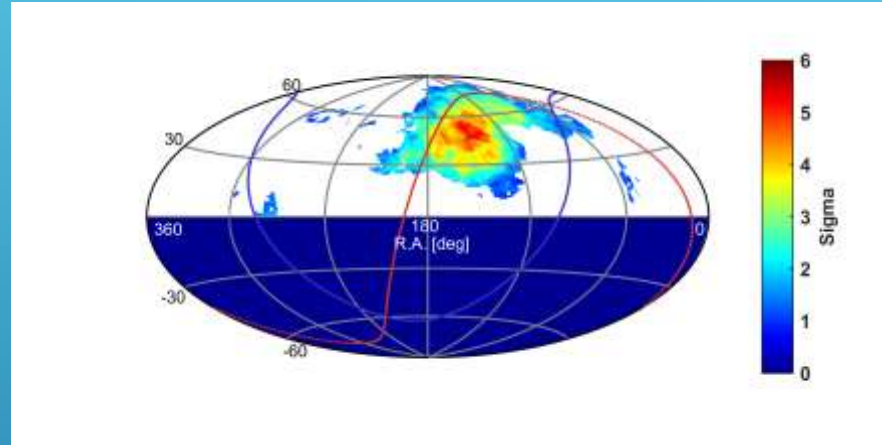
5000 random selections
of 368 events

HOT/COLD SOURCE SIGNIFICANCE – WINTER ONLY

368 events

Winter σ Combined

Max Hot/Cold: 5.52



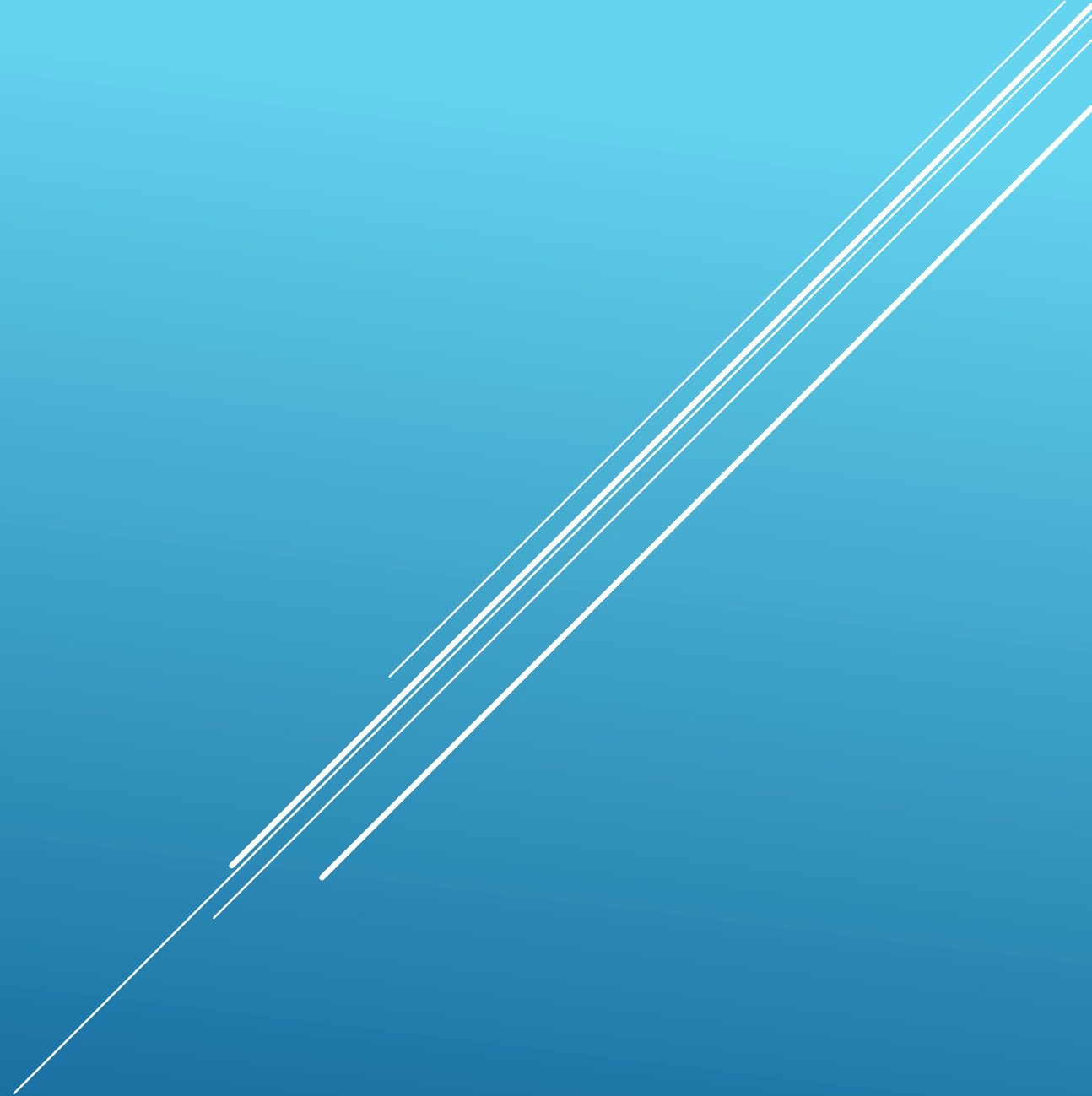
- ▶ Winter – October 16th to April, 14th

Rand data (same #) σ , Combined

Max: 4.64 – 0.55 + 0.63

Significance higher than random sampling by 1.4 sigma.
Change not significantly different from random sampling

DAY-NIGHT SPLIT

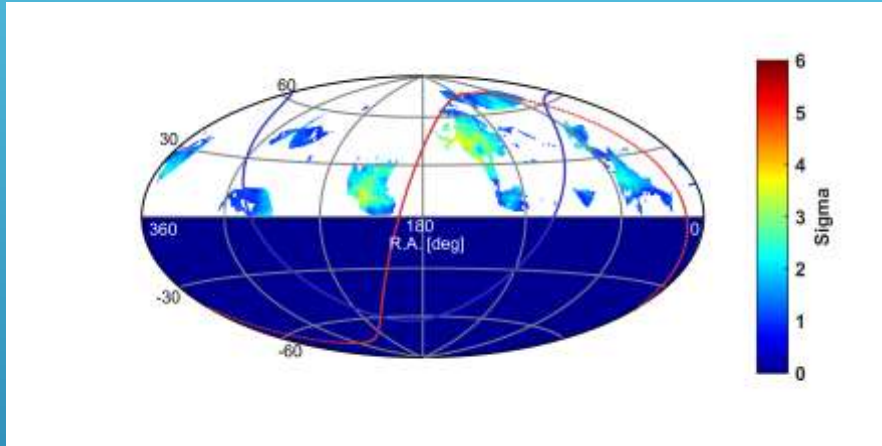


SPLIT DAY – NIGHT

432 events

Day σ Combined

Max: 3.95



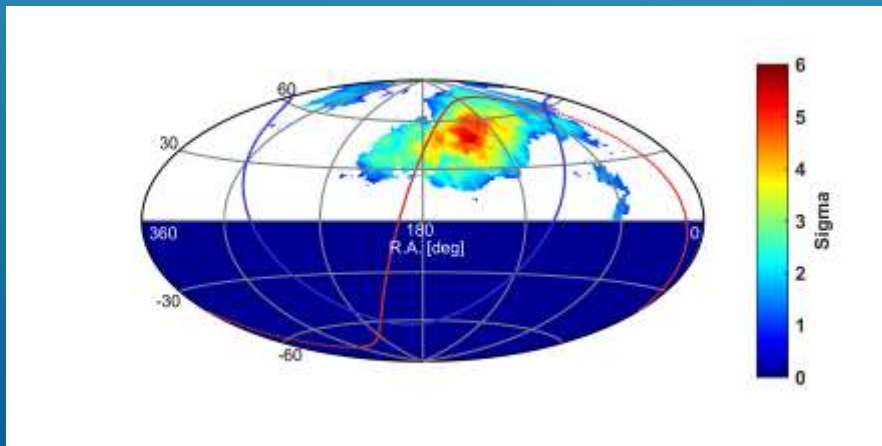
At max:
R.A. = 146
dec. = 42
Cold = -1.42
Hot = 3.29

Rand data (same #) σ , Combined
Hot/Cold Median: 4.87 - 0.57 + 0.58

Significance lower than random sampling
by 1.6 sigma.

420 events
Night σ Combined

Max: 5.82



At max:
R.A. = 139
dec. = 48
Cold = -3.30
Hot = 4.37

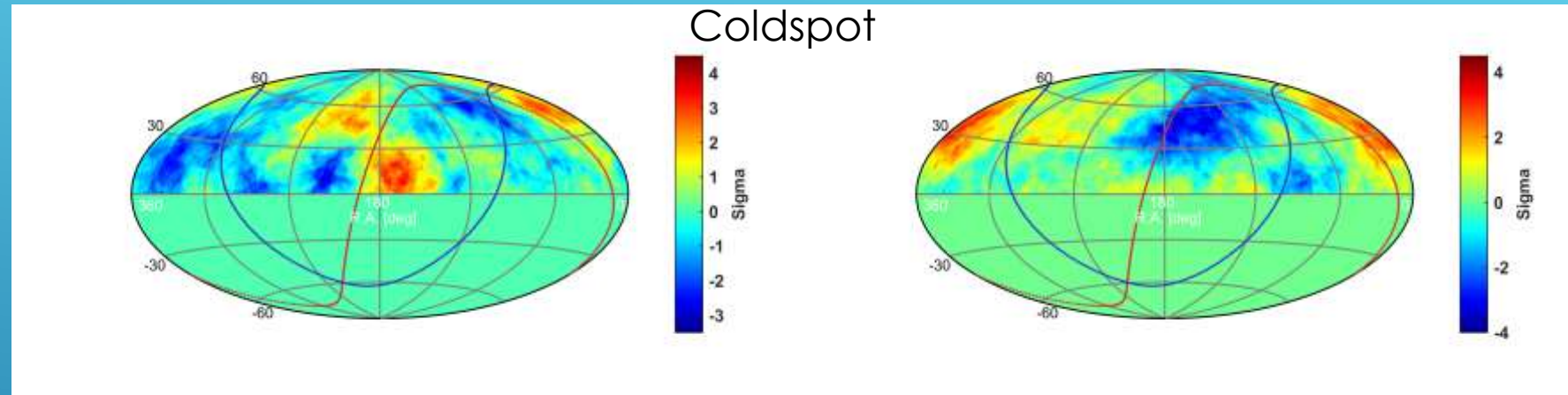
Rand data (same #) σ , Combined
Hot/Cold Median: 4.82 - 0.56 + 0.60

Significance higher than random sampling
by 1.7 sigma.

SPLIT DAY – NIGHT

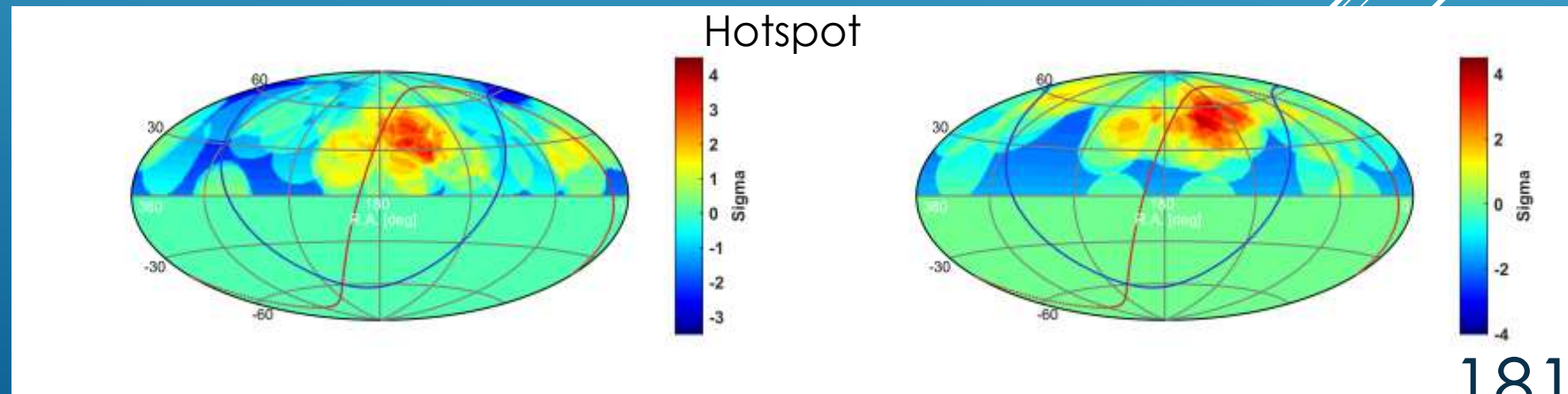
432 events
Day $\sigma E < 57$ EeV

420 events
Night $\sigma E < 57$ EeV



Day $\sigma E > 57$ EeV
Max: 3.63

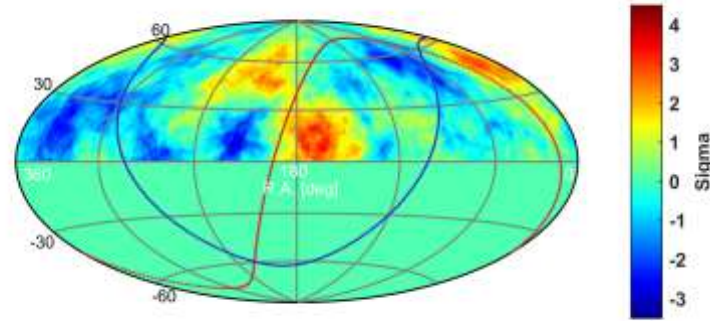
Night $\sigma E > 57$ EeV
Max: 4.37



HOT/COLD SOURCE SIGNIFICANCE – DAY ONLY

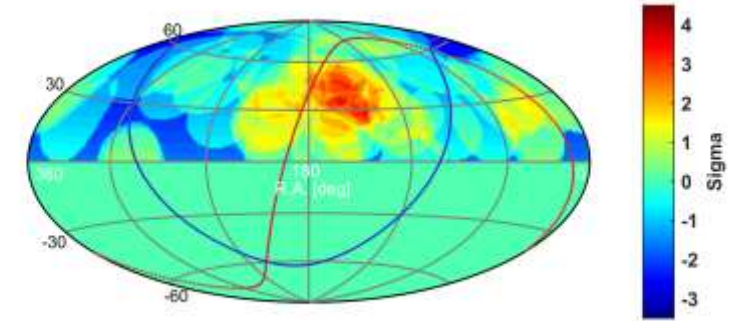
386 events
Day $\sigma E < 57$ EeV

46 events
Day $\sigma E > 57$ EeV



Coldspot

At Hot/Cold Spot: -1.39



Hotspot

At Hot/Cold Spot: 2.00

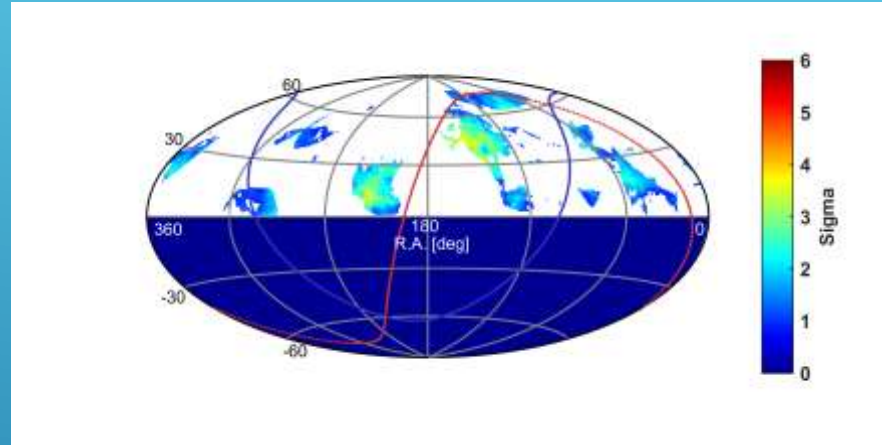
- ▶ Day – 9am to 9pm
 - ▶ 15 to 3 GMT

HOT/COLD SOURCE SIGNIFICANCE – DAY ONLY

432 events

Day σ Combined

Max: 3.95



► Day – 9am to 9pm

Rand data (same #) σ , Combined

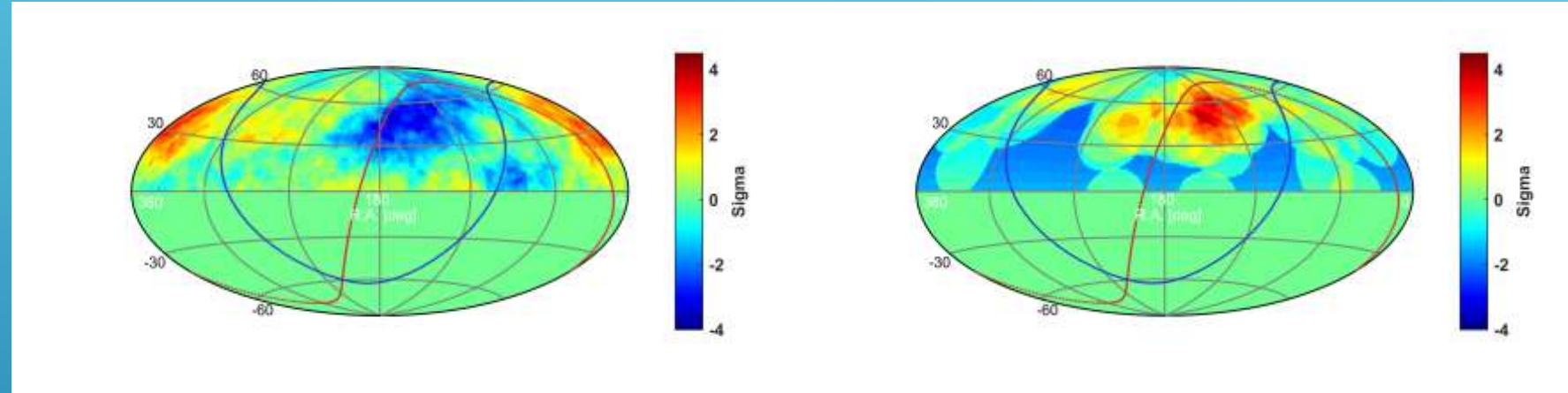
Max: 4.87 - 0.57 + 0.58

Significance lower than random sampling by 1.6 sigma.
Change not significantly different from random sampling

HOT/COLD SOURCE SIGNIFICANCE – NIGHT ONLY

382 events
Night $\sigma E < 57$ EeV

38 events
Night $\sigma E > 57$ EeV



Coldspot

Hotspot

► Night – 9pm to 9am

At Hot/Cold Spot: -3.30

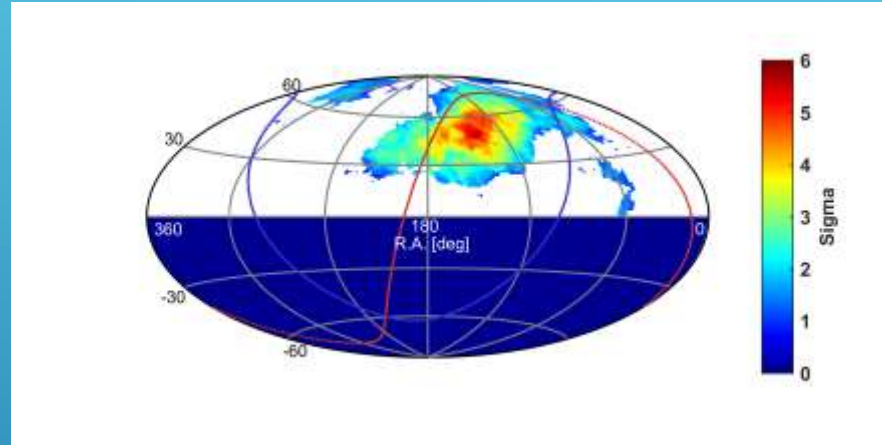
At Hot/Cold Spot: 4.37

HOT/COLD SOURCE SIGNIFICANCE – NIGHT ONLY

420 events

Night σ Combined

Max: 5.82



► Night – 9pm to 9am

Rand data (same #) σ , Combined

Max: 4.82 – 0.56 + 0.60

Significance higher than random sampling by 1.7 sigma.
Change not significantly different from random sampling

3 COMPONENT COMPOSITION – FIT XMAX AND S800

Jon Paul Lundquist

A series of several parallel white lines of varying thicknesses, slanted diagonally from the bottom-left towards the top-right, located in the lower right quadrant of the slide.

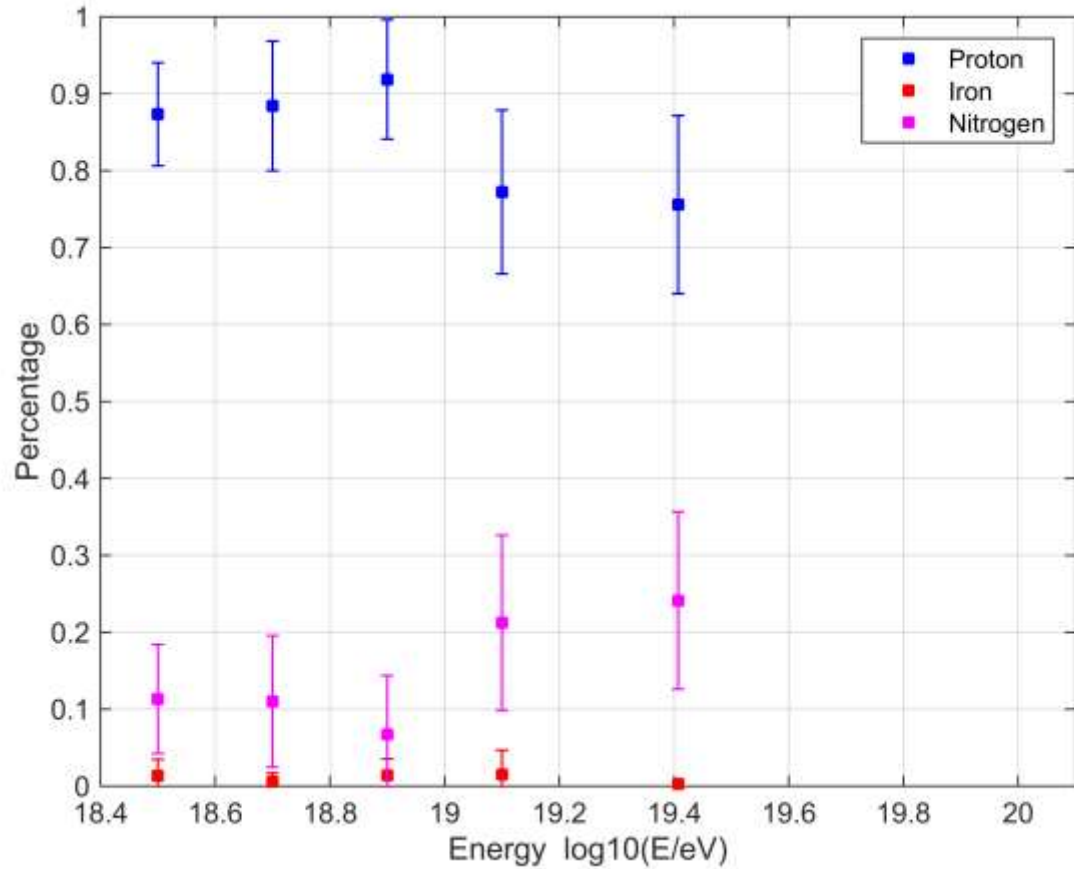
METHOD

- ▶ Use Proton, Iron, and Nitrogen primaries.
- ▶ Find best fit to X_{\max} and s_{800} distributions simultaneously
 - ▶ Maximize combined p-Value ($p_1 * p_2$) from CVM test.
- ▶ For each energy bin
 - ▶ For each ratio
 - ▶ Calculate combined p-Value for 100 different samples $N_{\text{data}} * 5$.
 - ▶ Find ratio which maximizes the mean combined p-value.
 - ▶ Iterate 100 times (using a different data sample with replacement – bootstrap) to find error on ratio which maximizes the p-value.

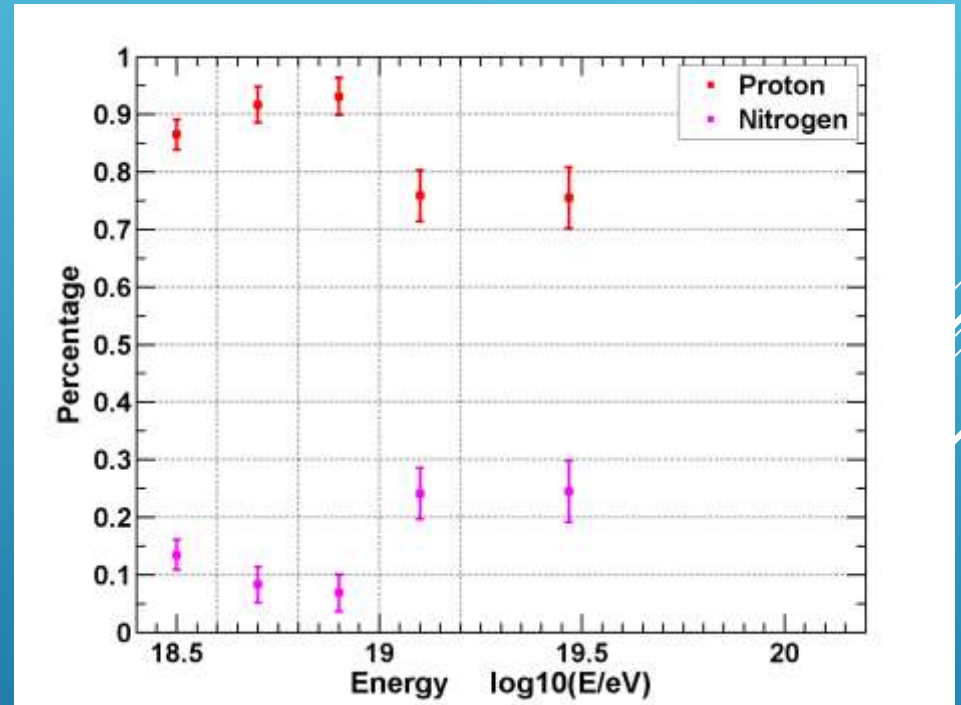
QGSJETII-03

A series of three parallel white diagonal lines extending from the bottom right towards the top right of the slide.

RESULT



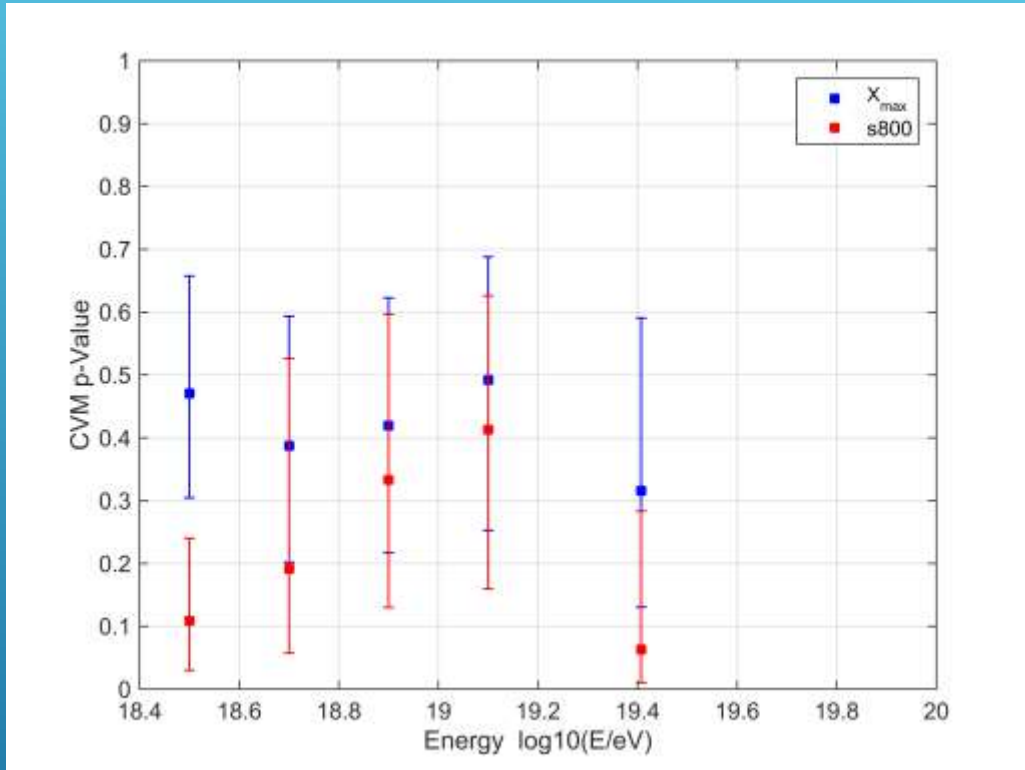
Consistent with zero iron.
Consistent with 2 component fit using only Xmax



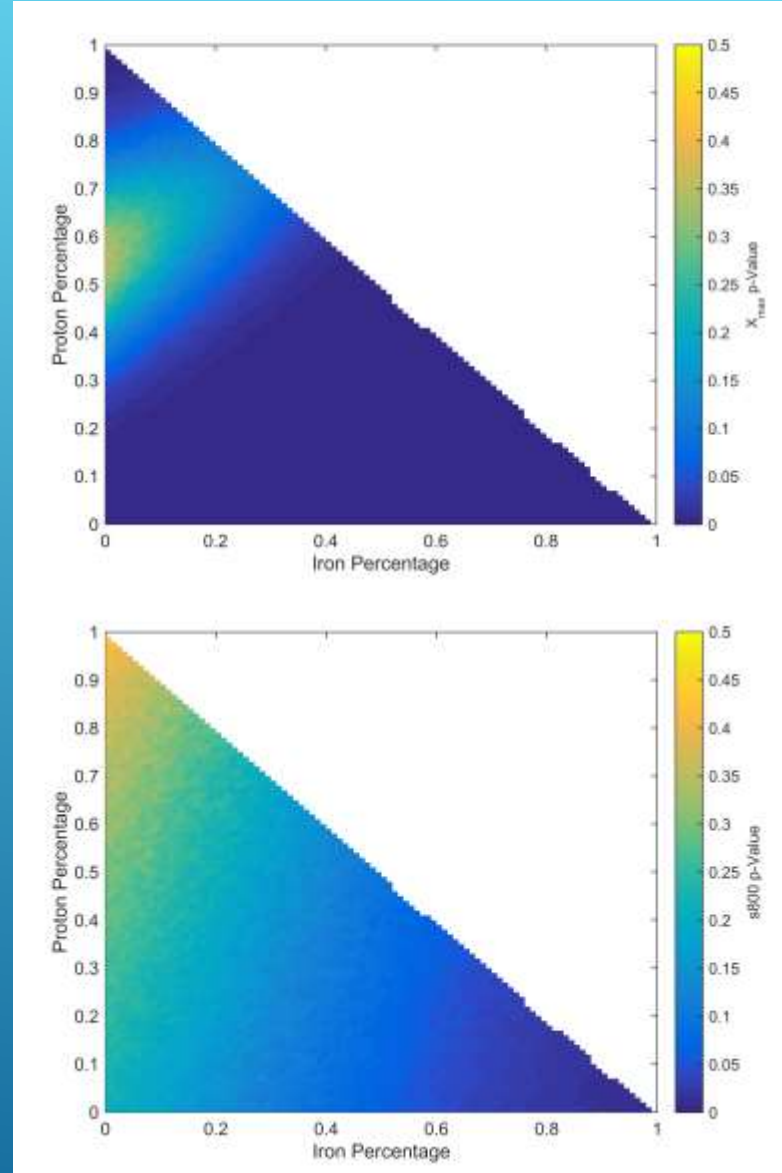
2 component

PVALUES

Log10(E/eV) > 19.2 – 1 iteration



Distribution p-Values Vs Energy



Xmax p-Values

s800 p-Values